

WestminsterResearch

<http://www.westminster.ac.uk/westminsterresearch>

Understanding the role of different strain types of *Fusobacterium necrophorum*: biofilms, glycans and metabolic pathways

Brimah, K.

This is an electronic version of a PhD thesis awarded by the University of Westminster.

© Ms Karima Brimah, 2019.

The WestminsterResearch online digital archive at the University of Westminster aims to make the research output of the University available to a wider audience. Copyright and Moral Rights remain with the authors and/or copyright owners.

**Understanding the role of different strain types of
Fusobacterium necrophorum: biofilms, glycans
and metabolic pathways**

Karima Brimah

A thesis submitted in partial fulfilment of the
requirements of the University of Westminster
for the degree of Doctor of Philosophy

November 2019

Abstract

Fusobacterium necrophorum an obligate Gram-negative anaerobe has been implicated in the cause of persistent severe throat infections and the systemic life-threatening Lemierre's syndrome; a potentially fatal periodontal disease, which results in abscess formation in the tonsils. The use of antibiotics had led to decreased incidence of *F. necrophorum* infections to a point that the bacterium became a forgotten pathogen; however, there has recently been a rise in interest. *F. necrophorum* is thought to survive the aerobic oropharynx by biofilm formation. Studies of optimal conditions for biofilm formation could be useful in improving therapeutic options. This current study determined that strains ARU 01 and JCM 3718 formed the most biofilm at 37 °C, with reduction in biofilm observed at 26 °C and 42 °C. Strain JCM 3724 on the other hand, formed most biofilm at 26 °C and 42 °C; this is an indication that strain JCM 3724 but not JCM 3718 or ARU 01 was able to survive in extreme temperatures by forming biofilms; all strains produced more biofilm at pH 4. Biofilm formation was observed in both mono and dual species culture of *F. necrophorum*, in dual culture the organisms became resistant to penicillin and ciprofloxacin.

As glycans are implicated in biofilm formation, bacterial adhesion to host cells and pathogenicity, the cell surface glycans and cell extracts of *F. necrophorum* were investigated using enzyme-linked lectin assays (ELLA) and lectin histochemical staining. No significant differences were seen in the staining patterns, but a patchy and variable staining was noted for *Sambucus nigra* that detects sialic acid. A surface lectin, the Galactose binding protein was identified and characterised as binding to unsubstituted beta galactosyl residues of the type carried by many bacteria suggesting a role in biofilm formation. Subsequent molecular and bioinformatic studies identified all but one key component of the lipid A pathway; *lpxI* was shown to substitute for *lpxH* in the pathway. The component genes required for expression of sialic acid on the cell surface of the organism were determined; a polymorphism, the presence or absence of *siaA*, suggested some but not all strains had the ability to express this sugar on the cell surface. Further studies are required to determine whether this is linked to pathogenicity.

Genomic and proteomic studies on type strains and clinical isolates revealed significant differences between subsp. *necrophorum* and *funduliforme* that will be useful in developing a simple molecular based subspeciation test. The subsp. *funduliforme* was split into 3 clusters (A, B and C) based on the genomic data; proteomic studies were used to determine the impact of the non-synonymous SNPs seen; two clusters were observed at the protein level, A and B+C. Most of the amino acid replacements that differentiated the clusters A from B +C were conservative or semi-conservative; more differences were noted between the two subspecies and these also included non-conservative changes that could affect protein structure and function. Clearly, there is scope for further work to elucidate the evolution of these clusters and their relevance to pathogenicity.

Acknowledgements

I would like to take this opportunity to express my deepest gratitude to Dr Pamela Greenwell for all her invaluable support and continuous guidance, help, time, understanding and most of all patience during the development of and throughout this research.

I would like to thank Professor Mike Wren and Antonia Batty for their generosity with the bacterial samples and advice. Thank you also to Mrs Val Hall for donation of reference strains used in this study.

I would like to extend my gratitude to Dr Lesley Hoyles for financial support and practical help throughout the bioinformatics part of this project.

Many thanks to Louise Usher for her support and help especially staying with me until the late hours after everyone has left. A big thank you to Nasrin for her sisterly support and being around to make sure that I was taking care of my well-being. Haddy, thanks for your sisterly support and laughs. Thank you also to all friends, both doctoral researchers and colleagues for their support and encouragement both in and out of the university premises.

I would like to thank Dr Lorna Tinworth and Chrystalla Ferrier for their continuous moral support and help throughout my time in the university.

I would also like to thank Dr Paul Curley my second supervisor for his encouragement and support.

I would like to express my thanks to the technical staff in the School of Life Sciences, especially Vanita Amin and Luisa Pitzulu. Many thanks also to colleagues and academic staff in the Biomedical and Life sciences department at the University of Westminster for their assistance in various aspects of this project.

I thank Almighty Allah for blessing me with the fortune and the opportunity to undertake this study. 'Alhamdulillah Ala Kulli Haal'.

I dedicate this to my beloved parents and my loving family for their continued support and unconditional love always. God Bless you always - Aameen.

Author's Declaration

I declare that all the material presented in this thesis, is wholly my own work, unless otherwise referenced or acknowledged. The document has not been submitted for qualifications at any other academic institution.

Table of Contents

Abstract.....	i
Acknowledgements.....	ii
Author’s Declaration	iii
Table of Contents.....	iv
List of Tables	ix
List of Figures.....	x
List of Abbreviations	xiii
1 Historical Introduction	1
1.1 General introduction	1
1.2 History of <i>F. necrophorum</i>	2
1.3 Issues associated with the detection of <i>F. necrophorum</i> in Humans	3
1.4 Animal infections with <i>F. necrophorum</i>	3
1.5 <i>F. necrophorum</i> subspecies.....	4
1.6 Phenotypic Identification of the organism.....	4
1.7 Antimicrobial susceptibility.....	6
1.8 Molecular identification	6
1.9 Evidence for biofilm formation	6
1.10 The role of glycans in biofilm formation	9
1.11 Sialic acid	11
1.12 Galactose binding lectin.....	11
1.13 Genome sequencing of <i>Fusobacterium</i>	12
1.14 Biochemical research on <i>Fusobacterium</i> in the last decade.....	12
1.15 Prevalence of <i>F. necrophorum</i> infection in the UK.	13
1.16 Study Aims	15
2 Materials and Methods.....	16
2.1 Materials.....	16
2.2 Bacterial isolates and type cultures.....	16
2.3 Methods	17
2.3.1 Preparation of media, buffers and stock solutions	17
2.3.2 Identification of <i>F. necrophorum</i> isolates.....	19
2.3.3 Molecular Analysis.....	20
2.3.4 RT-qPCR	27

2.4	Biofilm Formation Assays	27
2.4.1	Microtitre plate assay (MTP)	27
2.4.2	Preliminary Biofilm growth with <i>E. coli</i> and <i>S. aureus</i>	28
2.4.3	The effect of different conditions on Fusobacteria.....	29
2.4.4	BSAC disc susceptibility determination of <i>E. coli</i> and <i>S. aureus</i>	31
2.4.5	LIVE/DEAD BaLight Bacterial viability	34
2.5	Analysis of the bacterial cell surface utilising lectin staining.....	36
2.5.1	Cytochemistry staining with biotinylated lectins	38
2.5.2	Lectin cytochemistry for epifluorescent microscopy	39
2.5.3	Lectin ELISA (ELLA).....	39
2.6	Galactose binding protein – Study of function	40
2.6.1	Primer design.....	40
2.6.2	Haemagglutination assay	40
2.6.3	Bioinformatics	43
2.6.4	Sequence analysis.....	43
2.6.5	PCR and Sequencing	43
2.7	Whole genome sequencing.....	44
2.7.1	Preparation of anaerobic broth using anaerobic Hungate culture tubes	44
2.7.2	Growth of <i>F. necrophorum</i> in anaerobic BHI broth.....	44
2.7.3	Preparation of Genomic DNA (gDNA) for NG Sequencing	45
2.7.4	Next generation sequencing	45
2.7.5	Phylogenetic analyses	46
2.7.6	<i>16S rRNA</i> gene sequence analysis of strain F88.....	46
2.7.7	Quality control checks on genome sequence data	46
2.7.8	Determination of average nucleotide identity (ANI).....	47
2.7.9	Comparative and pangenome analyses of <i>Fusobacterium necrophorum</i> strains...	47
3	Typing and Subtyping of <i>F. necrophorum</i> strains and clinical isolates.....	49
3.1	Introduction	49
3.2	Methods	51
3.2.1	Identification methods	51
3.3	Results	51
3.3.1	Identification of isolates.....	51
3.4	Discussion	57
4	Biofilms	58
4.1	Introduction	58

4.2	Methods	59
4.3	Results	60
4.3.1	Biofilm formation	60
4.3.2	<i>F. necrophorum</i> and <i>S. aureus</i> biofilm formation under different conditions	61
4.3.3	BacLight viability.....	64
4.3.4	Single and Dual-species biofilm formation.....	65
4.3.5	Antibiotic disc susceptibility testing of <i>E. coli</i> and <i>S. aureus</i>	67
4.3.6	Antibiotic disc susceptibility testing of <i>F. necrophorum</i>	67
4.3.7	Minimum inhibition concentration (MIC) test using MTP	67
4.3.8	Single species biofilm with antibiotics.....	70
4.3.9	Dual-species biofilm with antibiotics	71
4.3.10	<i>16S rRNA</i> gene amplification from the DNA extraction from planktonic cells and biofilms. 73	
4.4	Discussion	74
5	Cell surface sugars and the Galactose-binding protein of <i>F. necrophorum</i>.	87
5.1	Introduction	87
5.1.1	Glycan-lectin interactions.....	87
5.2	Methods	88
5.2.1	Determination of specificity of the Galactose-binding protein.....	88
5.2.2	Protein modelling	90
5.3	Results	90
5.3.1	Cell surface glycans; ELISA lectin binding assay	90
5.3.2	Glycans present in whole cell extracts; ELLA assay	91
5.3.3	The <i>galactose-binding protein</i> gene; PCR based analysis	93
5.3.4	Rt qPCR analysis.....	95
5.3.5	DNA sequencing	95
5.3.6	Haemagglutination assays.....	96
5.3.7	Bead based lectin assay.....	96
5.3.8	Protein modelling	97
5.4	Discussion	102
6	LPS and lipid A biosynthesis	107
6.1	Introduction	107
6.2	Methods	111
6.2.1	Bacterial strains.....	111
6.2.2	Bioinformatics	111

6.2.3	PCR and Sequencing	111
6.2.4	Sequence analysis.....	111
6.3	Results	112
6.3.1	LPS and lipid IVA pathway of <i>F. necrophorum</i>	112
6.3.2	Identification of the <i>lpxI</i> gene in <i>Fusobacterium necrophorum</i>	123
6.4	Discussion	131
7	Genome Analysis of <i>F. necrophorum</i> reference strains and clinical isolates using NGS.	134
7.1	Introduction	134
7.2	Methods	135
7.2.1	Retrieval of whole genome sequences from public databases and microbesNG.	135
7.2.2	Preliminary phylogenetic analyses.	135
7.2.3	<i>16S rRNA</i> gene sequence analysis of strain F88.	136
7.2.4	Quality control checks on genome sequence data.	136
7.2.5	Determination of average nucleotide identity (ANI).....	136
7.2.6	Comparative and pangenome analyses of <i>Fusobacterium necrophorum</i> strains.	136
7.2.7	Impact of nucleotide changes on amino acid sequence.	137
7.3	RESULTS	145
7.3.1	Preliminary sequence analyses	145
7.3.2	ANI comparisons of <i>Fusobacterium necrophorum</i> genomes with other Fusobacteria	150
7.3.3	<i>Fusobacterium necrophorum</i> pangenome analysis.....	150
7.3.4	Impact of nucleotide changes on amino acid sequence.	156
7.4	Discussion	176
8	Sialylation pathways in <i>F. necrophorum</i>; the utility of <i>in silico</i> analysis of WGS data....	182
8.1	Introduction	182
8.2	Methods	185
8.3	Results	185
8.3.1	Interrogation of the Uniprot database.....	185
8.4	Discussion	192
9	General Discussion	196
9.1	Discussion	196
9.2	Future Work.....	199
9.3	Conclusion	199

Appendices	201
Appendix I: Biochemical tests.....	201
i-1 Gram stain and Microscopic appearance	201
i-2 Catalase test.....	201
i-3 Oxidase test	202
i-4 Spot Indole test	202
i-5 Lipase test	203
Appendix II: DNA Sequence [16S rRNA]	204
ii-1 ARU planktonic.....	204
ii-2 3718 planktonic	205
ii-3 3724 planktonic	206
ii-4 ARU biofilm	207
ii-5 3718 Biofilm	208
ii-6 3724 Biofilm	209
ii-7 Positive control.....	210
Appendix III: BLAST data analysis for <i>galactose binding</i> primers with <i>F. necrophorum</i>	
DNA samples.	211
iii-1 ARU 01- <i>gal binding</i> primer:.....	211
iii-2 JCM 3718 – <i>gal binding</i> primer:	212
iii-3 JCM 3724 – <i>gal binding</i> primer:	213
Appendix IV: Haemagglutination Assays.....	214
iv-1 Haemagglutination assay of human blood cells with commercial anti-sera.	214
iv-2 Haemagglutination assay of <i>F. necrophorum</i> cells with sheep red blood cells treated with neuraminidase.....	215
Appendix V: Q-RT-PCR for gene expression.....	217
Appendix VI: Formulae for estimation of biofilm assays.....	219
Appendix VII: Rpm (speed) to g (RCF)	220
Appendix VIII	222
References.....	223

List of Tables

Table 2.1 Clinical strains/isolates of <i>Fusobacteria</i> from UCLH, London, UK.....	17
Table 2.2 Strains of <i>Fusobacteria</i> from Anaerobic Reference Unit, Cardiff, UK.	17
Table 2.3 Control strains of bacteria used in this study.....	17
Table 2.4 Primers used for 16S rRNA, 23S rRNA and gyrB genes PCR	23
Table 2.5 List of primers used in the study of the function of Galactose (Gal) binding proteins.....	23
Table 2.6 Primers for genes involved in the lipid IV A biosynthetic pathway	24
Table 2.7 Primers used for amplification of genes involved in glycosylation of <i>F. necrophorum</i>	24
Table 2.8 Bacterial strains and antibiotics used for disc diffusion test of aerobes.	31
Table 2.9 Commonly used biotinylated lectins with their sugar specificity and abbreviations adapted from Afrough <i>et al.</i> , (2007).	37
Table 3.1 Characteristics of <i>F. necrophorum</i> isolates selected for future research	55
Table 3.2 Results of RT-PCR of <i>F. necrophorum</i> strains ARU 01, JCM 3718, JCM 3724 and <i>E. coli</i> with gyrase B and 16S rRNA primers:	56
Table 4.1 Comparisons of biofilm mean absorbance (MTP assay); adherent and planktonic cells.....	61
Table 4.2 Comparisons of crystal violet mean absorbance: adherent cells.....	61
Table 5.1 Results of lectin histochemistry using fluorescent-labelled lectins for <i>F. necrophorum</i> and <i>S. aureus</i>	91
Table 5.2 ELLA lectin assay for <i>F. necrophorum</i>	92
Table 5.3 qPCR results showing CT values and melting temperature analysis of <i>F. necrophorum</i> cDNA with the Gal binding primers.	95
Table 6.1 Output of the “Select neighbours” function of the Dali server	126
Table 6.2 Amino acids implicated by Raptor X in substrate binding.....	129
Table 7.1 Information for NCBI, NCTC and microbesNG genome assemblies used in preliminary phylogenetic.....	139
Table 7.2 Impact of non-synonymous SNPs on LpxI.....	157
Table 8.1 Candidate proteins for sialic acid pathways of <i>F. necrophorum</i>	186
Table 8.2 Analysis of gene encoded proteins in sialic acid pathways	190

List of Figures

Figure 2.1 Set up of bacterial cells and biotinylated lectin on slides.	38
Figure 3.1 Colony identification of <i>F. necrophorum</i> on FAA blood agar plates after 48 hours incubation under anaerobic conditions at 37 °C.	52
Figure 3.2 Gram stain images of <i>F. necrophorum</i> strains, A-ARU 01, B-JCM 3718 and C-JCM 3724	52
Figure 3.3 Electrophoretic separation pattern of amplicons of <i>F. necrophorum</i> DNA with 16S rRNA primers.	56
Figure 4.1 Quantification of biofilm formed by the 3 <i>F. necrophorum</i> isolates... ..	63
Figure 4.2 Representative images of BacLight viability staining with mixture of SYTO9 and PI.....	65
Figure 4.3 Comparison of biofilm formed by <i>F. necrophorum</i> strains (ARU 01, JCM 3718 and JCM 3724) as single or dual-species at absorbance of 600 nm..	66
Figure 4.4 Antibiotic susceptibility testing of <i>F. necrophorum</i> strains: ARU 01, JCM 3718 and JCM 3724 with three antibiotics (PEN-penicillin, KAN-kanamycin and MET-metronidazole) at concentration of 512 – 64 µg/ml... ..	69
Figure 4.5 Comparison of single-species biofilm with antibiotics.....	70
Figure 4.6 Comparison of dual-species biofilms of <i>F. necrophorum</i> strains with <i>S. aureus</i> with antibiotics.....	71
Figure 4.7 Gel electrophoresis of PCR amplicons of DNA extracted from planktonic cells and biofilms of <i>F. necrophorum</i> using 16S rRNA primers. ..	73
Figure 5.1 Glycan structures of the Human A, B and H antigens.	89
Figure 5.2 Glycan structures of sheep;.....	89
Figure 5.3 Gel electrophoresis of amplicons of <i>F. necrophorum</i> clinical Lemierre's strain ARU 01 and reference strains JCM 3718, JCM 3724 and clinical samples F1, F5, F11, F21, F24, F30, F39, F40, F41 & F42, amplified with <i>F. necrophorum</i> Gal-binding primers.	94
Figure 5.4 Protein sequence of the Galactose-binding protein of <i>F. necrophorum</i>	97
Figure 5.5 Suggested templates for modelling the Galactose-binding protein (Swiss-Model)	98
Figure 5.6 Results of modelling the Galactose- binding protein of <i>F. necrophorum</i>	99
Figure 5.7 N-acetyllactosamine (yellow) binding to the	100

Figure 5.8 Galactose binding (yellow) binding to the.....	101
Figure 5.9 Overlay of galactose (white) and N-acetyllactosamine (yellow) binding to the Galactose-binding protein.	101
Figure 6.1 Schematic of the basic structure of lipopolysaccharide.....	109
Figure 6.2 Biosynthetic pathway of lipid A in <i>E.coli</i>	113
Figure 6.3 Analysis of amplicons of <i>F. necrophorum</i> using <i>lpxA</i> and <i>lpxC</i> primer sets run on 1% agarose gel.....	114
Figure 6.4 Analysis of amplicons of <i>F. necrophorum</i> with the <i>lpxD</i> and	114
Figure 6.5 Multiple Alignment of the target sequence of <i>lpxA</i> of lipid A pathway for all samples.....	115
Figure 6.6 Multiple Alignment of the target sequence of <i>lpxD</i> of lipid A pathway for all samples.	116
Figure 6.7 Multiple Alignment of the target sequence of <i>lpxB</i> of lipid A pathway for all samples.	117
Figure 6.8 Multiple Alignment of the target sequence of <i>lpxC</i> of lipid A pathway for all samples.....	118
Figure 6.9 Impact of nucleotide deletions in <i>lpxC</i> on derived protein sequence.	118
Figure 6.10 The amino acids sequence alignment produced by ClustalW of LpxC.	119
Figure 6.11 Protein sequence analysis of the amino acid for the	120
Figure 6.12 Protein sequence analysis of the amino acid for the	120
Figure 6.13 Protein sequence analysis of the amino acid for the	121
Figure 6.14 The amino acids sequence alignment produced by ClustalW of LpxA.	122
Figure 6.15 Multiple sequence alignment of the LpxI proteins of <i>F. necrophorum</i> , <i>Caulobacter crescentus</i> and <i>Rhizobium galegae</i>	124
Figure 6.16 Structural alignment of models of LpxI from <i>F. necrophorum</i> generated using Swiss-Model (green) and RaptorX (red) using the Dali server.....	125
Figure 7.1 Phylogenetic (neighbour-joining) tree showing taxonomic placement of strains included in this study within the family Fusobacteriaceae.....	147
Figure 7.2 Representation of contaminating contigs in microbesNG-generated assembly of strain F80 genome.	148
Figure 7.3 Species assignment of F88.....	149

Figure 7.4 Heatmap summarizing ANI values for <i>Fusobacterium necrophorum</i> genomes and related species.	152
Figure 7.5 Pangenome analysis of <i>Fusobacterium necrophorum</i> subsp. <i>necrophorum</i> (FNN) and <i>Fusobacterium necrophorum</i> subsp. <i>funduliforme</i> (FNF).....	153
Figure 7.6 PCA of accessory genes (present in 5 – 95 % of strains) for <i>Fusobacterium necrophorum</i> subsp. <i>necrophorum</i> and <i>Fusobacterium necrophorum</i> subsp. <i>funduliforme</i>	154
Figure 7.7 PCA of accessory genes (present in 5 – 95 % of strains) for <i>Fusobacterium necrophorum</i> subsp. <i>funduliforme</i>	155
Figure 7.8 Venn diagram showing numbers of core and accessory genes shared by the three <i>Fusobacterium necrophorum</i> subsp. <i>funduliforme</i> clusters identified from PCA of accessory genes.	156
Figure 7.9 Clustal Omega analysis of the LpxI protein.....	159
Figure 7.10 Clustal Omega analysis of the Galactose binding periplasmic protein.	162
Figure 7.11 Clustal Omega alignment of a part of the Leukotoxin protein.....	163
Figure 7.12 Clustal Omega analysis of the Elongation factor Tu.....	165
Figure 7.13 Clustal Omega analysis of the Pyruvate synthase.	169
Figure 7.14 Clustal Omega analysis of the DNA polymerase III subunit tau. ..	172
Figure 7.15 Clustal Omega analysis of Threonine--tRNA ligase 2.	175
Figure 8.1 Overview of the major pathways for sialic acid utilization in bacterial pathogens.	183
Figure 8.2 Proposed major pathways for sialic acid utilization	187
Figure 8.3 Comparison of the gene order in <i>Fusobacteria</i> sp.	192

List of Abbreviations

A	Adenine
AB medium	Autoinducer Bioassay medium
AI	Autoinducer
AK	Amikacin
AMP	Ampicillin
ANOVA	Analysis of Variance
ARU	Anaerobe Reference Unit
AST	Antimicrobial Susceptibility Testing
ATCC	American Type Culture Collection
ATP	Adenosine Tri-phosphate
BGC	Biofilm Growth Check
BHI	Brain Heart Infusion
BLAST	Basic Local Alignment Search Tool
bp	Base pair
BSAC	British Society for Antimicrobial Chemotherapy
C	Cytosine
CAZ	Ceftazidime
cDNA	complementary DNA
CDS	Coding sequence
CFU	Colony Forming Unit
CHL	Chloramphenicol
CIP	Ciprofloxacin
CLSM	Confocal Laser Scanning Microscopy
Con A	<i>Concanavalin A</i>
CPS	Capsular polysaccharide
CV	Crystal Violet
CV %	Coefficient of Variation
DNA	Deoxyribose Nucleic Acid
DNase I	Deoxyribonuclease I
dNTP	deoxyribonucleotide triphosphate
eDNA	Extracellular DNA
EDTA	Ethylenediaminetetraacetic acid
ELISA	enzyme-linked immunosorbant assay
ELLA	Enzyme-Linked Lectinsorbent Assay
EPS	Extracellular Polymeric Substance

EUCAST	European Committee on Antimicrobial Susceptibility Testing
FAA	Fastidious anaerobe agar
FAB	Fastidious anaerobe broth
FITC	Fluorescein isothiocyanate
G	Guanine
GM	Gentamicin
<i>gyrB</i>	Gyrase B
H ₂ O ₂	Hydrogen Peroxide
HRP	horse-radish peroxidase
JAC	<i>Jacalin</i>
JCM	Japanese Collection of Microorganisms
KAN	Kanamycin
kb	Kilo bases
kDa	Kilo Daltons
lktA	leukotoxin
LB	Luria–Bertani
LEV	Levofloxacin
LPS	Lipopolysaccharide
M	Molar
Mb	Megabases
MBC	Minimum Bactericidal Concentration
MET	Metronidazole
MIC	Minimum Inhibitory Concentration
miRNA	microRNA
mM	milli–Molar
mRNA	Messenger ribonucleic acid
MTP	Microtitre Plate
NCBI	National Center for Biotechnology Information
NCTC	National Collection of Type Cultures
NGS	Next Generation Sequencing
nM	nanomolar
no-RT	no reverse transcriptase control
NS	non-structural
NSO	non-specific oligonucleotide
nt	nucleotide
OD	Optical Density
PBS	Phosphate Buffered Saline

PBST	Phosphate Buffered Saline/Tween 20
PE-LB	Protein Extraction & Lysis Buffer
PEN	Penicillin
PHA-L	Phaseolus Vulgaris Leucoagglutinin
PI	Propidium iodide
PMNs	Polymorphonuclear cells
PNA	<i>Peanut Agglutinin</i>
PNP	paranitrophenol-phosphate
PSTS	Persistent sore throat syndrome
PTA	Peritonsillar abscess
Q-RT-PCR	Quantitative real time PCR
QS	Quorum Sensing
QSI	Quorum Sensing inhibitor
RCA-I	Ricinus communis Agglutinin I
RFU	Relative fluorescence units
RNAi	RNA interference
RNase	Ribonuclease
rpm	Revolutions Per Minute
rRNA	Ribosomal Ribose Nucleic Acid
RT	reverse transcriptase
SEM	standard error of the mean
SD	standard deviation
SJA	<i>Sophora Japonica</i>
small interfering RNA	small interfering RNA
SNP	Single Nucleotide Polymorphism
sp.	Specie
spp.	Species (plural)
subsp.	Subspecies
T	Thymine
TBE	Tris-Borate-EDTA buffer
TET	Tetracycline
μl	microlitre
μM	micromolar
UTI	Urinary Tract Infection
UV	Ultra-violet
VAN	Vancomycin
v/v	Volume/Volume

w/v	Weight/Volume
WHO	World Health organisation
ZOI	Zone of Inhibition

Chapter 1

1 Historical Introduction

1.1 General introduction

Fusobacterium necrophorum is an obligate anaerobic Gram-negative rod known to colonise the mouth and respiratory tract in humans (as reviewed by Brazier, 2006). The most severe clinical presentation of infections due to *F. necrophorum* is septic jugular thrombophlebitis (also known as Lemierre's syndrome). Findings include sore throat, persistent fever, soft tissue or neck swelling and bacteremia (Handler *et al.*, 2011). *F. necrophorum* is implicated as a cause of endemic pharyngitis in adolescents and young adults, accounting for more than 20 % of acute pharyngitis and may also be the cause of intra-abdominal infections, peritonitis, septic arthritis, brain abscesses and infrequently, infective endocarditis (IE). There is strong evidence that *F. necrophorum* is also responsible for more than 20 % of recurrent, persistent or chronic sore throats known as persistent sore throat syndrome (PSTS), without resulting in full systemic infection. This bacterium is also implicated in otitis media in children, peritonsillar abscesses in adolescents and young adults and sinusitis in adults aged between 30-50 years; it has also been connected recently with tonsillitis (Jensen *et al.*, 2007). Studies by Batty *et al.*, (2005) and others have revealed that pharyngitis can progress to develop into Lemierre's syndrome, a severe and life-threatening infection, estimated to have a higher incidence, mortality and morbidity compared to rheumatic fever in adolescents and young adults in the Western world (Bank *et al.*, 2010). The disease progresses in several steps: primary infection, which is usually pharyngitis, local invasion of the lateral pharyngeal space and internal jugular vein (IJV) septic thrombophlebitis, and finally metastatic complications.

F. necrophorum infections were first noted in humans in 1898 by Hallé who examined a female with genitourinary tract infection and discovered that the bacteriological infection showed cocci shaped organisms. Further studies examining samples from patients suffering from otitis showed that they all had Gram-negative coccobacilli, and this led to Hallé naming the organisms as

'*Bacillus funduliformis*' (now referred to as *F. necrophorum* subsp. *funduliforme* (as cited by Brazier, 2006; Riordan, 2007).

In 1930, Lemierre, a French physician showed the association of *Bacillus funduliformis* with systemic infection (as cited by Brazier, 2006). Studies carried out by Lemierre in 1936 involving cases of anaerobic septicaemia, noted that the infected group consisted mainly of young adults. Their mortality rate from the onset of the infection was 7- 15 days, with symptoms ranging from mild fever to metastatic embolic pulmonary abscesses (as cited by Kristensen and Prag, 2000). This led Lemierre to provide a clear clinical description of postanginal septicaemia associated with *F. necrophorum*. In the late 1980s, the names necrobacillosis and postanginal septicaemia were replaced with Lemierre's syndrome (LS).

1.2 History of *F. necrophorum*

F. necrophorum was first described in animals, as it is a much more common and important pathogen in animals than in humans. This organism was first recognised in 1884 by Loeffler as the cause of diphtheria infection in a calf. He identified stained sections of diphtheric samples as negative rods with filamentous forms. This material was injected into mice, generating purulent lesions which were foul-smelling and contained similar bacilli. The isolate from calf serum broth could not be further sub-cultured. Flugge named the organism *Bacillus necrophorus* and coined the term necrobacillosis for the disease. The organism was first isolated in culture by Bang from liver abscess of cattle, and identified as the cause of hog cholera as cited by Riordan, (2007). Schmorl in 1891 described the first human infections involving an animal strain. Schmorl and his assistant working on rabbits with necrobacillosis developed abscesses on their fingers. Once resected, stained and analysed microscopically, the results demonstrated the characteristic filamentous Gram-negative bacilli that he observed earlier (as reviewed by Riordan, 2007).

1.3 Issues associated with the detection of *F. necrophorum* in Humans

Isolation and identification of obligate anaerobes such as *F. necrophorum* from the normal microbiota of the throat is difficult and time-consuming (Aliyu *et al.*, 2004). In diagnostic microbiology laboratories, isolating this bacterium requires adherence to the principles of good anaerobic bacteriology, due to its fastidious and strict growth requirements. Studies have shown that strict anaerobic conditions need to be adhered to when working with *F. necrophorum* with minimum exposure to air. The Centers for Disease Control and Prevention (CDC), USA, indicated that this microorganism may not survive exposure to air for more than 30 minutes (CDC, 2002).

This bacterium accounts for only a small proportion of cases of human infection compared to other non-sporing anaerobes, therefore is not well studied. However, there has been an increase in the isolation of the organism, which has stimulated research of this bacterium in microbiology laboratories in the UK (Brazier *et al.*, 2002; Brazier, 2006; Jones *et al.*, 2001). This increase may be due to increasing awareness, improved anaerobic diagnostic facilities and advice to general practitioners (GPs) not to prescribe empiric antibiotics for simple sore throats (Jones *et al.*, 2001; Hagelskjaer *et al.*, 1998; Brazier *et al.*, 2002; Department of Health Standing Medical Advisory Committee, 1998).

1.4 Animal infections with *F. necrophorum*

F. necrophorum is the cause of necrobacillosis in animals and is implicated in liver abscesses and footrot in cattle and sheep (Langworth, 1977; Zhou *et al.*, 2009a). The first description of *F. necrophorum* infection in animals was in 1876 by Dammann then studying calf diphtheria. He believed that the infection manifested due to *Bacillus diphtheria*, until Loeffler in 1884 analysed necrotic tissue of stained diphtheria material and labelled the causative agent as *F. necrophorum* (as cited by Brazier, 2006). *F. necrophorum* is a recognised opportunistic animal pathogen, causing a variety of diseases, including diphtheria in calf and mastitis in cattle, hepatic (liver) abscesses and foot rot. Liver abscesses have been described as the most common outcome of *F. necrophorum* infection found in cattle, and these infections are thought to start in the rumen and spread through septic emboli to

the liver. Footrot is a necrotic infection of the soft tissues on the foot and surrounding skin, and this can often lead to fever and lameness in cattle and other hooved animals. Predisposing factors include walking on damp ground and old injuries to the interdigital skin, with faecal secretions being the primary source of infection (Tan *et al.*, 1996). The incidence of hepatic abscesses reached up to 32 % in most feed yards (Brink *et al.*, 1990). Simon and Stovell, (1971) demonstrated that *F. necrophorum* was present in 97 % all of liver abscesses assessed. A total of 67 % of *F. necrophorum* were isolated in pure culture and 30 % isolated with other microorganisms such as streptococci.

These infections of livestock have a major economic impact on the farming industry as well as on the animals' welfare and this has led to the research on *F. necrophorum* mainly focused on the animal pathogen. The bacterium was initially described as more common and important in animals, but others later described it as a historical view due to the increasing importance of the infection in humans (Nagaraja and Chengappa, 1998; Riordan, 2007; Wright *et al.*, 2012).

1.5 *F. necrophorum* subspecies

F. necrophorum is taxonomically divided into two subspecies: *F. necrophorum* subsp. *necrophorum* (FNSN) and *F. necrophorum* subsp. *funduliforme* (FNSF). The *necrophorum* subspecies is the more virulent form associated mostly with infections in animals, whereas subsp. *funduliforme* infects mainly humans (Brazier, 2006; Zhang *et al.*, 2006; Jensen *et al.*, 2007).

1.6 Phenotypic Identification of the organism

F. necrophorum is a non-motile, non-sporing slow growing pleomorphic rod-shaped anaerobe. A few different agars can be used for culturing *F. necrophorum*, these include brain-heart infusion (BHI) agar, Columbia blood agar enriched with vitamin K, hemin and yeast extract (Brazier *et al.*, 1990). Studies by Batty and Wren (2005) and Brazier (2006) suggested that fastidious anaerobe agar (FAA) supplemented with 5 - 10% defibrinated horse blood is best for culturing *F. necrophorum*. FAA which has cysteine as a growth promoting agent provides all the nutritious medium for the growth of organism. Commercial kits such as the

API 20A, API Rapid ID 32A and RapID-ANA II strip tests can be used to identify *F. necrophorum*, although as many of the tests on each strip are negative, excluding the indole and alkaline phosphatase tests, it is often better to use specific tests when *F. necrophorum* is suspected (Batty *et al.*, 2005; Riordan, 2007).

The catalase test demonstrates the presence of the enzyme catalase which catalyses the release of oxygen from hydrogen peroxide (H₂O₂). This test differentiates bacteria that produces catalase enzyme from non-catalase producing bacteria. This enzyme breakdown hydrogen peroxide into oxygen and water, thus bacteria can protect themselves from the lethal effect of hydrogen peroxide which accumulates as end product of aerobic carbohydrate metabolism. Obligate anaerobes would be negative for catalase as they would die in the presence of oxygen. They do not produce this enzyme, as they do not use oxygen, so would not need to break it down. Although some obligate anaerobes produce these enzymes in very small quantities, they are totally absent in others (Hentges, 1996).

Anaerobic bacteria can be classified by the presence and absence of lipase among other things. One readily detectable feature of *F. necrophorum* is the production of lipase on egg yolk agar. Lipases are enzymes catalysing the breakdown of triglycerides (triacylglycerols) into glycerol and long chain fatty acids. Egg yolk agar is a differential and enriched medium used for the isolation and differentiation of different species based on their lipase and lecithinase activity. This non-selective egg yolk supplemented medium supplies lecithin and free fats, which are required for the detection of lipase and lecithinase production. If the enzyme is present, the microorganism hydrolyses the free fats present in the medium, forming glycerol and free fatty acids. The insoluble free fatty acids that is released, forms an iridescent sheen (oil on water) seen on the surface of the plate when angled at a light source (Tille, 2013). *F. necrophorum* subsp. *funduliforme* is less strongly positive for lipase than subsp. *necrophorum*. Tryptophanase enzymes which produce indole as a metabolite from tryptophan is also produced by *F. necrophorum*. The test for this uses spot indole reagent which produces a greenish-blue colour when positive for indole (Batty *et al.*, 2005). *F. necrophorum* colonies fluoresce a greenish-yellow under long wavelength Ultra-violet (UV) light of 365 nm (Barrow and Feltham, 2004).

1.7 Antimicrobial susceptibility

F. necrophorum is kanamycin and metronidazole sensitive and generally susceptible to penicillins, colistin, tetracyclines, lincosamides and macrolides, but resistant to vancomycin, gentamycin, neomycin and streptomycin (Nagaraja *et al.*, 1998).

1.8 Molecular identification

The use of molecular typing techniques to characterise bacterial strains is a very powerful tool, which contributes to our understanding and control of outbreaks and recurrent infections (Hollis *et al.*, 1999). *F. necrophorum* is thought to have a complex and unusual virulence and pathogenesis, which is poorly understood at present. In a small study in humans, 17 isolates from cases of systemic disease and from cases of persistent sore throat syndrome were compared using enterogenic repetitive intergenic consensus (ERIC) - PCR to determine whether strains of similar or different types were responsible for throat and systemic disease; similar strains were found in both diseases (Batty *et al.*, 2005). They identified at least twelve different band patterns and hence types. Interestingly, four proposed types were shared amongst clinical presentations (CPs) including a large proportion demonstrating the same band patterns as the type culture strain (JCM 3724), but the results also showed seven types that were exclusive to either persistent sore throat syndrome or Lemierre's syndrome samples.

Molecular typing studies by Okwumabua *et al.*, (1996) investigated differences between bovine strains of both subspecies of *F. necrophorum* using ribotyping. Narayanan *et al.* (1997) expanded on the work and discovered different strains and subspecies from different lesions in the same animal, indicating different strains actively causing independent lesions. They also identified the same strain in different sites, possibly suggesting that only certain strains are able to colonise and spread, which indicates a potential route of pathogenesis of the bacterium. This work has not been carried out for the human pathogen.

1.9 Evidence for biofilm formation

Fusobacteria are likely to reside in biofilms alongside other microbes that can decrease the available oxygen and provide a stable anaerobic environment.

Biofilms are defined as structured communities of bacterial cells enclosed in a self-produced polymeric matrix. They are ubiquitous masses of cells capable of surviving on a wide range of surfaces by adhering to an inert or living surface such as water pipes and chronic wounds. This mode of growth is a strategy used by microorganisms to survive harsh growth conditions and exposure to antimicrobial agents (Stewart and Costerton, 2001). Biofilms are surrounded with self-generated exopolysaccharides known as the extracellular polymeric substance (EPS). The EPS is made up of polysaccharide biopolymer, protein and DNA, but the structural components vary among different bacterial species and strains (Branda *et al.*, 2005). These are tightly attached to the underlying surface and inactivate the defence molecules, thus contributing to the persistence of the biofilm and difficulty in treatment (Vu *et al.*, 2009). There is evidence that biofilms play an important role in the development of antimicrobial resistance. Since their complex structure provides a barrier to the penetration of antimicrobial agents. The EPS protects the bacteria from killing by antimicrobial agents and enables evasion from the host immune response, resulting in chronic upper respiratory infections and in the case of *F. necrophorum* biofilm and antibiotic resistance (Mohammed *et al.*, 2013). It has been shown that the resultant biofilms have altered phenotypes with respect to growth, gene expression and protein production. This is as a result of communication among the bacteria in this sessile environment known as quorum sensing (QS) (Donlan *et al.*, 2002). Most bacteria during stressful changes in the environment, secrete small QS signalling molecules also called autoinducers, at a concentration (threshold) corresponding to the density of cells (Raina *et al.*, 2009; Jang *et al.*, 2012). Stress response gene expression is triggered at a threshold causing a change in cell surface proteins, which increases cell surface hydrophobicity (Stanley and Lazazzera, 2004). QS is implicated in the regulation of processes such as antibiotic resistance, antibiotic production, biofilm formation, bioluminescence and virulence expression (Engebrecht and Silverman, 1984; Haas *et al.*, 2002).

The human upper respiratory tract has abundant oxygen, yet facultative and obligate anaerobes have been shown to thrive in this niche (Ahn and Burne, 2007). Anaerobes such as *F. necrophorum* are thought to survive in this oxygen rich environment by forming polymicrobial biofilms, where oxygen is consumed by aero-tolerant species; this creates an oxygen gradient in the biofilm, allowing anaerobes to survive deep within (Bradshaw *et al.*, 1998). It is unusual to find a

single bacterial species in an infection and the microbes tend to form biofilms that act synergistically, affecting, for example, the antibiotic sensitivity of the organisms involved. Biofilms have been associated with a wide variety of microbial infections in the body, estimated to be as high as 80% of all infections according to the National Institutes of Health (NIH) (Davies, 2003; Joo and Otto, 2012; Jamal *et al.*, 2018).

Many biofilms are detrimental to humans, the clinically important ones are formed in response to stresses from the host defence mechanisms and antibiotics (Anderson and O'Toole, 2008). Biofilms have increased resistance to antimicrobials and are more resistant to host defence mechanisms than free-living planktonic cells; indeed bacteria in a biofilm growth state can be up to 1000 times more resistant than their planktonic counterparts (Mah and O'Toole, 2001; López *et al.*, 2010). Thus, biofilm formation is a mechanism that promotes bacterial attachment to host surfaces. Bacteria within biofilms communicate with one another through soluble signalling molecules to optimize gene expression for survival and live in conditions of limited nutrients in a dormant state, in which defence molecules produced by the immune system and pharmacologic antibiotics are less effective. Research into the formation of *F. necrophorum* biofilms may shed light on the behaviour and requirements of this obligate anaerobe.

Bacteria in biofilms usually use surface proteins and sugars for attachment to each other, host cells or to the extracellular matrix. Oligosaccharide residues on cells, such as surface proteoglycans, glycoproteins and glycolipids, are specific to different cells. Fimbriae and other cell surface appendages expressed by bacteria such as *Escherichia coli* are involved in providing structural stability during biofilm formation (López *et al.*, 2010; Donlan, 2002). Bacterial lectins are carbohydrate-binding proteins first described in 1970 by Nathan Sharon and colleagues. They specifically identify and bind to sugar moieties to help in the process of cell-cell or cell-matrix attachments during biofilm formation; these lectins also bind with glycan ligands on host surface receptors. Lectins are also useful as primary diagnostic tools for the identification of bacterial glycans (Afrough *et al.*, 2007; Munoz *et al.*, 1999; Munoz *et al.*, 2003; Slifkin and Doyle, 1990).

1.10 The role of glycans in biofilm formation

In the last 15 years, interest in the glycans of bacteria has increased substantially. These glycans can be found in polysaccharides, glycoproteins glycolipids, lipopolysaccharides and peptidoglycans (reviewed by Comstock and Kasper, 2006). The lipopolysaccharides and peptidoglycans have been well documented but more recently the focus has moved towards glycolipids and glycoproteins (Zhou and Wu, 2009), some of which carry sugars identical to those of the host implying that molecular mimicry could be a colonisation strategy (reviewed by Varki *et al.*, 2009). Additionally, bacterial glycans can facilitate binding to other bacteria or to host cells via glycan-lectin interactions. A number of pathogens have been investigated and the data supporting the role of glycans and lectins in colonisation, adherence and biofilm formation is compelling (Esko and Sharon, 2009).

Glycan-lectin binding plays a role in biofilm formation with for example, lectins on organisms binding to host glycans, lectins on the host binding bacterial glycans and lectin-glycan binding between organisms of the same or different species. The understanding of the mechanisms of biofilm formation in *F. necrophorum* infection could lead to the development of ways of inhibiting biofilm formation and potential therapeutic strategies based on glycan and biofilm formation (Lesman-Movshovich *et al.*, 2003; Ofek *et al.*, 2003; Wu *et al.*, 2007; Rachmaninov *et al.*, 2012).

Oligosaccharides containing *N*-acetylneuraminic acid (sialic acid) on the cell surface of some pathogenic bacteria are known to be important for host-microbe interactions. Studies have shown *N*-acetylneuraminic acid (Neu5Ac) has a major role in the pathogenicity of bacterial pathogens, such as cell surface sialyloligosaccharide moieties of the human pathogen *Haemophilus influenzae* which are involved in virulence and adhesion to host cells. Little is known about glycosylation of *F. necrophorum*; indeed, bacterial glycosylation is a fairly novel area and glycans have not yet been given a definitive function. However, many discoveries have been made on appendages of pathogenic bacteria indicating glycans may influence pathogenicity (Vimr, 2004; Vimr *et al.*, 2013).

By imitating the carbohydrates of human host cells, which are crucial for self/non-self-recognition, a bacterial pathogen can escape the host immune system. The

terminal oligosaccharide moieties of some bacteria are identical to those of gangliosides, which are compounds composed of a glycosphingolipid with one or more sialic acid linked to the sugar chains; these moieties are thought to be involved in virulence and adhesion to host cells (Yuki *et al.*, 2004). Important information in the understanding of the role of bacteria in chronic infections will be obtained from an investigation of the mechanisms of glycan-lectin interactions during biofilm formation. The inhibition of glycan-lectin interactions and quorum sensing have been considered as alternative strategies to antibiotic treatment that can be useful in the treatment of chronic infections through the prevention and disruption of biofilm formation (Brackman *et al.*, 2011).

Extracellular products such as lipopolysaccharide (LPS) endotoxins confer pathogenicity to *Fusobacteria*; LPS is the major component of the outer membrane of Gram-negative bacteria. In the late 19th century Richard Pfeiffer discovered a heat-resistant toxic component released from *Vibrio cholerae* only after the destruction of the bacterial cell wall (as cited by Lerner *et al.*, 2003). This structure is essential for the majority of Gram-negative organisms and confers protection in hostile environments and antibiotic resistance (Dong *et al.*, 2014). LPS is the most powerful natural immunogen able to trigger strong immune response in animals. This complex molecule of about 30 KDa is composed of three different regions: O-antigen, core oligosaccharide and lipid A.

The O-antigen or O-polysaccharide is the most heterogenous part of the LPS consisting of many sugar unit repeats, and it is bound to the core oligosaccharide. It is the outer part of the LPS that is the first target of the host immune system and is also important in serological classification of bacteria strains (Atlas, 1997). The core part of the LPS is the hetero-oligosaccharide containing sugars such as: acid 2-keto-3-deoxyoctulosonate (KDO), L-glycerol-D-manno-heptose, D-galactose and D-glucose; this connects the O-antigen repeats with lipid A (Henderson, 2013).

Lipid A is hydrophobic and allows anchorage of the whole molecule to the bacterial outer membrane. It is highly conserved in Gram-negative bacteria and is the toxic component of the LPS. This structure and the biosynthetic pathway of lipid A is widely researched and studied; it is the most conserved part of the LPS in bacteria

and responsible for endotoxic activity and growth. Studies in *Escherichia coli* have shown involvement of enzymes and genes in lipid A biosynthesis which are shared by many Gram-negative bacteria (Wang and Quinn, 2010). The elucidation of the lipid A pathway in *F. necrophorum* would help clarify its importance in bacteria expressing the endotoxin.

1.11 Sialic acid

Sialic acids are important components of carbohydrate chains, they commonly occur at the terminal position to form glycoconjugates, including glycoproteins and glycolipids (Vimr *et al.*, 2004). A major sialic acid linked to glycoconjugates, and the sialyloligosaccharides of glycoconjugates is *N*-acetylneuraminic acid (Neu5Ac). It plays important roles in many biological processes including cell–cell recognition, inflammatory and immunological responses, cancer metastasis and viral infection. Lipopolysaccharides, lipooligosaccharides, and glycoproteins are among the glycoconjugates located on the surface of bacteria pathogenic to humans such as *Haemophilus influenzae* and *Campylobacter jejuni*, and their sugar chain structures have been determined (Kajiwara *et al.*, 2010).

1.12 Galactose binding lectin

F. necrophorum surface is decorated with many glycan-binding proteins, which, as well as helping with attachment to the host also protect them from host defences. These glycan-binding proteins also known as lectins were first described in bacteria by Nathan Sharon and colleagues in 1970. These lectins are adhesins, some of which have haemagglutination activity, and bind with glycan ligands on host receptor surface. Scientists have analysed the structure of these adhesins in Gram-negative anaerobes; the main interest is in those adhesins (lectins) important for bacterial internalisation or for colonisation (Nobbs *et al.*, 2009). Several studies have shown the expression adhesins of *Fusobacterium nucleatum* that mediate galactose-sensitive binding to various mammalian cells and lectin-like adhesins that enabled galactose-sensitive coaggregation with other periodontopathogenic bacteria (Shaniztki *et al.*, 1997).

1.13 Genome sequencing of *Fusobacterium*

Kapatral *et al.*, in 2002 completed a study to understand the genetic, metabolic and pathogenesis of *Fusobacterium*, by assembling the *F. nucleatum* strain ATCC 25586 genome from shotgun sequences; this was the first determination of *Fusobacterium* species genome sequence. From the genome analysis, they revealed several important pathways including amino acid, carbohydrate, organic acid and lipid metabolism. They were able to predict for the first time some outer membrane proteins of very high molecular weight, and also identified several transporters which are used for uptake of different substrates including sugars, peptides, metal ions and cofactors.

The annotated genome of *F. nucleatum* has been used to predict the genome of *F. necrophorum*, as they are both thought to occupy similar niches and may therefore share some virulence mechanisms. The first genome for *F. necrophorum* was lodged in 2012 in the GenBank database, but now there are many more genomes available, which include strains from deer, bovine and human origin.

1.14 Biochemical research on *Fusobacterium* in the last decade

A survey of the PubMed database (22/01/2019) using the interrogation terms "*Fusobacterium necrophorum*" and "human" and limiting the search to the past decade retrieved 280 publications. Of these, the vast majority were medical case studies, and a few were epidemiological surveys. This underlines a strong interest in the medical consequences of infection and the number of cases worldwide. Only one publication addressed biochemical aspects of the organism (Holm *et al.*, 2017). In this study of 220 human isolates of *F. necrophorum*, the authors determined that there were 3 variants of the *leukotoxin* gene; 2 of which had not been previously described. They also noted that the majority of isolates had novel sequence types and that these were related to the site of infection. Clearly there is scope for in-depth biochemical and molecular analyses of the organisms to gain an understanding of metabolic processes, molecular diversity and the relationship to pathogenicity.

1.15 Prevalence of *F. necrophorum* infection in the UK.

There are issues surrounding determination of organism prevalence as this would rely on the reporting of all infections: this is not current practise in the UK. A large retrospective study of symptomatic patients was carried out at the Royal Hampshire County Hospital (Pett *et al.*, 2014). They reported 18 patients diagnosed with Fusobacterial infections; 0.76 cases/100,000/year, of which half were infected with *Fusobacterium necrophorum*. This study indicated a relatively low number of infections seen in the UK.

The relative importance of *F. necrophorum* was highlighted by Centor *et al.*, (2015) in a cross-sectional study of 312 university students in the USA aged 15-30 years who presented with acute sore throat and 180 asymptomatic controls. They isolated *Fusobacterium necrophorum* in 20.5 % of patients and 9.4 % of asymptomatic students; group A β -haemolytic *Streptococcus* in 10.3 % of patients and 1.1% of asymptomatic students; group C/G β -haemolytic *Streptococcus* in 9.0 % of patients and 3.9 % of asymptomatic students and *Mycoplasma pneumoniae* in 1.9 % of patients and 0 % asymptomatic students. Likewise, Klug *et al.*, (2016) undertook a systematic literature search to investigate 498 records of patients with acute tonsillitis and associated controls. Patients were found to be more likely to carry *F. necrophorum* than healthy controls (21 % vs 8 %).

Holmes *et al.*, (2016) reviewed the role of *F. necrophorum* in pharyngotonsillitis. Having determined that it was an important pathogen in 13 - 40 years old suffering from pharyngotonsillitis, he suggested that throat swabs from such patients should be routinely tested for the presence of the organism. This is important given the reported cases of Lemierre's disease in teenagers and young adults. In a study of patients in Sweden, Dapefrid *et al.*, (2017) also reported a high prevalence of *Fusobacterium necrophorum* in 126 patients in the age group 15-23 years diagnosed with chronic tonsillitis undergoing tonsillectomy. Interestingly, *F. necrophorum* was the most common pathogen (19 %) and was detected at both the surface and in the core of the tonsils; even though *F. necrophorum* is a strict anaerobe. In the same age group of patients, streptococci group G and C were also detected (30 %).

In a study by Atkinson *et al.*, (2018) a comprehensive microbiome analysis of students in the USA suffering from pharyngitis confirmed that *F. necrophorum* was a more common cause (18 patients) than *Streptococcus pyogenes* (Group A streptococci) (9 patients). It was also noted that the development of a productive mucosal infection with *F. necrophorum* was associated with a significant decrease in the microbial diversity. Yusuf *et al.*, (2015) investigated cultures from 230 patients in Belgium (median age of 28 years, 61.7 % men). *F. necrophorum* was found in 37/57 of patients suffering from acute tonsillitis or peritonsillar abscess, whilst *Fusobacterium* spp. other than *F. necrophorum* were found in 35/45 of patients with acute otitis.

However, in a cohort of fifty-seven patients aged 15-52 years who were to undergo tonsillectomy due to recurrent or persistent throat pain, Björk *et al.*, (2015) assessed oropharyngeal colonisation with *F. necrophorum* and β -haemolytic streptococci. Follow-up samples were also assessed for bacterial colonisation post-surgery. In the samples harvested pre-surgery, during surgery and at follow up, *F. necrophorum* was detected in 28, 30 and 16 % of the patients respectively. By comparison, the results for β -haemolytic streptococci were 5, 9 and 5 % respectively. Interestingly, patients with and without colonisation with *F. necrophorum* at follow-up both reported relief from pain: this suggested that *F. necrophorum* was not the sole cause of the symptoms seen and hence further work is required to determine its' role in pathogenicity. However, the reporting of the levels of pain is subjective and there were issues associated with storage of samples prior to testing. In support, Hayawaka *et al.*, (2018), studied 32 Japanese patients undergoing elective tonsillectomy between 2014 and 2015, and determined the prevalence of *F. necrophorum* by either culture or *gyrB* PCR. *F. necrophorum* was not significantly different between patients with infectious and non-infectious indications. However, the authors themselves raised issues on this study; the cohort number was too small for robust statistical analysis, qPCR was not performed, and the MIC determination was carried out in broth rather than on agar. More importantly, exposure of the patients to recent antimicrobial therapy was collected retrospectively resulting in a likely underestimation of infection.

There are some researchers who feel that *F. necrophorum* plays an important role in pathogenesis and others whose studies do not support this. It is difficult to

reconcile these views, however, the work of Björk *et al.*, (2015) does suggest that in tonsillitis, symptoms were alleviated even when *F. necrophorum* was detected post-surgery suggesting that the organism is not the prime cause of the associated pain. Differences noted in different racial groups (cohorts) may be due to ethnic variations in cell surface receptors required to enable attachment of the organism or differences in immune response.

1.16 Study Aims

The aims of this research project were to:

1. investigate biofilm formation in *F. necrophorum*, to determine optimal conditions, to assess antibiotic resistance of biofilm and confirm the organism present by DNA sequencing.
2. analyse the glycan-lectin profiles of the organisms.
3. investigate the LPS/lipid A pathways utilising *in silico* methods.
4. sequence whole genomes of type strains and clinical isolates.
5. analyse whole genome sequences (WGS) of clinical strains to confirm presence of genes involved in glycan pathways.
6. determine sialic acid related metabolic pathways utilising *in silico* methods to interrogate WGS of *Fusobacteria* sp.
7. to provide evidence for a future robust typing system for *F. necrophorum*.

Chapter 2

2 Materials and Methods

2.1 Materials

Materials used in this study were purchased from various selected companies including Sigma–Aldrich (Dorset, UK), VWR Ltd (East Grinstead, UK), Qiagen (Crawley, UK), and Fisher Scientific Ltd (Loughborough, UK). Solid media, including Fastidious anaerobe agar (FAA), Fastidious anaerobe broth (FAB), Brain Heart Infusion (BHI) broth, Luria–Bertani (LB) agar, and blood used for culturing bacterial strains were obtained from Sigma–Aldrich (Dorset, UK), VWR Ltd (East Grinstead, UK), LabM Ltd., Heywood, UK, Oxoid Ltd (Basingstoke, UK) and Fisher Scientific Ltd (Loughborough, UK). Biofilm assays were performed using conventional microtitre plates (Nunc™, Denmark). All PCR and DNA sequencing kits were obtained from Qiagen and Sigma–Aldrich Ltd, UK.

2.2 Bacterial isolates and type cultures

Human isolates of *Fusobacterium necrophorum* harvested from patients with persistent sore throat were obtained from the HPA laboratory at University College Hospital London (UCLH), UK (Table 2.1); no clinical data was provided. One clinical *F. necrophorum* isolate (ARU 01) from a human with Lemierre’s disease and two bovine (from bovine liver abscesses) reference strains from the Japanese Collection of microorganisms (JCM): *F. necrophorum* subsp. *necrophorum* (JCM 3718) and *F. necrophorum* subsp. *funduliforme* (JCM 3724), were obtained from Mrs V. Hall, at the Anaerobe Reference Unit, Cardiff. Whilst all cultures obtained had been sub-cultured and grown within an anaerobic cabinet, all the results presented in this thesis were obtained in experiments carried out in anaerobic gas jars (section 2.3.2.1), microtitre plates with oil overlay (section 2.4.4.4) or Hungate tubes (section 2.7.1).

E. coli NCTC 10418 and *S. aureus* NCTC 6571 used in this study were obtained from stock cultures held at the University of Westminster, London. At the time of this research, the cultivation of *Clostridium perfringens*, an anaerobic control, was not allowed at the University of Westminster.

Table 2.1 Clinical strains/isolates of *Fusobacteria* from UCLH, London, UK.

Collection	Isolate numbers
Clinical isolates of <i>Fusobacterium necrophorum</i>	1, 5, 11, 21, 24, 30, 39, 40, 41, 42, 52, 59, 62, 70, 80, 82, 86, 87, 88, 89, 90, 91, 92, 93, 94, 95.

Table 2.2 Strains of *Fusobacteria* from Anaerobic Reference Unit, Cardiff, UK.

Strain/ Isolate	Subspecies	Source
ARU 01	<i>Fusobacterium necrophorum</i> subspecies <i>funduliforme</i>	Human
JCM 3718	<i>Fusobacterium necrophorum</i> subspecies <i>necrophorum</i>	Bovine liver
JCM 3724	<i>Fusobacterium necrophorum</i> subspecies <i>funduliforme</i>	Bovine liver

(JCM –Japan Collection of Microorganisms (Microbe Division (Riken Brc, 2015))

Table 2.3 Control strains of bacteria used in this study.

Culture Strain	NCTC Number
<i>Escherichia coli</i>	NCTC 10418
<i>Staphylococcus aureus</i>	NCTC 6571

(NCTC – National Collection of Type Cultures (Culture Collections, 2015))

2.3 Methods

2.3.1 Preparation of media, buffers and stock solutions

2.3.1.1 Solid media

Solid media used in this study were prepared following the manufacturer's instructions. The desired amounts of the powdered agar were weighed and dissolved in deionised water and thoroughly mixed either by heating on a hot plate or gently stirring and swirling until all the powdered agar was dissolved. The media were then sterilised by autoclaving at 121 °C for 15 minutes at 15 psi. For the preparation of solid media supplemented with blood, antibiotics or sugars, the autoclaved media were cooled to 50 °C after which the supplements were added.

Blood agar was normally prepared by the addition of horse, sheep or human blood (7 % (v/v)) Fastidious anaerobe agar (FAA). LB agar without supplements was used for growth of the control aerobic bacteria.

2.3.1.2 Liquid media

Liquid media were also prepared according to manufacturer's instruction and sterilised by autoclaving at 121 °C for 15 minutes at 15 psi before use. The same method as above was followed for the addition of supplements. Liquid media used included FAB, BHI broth and LB broth.

2.3.1.3 Solutions

All solutions used were prepared according to the manufacturer's instructions and sterilised by autoclaving or where appropriate, by filtration. Solutions included 1X phosphate buffered saline (PBS), TE (10 mM Tris-HCl, 1 mM EDTA, pH 8.0) buffer, 10X Tris-Borate-Ethylene-diamine-tetra-acetic acid (EDTA 0.5 M) (TBE), Elution buffer (10 mM Tris-HCl, pH 8.5, 10X Tris-Acetate-Ethylene-diamine-tetra-acetic acid (EDTA 0.5 M) (TAE), physiological saline (0.85% NaCl), 10% SDS, 4% formaldehyde, 8mM NaOH, 5M NaCl and 0.1M sodium citrate in 10% ethanol.

2.3.1.4 Preparation of antibiotics

Antibiotics stock solutions used in this study were prepared using their respective solvents according to the manufacturer's instructions. These included ampicillin (AMP), ciprofloxacin (CIP), gentamicin (GM), kanamycin (KAN), tetracycline (TET), vancomycin (VAN), levofloxacin (LEVO), ceftazidime (CEF), and chloramphenicol (CHL). Stock solutions for all antibiotics used were prepared following the guidelines of Clinical Laboratory Standards Institute (CLSI, document M100-S24) and the British Society for Antimicrobial Chemotherapy (BSAC) methods for antimicrobial susceptibility testing guidelines, filter-sterilised and stored at -80 °C (Clinical Laboratory Standards Institute, 2014; British Society for Antimicrobial Chemotherapy, 2013). EUCAST (European Committee on Antimicrobial Susceptibility Testing) breakpoints were used where BSAC had no established breakpoints for the interpretation of zones of inhibition for some

antibiotics. It is recommended that, as disc diffusion methods are not so robust in anaerobes, that in future work gradient strips (e.g. E-test) should be used. Working solutions of each antibiotic used for minimum inhibitory concentration (MIC) determination were prepared as 10, 100 and 1000-fold concentrations using the MIC range (512, 256, 128, 64, 32, 16, 8, 4, 2, 1, 0.5 and 0.25 µg/mL) as a guide and stored at -20 °C. Stock concentrations of each were prepared at 5120 µg/ml; these were diluted with sterile LB broth to make working concentrations.

2.3.2 Identification of *F. necrophorum* isolates

2.3.2.1 Bacterial culture

Cultures were suspended in sterile 15 % (v/v) glycerol solution (Sigma, Gillingham) and frozen at -80 °C for long-term storage. Using these stocks, all *F. necrophorum* isolates were cultured on fastidious anaerobe agar (FAA) (LabM Ltd., Heywood, UK) supplemented with 5-7 % defibrinated horse, sheep blood (Oxoid Ltd., Basingstoke, UK) or whole human blood (NHS Blood Transfusion Lab, London, UK) and incubated anaerobically at 37 °C for 48 hours in an anaerobic jar (Oxoid Ltd., Basingstoke, UK) with AnaeroGen™ sachet (Oxoid Ltd., Basingstoke, UK) generating anaerobic growth conditions (oxygen level <1 % and 9-13 % carbon dioxide and 85 % nitrogen). An oxygen detector strip was used to monitor anaerobe conditions. Colonies obtained were subsequently sub-cultured in Brain Heart Infusion (BHI) broth (Lab M Ltd., Heywood, UK) and grown anaerobically at 37 °C with shaking at 85 rpm in the Innova 42 incubator shaker (Eppendorf Inc., CT, USA) for 48 hours, until an optical density (OD) of 0.6 to 0.7 at wavelength of 600 nm was achieved. *E. coli* and *S. aureus* (provided by the University of Westminster, London, UK) were used as positive controls throughout this study. *E. coli* and *S. aureus* were cultured on Luria Bertani (LB) agar under aerobic conditions at 37 °C overnight and sub-cultured in LB broth with shaking at 200 rpm and 37 °C overnight.

2.3.2.2 Biochemical identification of bacterial strains

Identification tests were carried out on all the *Fusobacterium* strains isolated on the FAA. They were analysed macroscopically by observing the colony morphologies and microscopically by performing Gram staining on all cultured

isolates using the method described by Halebain *et al.*, (1981). Biochemical identifications included the Catalase Test (Sigma Aldrich Ltd, Dorset, UK), Oxidase Test using N, N, N', N'- tetramethyl-p-phenylenediamine (TMPD) and Spot Indole Test (Remel™; Thermo Scientific, DE, USA). Lipase production was tested by the egg yolk agar plate method. Briefly, egg yolk saline solution (1:1) was added to FAA (instead of GAM - Gifu Anaerobe Medium agar) at a concentration of 10% and the strains were inoculated as streaks and incubated as described above. The formation of an oily iridescent sheen over and immediately around growth indicated lipase production (Amoaka *et al.*, 1993). Identification was also carried out on type strains used in this study even though they had been identified in previous studies. Some, but not all cultures were examined under UV light for fluorescence. The isolates had been analysed by API and fatty acid analysis by our collaborators.

2.3.2.3 Primer design

Primers were designed to target the *gyrase B* gene of *Fusobacteria* and for the highly conserved areas of bacterial 16S, 23S *rRNA* genes. Sequences were taken from the literature (Chakravorty *et al.*, 2007) and BLASTN, CLUSTALW (www.ebi.ac.uk/Tools/msa/) were used to identify highly conserved areas suitable for primer design. Primers were designed using Primer 3 (www.primer3.ut.ee) and synthesised by MWG Eurofin, Germany.

2.3.3 Molecular Analysis

2.3.3.1 16S rRNA gene identification

Genotypic identification of microorganisms using 16S *rRNA* gene sequencing is a more objective, accurate and reliable method for identification of bacteria compared to phenotypic methods such as Gram staining and colony morphologies. The genotypic identification method enables defining the taxonomical relationships among bacteria (Petti *et al.*, 2005).

2.3.3.2 Bacterial culture for molecular analysis

The *F. necrophorum* reference and clinical strain isolates were plated on FAA (LabM Ltd., Heywood, UK) supplemented with 5 % defibrinated horse blood. The

plates were incubated anaerobically at 37 °C for 48-72 hours as described above (see 2.2.2.1). The resulting bacterial colonies were sub-cultured in brain heart infusion (BHI) broth (LabM Ltd., Heywood, UK) and grown overnight at 37 °C anaerobically in the Innova 42 incubator shaker (Eppendorf Inc., CT, USA) at 85 rpm until the stationary phase, OD₆₀₀ of 0.6 to 0.7. *E. coli* and *S. aureus* cultures used as controls were grown on LB agar plates for 16 hours at 37 °C and sub-cultured in LB broth aerobically. DNA extraction was performed based on the boiling lysis method utilised by Millar *et al.*, (2000).

2.3.3.3 DNA extraction and amplification of 16S, 23S rRNA and gyrase B genes

Bacterial cultures were centrifuged at 3000 rpm for 10 minutes and the liquid removed. DNA was extracted from the bacterial pellets and frozen at -20 °C as described by Millar *et al.*, (2000). The pellets were re-suspended in 500 µl sterile distilled water and the tubes incubated at 100 °C using boiling water or a heat block for 10 minutes. The tubes with the suspensions were then centrifuged at 10,000 rpm for 5 minutes. The resulting supernatant contained the crude DNA extracts, whose concentrations were determined using the NanoDrop 1000 spectrophotometer (Thermo Scientific, Loughborough, UK); these were used as templates for the PCR. DNA template (1 µl) was mixed with 12.5 µl Master Mix (Qiagen, Crawley, UK; Sigma-Aldrich, MO, USA), 2.5 µl of each primer (0.5 µM) and 6.5 µl of sterile distilled water giving a total volume of 25 µl. PCR amplifications were performed using either the Techne Touchgene Gradient thermal cycler (Barloworld Scientific Ltd, Stone, UK) or the Peltier thermal cycler, DNA Engine®, BIO-RAD using the *Taq* PCR Master Mix kit according to the manufacturer's instructions (Qiagen, Crawley, UK). PCR conditions were an initial denaturation step at 95 °C for 5 minutes, followed by 35 cycles of denaturation at 95 °C for 30 seconds, annealing at 55 °C for 30 seconds and extension at 72 °C for 30 seconds, and a final extension step at 72 °C for 5 minutes.

2.3.3.4 Phenol-chloroform extraction

Due to the growth of the isolates on blood agar plates, some of the extracted crude DNA was contaminated with haem; therefore, the samples were further purified using phenol-chloroform extraction.

The phenol-chloroform extraction procedure involved adding 500 µl phenol: chloroform: isoamylalcohol (25:24:1, v/v; Sigma-Aldrich, Dorset, UK) to an equal volume of bacterial suspension. The mixtures were shaken vigorously and centrifuged at 10,000 rpm for 10 minutes to separate the aqueous and organic layers. The upper aqueous layer was transferred to a clean microfuge tube and 500 µl of chloroform was added. The mixtures were shaken vigorously and centrifuged at 10,000 rpm for 10 minutes to separate the aqueous and organic layers. The upper aqueous layer was transferred to a clean microfuge tube. The nucleic acids in the aqueous layer were precipitated with a 1:10 v/v solution of 3 M NaOAc (Sigma-Aldrich, Dorset, UK) and 2 volumes of 100 % ethanol (Thermo Scientific, USA). The samples were stored at -80 °C for 20 minutes and then centrifuged at 10,000 rpm for 10 minutes. The DNA pellets were washed once with 70 % ethanol, air-dried at room temperature and then re-suspended in 50 µl of sterile distilled water. The concentration of DNA was measured using the NanoDrop 1000 spectrophotometer.

2.3.3.5 Gel Electrophoresis

All amplified PCR products were resolved on 1% (w/v) agarose gels in 1 x TBE buffer. Agarose powder (Sigma–Aldrich, Dorset, UK) was dissolved in 1 x TBE buffer and heated in a microwave until fully dissolved; the mixture was allowed to cool to about 60°C and then poured in the gel cast. PCR amplicons were mixed with loading dye, loaded onto the gel along with DNA marker in one of the wells, and electrophoresed with 1 x TBE buffer at 100 volts for about 60 minutes. The amplicons resolved on the gel were stained with ethidium bromide (20 µg/ml) and the bands visualised using the UVITEC PRO gel imaging system (UVITEC, Cambridge, UK).

Table 2.4 Primers used for 16S rRNA, 23S rRNA and gyrB genes PCR

Primer name	Oligonucleotide sequence
339F	5' ACT CCT ACG GGA GGC AGC AGT 3'
907R	5' CCG TCA ATT AMT TTG AGT TT 3'} DEGENERATE
533F	
CDR	
23S rRNA-F	5' GCG ATT TCY GAA TGG GGR AAC CC 3'} DEGENERATE
23S rRNA-R	5' TTC GCC TTT CCC TCA CGG TAG 3'
GyrB-F	5' AGG AAT TTC CGT CGT GAA TC 3'
GyrB-R	5' TGG TTC CTG TTG TTT CTC CA 3'

Where M = A, C; Y = C, T; R = A, G.

The 16S rRNA primers were used for the confirmation of identity of all strains. These primers described by Chakravorty *et al.*, (2007) are specific for the conserved regions of the 16S rRNA gene sequences in all bacteria and, following sequencing of the PCR products, BlastN analysis was used for identification purposes.

Table 2.5 List of primers used in the study of the function of Galactose (Gal) binding protein genes.

Primer name	Sequence
Gal1F	5' GGA TGC ATG GTT GTC AGG AC 3'
Gal1R	5' TTG CTT GAC CTT TTG CGT CA 3'
Gal2F	5' AAGCATGGCAAATCCT 3'
Gal2R	5' GTCCTGACAACCATGCATCC 3'
Gal3F	5' GGCTATGATCCGTGGTTATG 3'
Gal3R	5' AGCACCCAATATGATTCCA 3'

Table 2.6 Primers for genes involved in the lipid IV A biosynthetic pathway

LPX primers	Sequence	Gene
Primer1-F Primer1-R	5'-GGCGGTTGTTTCGAGGTTTAA-3' 5' TTCAAATTGCTCTTCCGCC-3'	<i>LpxA-UDP-N-ACETYLGLUCOSAMINE-O-ACYL TRANSFERASE</i>
Primer2-F Primer2-R	5'-TGAAGAGGCGGGAATACAAGA-3' 5'-AAGCCGAAAGTTCTTGCAGG-3'	<i>LpxC-UDP-3-O-[HYDROXYMYRISTOLYL]-N-ACETYLGLUCOSAMINE DEACETYLASE</i>
Primer3-F Primer3-R	5'-TCGAGAAGGTGCTGTGATT-3' 5'-TACAGTCGTATTTGCCCGA-3'	<i>LpxD-UDP-3-O-[3HYDROXYMYRISTOYL] GLUCOSAMINE-N-ACETYLTRANSFERASE</i>
Primer4-F Primer4-R	5'-GGATGTTCCGACTGTGGTTG-3' 5'-CTCTCACTGCCCGCAATTTT-3'	<i>LpxB-LIPID-A-DISACCHARIDE SYNTHETASE</i>

Table 2.7 Primers used for amplification of genes involved in glycosylation of *F. necrophorum*.

Target Gene	Sequences
UDP-N-acetylenolpyruvoylglucosamine reductase	5' ccctaaactgggttgcca 3' 5' ttcggaacggaattttga 3'
Mannosyl-glycoprotein endo-beta-N-acetylglucosaminyl transferase	5' gaattccccctgtaagctc3' 5' gggagctctaaattggcaca3'
N-acetylglucosaminyltransferase	5 'ggaataattaccgccggtt 3' 5' tatactgggcaaccggaag 3'
Glycosyltransferase II	5' tcttcgctcctctgtgt 3' 5' ggaagcggagcatttaatca 3'
Lipopolysaccharide heptosyltransferase II	5' tcttcgctcccaacgactt 3' 5' agacgttgctgcctttgt 3'
Lipopolysaccharide heptosyltransferase I	5' tcagagccttctcatccac 3' 5' tttggagggttcgacaggac 3'
Acylneuraminate cytidyltransferase	5' ttacgccctgtcgaattagc 3' 5' catcaaatcgggtgctctt 3'

All products were analysed by agarose (1 %) gel electrophoresis in 1X TBE buffer with appropriate DNA ladders. The amplicons resolved on the agarose gels were stained with ethidium bromide (20 µg/ml) for 5 minutes before being viewed on a UV transilluminator. Results were recorded using the UVITEC PRO software.

2.3.3.6 Gel/PCR purification and DNA Sequencing

PCR products showing clear single bands were purified prior to sequencing using a QIAquick PCR purification kit (Qiagen, Crawley, UK) following the manufacturer's instructions. Amplicons showing multiple bands were extracted and gel purified, by excising the band of interest and then purifying using the QIAquick Gel Extraction kit (Qiagen, Crawley, UK) following the manufacturer's instructions with slight modifications. Briefly, PB buffer was used for the PCR products and QC buffer was used for the excised gel to provide optimal salt concentration and low pH necessary for the DNA to adsorb to the silica gel membrane. Samples were applied to the QIAquick silica-gel spin column and centrifuged at maximum speed (13,000 rpm (15,115 x g*)) for 1 minute to remove contaminants from the sample. PE wash buffer was used to thoroughly wash the samples and the purified samples were finally eluted with sterile distilled water. The amplicons were then sequenced using dideoxy sequence methods by GATC Biotech AG, Constance, Germany. The resulting sequences were analysed using bioinformatics tools such as BLAST and CLUSTALW to determine similarities with strains in the databases.

*Please refer to the appendix for conversion table of speed to rcf (g) for the centrifuge used.

2.3.3.7 RNA Extraction

The RNA was extracted using TRI Reagent® RNA Isolation Reagent (Sigma-Aldrich, UK) combined with RNeasy kit (Qiagen, UK). 500 µl of TRI Reagent was added to frozen bacterial cell pellets (stored at -20 °C) and homogenised. Chloroform (500 µl) was then added and mixed using a vortex for 10 seconds. The mix was then centrifuged at 10,000 x g at 4 °C for 30 minutes. Approximately 500 µl of the colourless upper aqueous phase of the supernatant was transferred to a new tube and an equal volume of 70 % ethanol was added, the sample was vortexed for 5 s. To precipitate the RNA, 500 µl of 80 % ethanol was added to the spin column before the sample was centrifuged at 10,000 x g for 2 minutes. To

remove any carryover of ethanol, the lid of each tube with a sample was left opened, and the tubes were re-centrifuged at maximum speed for 5 minutes. To elute the RNA, 50 μ l of RNase-free water were added to each sample and then the tubes centrifuged at maximum speed for 1 minute. The concentration and purity of the purified total RNA was measured with NanoDrop spectrophotometer at wavelengths of 260 and 280 nm (NanoDrop 1000, Thermo Scientific). An accepted RNA yield is about 150-300 ng and accepted 260:280 and 260:230 ratios is approximately 2.00 and 2.0-2.2 respectively. The samples were either used directly to make complementary DNA (cDNA) or stored at -80 °C.

2.3.3.8 DNase Treatment

Using 5 μ l of the extracted RNA from above, 1 μ l of DNase (1 unit/ μ l) plus 1 μ l of (10x) DNase buffer and 3 μ l of sterile distilled water was added in a 0.5 ml microfuge tube. The mix was incubated for 30 minutes at 37 °C. The quality of the cleaned RNA was checked using agarose gel electrophoresis and the quantity and quality of the extracted RNA checked using NanoDrop spectrophotometer. Controls with no DNase, using water instead, were also set up.

2.3.3.9 cDNA synthesis

QuantiTect® Reverse Transcription protocol for cDNA synthesis was followed (Qiagen®, UK). Genomic DNA elimination reaction was first prepared. A 14 μ l reaction volume in each tube contained: ~300 - 500 ng RNA. RNA (2 μ l) was mixed with 2 μ l of gDNA Wipeout buffer and 10 μ l of sterile distilled water to give a total volume of 14 μ l. The tubes were incubated at 42 °C for a minimum of 2 minutes (maximum 10 minutes), then immediately chilled on ice for 2 minutes. To clean 1.5 ml tubes was added 1 μ l of Reverse Transcriptase (RT), 4 μ l RT buffer and 1 μ l RT primer mix. The template RNA from above (all 14 μ l) was then added to each appropriately labelled tube. The tubes were incubated at 42 °C for 15 minutes and then at 95 °C for 3 minutes to inactivate the enzyme. After this, the tubes were chilled on ice. Samples were then either used for real-time PCR mix or stored at -20 °C until ready to use. The cDNA was then stored at -80 °C until required for RT-qPCR.

2.3.4 RT-qPCR

qPCR was performed in a 25 µl total volume comprising of 12.5 µl SYBR Green Master Mix (Qiagen, QuantiFast, UK), 2.5 µl of each forward and reverse primers (0.5 µM), 2 µl of cDNA template and 5.5 µl of sterile distilled water. Negative controls with samples with no cDNA and another with no reverse transcriptase were also set up. The qPCR cycling using the Rotor GeneQ thermocycler (Qiagen, UK) was performed with an initial activation step at 95 °C for 5 minutes, followed by 35 cycles of: denaturation at 95 °C for 10 seconds; annealing at 55 °C for 30 seconds and extension at 72 °C for 30 seconds. A melt curve analysis was also produced at the end of each run to check the specificity of the reaction.

2.4 Biofilm Formation Assays

2.4.1 Microtitre plate assay (MTP)

Formation and development of biofilm by bacteria have been studied using a variety of systems, which are categorised into static and continuous flow systems. The system of choice determines the kind of data that needs to be extracted from the study, and care is necessary in selection of the platform in order to fulfil the experimental requirements. All platforms have some advantages and disadvantages. Biofilm formation using static systems like microtitre plates are common and useful for the study of early events during the formation of biofilms (Azeredo *et al.*, 2017). Originally developed by Madilyn Fletcher (1977) for the investigation of bacteria attachment and was also proved to be suitable for studying sessile development (Azeredo *et al.*, 2017). The polystyrene microtitre plate (static) biofilm system is simple to use, inexpensive and has a high-throughput, therefore are easily adaptable for studying biofilms under difficult conditions.

Formation of biofilm in this study was determined using the conventional microtitre plate (MTP) assay previously described (O'Toole *et al.*, 1999; Stepanovic *et al.*, 2001; Merritt *et al.*, 2011; O'Toole, 2011), with slight modifications. The technique used is suitable for growing biofilms in a wide range of bacteria. Water was replaced with 1X phosphate buffered saline (PBS) and 33 % (v/v) acetic acid was used as solubiliser in addition to 80 % and 95 % ethanol and 20 % acetone. Other

modifications include careful aspiration of unbound cells from the 24 or 48-hour-old biofilm cultures before washing and fixing with 4 % formaldehyde then staining.

2.4.2 Preliminary Biofilm growth with *E. coli* and *S. aureus*

Initial experiments for biofilm formation were set up using *E. coli* and *S. aureus* to determine the biofilm thickness under different conditions.

2.4.2.1 Temperature

Overnight bacterial cultures in LB broth were diluted 1:100 in fresh LB broth. 200 µl of single culture and 200 µl of mixed cultures of *E. coli* and *S. aureus* (100 µl of each culture) were plated into 3 sets of 96-well plates in duplicate and incubated at three different temperatures: 26 °C, 37 °C and 42 °C for 24 hours.

2.4.2.2 pH

Using the method above, the ability to form biofilms under acidic and alkaline environmental conditions was tested. The pH of the LB broth were adjusted to 4, 7 and 10 without altering the nutrient strength of the growth media. The bacterial cultures were inoculated as above and incubated for 24 hours at 37 °C. Growth at pH 7 was used as control for comparison of the extent of biofilm formation in normal, acidic and alkaline growth medium.

2.4.2.3 Nutrient concentration

The third condition to be tested was nutrient concentration of the LB broth media used for growth of the bacteria. The ability for biofilm formation with different concentration of nutrient: stock (full) concentration (25 g/L), half concentration (12.5 g/L) and quarter concentration (6.25 g/L) of LB broth were tested. Except for the concentration of the LB broth used, the method was as above (see section 2.2.1.2.).

2.4.3 The effect of different conditions on Fusobacteria

2.4.3.1 pH

The ability of the selected clinical isolates to form biofilm was tested in growth media with different pH. *F. necrophorum* isolates were inoculated in FAB, BHI or LB broth respectively of pH 4, 7 and 10 and incubated anaerobically at 37 °C.

2.4.3.2 Temperature

Biofilm assays were also performed under different incubation temperatures namely, 26 °C, 37 °C and 42 °C.

2.4.3.3 Nutrient concentration

This test was performed to determine whether *F. necrophorum* had preference for specific media and/or could form biofilm in diluted concentrations of nutrients in the media used to support their growth. The strains were grown in FAB, BHI and LB and their ability to form biofilms in these media were compared. In the reduced nutrient concentration assay, stock concentration (full) (37 g/L) of BHI broth was diluted to (half) 18.5 g/L and (quarter) 9.25 g/L and used to grow biofilms.

All the assays were performed in duplicate, repeated at least three times for reproducibility, and used the conventional MTP biofilm assay (O'Toole *et al.*, 1999; Merritt *et al.*, 2011; O'Toole 2011; Stepanovic *et al.*, 2001). Results were classified according to biofilm production described by Pye *et al.*, (2013). Definition of biofilm producers: weak biofilm producers at OD₅₇₀ were ≥ 0.05 but < 0.13 , moderate producers at OD₅₇₀ were ≥ 0.13 but < 0.25 and strong producers at OD₅₇₀ were ≥ 0.25 .

2.4.3.4 Inhibition of biofilm formation in *F. necrophorum*

In this biofilm experiment, three species of bacteria were used: *E. coli* NCTC 10418, *S. aureus* and *F. necrophorum*. The control strain, *E. coli*, was chosen because it had been demonstrated to be a biofilm producer in previous studies (López *et al.*, 2010). The clinical and reference strains of *F. necrophorum* were checked for their ability to form biofilms under both normal and different environmental conditions such as change in pH and temperature, reduced nutrient

concentration in the environment and in the presence of increasing concentrations of antibiotics. These conditions were studied using the 96-well microtitre plate. Culture media used to support the growth of the bacterial cells were fastidious anaerobe broth (FAB), BHI and LB broth (for aerobic cultures). Briefly, broth culture of *F. necrophorum* strains harvested at the stationary growth phase and the control *S. aureus* (or *E. coli*) grown overnight with shaking at appropriate speeds were diluted 1:10 in BHI (or FAB) broth or LB broth respectively. 100 μ l aliquots of each diluted strain, 8 replicates of each were pipetted into the wells of the 96-well microtitre plate (NUNC; Fisher Scientific Ltd., Loughborough, UK). The cells were then overlaid with 50 μ l of mineral oil (*F. necrophorum* cultures only) to provide anaerobic conditions (Ahn and Burne, 2007). Positive control for the biofilm assay was *S. aureus*. Negative control with BHI broth only with no cells was also set up. The plates with cultures were incubated statically at 37 °C for 48 hours. Unbound cells were aspirated, and the biofilm fixed with 4 % formaldehyde for 10 minutes. The wells were washed with 1X PBS and stained with 0.1 % crystal violet (CV) for 10 minutes. The stained biofilm was washed again with 1X PBS, allowed to air-dry and solubilised with the appropriate solvent, in this case 33 % acetic acid. Absorbance was measured at 600 nm with a microtitre plate reader. All tests were performed and repeated for reproducibility as mentioned above.

2.4.3.5 Biofilm estimation – Crystal violet assay

Quantification of biofilm formation used the method demonstrated by Merritt *et al.*, (2011). The crystal violet assay provides a quantitative assessment of biofilm growth as well as allowing motile and non-motile cells to be distinguished by their adherence to plate wells. Biofilm liquid containing planktonic (unbound) cells was carefully removed ensuring the biofilm itself was not disrupted. The remaining biofilm was carefully washed 3 times with 1X PBS buffer and then fixed with 4 % formaldehyde for 15 minutes at room temperature. A wash step with 100 μ l 1X PBS buffer was carried out twice. The PBS was removed and 125 μ l 0.1 % crystal violet stain solution was added to each well using a multi-tip Gilson pipette. The solution was left to stain the well contents at room temperature for 10 -15 minutes. The washing step was repeated, and the plate was allowed to air dry before solubilisation of the biofilm. Acetic acid (150 μ l of 33 %) was pipetted into each

well to elute the dye bound to the biofilm. To allow solubilisation, the plate was covered and incubated at room temperature for 15 minutes. A pipette was used to ensure the well contents were mixed. Aliquots of 125 µl of the crystal violet/acetic acid solution from each well was transferred into a flat bottom 96-well plate (Sterilin; Barloworld Scientific Ltd, Stone, UK). Optical density was measured at 570 nm and 600 nm with 33 % acetic acid as the blank, using a microtitre plate reader (Versamax; Molecular devices, CA, USA). The amount of crystal violet bound to each well is proportional to the amount of biofilm produced (O'Toole, 2011).

2.4.4 BSAC disc susceptibility determination of *E. coli* and *S. aureus*

Bacterial cell cultures were grown in LB broth aerobically overnight and about 4 colonies were picked and diluted 1:100 with sterile Iso-Sensitest broth (Oxoid, Basingstoke, UK), using direct colony suspension method according to the BSAC method for antimicrobial susceptibility testing (AST). AST was performed on Iso-Sensitest agar (Oxoid, Basingstoke, UK) by streaking the suspension of cells evenly on the entire plate using a sterile cotton swab to achieve a lawn of growth. Antibiotic discs were placed on the inoculated agar plate above and the plate was incubated aerobically at 37 °C for 24 hours. The zones of inhibition (ZOI) were determined to the nearest mm with a ruler and interpreted using the BSAC and EUCAST guidelines.

Table 2.8 Bacterial strains and antibiotics used for disc diffusion test of aerobes.

Bacteria Strains	Antibiotic Used
<i>E. coli</i>	AK (30 µg), CAZ (30 µg), CHL (30 µg), CIP (5 µg), GM (10 µg)
<i>S. aureus</i>	AMP (30 µg), CIP (5 µg), GM (10 µg), TET (30 µg), VAN (5 µg), LEV (5 µg), KAN (30 µg)

Key: AK (Amikacin), AMP (Ampicillin), CAZ (Ceftazidime), CHL (Chloramphenicol), CIP (Ciprofloxacin), GM (Gentamicin), KAN (Kanamycin), LEV (Levofloxacin), TET (Tetracycline), VAN (Vancomycin).

2.4.4.1 Antibiotic Susceptibility (Bacteriostatic) testing of Fusobacteria

Disc diffusion method of Lakhssassi *et al.*, (2005) was used for the testing of antibiotic susceptibility and determine zones of inhibition. Blood agar plates were inoculated with diluted *F. necrophorum* cell culture as described above for *E. coli* and *S. aureus*. The inoculum was spread over the entire plate and antibiotic discs were carefully place on the agar and the plates were incubated anaerobically at 37 °C for 48 hours.

2.4.4.2 Antibiotic susceptibility testing on planktonic cells and biofilm *E. coli* and *S. aureus* (MIC determination).

Overnight cultures of *E. coli* and *S. aureus* in LB broth were set up as described above and 100 µl of 1:100 fresh diluted cultures were plated into 96-well plates and then incubated at 37 °C for 24 hours. After the incubation period, 100 µl of diluted antibiotics were added to the cells and incubated at 37 °C for another 24 hours. Antibiotics used were AMP, CIP, GM, TET and VAN for *S. aureus* and AK, CAZ, CHL, CIP, GM, and LEV for *E. coli*. For mixed cultures of the two bacteria, AMP, CIP, GM, LEV and VAN were added. Antibiotics were added at four different concentrations: 512, 256, 128 and 64 µg/ml, to test their effects on planktonic cells and biofilms produced.

2.4.4.3 Antibiotic susceptibility testing on *F. necrophorum* biofilm

2.4.4.3.1 Minimum inhibition concentration (MIC) test using MTP

To determine the lowest antibiotic concentration that inhibits growth of *F. necrophorum* planktonic cells and biofilm formation, 96-well microtitre plates were used to set up the experiment. Appropriate dilutions of the overnight (*S. aureus*) and stationary phase (*F. necrophorum*) cultures were diluted 1:100 in BHI corresponding to 0.5 McFarland ($1.5 - 3.0 \times 10^8$ CFU/ml) and 100 µl of bacterial cell culture were aliquoted into each well of the 96-well plates. Aliquots of 50 µl of the different antibiotics (ciprofloxacin, kanamycin, metronidazole and penicillin) were added to appropriate wells and each well was overlaid with 50 µl of sterile mineral oil to achieve an anaerobic environment. A control was set up using 50 µl of sterile 1X PBS instead of antibiotics. The plate was sealed with parafilm and

incubated at 37 °C for 48 hours. After 48 hours, the plates were observed for the presence or absence of growth (turbidity of broth was indicative of cell growth). Optical density at OD₆₀₀ was measured using a plate reader. Antibiotics were added at four different concentrations: 512, 256, 128 and 64 µg/ml, to test the minimum antibiotic concentration required for inhibition or elimination of biofilms produced.

2.4.4.4 Single and Dual-species biofilm formation

The two reference strains (JCM 3718 and JCM 3724) and the clinical isolate (ARU 01) were sub-cultured in BHI and diluted as describe above. *E. coli* and *S. aureus* were subcultured in LB broth and diluted as above. Single-species biofilm assays were set up in 96-well microtitre plates by aliquoting 100 µl of ARU 01, 3718 and 3724 in duplicates into appropriate wells. A negative control was BHI only, no added cells. For dual-species biofilm assay, the volume of ARU 01, 3718 and 3724 cell cultures were reduced to 50 µl per well and 50 µl of either *E. coli* or *S. aureus* were added to the *Fusobacterium* cultures. The wells were overlaid with 50 µl of sterile mineral oil to achieve an anaerobic environment. The plates were sealed with parafilm and incubated at 37 °C for 48 hours. After 48 hours, the optical density at 600 nm wavelength (OD₆₀₀) was determined using a plate reader. Microtitre plates with bacterial species showing growth after overnight incubation with antibiotics were then quantified for residual biofilms. The amount of biofilm formed was quantified using the crystal violet assay. The percentage inhibition or antibiotic efficacy was estimated by comparison of the optical density of the residual biofilm of bacterial species that had been challenged with antibiotics to that of a positive control, i.e. the same species without antibiotics.

2.4.4.5 Statistical analysis

Each experiment was performed in 16 replicates and repeated 3 times at different time points and the results were averaged where necessary. The mean absorbance of the negative control was subtracted from the mean absorbance values to determine the actual values. In the current study, the main statistical used was one-way analysis of variance (ANOVA) followed by Bonferroni multiple comparison and was performed using GraphPad Prism® version 5.00 for Windows. This test was used to determine whether there were any differences in

the degree of biofilm formation under different environmental conditions (three parameters compared each time). A p value of <0.05 was considered statistically significant. The mean value obtained for each strain forming single/dual-species biofilm was determined using Microsoft Office Excel software. The confidence interval of the mean was calculated by setting the significance limit to $p = 0.05$ at 95 % confidence interval.

See Appendix V for the formulae for estimating percentage efficacy and residual biofilm of the antibiotics that inhibit biofilm. Percentage residual biofilms of ≤ 0.05 at OD_{600} were considered as complete inhibition.

2.4.5 LIVE/DEAD BacLight Bacterial viability

This method is a quantitative fluorescent microscopy technique for the determination of viability of bacterial cells. The kits consist of SYTO 9, a green fluorescent nucleic acid dye which stains live cells and propidium iodide, a red fluorescent nucleic acid dye which stains dead or dying cells.

2.4.5.1 Bacterial Viability assay

LIVE/DEAD BacLight Bacterial Viability [Live/Dead[®]BacLight[™] kit L7012] - 3.34 mM SYTO 9 dye (component A), 20 mM Propidium iodide dye (PI-component B), mounting oil] (Life technologies, NY, USA & Molecular Probes, USA), is a fluorescent staining method which was applied to each of the bacterial samples to assess the ratio of viable to total cell counts. The two fluorescent components are nucleic acid stains, which fluoresce depending on cell viability. SYTO 9, a green fluorescent nucleic acid dye, penetrates all live bacterial cells, which produces the green colour. PI, which is a red fluorescent nucleic acid dye, will only combine with SYTO 9 to form the red fluorescent colour if the cell has damaged membranes, i.e. dead or dying cells. In preparing for the BacLight procedure, the cells had to be grown in broth cultures according to the manufacturer's protocol with slight modifications. 100 μ l of each bacterial sample extracted with 0.85 % NaCl to obtain the desired bacterial density, was pipetted into a labelled Eppendorf tube and an equal volume of component A (SYTO 9) and component B (PI) were vortexed in a new Eppendorf tube. The dye mixture was covered in foil to avoid photodegradation. Dye mixture (0.5 μ l) was then added to each bacterial sample, ensuring minimal exposure to light. Samples were incubated in the dark for 15

minutes at room temperature. 5 µl of each dye/bacteria solution sample was pipetted onto a separate glass slide. The samples were covered in a layer of BacLight mounting oil (component C) before an 18 mm glass cover slip was applied. Slides were viewed with Leica epifluorescence microscope (Leica Microsystems Ltd, Milton Keynes, UK).

2.4.5.2 Cytospin procedure

For the cytospin procedure, the dye mixture was prepared and added to the samples as mentioned above. The sample were mounted into a cytocentrifuge and spun at 500 rpm for 3 minutes, to produce a discrete area of cells on the slide using a Shandon Cytospin 3 (Thermo Scientific, DE, USA). BacLight mounting oil and glass cover slip were then applied as above.

2.4.5.3 Viability of biofilm forming cells

Planktonic cells from biofilms formed in 96-well plates were discarded, and 150 µl of 0.85 % NaCl was pipetted into each well. The contents of each well were thoroughly mixed by pipetting up and down several times to extract the biofilm, and the content was transferred to appropriately labelled microfuge tubes. The tubes and contents were centrifuged at 1000 rpm for 15 minutes and the supernatant discarded. Bacterial suspensions were prepared following the manufacturer's protocols with slight modifications. Isopropyl alcohol was omitted and only 0.85 % NaCl was used, also the amount of cell culture used was 1.2 ml instead of 25 ml. Briefly, the two dyes (SYTO 9 and propidium iodide) were mixed in a 1:1 ratio, and 0.5 µl of the mixture added to 100 µl of each bacterial suspension. The samples were thoroughly mixed, covered and incubated in the dark at room temperature for 15 minutes.

For microscopy, the cells were then immobilised onto slides by cytocentrifugation at 500 rpm using a Shandon Cytospin 3 (Thermo Scientific, DE, USA). A drop of BacLight mounting oil was applied to each slide and coverslips applied. The stains were examined under epifluorescent microscope (Leica Microsystems Ltd, Milton Keynes, UK). The percentage of Live/Dead cells was estimated.

2.5 Analysis of the bacterial cell surface utilising lectin staining

Biotinylated lectins used in this study were purchased from Vector Labs, UK and were chosen to cover a range of sugar specificities. The lectins were (1 mg) were re-suspended following the manufacturer's instructions to a stock concentration of 1 mg/ml. The assay used a final concentration of 0.6 µg/ml.

Table 2.9 Commonly used biotinylated lectins with their sugar specificity and abbreviations adapted from Afrough *et al.*, (2007).

Lectins	Abbreviation	Source	Carbohydrate Specificity
<i>Concanavalin A</i>	Con A	Jack bean	Glucose/Mannose
<i>Peanut Agglutinin</i>	PNA	Peanuts	Galactose
<i>Jacalin</i>	JAC	Jackfruit seed	Galactose/GalNAc ^a
<i>Erythrina cristagalli</i>	ECA	<i>Erythrinacristagalli</i> seeds	Galactose/GlcNAc ^b
<i>Sophora japonica</i>	SJA	Japanese pagoda seeds	GalNAc/Galactose
<i>Ricinus communis Agglutinin I</i>	RCA-I	Castor bean	GalNAc/Galactose
<i>Griffonia simplicifolia Lectin I</i>	GSL-I	Griffonia seeds	GalNAc/Galactose
<i>Soybean Agglutinin</i>	SBA	Soybean	GalNAc
<i>Dolichos biflorus</i>	DBA	Horse gram seeds	GalNAc
<i>Vicia villosa Lectin</i>	VVA	Hairy vetch seed	GalNAc
<i>Griffonia simplicifolia Lectin II</i>	GSL-II	Griffonia seeds	GlcNAc
<i>Wheat Germ Agglutinin</i>	WGA	Wheat gem	GlcNAc/NANA (N-Acetylglucosamine/N-Acetylneuraminic acid.
<i>Succinylated Wheat Germ Agglutinin</i>	SWGA	Wheat gem	GlcNAc
<i>Lycopersicon esculentum</i>	LEA	Tomato fruit	GlcNAc
<i>Solanum tuberosum</i>	STA	Tomato fruit	GlcNAc/Sialic acid
<i>Lens culinaris Agglutinin</i>	LCA	Lentil seeds	Glucose/Mannose
<i>Sambucus nigra Agglutinin</i>	SNA	Elder bark	α -2,6 sialic acid
<i>Pisum sativum Agglutinin</i>	PSA	Garden pea	Glucose/Mannose
<i>Phaseolus vulgaris Leucoagglutinin</i>	PHA-L	Red kidney beans	Complex Sugars
<i>Phaseolus vulgaris Erythroglubulin</i>	PHA-E	Red kidney beans	Complex Sugars
<i>Datura stramonium</i>	DSA	Thorn apple	LacNAc ^c
<i>Ulex europaeus Agglutinin I</i>	UEA-I	Furze seed	Fucose

^a – GalNAc – N-acetyl D-galactosamine

^b – GlcNAc – N-acetyl D-glucosamine

^c – LacNAc – N-acetyllactosamine

2.5.1 Cytochemistry staining with biotinylated lectins

Bacterial cell pellets were re-suspended in 50 μ l of sterile distilled water and three small aliquots was smeared onto glass microscope slides (see below). The slides were air-dried and a paraffin (PAP) pen was used to draw circles around the air-dried spots to contain the reagents. The cells were fixed with 4 % paraformaldehyde (PFA) at room temperature for 30 minutes, and the slides were washed 3 x 5 minutes with 1X PBS. The fixed cells were then blocked using 4.5 % human serum albumin (HSA) (Zenlab, UK) at room temperature 30 minutes. Slides were washed with 1X PBS for 3 x 5 minutes.

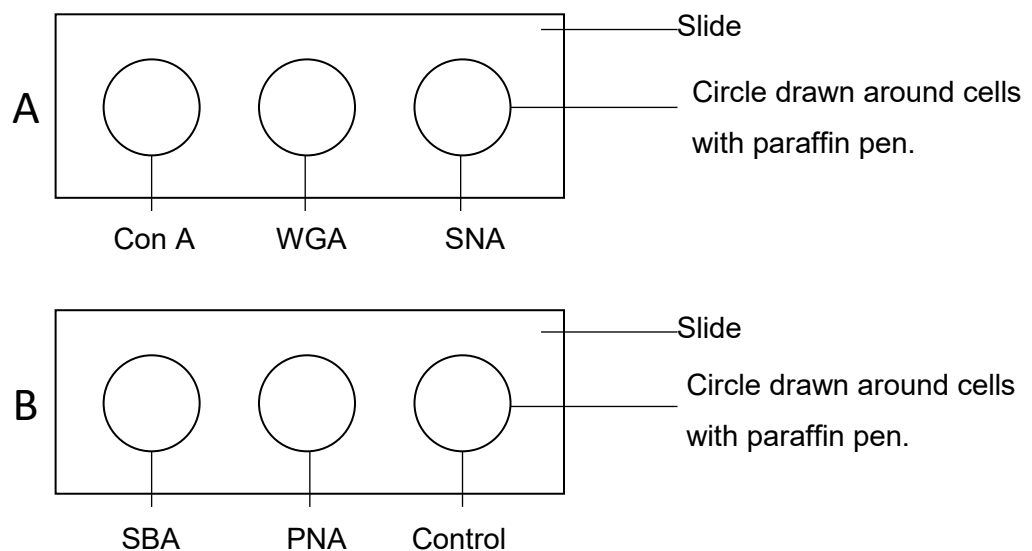


Figure 2.1 Set up of bacterial cells and biotinylated lectin on slides.

Five lectins were used per strain of bacterium plus one lectin free control, containing cells only.

Diluted lectin (50 μ l of 6 μ g/ml) was pipetted onto the bacteria on each slide. The slides with the lectins were incubated for 1 hour at room temperature then rinsed with 1X PBS/Tween™20 (0.05 % v/v) (PBST). Streptavidin-peroxidase (Sigma) was diluted according to the manufacturer's instructions and 50 μ l was placed on the bacteria on the slides for 1 hour at room temperature. The slides were rinsed with solution of 1X PBST. The substrate solution for peroxidase prepared as according to the manufacturer's instructions (Vector Laboratories (SK-4200)), was then pipetted onto each circle and incubated at room temperature for 30 minutes and removed by tilting the slides. Finally, the cells were counter stained with Mayer's haematoxylin for 30 minutes at room temperature and then rinsed by

pipetting PBST onto the slides. Results were then observed using a light microscope.

2.5.2 Lectin cytochemistry for epifluorescent microscopy

The fluorescein isothiocyanine (FITC) conjugated lectins used in the staining include Concanavalin A (Con A), Wheat Germ Agglutinin (WGA), Peanut Agglutinin (PNA), Soybean Agglutinin (SBA) and *Sambucus nigra* Agglutinin (SNA). (Vector Laboratories, UK). The staining protocols were similar to those described above for the biotinylated lectins with some modifications. The slides with the fluorescent lectins were incubated for 1 hour in the dark at room temperature. After incubation, the slides were rinsed with solution of 1X PBS and Tween™20 (0.05 % v/v) (TPBS). Mounting medium was applied to the slides and coverslips placed on top. The slides were viewed under an epifluorescent microscope with a FITC filter (Zeiss Axiovert).

2.5.3 Lectin ELISA (ELLA)

This enzyme –linked lectinsorbent assay (ELLA) procedure was used to highlight which glycans were present in the bacteria (intra and extracellular). 1 ml of each broth culture sample was centrifuged at 10,000 rpm for 3 minutes, the supernatant was discarded, and the pellet was mixed via vortex in 1.5 ml PE-LB buffer solution (G-biosciences Tissue PE LB™). After a 30 minutes incubation period at room temperature, the samples were centrifuged at 10,000 rpm for 5 minutes. The protein extract (supernatant) was pipetted into labelled centrifuge tubes. 50 µl was removed for spectrophotometric analysis (NanoDrop™) to assess the protein content of the extract. 100 µl of the extracts were pipetted into wells of the 96-well plate, with PE-LB buffer used as the negative control. The plate was left in a fridge for at least 24 hours. The extracts were removed, and the wells were washed by using 200 µl PBS buffer and shaking the plate for 10 minutes. The PBS buffer was removed and 200 µl of 4.5 % human serum albumin (HSA) was added to each well as the blocking agent and left at room temperature for 60 minutes. The blocking agent were then removed and 100 µl of the diluted biotinylated lectin solutions (6 µg/ml) were added to duplicate wells for each lectin (see Table 2.9). The plate was incubated at room temperature for 60 minutes before lectin solutions were removed and the washing step was repeated. 100 µl of

streptavidin-alkaline phosphatase (diluted as recommended by the manufacturer) was then added to each well and left for 60 minutes at room temperature before the washing step was repeated. 100 µl of pnp-phosphate solution (10 mM) was pipetted into each well and incubated for 60 minutes at room temperature. 50 µl of 3 M NaOH solution was added to stop the reaction and the plate was read at 405 nm on a microtitre plate reader (VersaMax; Molecular devices, CA, USA).

2.6 Galactose binding protein – Study of function

2.6.1 Primer design

The FUS007_00675 gene sequence encoding the *F. necrophorum* D-galactose-binding protein was obtained from the UniProt (Universal protein resource database) Knowledgebase, and the gene specificity was compared to all microbes using NCBI BLAST to evaluate all homology. Clustal Omega was utilised to determine conserved areas suitable for primer design. Using Primer3 software (Koressaar and Remm, 2007; Untergrasser *et al.*, 2012), three primer sets for Galactose binding (Gal-binding) protein were designed for the candidate sequence:

1) Forward: 5' GGA TGC ATG GTT GTC AGG AC 3' and the reverse: 5' TTG CTT GAC CTT TTG CGT CA 3'.

2) Forward: 5' AAGCATGGCAAATCCT 3' and the reverse:

5' GTCCTGACAACCATGCATCC 3'.

3) Forward: 5' GGCTATGATCCGTGGTTATG 3' and reverse:

5' AGCACCCAATATGATTCCA 3'.

The above primers were based on nucleotide sequence of the FUS007_00675, FSEG_00004 gene and *F. necrophorum* D-12 strain on the BioCyc database. All the primers were synthesised by MWG Eurofin, Germany. DNA Extraction and PCR were as previously described (see section 2.2.3.3 in methods).

2.6.2 Haemagglutination assay

2.6.2.1 Blood typing

Agglutination tests were carried out in 96-well microtitre plates using Human blood obtained from the National Blood Transfusion Services. Anti-A and anti-B monoclonal antibodies were tested against blood group A, B, O and AB. This was

used to demonstrate the appearance of positive and negative agglutination in 96-well microtitre plate, which was rated from 0-4+, with 0 meaning no haemagglutination (cells homogenously distributed) and 4+ meaning 100 % haemagglutination (grape-like clusters of cells).

Single drops of anti-A and anti-B monoclonal antibodies were added to individual wells of the microtitre plate and 50 µl of sterile 1X PBS was added. Serial double dilution of the blood typing sera was conducted. Red blood cells were diluted to 2 % (v/v) with sterile PBS and 50 µl of the red cell suspension was added to each well containing the serially diluted antibodies. The microtitre plate was incubated at 37 °C for 1 hour before assessment of the results.

2.6.2.2 Human erythrocyte agglutination by bacteria

Several examples of haemagglutination of bacteria have been shown to involve appendages such as pili or flagella on the surface of the cells. Some strains of *E. coli* were shown to attach to cells by means of pili. Studies using electron microscopy of whole organisms or cell fragments did not show the presence of these appendages, thus have not associated haemagglutination of *F. nucleatum* with pili or flagella. Others were able to show *F. nucleatum* can agglutinate A, B and O human erythrocytes and that of other species (Dehazya and Coles, 1980). To determine whether the Galactose binding protein bound to the alpha galactosyl residue on Human blood group B red cells, A, B, O and AB red cells were diluted to 1 % in PBS (v/v) and 100 µl of the diluted red blood cells was added to each well of a microtitre plate and incubated at room temperature for 1 hour. Three different strains of *F. necrophorum*: ARU 01, JCM 3718 and JCM 3724 were each diluted to ratio of 1:1 in PBS and aliquoted into appropriate wells. The strains were tested against each blood type. The microtitre plate was incubated anaerobically in an anaerobic jar with an AnaeroGen sachet for 1 hour at 37 °C. Agglutination was scored as above, i.e. from 0-4+.

2.6.2.3 Sheep erythrocyte agglutination

To determine whether the galactose binding protein bound to β-galactosyl residues, neuraminidase (Sialidase) type V from *Clostridium perfringens* diluted in PBS and was used to cleave the terminal sialic acid residues of sheep erythrocytes, so that the β-galactose molecules could be exposed. 5 %

erythrocyte suspension in PBS was added to a neuraminidase solution consisting of 1 µl neuraminidase in 49 µl of diluent (1X PBS) and incubated at room temperature for 1 hour. After incubation, erythrocytes were washed by centrifugation with PBS at 3000 rpm for 5 minutes. Strains of *F. necrophorum* were diluted 1:1 with PBS and used for serial doubling dilution of the bacteria. The microtitre plate was incubated anaerobically with an AnaeroGen sachet at 37 °C for an hour. The same criteria and scoring as above was used for observing haemagglutination under the microscope.

2.6.2.4 Bead based lectin assay

Galactose binding proteins play an important part in biofilm formation and attachment of bacteria to the host receptor cells. To evaluate the specificity of the galactose binding protein, a series of immobilised glycans were investigated in an interaction assay.

Five beads with attached sugars: *P*-Aminophenyl β-D-thiogalactopyranoside agarose (Thio-Gal), Glucose agarose, N-Acetyl-D-Glucosamine agarose (GlcNAc), *P*-Aminophenyl oxalic acid agarose (Sialic acid), N-Acetylgalactosamine agarose (GalNAc) and two controls Sepharose CL and Sepharose 2B, which had no attached sugars (Sigma Aldrich, UK), were equilibrated in 0.15 M NaCl. *F. necrophorum* samples used were ARU 01, JCM 3718 and JCM 3724, which were grown until they were confluent. In a further experiment, the following sugars, 0.1 M xylose, 0.01 M xylose, 0.1 M galactose and 0.01 M galactose were added to the bead to inhibit binding of bacteria to the beads. In principal, the sugars would lead to competition for binding and therefore the bacterial binding to the beads would be reduced if inhibition occurred.

2.6.2.5 Methodology for bead assay

Agarose beads were suspended in 1 part beads and 5 parts of 0.15 M NaCl to a working volume of 1.5 ml in a 1.5 ml Eppendorf tube. 20 µl of the agarose beads were transferred into another 1.5 ml Eppendorf and 50 µl of the confluent bacterial cultured cells and 50 µl of 0.15 M NaCl were added to the tube. 50 µl of mineral oil was used to overlay the contents of the tube to create an anaerobic environment. The samples were incubated at 37 °C for 4 hours, with the tubes gently inverted every hour to re-suspend the beads. After 4 hours, 1 ml of 0.15

NaCl was added to each tube and carefully mixed, then incubated undisturbed at room temperature for 30 minutes. Most of the liquid above the agarose beads was removed leaving only about 100 µl to prevent the beads from drying out. The beads were re-suspended and 50 µl were transferred into wells of a 96-well microtitre plate and observed under a light microscope. The remaining bacterial cell cultures were stained with Live/Dead BacLight Bacterial Viability stain (Thermo Scientific) described above. The result was observed under fluorescent microscope.

2.6.3 Bioinformatics

The nucleotide sequence of the enzymes were obtained from the BioCyc database (<http://www.biocyc.org>). Primers for the genes were designed using 'Primer 3' and the sequences were confirmed by BLAST (The Basic Local Alignment Search Tool).

2.6.4 Sequence analysis

F. necrophorum isolates grown on blood agar plates were used to extract bacterial DNA using the boiling method (section 2.2.2.4). The resulting supernatants contain DNA templates used to validate the primers, by standard PCR and gel electrophoresis (section 2.2.2.4).

2.6.5 PCR and Sequencing

A PCR reaction was set up as described for *16S rRNA*, with slight modifications. Aliquots of 2 µl of DNA template was used in a 25 ul PCR reaction mix. 5 µl of the PCR amplicon was run on a 1 % agarose gel (see section 2.2.3.3 and 2.2.3.5). The resulting gel was stained with ethidium bromide and the bands visualised under a UV transilluminator comparing the bands with DNA ladder with fragments of defined lengths (Peqlab, Erlangen, Germany) run on the same gel.

The remaining PCR amplicon was purified using QIAquick PCR Purification kit (Qiagen, Hilden, Germany) according to the manufacturer's instructions. Purified samples were sequenced using Sanger sequencing by GATC Biotech Ag, Germany. Using online alignment tool BLAST, each of the sequence obtained were compared with those in GenBank database. CLUSTALW program was used to search similarity of sequence in the different isolates of *F. necrophorum*.

Sequences were translated with ExPASy (<http://web.expasy.org/translate/>) to confirm whether the nucleotide sequence differences resulted in changes to primary amino acid structures.

Comparative studies were undertaken between *E. coli* K12 and *F. necrophorum* D12 using bioinformatics databases to see if there were differences in the amplified sequences and if these were conserved domains and located in the catalytic regions.

The RaptorX server (<http://raptorx.uchicago.edu/>) was also used to predict the 3D structure of the enzymes involved in lipid A biosynthesis.

2.7 Whole genome sequencing

2.7.1 Preparation of anaerobic broth using anaerobic Hungate culture tubes

Brain heart infusion (BHI) broth was made following the manufacturer's instructions, and resazurin solution at a concentration of 0.1 g/50 ml was added. This was heated to boiling and then L-cysteine hydrochloride (0.5 g/L) was added which changed the colour of the medium from pink to yellow. The media were aliquoted into Hungate culture tubes, placed in a boiling water bath until the media turned from pink back to yellow. The tubes were closed with the butyl rubber septum and the screw caps tightened to prevent leakage of the anaerobic atmosphere during autoclaving. The samples were autoclaved at 121 °C for 15 minutes at 15 psi. The media undergoes further oxygen purging during autoclaving. The samples were then allowed to cool and the stored at room temperature until ready to use.

2.7.2 Growth of *F. necrophorum* in anaerobic BHI broth

Single colonies of *F. necrophorum* cultures grown anaerobically on FAA blood agar plates as described above were subcultured in 10 ml of anaerobic BHI broth in Hungate tubes using aseptic microbiological techniques. The tubes were tightly closed, and cultures grown anaerobically at 37 °C until mid-log phase (optical density (OD) of 0.6 to 0.7 at 600 nm) using 'Ultrospec 10' spectrophotometer. A

Hungate tube containing only anaerobic BHI broth was used as a blank for calibration of the spectrophotometer.

2.7.3 Preparation of Genomic DNA (gDNA) for NG Sequencing

Genomic DNA was extracted using Sigma GenElute Bacterial Genomic DNA Kit (Sigma-Aldrich, UK), following the manufacturer's instructions with some slight modifications. *F. necrophorum* culture samples grown to mid log phase (OD of approximately 0.3 – 0.5) were aliquoted and the cells pelleted and stored at -20 °C until they were used for preparation of gDNA. The gDNA was eluted in 10 mM Tris-HCl buffer pH 8.5 (no EDTA). Samples were then aliquoted and stored at -20 °C to prevent degradation.

The concentration of gDNA necessary for NGS library preparation was 1-30 ng/ul in 30 - 100 ul volume. The concentrations of gDNA were quantified using a Qubit and NanoDrop spectrophotometer. When NanoDrop was used for quantification, the minimum concentration of DNA required for NGS library preparation was 10 ng/ul in 30 – 100 ul volume (as NanoDrop usually overestimates concentration of DNA, usually by 10-fold).

The integrity of the gDNA was checked by electrophoresis on a 0.8 % agarose gel to verify that the gDNA was not degraded which may jeopardise the outcome of the NGS library preparation. Non-degraded genomic DNA samples were then aliquoted into 1.5 ml microfuge tubes, prepared according to the company's instructions and sent for sequencing.

2.7.4 Next generation sequencing

The two *F. necrophorum* reference strains, Lemierre's syndrome (LS) isolate and 17 other clinical isolates were commercially sequenced by microbesNG (Edgbaston, Birmingham, UK), using Illumina next generation sequencing technology (on the Illumina HiSeq. The raw sequence data was processed with their automated analysis pipeline.

They used Kraken (a taxonomic sequence classification system) to identify the closest available reference genome and the reads were mapped using Burrows-Wheeler Aligner (BWA mem), a software package for mapping low-divergent sequences against a large reference genome, to assess the quality of the data.

BWA-MEM is the latest of one of three algorithms, and is generally the one recommended for high-quality queries, it is also faster and more accurate as well as its use for longer sequences ranging from 70 bp to 1 Mbp.

De novo assembly of the reads using SPAdes was also performed and these were mapped back to the resultant contigs using BWA mem to get more quality metrics.

2.7.5 Phylogenetic analyses

Information from assemblies obtained from microbesNG, NCBI and NCTC were used in the phylogenetic analysis, and genes encoded within genomes were predicted using Prokka 1.13 (Seemann, 2014).

2.7.5.1 Preliminary phylogenetic analyses

Prokka 1.13 (Seemann, 2014) software was used to predict genes encoded within genomes. All protein sequences were analysed with PhyloPhlAn 0.99, to determine the placement of the whole-genome within the *Fusobacterium* genus (Segata, *et al.*, 2013). The resulting multiple-sequence alignment was imported into R and phangorn v.2.3.1 (Schliep, 2011) was used to construct a neighbour-joining tree. FigTree v1.4.2 (<http://tree.bio.ed.ac.uk/software/figtree/>) was used to visualize the phylogenetic tree and annotated using Adobe Illustrator.

2.7.6 16S rRNA gene sequence analysis of strain F88

Using RNAmmer 1.2 (Lagesen *et al.*, 2007) the 16S rRNA gene sequence of strain F88 was predicted, with a partial (1229 nt) sequence recovered that was extended to 1514 nt by comparison with other *Fusobacterium* spp. Accession numbers for 16S rRNA gene sequences of type strains of the genus *Fusobacterium* were obtained from the List of Prokaryotic Names With Standing In Nomenclature (<http://www.bacterio.net/fusobacterium.html>) and De Witte *et al.*, (2017). The sequences were imported into Geneious 8.1.4. A multiple-sequence alignment was created using CLUSTAL W, and this used to create a neighbour-joining tree (Jukes Cantor). Bootstrap values were generated from 1000 replicates.

2.7.7 Quality control checks on genome sequence data

For all *Fusobacterium necrophorum* genomes listed in **Table 1**, the size of genome, number of CDS and number of scaffolds were examined. Potential

contaminants within genomes were identified by running the questionable *Fusobacterium necrophorum* assemblies against the nt (NCBI non-redundant nucleotide) database (created 3 March 2018) of Centrifuge 1.0.3 (Kim *et al.*, 2016).

2.7.8 Determination of average nucleotide identity (ANI)

This was determined between pairs of genomes using OrhtoANI implemented in OAT 0.93 (≤ 10 sequences to compare) or OAT_cmd 1.30 (Lee *et al.*, 2016). Outputs from OAT_cmd were imported into R to generate a heatmap (heatmap.2 function in package gplots).

2.7.9 Comparative and pangenome analyses of *Fusobacterium necrophorum* strains.

The 49 whole-genome sequences identified as *Fusobacterium necrophorum sensu stricto* were subject to further analyses. ANI was determined for the 49 genome sequences and other *Fusobacterium* species using OAT_cmd 1.3.0. A pangenome analysis was carried out on the 49 *Fusobacterium necrophorum* strains using Roary (Page *et al.*, 2015).

Using Roary, coding sequences (CDSs) were extracted from the input files and translated to protein sequences, filtered to remove partial sequences and iteratively pre-clustered using CD-HIT (Fu *et al.*, 2012). This resulted in a substantially smaller dataset of protein sequences, which were then clustered with TRIBE-MCL (Enright, *et al.*, 2002). Finally, results from CD-HIT and TRIBE-MCL were merged together and used to make a core gene alignment with MAFFT (Kato, *et al.*, 2002), outputting a core cluster alignment file. A maximum-likelihood tree (GTR model) was created using FastTree with the core alignment file. The phylogenetic tree was visualized using FigTree v1.4.2. phandango (Hadfield, *et al.*, 2017) was used to visualize pangenome data. Single nucleotide polymorphism (SNP) sites in the core cluster alignment file generated by Roary were identified using *SNP-sites* (Page *et al.*, 2016). Principal component analysis (PCA) of the presence/absence of accessory genes within *Fusobacterium necrophorum* subsp. *funduliforme* genomes was done using the R package FactoMineR (Lê *et al.*, 2008). Representative sequences of the 6819 genes detected in the Roary analysis were submitted to eggNOG-mapper v4.5.1

<http://eggnogdb.embl.de/#/app/home>; Huerta-Cepas, *et al.*, (2016) to obtain additional functional information. progressiveMauve (Darling, *et al.*, 2010) was used to visualize genome arrangements, using the .gbk files produced by Prokka.

Chapter 3

3 Typing and Subtyping of *F. necrophorum* strains and clinical isolates

3.1 Introduction

The two major subspecies of *F. necrophorum* are biotype A, *F. necrophorum* subsp. *necrophorum* and biotype B, *F. necrophorum* subsp. *funduliforme* (Shinjo *et al.*, 1991). In the past, *F. necrophorum* has been divided into three biotypes: the two mentioned above and the third biotype C which has been placed in a new species as *Fusobacterium pseudonecrophorum*. Biotype A is the virulent form of *F. necrophorum*, and is predominantly isolated from bovine hepatic abscesses, biotype B is benign and is isolated mainly from ruminal contents, but also from lesions caused by a mix of biotypes. Biotype C is non-pathogenic and can be isolated from abscesses and faecal material. There is also a fourth intermediate biotype known as AB: this is mainly isolated from ovine and bovine foot lesions (Nicholson *et al.*, 1994). Their classifications were based on cellular and colonial morphology, characteristic growth in broth medium, toxin production, their ability to agglutinate chicken erythrocytes and virulence in mice. Differences in production of certain extracellular enzymes such as lipase, DNase and alkaline phosphatase have been demonstrated, however, these have not been shown to be useful to distinguish between the two major subspecies (Okwumabua *et al.*, 1996). Narongwanichgarn *et al.*, (2001) were able to characterise nineteen strains of *F. necrophorum* using the API 20A test kit for identification of anaerobes, which had been previously identified as *F. necrophorum* by the VPI method. Of the 19 strains tested, only 7 of them were identified as having haemagglutinating activity; these were classified as *F. necrophorum* subspecies *necrophorum*. Those strains lacking haemagglutinating activity were classified as *F. necrophorum* subspecies *funduliforme*. All the strains tested were shown to be β -haemolytic on blood agar plates (Narongwanichgarn *et al.*, 2001).

Both cellular morphology and total DNA homology data have provided convincing evidence for relatedness of *F. necrophorum* subspecies, but it has been shown that comparing 16S *rRNA* sequences is a better and more sensitive method for verification of the taxonomic identity. Over the years, the increasing use of PCR, rapid template purification and automated DNA sequencing has dramatically

reduced the time necessary to yield a high-quality sequence. The use of 16S *rRNA* gene sequencing to identify strains and to study the relatedness of prokaryotic species is well established and this has resulted in increased availability of 16S *rRNA* databases. Reports have shown that subtle differences in the 16S *rRNA* gene can be used for species identification and for subtyping and identifying hypervirulent bacterial clones (Gee *et al.*, 2003).

Molecular techniques such as 16S and 23S *rRNA* intergenic spacer region sequence analysis, random amplified polymorphic DNA-PCR and ribotyping analysis are used to discriminate between the two *F. necrophorum* subspecies. Random Amplified Polymorphic DNA PCR (RAPD-PCR) using a 10-mer oligonucleotide primer, W1L-2 has also been used for discriminatory tests (Narongwanichgarn *et al.* 2001).

A real-time quantitative PCR assay was developed by Jensen, *et al.*, (2007) for the detection of *F. necrophorum* subspecies. For confirmation that the strains were indeed *F. necrophorum*, they initially identified colonies on agar plate by colony morphology, odour, Gram stain, green fluorescence with UV light irradiation, β -haemolysis on blood agar plates and antimicrobial susceptibility testing. This was followed by targeting the gyraseB (*gyrB*) gene of both subspecies using subspecies-specific PCR primers, which amplified a region of 306 bp. Results of the *gyrB* species assay were verified with TaqMan-based quantitative PCR-probe assay to bind within the amplified region. The assay used was based on the *RNA polymerase β -subunit* (*rpoB*) gene, consisting of PCR primers and a single probe specific to *F. necrophorum*. All the *F. necrophorum* strains tested were amplified with the primers-probe set, resulting in the correct subspecies assignment of the isolates, based on previous records of the strains (Jensen *et al.*, 2007).

The aim of this chapter was:

1. To identify, based on biochemical and PCR/Sanger sequencing-based analysis of *F. necrophorum* isolates from clinical samples.

3.2 Methods

3.2.1 Identification methods

3.2.1.1 Colony morphology and macroscopic appearance

Initial identification of *F. necrophorum* was based on colony morphology. Isolates were cultured on fastidious anaerobe agar (FAA) (LabM Ltd., Heywood, UK) supplemented with 5 % (v/v) defibrinated horse blood (Oxoid Ltd., Basingstoke, UK) and incubated anaerobically at 37 °C for 48 hours in an anaerobic jar (Oxoid Ltd., Basingstoke, UK) with AnaeroGen™ sachet (Oxoid Ltd., Basingstoke, UK) generating anaerobic growth conditions (oxygen level <1 % and 9-13 % carbon dioxide and 85 % nitrogen). β -haemolysis was recorded, where present, on the blood agar plates.

3.2.1.2 Biochemical tests

The methods for these tests, including Gram staining and tests for catalase, oxidase, indole and lipase are presented in the Appendix I.

3.2.1.3 Molecular Analysis

Methods for bacterial growth, harvesting, DNA extraction, PCR, DNA sequencing, RNA extraction, cDNA synthesis and rt-qPCR are described in the Methods sections 2.3.3.9 and 2.3.4 (chapter 2).

3.3 Results

3.3.1 Identification of isolates

3.3.1.1 Morphology and Biochemical tests

F. necrophorum isolates were incubated anaerobically for 48 hours as described above, and the colonies macroscopically observed. All strains produced colonies that were either translucent or opaque cream colour with waxy or matt appearance. The size of the colonies varied with some being very small, and others medium to large. Most were β -haemolytic on 5 % blood agar, even though

this was not always clear with some of the isolates. They all produced a characteristic, offensive 'boiled cabbage' odour.

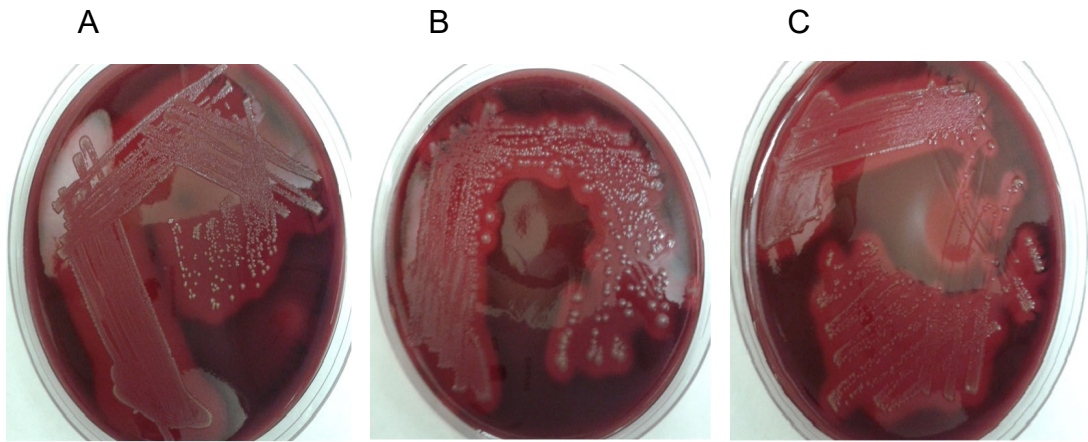


Figure 3.1 Colony identification of *F. necrophorum* on FAA blood agar plates after 48 hours incubation under anaerobic conditions at 37 °C.

A) ARU 01, B) JCM 3718 and C) JCM 3724

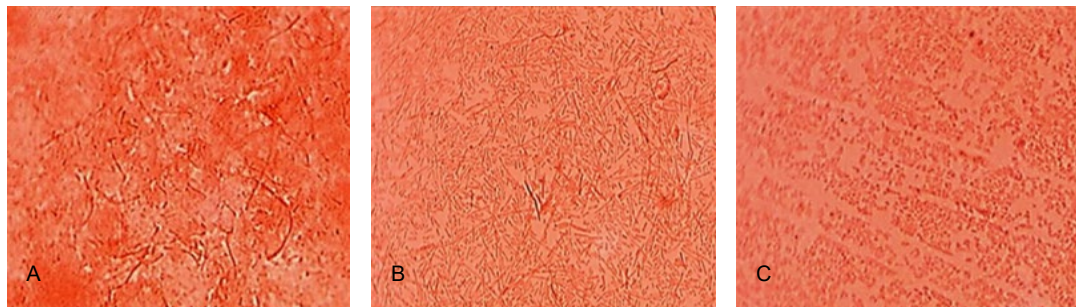


Figure 3.2 Gram stain images of *F. necrophorum* strains, A-ARU 01, B-JCM 3718 and C-JCM 3724

Showing pink Gram-negative rods with characteristic pleomorphic morphology consisting of short rods, long filaments and coccoid elements. Under the light microscope, ARU 01 and JCM 3718 strains displayed long and short rods, while JCM 3724 had coccoid forms (Magnification x1000).

All the strains tested were Gram-negative, pleomorphic in nature consisting of mainly short rods and longer filamentous coccoid elements when examined under the microscope (Figure 3.2). The pleomorphism is likely to be a consequence of stress reaction to oxygen in the media. They were all catalase negative as they gave off little or no oxygen with hydrogen peroxide. The strains were mainly negative for the oxidase test (52 isolates out of the initial 80 isolates tested), but

a few of the isolates appeared to be positive; as an obligate anaerobe, *F. necrophorum* is unable to produce energy aerobically and should not express oxidase enzyme. Some of the positive results were noted after 30 seconds (data not shown) and thus were classified as false positive and inconclusive. *S. aureus* was used as a control for most of the tests, and despite the fact that it prefers aerobic respiration, was oxidase negative, confirming studies that have shown that the enzyme is not expressed by this species (Baker, 1984). The indole test was positive for all of the isolates, which was in agreement with results from previous studies (Bennett & Eley, 1993); El-Hadedy and El-Nour, 2012). Studies have shown indole to be an important molecule in cell signalling (quorum sensing) that controls biofilm formation (Hu *et al.*, 2010). Some isolates produced lipase on egg yolk agar: this test has been used in some studies to differentiate subspecies of *F. necrophorum* (Morgenstein *et al.*, 1981; Amoako *et al.*, 1993).

3.3.1.2 16S and 23S rRNA analysis

Genotypic identification of microorganisms using 16S rRNA gene sequencing is known to be a more objective, accurate and reliable method for identification of bacteria compared to phenotypic methods such as Gram staining and colony morphologies. The genotypic identification method has the added capability of defining the taxonomical relationships among bacteria. Phenotypic methods have many strengths but may fail because the phenotype can inherently be mutated, and interpretations can be biased (Petti *et al.*, 2005).

In the current study, microbiological and biochemical identification results were confirmed by 16S rRNA PCR and DNA sequencing, 21 isolates were selected for future research. 16S (533F/CDR) and 23S (universal) primers (Rudi *et al.*, 1997) were used to amplify rRNA from *F. necrophorum* strains JCM 3718, JCM 3724 and ARU 01. The results for 10 isolates amplified using 16S rRNA primers are shown in Figure 3.3. Amplicons were the expected 425-450 bp and about 400 bp with the 23S rRNA primers (results not shown).

Biochemical tests had only confirmed that the isolates were *F. necrophorum* species, but 16S rRNA PCR and sequencing of the amplicons produced was able to identify different species and subspecies of *Fusobacterium* after sequence analysis using the BlastN function at the NCBI. The *gyrase B* primers amplified

the expected amplicons of 125bp (results not shown) and amplicons were identified BlastN.

Table 3.1 Characteristics of *F. necrophorum* isolates selected for future research

Strains	Colony Morphology	Haemolysis	Gram Stain	Catalase	Oxidase	Indole	Lipsae
ARU 01	Creamish in colour, medium to large shiny smooth appearance.	Positive	-ve Rods	Negative	Negative	Positive	-
JCM 3718	Opaque-creamish, smooth and irregular edges, tiny to medium and raised.	Positive	-ve Rods	Negative	Negative	Positive	+/-
JCM 3724	Small in size, shiny, creamish-yellow and waxy appearance.	Positive	-ve Rods	Negative	Negative	Positive	-
F1	Creamish colour, very tiny approx, 2mm - raised, regular shape and smooth appearance. }	Positive	-ve Rods	Negative	Negative	Positive	+/-
F5		Positive	-ve Rods	Negative	Negative	Positive	+/-
F11		Positive	-ve Rods	Negative	Negative	Positive	+/-
F21	Same as F1, F5 and F11 above.	Positive	-ve Rods	Negative	Negative	Positive	+/-
F24	White 1-6 mm colonies, shiny, smooth appearance.	Positive	-ve Rods	Negative	Negative	Positive	+/-
F30	Creamish small colonies, same as F1-F21.	Positive	-ve Rods	Negative	Negative	Positive	+/-
F39	Mix of small and large colonies, 2-3 mm in size with similar colour, shape and appearance to strains F1-F21. }	Positive	-ve Rods	Negative	Negative	Positive	-
F40		Positive	-ve Rods	Negative	Negative	Positive	+/-
F41	Same as F39 and F40.	Positive	-ve Rods	Negative	Negative	Positive	-
F42	Small creamish tiny colonies 1 mm approximately, smooth, shiny and raised.	Positive	-ve Rods	Negative	Negative	Positive	N/T
F52	Small creamish tiny colonies 1 mm approximately, smooth, shiny and raised.	Positive	-ve Rods	Negative	Negative	Positive	N/T
F59	Tiny creamish-yellow translucent colonies.	Positive?	-ve Rods	Negative	Negative	Positive	N/T
F62	Large creamish colonies, smooth and raised.	Positive	-ve Rods	Negative	Negative	Positive	N/T
F70	Creamish, very tiny 2 mm, same as F1 -F21	Positive	-ve Rods	Negative	Negative	Positive	N/T
F80	Tiny - medium creamish shiny, smooth and regular colonies.	Positive	-ve Rods	Negative	Negative	Positive	N/T
F82	Tiny - medium creamish shiny, smooth and regular colonies.	Positive	-ve Rods	Negative	Negative	Positive	N/T
F86	Same as F80 and F82	Positive	-ve Rods	Negative	Negative	Positive	N/T
F88	Whitish medium size colonies.	Positive?	-ve Rods	Negative	Negative	Positive	N/T

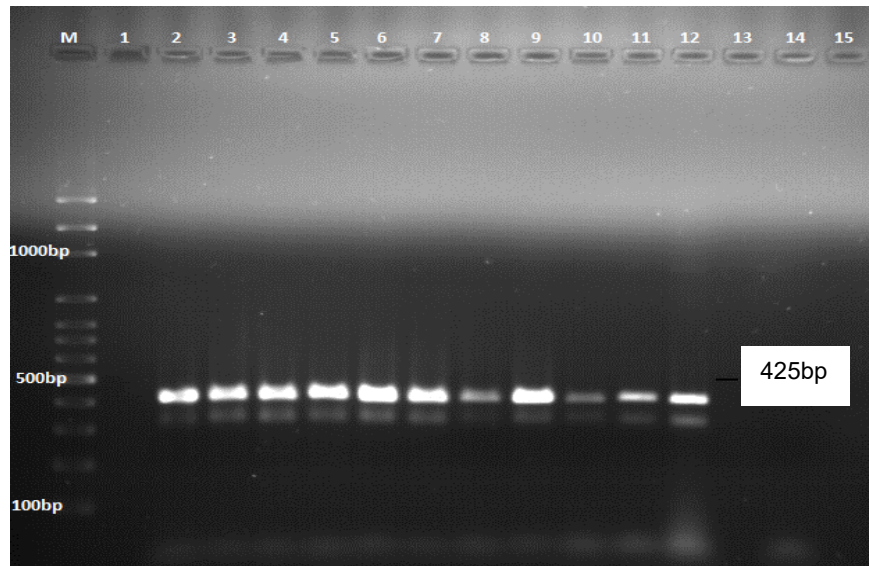


Figure 3.3 Electrophoretic separation pattern of amplicons of *F. necrophorum* DNA with 16S rRNA primers.

Lane M 100 bp marker, lane- 1 Empty, lane 2- ARU 01, lane 3- JCM 3718, lane 4- JCM 3724, lane 5- F1, lane 6- F5, lane 7- F11, lane 8- F21, lane 9- F24, lane 10- F30, lane 11- F40, lane 12- *S. aureus* and lane 13- negative control.

3.3.1.3 Real-time PCR (RT-PCR/qPCR)

Table 3.2 Results of RT-PCR of *F. necrophorum* strains ARU 01, JCM 3718, JCM 3724 and *E. coli* with *gyrase B* and 16S rRNA primers:

ARU 01; JCM 3718; JCM 3724; *E. coli*, +ve (positive control) and -ve (no template control).

Samples	CT Values	Melting Temperature
ARU 01	22.72	77.2
JCM 3718	27.31	77.3
JCM 3724	26.55	77.5
<i>E. coli</i>	27.79	77.5
<i>GyraseB</i> -ve	31.68	77.5
16S rRNA +ve	19.22	90
16S rRNA -ve	30.05	90.2

3.4 Discussion

The strains obtained from the UK Anaerobe Reference Unit (UKARU), Cardiff, consisted of two reference type strains (one subsp. *funduliforme* and the other *necrophorum*) and a clinical isolate from a Lemierre's patient identified to subspecies level as *F. necrophorum* subsp. *funduliforme*. The results in the current study fully supported their findings. Of the 80 clinical samples available for the current studies (obtained from University College Hospital, London), due to financial constraints, only 21 were selected for further study based on biochemical and molecular methods; these were unequivocally *F. necrophorum*.

The PCR based methods used to confirm the biochemical identification tests used *16S rRNA*, *23S rRNA* and *gyrase B* primers. The primers used successfully validated most of the 80 isolates as *F. necrophorum*, but there were some isolates that were not *F. necrophorum*, suggesting contamination. The issues with these isolates were not picked up by the biochemical tests used in this study, therefore additional tests would have been required if molecular techniques had not been used. Primers targeting the *rpoB* gene specific for *F. necrophorum* could have been used instead of *16S rRNA* primers which target *16S ribosomal RNA* genes found in all bacteria (Aliyu *et al.*, 2004). Jensen *et al.*, (2007) used a *gyrB* TaqMan probe-based method to sub-speciate *F. necrophorum* type strains ATCC 25286 and ATCC 51357 (JCM 3718 and JCM 3724 respectively): these strains subsequently served as positive and negative controls for their differentiating probes in further studies.

Care taken in the validation of isolate identity is key to successful research, though it will become apparent in subsequent chapters that, during the Whole Genome Sequencing work, one isolate was found to have been misidentified.

Chapter 4

4 Biofilms

4.1 Introduction

The oral environment exposes bacteria to various physio-chemical challenges such as nutrient limitation, variation in oxygen tension, fluctuations in temperature and pH. Biofilms are sessile architecturally complex communities of microorganisms (Vlamakis *et al.*, 2008) adhering to each other and to solid surfaces. They are enclosed in a self-produced hydrated matrix of extracellular polysaccharide, protein and DNA (Stewart & Costerton, 2001; Bassler & Losick, 2006; Hadju *et al.*, 2010). Almost all microorganisms (nearly 99 %) exist as biofilms in their natural habitats due to environmental stresses such as hostile environmental conditions and exposure to antimicrobial substances (Stewart and Costerton, 2001). Studies have shown the importance of appendages such as flagella, fimbriae and pili which influence the rate of attachment to temporary surfaces until a permanent mechanism is achieved (Donlan, 2002; López *et al.*, 2010). Most bacteria secrete small signalling molecules known as auto-inducers for cell to cell signalling that mediate quorum sensing (QS) (Jang *et al.*, 2012). Stress response gene expression is triggered when these molecules reach a threshold, causing a change in cell surface proteins, increasing cell surface hydrophobicity (Stanley & Lazazzera, 2004). This leads to induction of the first stage of the biofilm cycle where the primary reversible adherence between cells and attachment of the cell to a surface occurs. This is followed by secretion of the extracellular matrix, which is associated with a decrease in hydrophobicity resulting in irreversible attachment (Jefferson, 2004). Finally, the biofilm matures giving rise to complex micro-colonies and the dispersal of very motile planktonic (free-floating) cells under unfavourable conditions (McDougald *et al.*, 2012). The detached planktonic cells are then free to infect other areas, playing a key role in systemic infection, which is also dependent on the host immune response (Donlan, 2001; Taj *et al.*, 2011).

Bacteria in biofilms are protected from being killed by antimicrobial agents by their extracellular polymeric substances (EPS), that help them to evade the host immune responses, leading to chronic infections such as those of the upper

respiratory tract in the case of *F. necrophorum* biofilm (Mohammed *et al.*, 2013). Bacteria of the same strain existing in a biofilm growth state are 10 - 1000 times more resistant to antibiotics than their planktonic counterparts. Suggestions for this antibiotic resistance include: slow growth rate, nutrient limitation, poor antibiotic penetration, stress responses and formation of persister cells (Mah & Toole, 2001). Biofilms are reported to be responsible for up to 80 % of human bacterial infections, including dental plaques, upper respiratory tract infections and medical implant associated infections (Schachter, 2003b; Römling & Balsalobre, 2012).

Research into biofilm has focused mainly on mono-species biofilms, but this is not the normal occurrence in nature; biofilms are often made up of many bacterial species, and sometimes contain algae, protozoa and fungi (Burmølle *et al.*, 2014). Several studies have investigated ways of preventing biofilm formation including the use of enzymes to dissolve the biofilm matrix and compounds such as furanones (Licking, 1999).

The study in this project included *in vitro* examination of mono-species biofilm production of the three *F. necrophorum* strains under various conditions of nutrient concentration, temperature and pH and dual-species biofilm assays of *F. necrophorum* and *Staphylococcus aureus*. Any findings in this study could help in the understanding of the behaviour of *F. necrophorum* biofilms and in finding novel antimicrobial treatment.

Aims of this study included:

1. the determination of the optimal conditions for biofilm formation by *F. necrophorum* in mono-species culture.
2. the investigation of *F. necrophorum* biofilm formation in dual culture with *S. aureus* an aerobic bacterium using the MTP assay.
3. the determination of the impact of biofilm formation on antibiotic resistance.

4.2 Methods

All methods are described in methods sections 2.4.1, 2.4.2, 2.4.3, 2.4.4.2, 2.4.4.3 and 2.4.4.4 (chapter 2).

4.3 Results

4.3.1 Biofilm formation

At 37 °C under anaerobic conditions *F. necrophorum* formed biofilms in both mono- and dual-culture. Using absorbance in the MTP assay as a measure of adherent and planktonic cells in biofilm formation (Table 4.1), *S. aureus* grown in mono-cultures without mineral oil yielded more biofilm than *S. aureus* with mineral oil, 0.108 and 0.701 respectively, demonstrating that although *S. aureus* was able to generate ATP in both conditions as it is a facultative anaerobe, its growth was decreased slightly by the anaerobic environment created by the mineral oil. The mean growth value for the *F. necrophorum* was higher than that obtained for *S. aureus* grown under aerobic conditions; 1.17 and 0.701 respectively. The highest mean biofilm growth was seen in the co-culture of *S. aureus* with the reference JCM 3724 strain, the dual-culture of *S. aureus* and the ARU 01 strain had a slightly lower mean biofilm when compared to the dual culture of *S. aureus* and JCM 3724, but JCM 3718 exhibited the least biofilm growth; 1.23, 1.20 and 1.14 respectively. Mono-cultures formed less biofilm than dual-cultures; (volume corrected). The reference strain JCM 3724 in co-culture generated the greatest mean biofilm growth, with JCM 3718 showing the least mean biofilm growth (Table 4.2).

Using crystal violet (CV) as a measure of adherent cells in the biofilm (Table 4.2), whilst the *F. necrophorum* mono-cultures gave higher absorbance than did *S. aureus*, the difference (0.132 vs 0.129) was not as pronounced as that seen by MTP absorbance measurements (1.17 vs 0.701), which are for both planktonic cells and biofilms. Although there was a difference between the measurement for *S. aureus* in the presence and absence of mineral oil, this was not as pronounced in the CV assay. The highest absorbance in dual culture was for JCM 3724 and *S. aureus*, whilst the co-culture of ARU 01 with *S. aureus* yielded the lowest value in the CV assay whereas, in the MTP absorbance assay the poorest biofilm producing dual cultures were JCM 3718 and *S. aureus*. In both assays, the absorbance obtained in dual culture was significantly higher than the additive absorbances of the single strains (volume corrected) with the exception of the ARU 01 co-culture assayed by the CV assay.

As the MTP assay was assessing both planktonic and sessile cells, true biofilm formation can only be determined by the CV assay; hence, all subsequent results presented refer to the CV assay.

Table 4.1 Comparisons of biofilm mean absorbance (MTP assay); adherent and planktonic cells

Bacteria - conditions	Mean absorbance (nm) ± standard deviation (SD)
JCM 3718 + <i>S. aureus</i>	1.14 ± 0.040
JCM 3724 + <i>S. aureus</i>	1.23 ± 0.047
ARU 01 + <i>S. aureus</i>	1.20 ± 0.140
<i>S. aureus</i> + mineral oil	0.701 ± 0.179 (0.35*)
<i>F. necrophorum</i> strains + mineral oil	1.17 ± 0.313 (0.585*)
<i>S. aureus</i>	1.08 ± 0.258 (0.54*)

*corrected to 50µL n=36

Table 4.2 Comparisons of crystal violet mean absorbance: adherent cells

Bacteria - conditions	Mean absorbance (nm) ± standard deviation (SD)
JCM 3718 + <i>S. aureus</i>	0.134 ± 0.033
JCM 3724 + <i>S. aureus</i>	0.168 ± 0.034
ARU 01 + <i>S. aureus</i>	0.103 ± 0.003
<i>S. aureus</i> + mineral oil	0.119 ± 0.018 (0.060*)
<i>F. necrophorum</i> strains + mineral oil	0.132 ± 0.041(0.065*)
<i>S. aureus</i>	0.129 ± 0.066 (0.065*)

*corrected to 50µL n=36

4.3.2 *F. necrophorum* and *S. aureus* biofilm formation under different conditions

All three *F. necrophorum* isolates (JCM 3718, JCM 3724 and ARU 01) in the present study were found to be biofilm producers at the ranges of temperatures, pHs and nutrient concentrations which were under study (Figure 4.1). The mean

absorbance corresponded to the amount of biofilm formed under each condition (experiment done in replicates and repeated three times).

As pH increased strains JCM 3724 and ARU 01 in the biofilm assay, showed reduction in biofilm formation and the most amount of biofilm was formed at pH4 (Figure 4.1a). Statistically, biofilm reduction in strains ARU 01 and JCM 3718 was not significant (p value=0.13 and 0.17 respectively). In the case of strain JCM 3724, the p value was 0.003, which was statistically significant. However, although the pH of BHI in the biofilm assay after 48 hours incubation remained at 4 in case of the pH 4 medium, it decreased to 6 in case of the pH 7 medium and decreased to 8 in case of the pH 10 medium.

Strain JCM 3718 was affected by low (26 °C) and high (42 °C) temperatures and formed less biofilm than at 37 °C (Figure 4.1b). All other strains and the *S. aureus* control produced more biofilm at 26 °C than 37 °C and the least at 42 °C (Figure 4.1b). Statistical analysis showed no significant difference in the amount of biofilm produced at each temperature for all three strains (JCM 3718, JCM 3724 and ARU 01), with absorbances of 0.02, 1.63 and 0.01 respectively (p value = 0.47, 0.24 and 0.08 respectively).

For the nutrient concentration biofilm assay, decreased biofilm formation in strains ARU 01 and JCM 3718 was observed as the nutrient concentration was reduced; the largest amount of biofilm was formed at full BHI concentration (Figure 4.1c). More biofilm was produced with strain JCM 3724 at half BHI concentration, followed by quarter BHI concentration and then full BHI concentration (Figure 4.1c). There were no statistical significance in the differences in the amount of biofilm produced at decreasing nutrient concentration for strains JCM 3718, JCM 3724 and ARU 01 (p value = 0.86, 0.65 and 0.29 respectively).

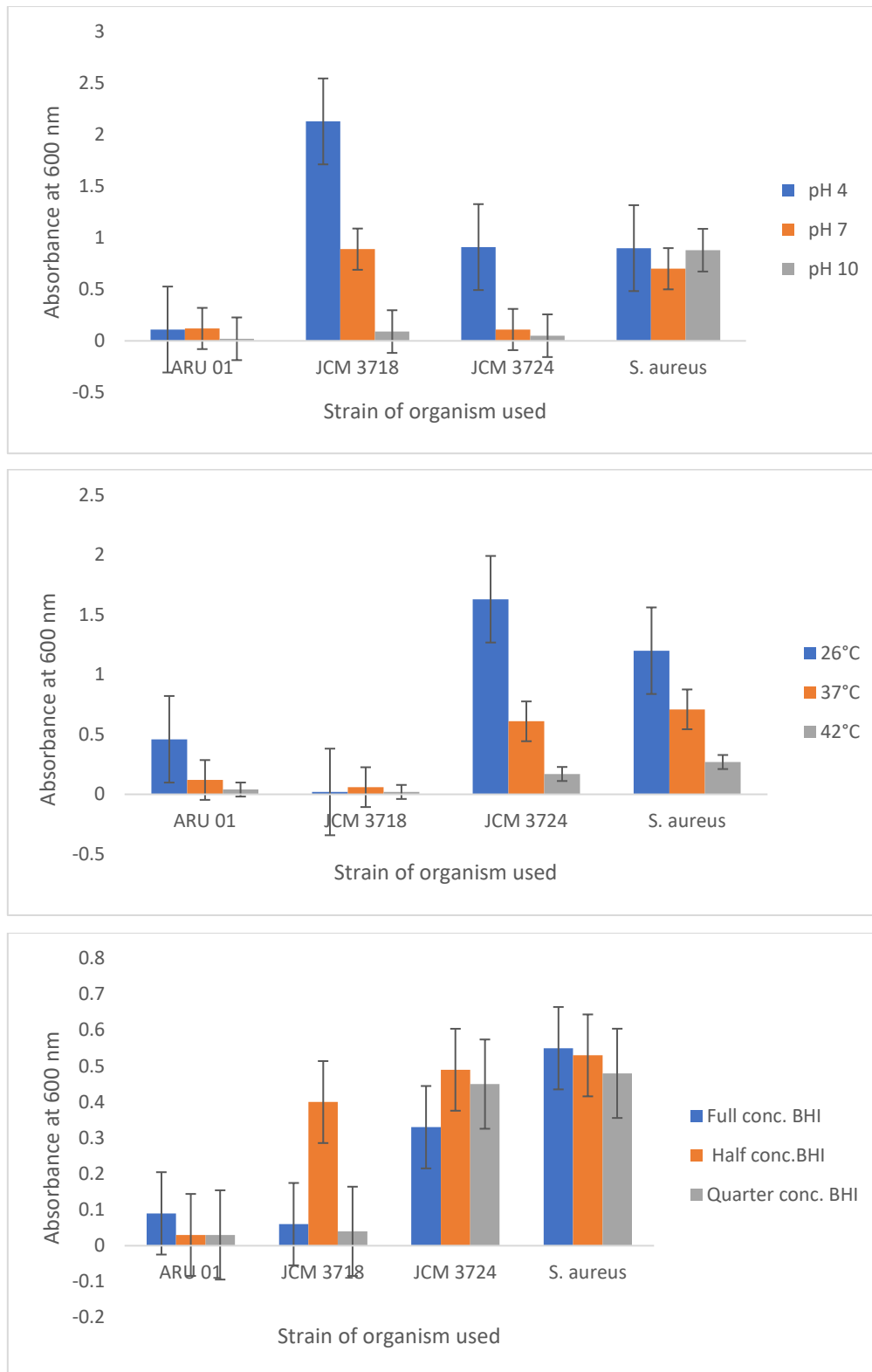


Figure 4.1 Quantification of biofilm formed by the 3 *F. necrophorum* isolates (ARU 01, JCM 3718 and JCM 3724) under different conditions:

pH, temperature and nutrient concentration, to study the amount of biofilm formed under different conditions and examine the optimum conditions for biofilm formation by *F. necrophorum*. (a) Mean biofilm formed at pH 4,7 and 10, (b) mean biofilm formed at 26°C,37°C and 42°C and (c) mean biofilm formed under different nutrient concentrations (full, half and quarter). Data represent n=48. {Error bars represent standard error.}

4.3.3 BacLight viability

BacLight viability assay was initially carried out on mixed cultures of known ratios of live and dead cells; results showed that viable to dead cells ratios were as expected (results not shown). ARU 01 cells killed by treatment with 70 % isopropyl alcohol (used for preparing dead bacteria as a control) showed mostly dead cells (see Figure 4.2b).

The assay was applied to biofilms formed to determine the ratio of Live/Dead cells within the biofilms. A high proportion (greater than 70 %) of viable cells were shown to be present in the reference strain JCM 3718 and ARU 01 Lemierre's strain, whereas JCM 3724 showed equal numbers of Live/Dead cells. *S. aureus* showed higher proportion of live cells (ratio of Live/Dead of approximately 95:5 %).

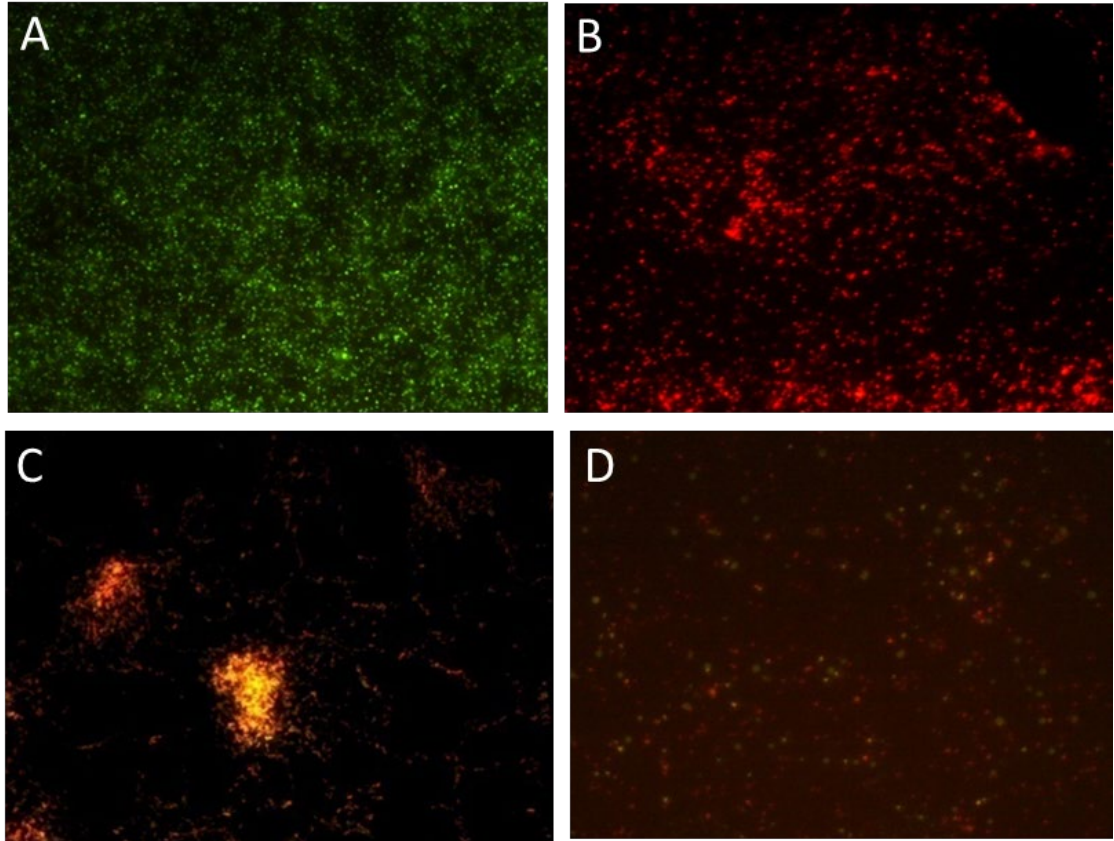


Figure 4.2 Representative images of BacLight viability staining with mixture of SYTO9 and PI

(a) Live cells of *S. aureus* stained green, (b) Dead cells of ARU (treated with 70% isopropyl alcohol) which are stained red, (c) JCM 3724 cells yellowish-orange staining (showing cells that have taken up both dyes) and (d) JCM 3718 showing mixed fluorescence micrograph of both live (green) and dead (red) stained cells.

4.3.4 Single and Dual-species biofilm formation

After growing of *F. necrophorum* samples anaerobically for 48 hours, biofilm formation in 96-well microtitre plates were quantified as described. The absorbance of single and dual-species biofilms was measured using the microtitre plate reader at OD₆₀₀ (Figure 4.3).

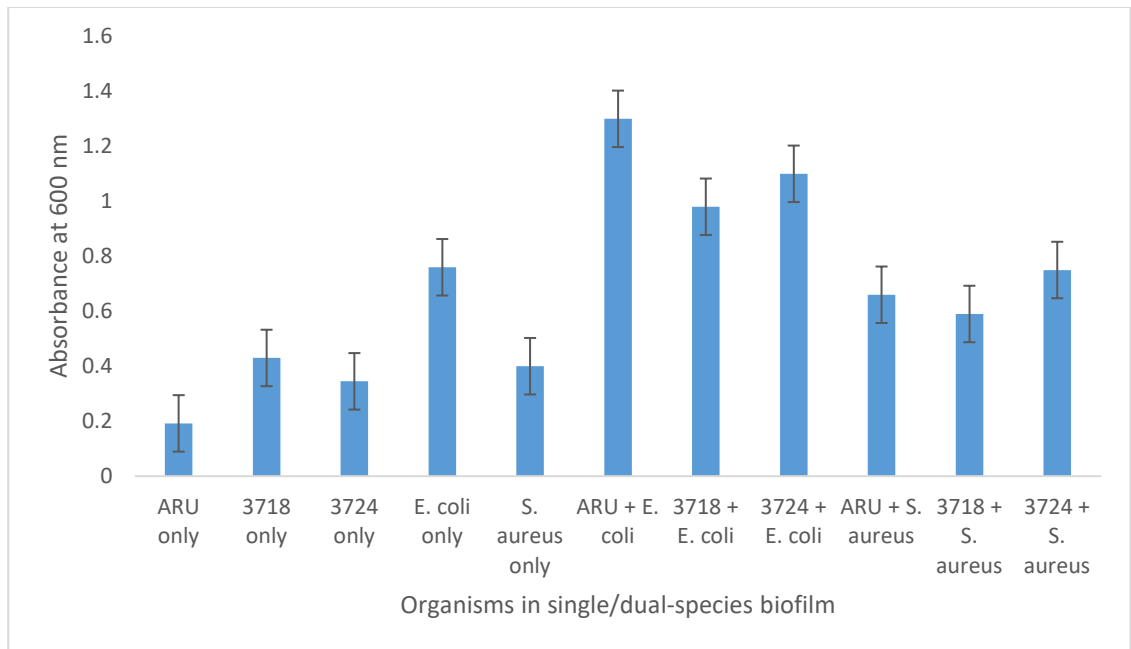


Figure 4.3 Comparison of biofilm formed by *F. necrophorum* strains (ARU 01, JCM 3718 and JCM 3724) as single or dual-species at absorbance of 600 nm.

The graph represents the absorbance values of biofilm formed by the strains. The single species values represent the results for 50 ul. Data represent n=24. {Error bars represent standard error.}

The absorbance values correspond to the amount of biofilm formed by each bacterial strain. The quantification of biofilm formation using the crystal violet staining method does not identify individual strain/species in a dual-species biofilm. In the single species biofilm assay, JCM 3718 was observed to form the most biofilm, having a mean absorbance (OD₆₀₀ of 0.85). JCM 3724 and ARU 01 produced less biofilm with mean absorbance of 0.67 and 0.35 respectively at OD₆₀₀. *E. coli* single-species was observed to form the most biofilm (OD₆₀₀ 1.52), compared to *S. aureus* single-species biofilm (OD₆₀₀ 0.8). For dual-species, ARU 01 and *E. coli* formed the most biofilm giving a high absorbance of 1.28 at OD₆₀₀, this was followed by JCM 3724 and *E. coli* (OD₆₀₀ 1.1) and the lowest dual-species biofilm was observed with JCM 3718 and *E. coli* (OD₆₀₀ 0.98). Dual-species of *F. necrophorum* with *S. aureus* produced less biofilm with all the strains when compared to *F. necrophorum* strains with *E. coli*. With the exception of ARU 01 and *E. coli*, there was no evidence of enhanced biofilm formation in dual culture.

4.3.5 Antibiotic disc susceptibility testing of *E. coli* and *S. aureus*

Antibiotic discs applied to the agar plates were examined after 24 hours incubation at 37 °C. Zones of inhibition (ZOI) were measured to the nearest mm and the results were compared to a standard interpretation chart using BSAC guide (Andrews, 2001). *S. aureus* was observed to be susceptible (S) to all the antibiotics tested, *E. coli* was seen to be susceptible to amikacin (AK) and ceftazidime (CAZ), but resistant (R) to ciprofloxacin (CIP), chloramphenicol (CHL) and gentamycin (GEN).

4.3.6 Antibiotic disc susceptibility testing of *F. necrophorum*

The disc diffusion test was interpreted using BSAC (2015) and EUCAST (2014) methods for antimicrobial susceptibility testing. This was demonstrated by clear zones of inhibition (ZOI) on the agar plates, indicating that growth of both reference strains (JCM 3718 and 3724) and the clinical strain ARU 01 were inhibited by the antibiotics used (photos not included). Imipenem (IMP) was seen to be the least efficient of the antibiotics used with a small zone of inhibition (this can be classified as resistant) and the other four antibiotics: CIP, PEN, MET, and tazobactam/piperacillin (TZP) were all equally effective on the strains of *F. necrophorum* tested, with similar size zones of inhibition. It should be noted that, as yet, the disc diffusion test is not recommended for anaerobes.

4.3.7 Minimum inhibition concentration (MIC) test using MTP

Antibiotics were selected to test their efficacy to inhibit and or eradicate biofilm of *F. necrophorum*. The optical density of cultured cells treated with different concentrations (64 -512 µg/ml) of antibiotics were measured at 600 nm. For the clinical strain ARU 01, penicillin and kanamycin were seen to be most effective at 512 µg/ml, with the efficacy of inhibiting biofilms ranging from 72 % for penicillin and 77 % for kanamycin. Metronidazole had a lower efficacy of 55 % with the clinical strain. The antibiotics penicillin and kanamycin, in inhibiting reference strain JCM 3718 of *F. necrophorum*, were more effective than metronidazole, with percentage inhibition of 64 %, 60 % and 53 % respectively. Penicillin was more

effective for JCM 3724 at 55 % inhibition, with kanamycin and metronidazole having similar efficacies of 45 % and 44 % respectively. Overall penicillin and kanamycin were seen to significantly inhibit the formation of biofilm. For all the strains tested, metronidazole was observed be the least effective at inhibiting biofilm formation at all the concentrations of antibiotics used (see Figure 4.4).

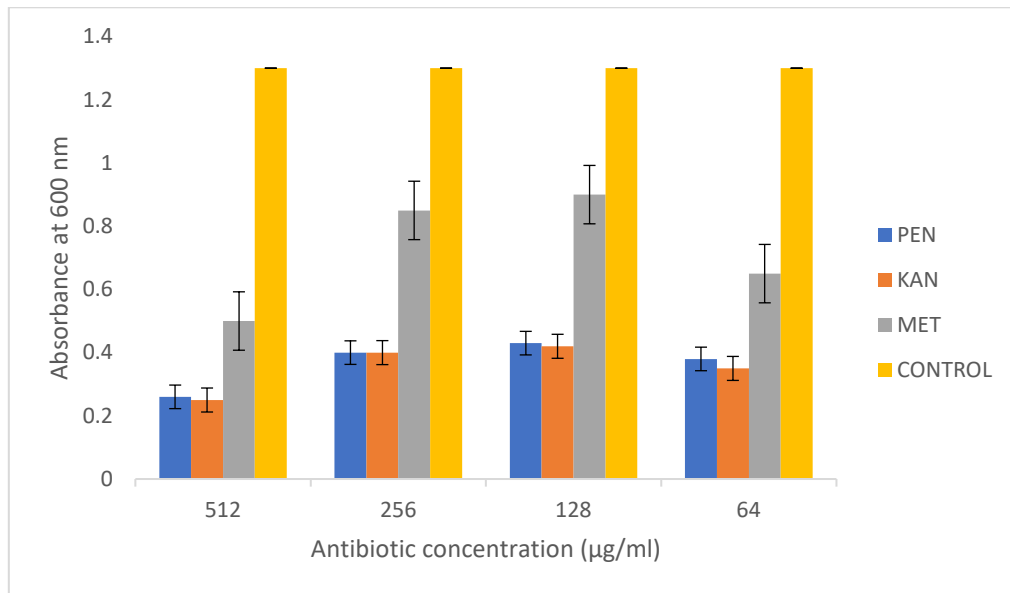


Figure 4.4a Strain ARU 01

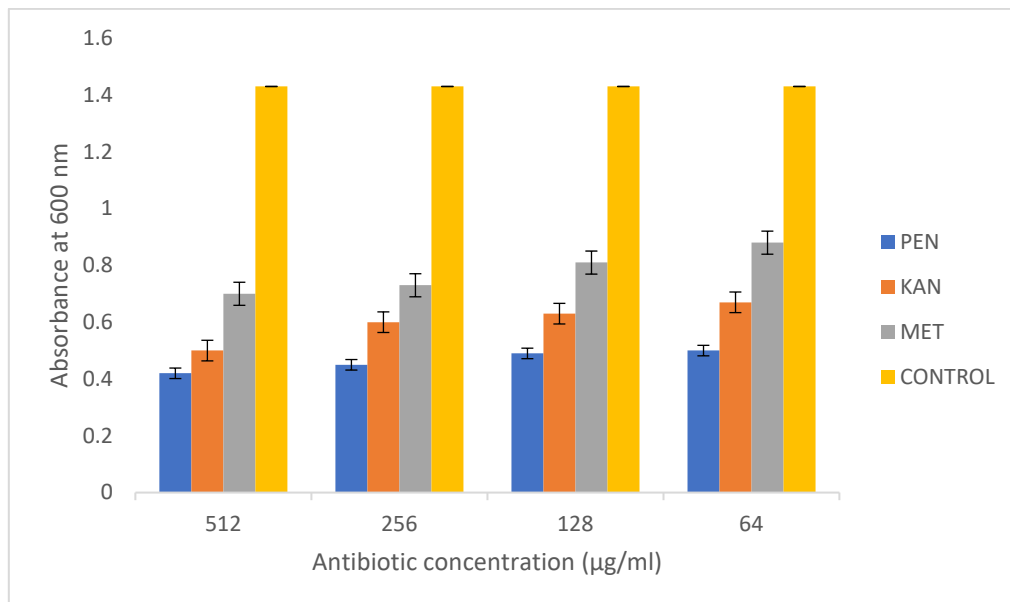


Figure 4.4b Strain JCM 3718
(Continued below on page 69.)

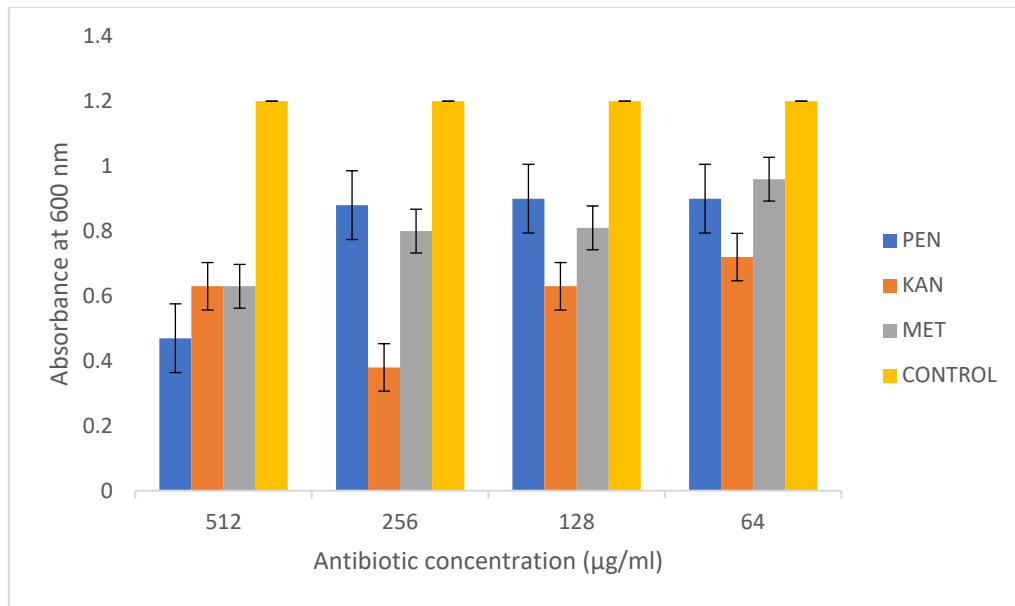


Figure 4.4c Strain JCM 3724

Figure 4.4 Antibiotic susceptibility testing of *F. necrophorum* strains: ARU 01, JCM 3718 and JCM 3724 with three antibiotics (PEN-penicillin, KAN-kanamycin and MET-metronidazole) at concentration of 512 – 64 µg/ml. Data represent n=24. {Error bars represent standard error.}

Penicillin and kanamycin were shown to produce significant inhibition of biofilm formation on ARU 01 cells at all the four concentrations of antibiotics (Figure 4.4a). For JCM 3718, kanamycin and penicillin were seen to be better inhibitors when compared to metronidazole at the same concentrations (Figure 4.4b). Penicillin was more effective in inhibiting biofilm formation of JCM 3724 at a concentration of 512 µg/ml than kanamycin and metronidazole (Figure 4.4c).

4.3.8 Single species biofilm with antibiotics

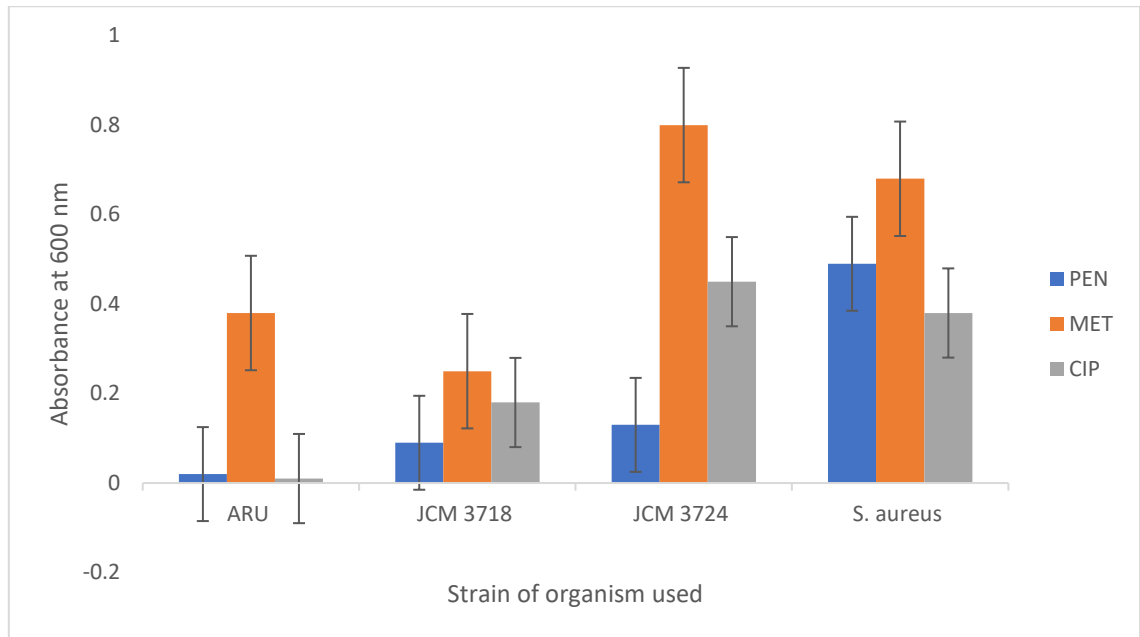


Figure 4.5 Comparison of single-species biofilm with antibiotics.

Biofilm assay with single species *F. necrophorum* strains (ARU 01, JCM 3718 and JCM 3724) and *S. aureus* used as a control. PEN- penicillin, MET- metronidazole and CIP- ciprofloxacin were used at concentration of 512 $\mu\text{g/ml}$, to compare the biocidal activity of the antibiotics on biofilm formation of the single-species bacteria used. Mean amount of biofilm formed was calculated (n=12). {Error bars represent standard error.}

4.3.9 Dual-species biofilm with antibiotics

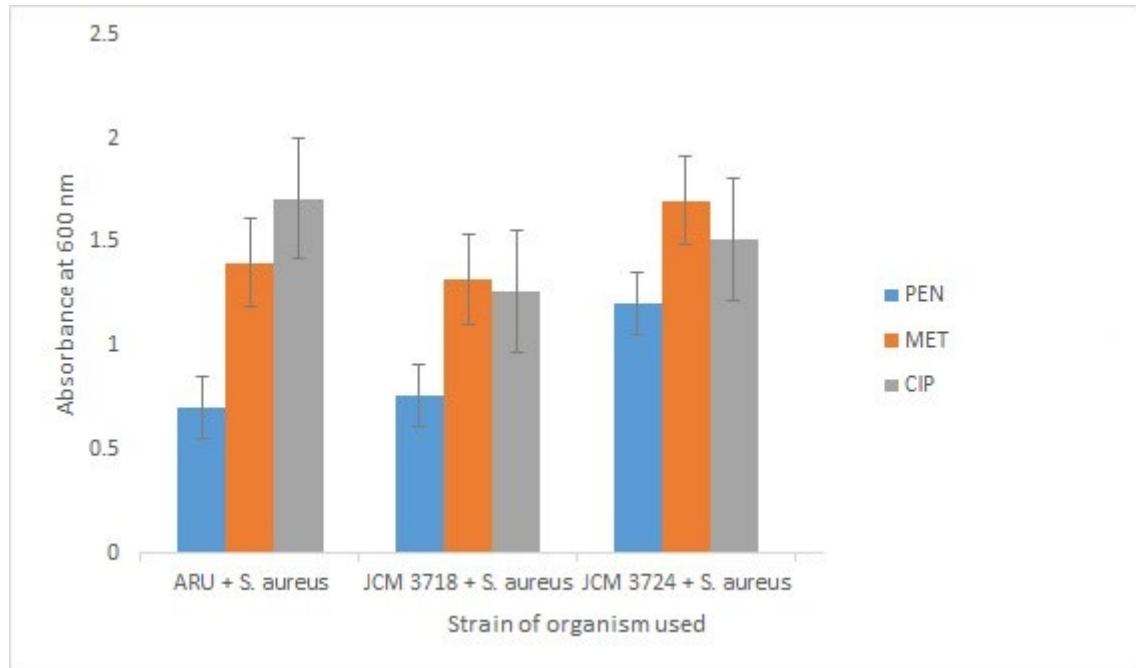


Figure 4.6 Comparison of dual-species biofilms of *F. necrophorum* strains with *S. aureus* with antibiotics.

Dual-species biofilm of ARU 01, JCM 3718 and JCM 3724 with *S. aureus* in the presence of 512 $\mu\text{g/ml}$ concentration of PEN, MET or CIP antibiotics, to study the effect of the antibiotics on biofilm formation. The data is representative of three independent experiments in 4 replicates each (n=12). {Error bars represent standard error.}

All strains and isolates of *F. necrophorum* used for single and dual-species were observed to form biofilm to some extent. Figure 4.5 shows the amount of biofilm formed in single and dual-species both in the presence and absence of antibiotics. Strain ARU 01 yielded the lowest amount of biofilm when grown alone as a single-species compared to JCM 3718 and JCM 3724 strains. The same strains in single-species biofilm with antibiotics resulted in less biofilm production for ARU 01 and JCM 3724 suggesting the antibiotics had some inhibitory effect on these strains. JCM 3718 did not show significant change in the amount of biofilm formed in single-species with or without antibiotics. ARU 01 in dual-species combination with *S. aureus* resulted in good growth when compared to ARU 01 only. The growth in all the dual-species biofilm were modest, but slight increases were observed in dual-species biofilm for JCM 3718 and JCM 3724 when compared to their single-species growth. There was a slight decrease in ARU 01 biofilm in dual-species assay. All three of the *F. necrophorum* strains grown with antibiotics

showed increased yield in biofilm formation. Statistically, there were no significant difference between three strains ($p = 0.56$), however, a significant difference was observed in the different conditions tested: single-species with or without antibiotics, and dual-species with or without antibiotics ($p = <0.0001$).

The biocidal activity of antibiotics, PEN, MET and CIP on single-species *F. necrophorum* strains was also compared with *S. aureus* for biofilm formation. The clinical strain ARU 01 only grew in the presence of MET, but no growth was observed with PEN and very little growth in the presence of CIP. Penicillin was the most effective antibiotic against all three strains of *F. necrophorum* tested, having high biocidal activity. MET allowed growth in all the strains examined, thus showed the least biocidal activity. *S. aureus* biofilm had reduced growth in the presence of CIP compared to PEN and MET. The efficacy of the antibiotics to eradicate most of the strains in single-species biofilm was found to be statistically significant ($p = 0.0082$), and significant difference were observed between the different strains with antibiotics ($p = 0.013$) (Figure 4.5).

The other part of this study examined the effect of antibiotics (PEN, MET and CIP) on dual-species biofilms (Figure 4.6). The antibiotics PEN was seen to produce the least amount of biofilm, thus showing the highest efficacy in eradicating biofilms in the strains tested. MET enabled the production of consistent biofilms in all strains tested in the dual-species assay, but CIP was only able to slightly inhibit JCM 3718 in a dual-species biofilm. Overall, there was little difference in the efficacy of the antibiotics used in the dual-species biofilm, and no statistical significance on biofilm growth ($p = 0.077$) was shown. There was also no statistical significance ($p = 0.516$) between the *F. necrophorum* strains in the presence of antibiotics.

4.3.10 16S rRNA gene amplification from the DNA extraction from planktonic cells and biofilms.

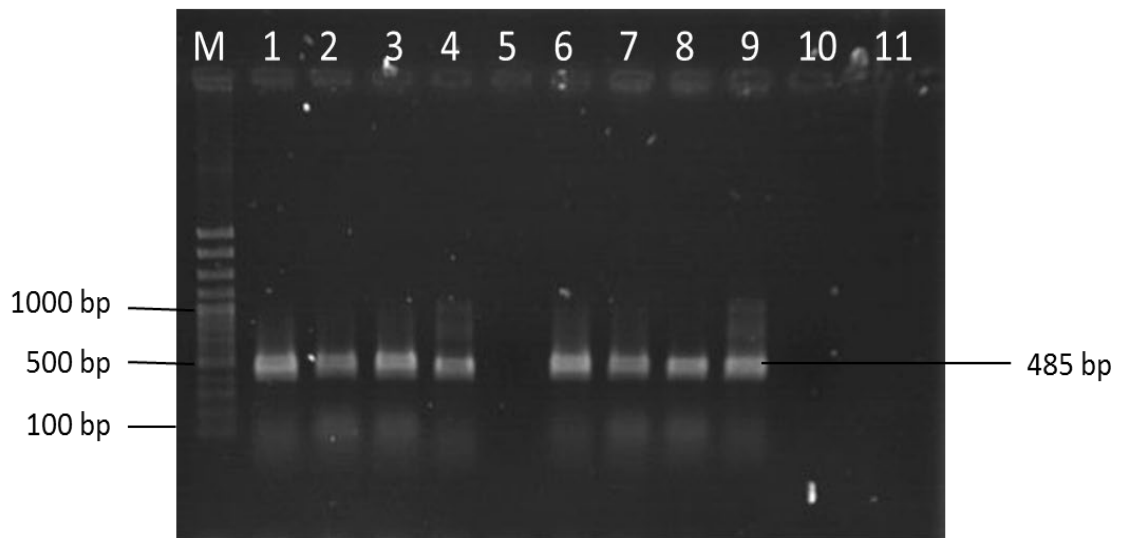


Figure 4.7 Gel electrophoresis of PCR amplicons of DNA extracted from planktonic cells and biofilms of *F. necrophorum* using 16S rRNA primers.

DNA were extracted from the biofilm assay samples (*F. necrophorum* strains: ARU 01, JCM 3718 and JCM 3724) 48 hours after anaerobic incubation at 37°C. Samples were amplified with 16S rRNA primers and the products resolved on 1 % agarose gel using a standard DNA marker. Lane M – 100 bp DNA marker; Lane 1 – ARU 01 planktonic cells (PC); Lane 2 – JCM 3718 PC; Lane 3 – JCM 3724 PC; Lane 4 – ARU 01 positive control; Lane 5 – negative control; Lane 6 – ARU 01 biofilm; Lane 7 – JCM 3718 biofilm; Lane 8 – JCM 3724 biofilm; Lane 9 – ARU 01 positive control; Lane 10 – negative control; Lane 11 – empty.

Analysis of the DNA samples extracted from the planktonic cells and biofilm of the three strains of *F. necrophorum* by PCR resulted in products of the expected sizes of 485 bp. All observed bands had the same intensity for both planktonic cells and biofilm amplified DNA. The positive controls also had bands of the expected sizes, in addition to faint multiple bands. No bands were observed in the negative controls. After sequencing the purified PCR products, the resulting sequence data were compared to those in the GenBank database using BLAST search, and this revealed all the strains as *F. necrophorum* (see Appendix II for sequencing data and BLAST results). The DNA analysis was only carried out on single-species biofilms and not for the dual-species due to time constraints.

Primers could be designed specifically for each of the microorganism species, though a qPCR method would need to be developed for quantitation.

4.4 Discussion

Infections caused by *F. necrophorum* are chronic and recurrent in the upper respiratory tract in humans are not fatal, but account for significant costs in the healthcare system due to their common presentation at general practitioner's (GP's) surgeries (Nord, 1995). Decades of studies by scientists on bacteria in liquid suspension have provided many insights into the physiology and genetics of these microorganisms. They are now known to exist naturally as sessile aggregates and not as planktonic cells as was original thought. Biofilms are abundant in healthcare, industry and other settings and these have led to increased interest and research over the last few decades. EPS of biofilms are thought to result in antibiotic resistance and persistent upper respiratory tract infections. The cost of treating biofilm related infections are reported to be around \$7 billion per year in the United States alone, with limited success (Licking, 1999). According to the National Institutes of Health, 80 % of human infections are due to biofilms, yet antibiotics have all been designed for planktonic cells (Schachter, 2003b). Collective biofilms provide their inhabitants with resistance to antimicrobials and host defence mechanisms through quorum sensing and horizontal gene transfer and this is one of the rationales behind this study. The lack of studies on *F. necrophorum* and its resurgence also justifies the need for further research on this microorganism.

Due to circumstances outside our control, only preliminary work was carried out in an anaerobic cabinet. Subsequently, microtitre plate-based assays, overlaid with mineral oil were used. All results presented here were from these experiments.

The mineral oil overlay used in the microplate-based assays was shown to provide a suitable environment, achieving the anaerobic condition needed for the growth of *F. necrophorum* an obligate anaerobic organism. The oil reduced growth of the facultative anaerobe *S. aureus* significantly, this reduction in growth indicates a change in respiratory conditions, as anaerobic respiration yields less ATP than aerobic respiration, thus less energy is available for cellular proliferation. The theory for biofilm co-culture was that mineral oil would result the production of an

environment with greatly reduced oxygen, which would be reduced further by the presence of *S. aureus*. It was important that *F. necrophorum* did not completely dominate the anaerobic culture. Readings were taken after 48 hours incubation, at a point where the organisms were still in log phase. Recording absorbance of samples in the microtitre plates at regular time intervals, and comparing bacterial growth under mineral oil and in an anaerobic jar would have improved analysis and allow clarification of which method was more effective; however, it was difficult to use the microtitre plates within the anaerobic jars and handling of the plates for repetitive absorbance readings could have affected the biofilms or, if the mineral oil layer was displaced, could have compromised the anaerobic culture. An adaptation of the crystal violet method by Merritt *et al.*, 2005 used for quantification of biofilm formed in this study could be used to assess growth over time. Other studies have been able to show that the mean absorbance (i.e. biofilm formation) increases with extension of incubation times (Adetunji and Isola, 2011).

The BacLight viability assay used for *F. necrophorum* proved to be an effective method for the detection of viable cells from the biofilm produced. The procedure allowed for qualitative assessment of Live/Dead cells after biofilm formation and gave an indication of the survival of bacteria grown under different conditions. However, the results rendered interpretation of the data obtained from the absorbance assays difficult. For example, although JCM 3724 appears to grow well at 26 °C many of those cells were shown to be dead. There are three potential explanations; 1- cells had grown well, reached a maximum and then died *in situ*; 2-during the harvesting of the cells for the BacLight assay they were exposed to oxygen in the environment and died; 3-the biofilms were less tolerant to exposure to oxygen and died during processing. As all experimental wells for one strain were seeded with the same original culture, and different results were obtained for the varied conditions, option 1 is unlikely. It would be prudent to investigate this problem experimentally, exposing the cells from the biofilms and from standard culture to air for varying times prior to processing. A further option (option 4) is that they did not grow at all but died immediately and stuck to the surface of the well. However, dead cells do not adhere, and this is therefore an unlikely explanation. It is noteworthy that *S. aureus* that is tolerant to air showed 95 % viability during the experiments.

It was not possible to identify specific cells in the dual cultures in the BacLight assay, as there were no Gram stained references from some of the earlier co-cultured biofilms. Limitations also include an assumption that the viable cells in biofilm co-culture included both *F. necrophorum* strains and *S. aureus*, based on the fact that both organisms grew separately under mineral oil conditions. It is possible that one species predominated; this could be checked using a qPCR assay with species-specific primers and standard curves.

Under “conventional” *in vitro* conditions of incubation at pH 7, 37 °C and full nutrient concentration, all the strains of *F. necrophorum* formed biofilm. Conditions encountered by microorganisms in the human host are clearly different from those *in vitro* (Di Bonaventura *et al.*, 2007). It is widely known that environmental factors such as pH, temperature and nutrient availability all influence biofilm formation (Hadju *et al.*, 2010), thus the experiments undertaken in this study allowed the quantification of biofilm formed by *F. necrophorum* strains (ARU 01, JCM 3718 and JCM 3724) on abiotic surfaces under different pHs, temperatures and nutrient concentrations. It was believed that this was the first study investigating biofilm formation by *F. necrophorum*.

Marked differences were observed in inhibition in biofilm formation by the three *F. necrophorum* strains studied at growth media pH 10. Nostro *et al.*, (2012), observed similar association between increased pH and biofilm formation, they demonstrated that Staphylococcal biofilm formation was obstructed at alkaline pH. The effect of inhibition by alkaline pH on the ability of *F. necrophorum* to form biofilm by bacterial attachment could be related to the effect of pH on attachment due to surface charge properties (Nostro *et al.*, 2012). There is an interest to study the effect of alkaline conditions together with antimicrobials in order to find effective antimicrobial therapy to eradicate bacteria colonisation and survival in biofilm which would lead to decrease in biofilm-related hazards. On the other hand, increase in pH has been shown to result in increase in biofilm production in *Pseudomonas aeruginosa*, *Klebsiella pneumoniae* and *Vibrio cholera* (Hořtacká *et al.*, 2010). Increased biofilm production in *P. aeruginosa* at a higher pH of 8 is explained by the higher production of alginate, similar association has also been demonstrated in *S. maltophilia* (Harjai *et al.*, 2005; Di Bonaventura *et al.*, 2007; Hořtacká *et al.*, 2010).

This study showed all three strains of *F. necrophorum* produced the greatest amount of biofilm at acidic pH (pH 4), suggesting that the formation of biofilm could be due to the response to stress signals which results in the production of extracellular matrix allowing survival at low pH. Another interesting finding in this study was after 48 hours incubation of the biofilm under different pH conditions, the pH of the growth medium decreased from pH 10 to 8, and in the growth medium with pH 4, it decreased to pH 2. The explanation for these findings may be due to the production of butyric acid by *F. necrophorum* as the main end product of its metabolism (Carlier *et al.*, 1997). It would be interesting to assess butyric acid production, using NMR/MS for biofilm and planktonic cells.

One of the basic requirements for bacterial growth is temperature (Hadju *et al.*, 2010). It was observed in this study that the relationship between incubation temperature and biofilm formation in *F. necrophorum* strains used did not show consistent behaviour. At 37 °C incubation, ARU 01 and JCM 3718 strains formed the most biofilm, with reduction in biofilm observed at 26 °C and 42 °C, indicating that these two strains are unable to form biofilm to help them survive at extreme temperatures. Strain JCM 3724 on the other hand, formed most biofilm at the lower temperature of 26 °C and also a significant amount of biofilm at the higher incubation temperature of 42 °C. This is an indication that strain JCM 3724 might be able to survive in extreme temperatures by forming biofilms.

It can be seen that biofilm formation on abiotic surfaces was favoured by environment that is limited nutritionally as observed for *F. necrophorum* strain JCM 3724. This indicates that sessile growth during biofilm formation may be a survival strategy. This has also been observed by Loo *et al.*, 2000, where biofilm formation by *Streptococcus gordonii* was increased in low concentration nutrient medium but not in a rich nutrient medium. This increase in biofilm formation in low nutrient medium could be associated with increase in the production of EPS by the organism. The process usually demands high energy, therefore more nutrients would be required for increased EPS production (Allan *et al.*, 2002). In this study, results for strain ARU 01, was shown to form the most amount of biofilm at pH 7, 26 °C and full nutrient concentration. Strain JCM 3718 formed the most biofilm at pH 4, 37 °C and half nutrient concentration. The observed results could be due to stress response where low pH enhances biofilm formation of strain JCM 3718. Most biofilm production for strain JCM 3724 was observed at pH 4, 26 °C and half

nutrient concentration. The experiments in this study showed that the quantity of biofilm formed is dependent on all three conditions tested (pH, temperature, and nutrient concentration). Change in any of these factors can dramatically affect biofilm formation, therefore the results shown in this study can reveal that *F. necrophorum* biofilm behaviour *in vivo* is dependent on the environmental conditions and most probably host immune responses at the site of infection. In the production of biofilm in *Pseudomonas*, *Klebsiella* and *Vibrio*, there was a positive relationship observed between pH of incubation media and biofilm formation (Hošťacká *et al.*, 2010).

Two major regulatory genes, *rpoS* and *algT* found in *P. aeruginosa* and *E. coli* are thought to be responsible for the initiation of stress response during biofilm formation (Cochran *et al.*, 2000). These regulatory genes can be upregulated and thus moderate physiological changes that protect the biofilm structure from environmental stresses such as heat shock, cold shock, oxidative stress and other chemical agents. *P. aeruginosa* has the ability to form biofilm under extreme environmental conditions due to the production of the EPS known as alginate (Stapper *et al.*, 2004; Cotton *et al.*, 2009). Alginate in *P. aeruginosa* has been shown to provide specific protection to bacterial biofilms from antibiotics and immune responses, thus it is important to target this polymer in medical research (Cotton *et al.*, 2009).

The genetic background of the organism seems to play a more important role than the natural habitat with the environmental stress factors, which are less important in the role of biofilm production. In the clinical setting, alkaline solutions or cleaners could be promising in preventing bacterial colonisation, by treating surfaces such as catheters or indwelling medical devices, reducing the risk of biofilm related infections.

The bacteriostatic method for assessing antibiotic resistance for *F. necrophorum* in this study, demonstrated clear zones of inhibition showing susceptibility of *F. necrophorum* to PEN (penicillin), MET (metronidazole), CIP (ciprofloxacin) and TZP (tazobactam/piperacillin). The study continued to investigate the ability of *F. necrophorum* strains to form biofilm in single and or dual-species using the MTP assay set up under “normal” *in vitro* settings for 48 hours under anaerobic conditions. The results showed that all the strains (ARU 01, JCM 3718 and JCM

3724) were able to produce biofilms when grown as single-species. ARU 01 was able to produce the most biofilm when grown as a single species but did not produce much biofilm when grown in combination with *S. aureus*. When comparing the individual species forming biofilms with those of dual-species, we could estimate the amount of expected biofilm formed in co-culture, such as in the case of *S. aureus*, which produced low biofilm when compared to *E. coli* in single-species biofilm. Among the three *F. necrophorum* strains studied, ARU 01 produced the lowest biofilm mass, so would be expected to be a poor biofilm producer in co-culture. Co-culture of ARU 01 with *S. aureus* produced a low mean absorbance value of 0.66 at OD₆₀₀ (Figure 5.6) when compared with ARU 01 and *E. coli* co-culture with absorbance value of 1.12 (at OD₆₀₀). The expectation in this investigation was that dual-species biofilm would thrive due to the presence of *S. aureus*, which would consume the oxygen allowing for the survival of *F. necrophorum*, a fastidious anaerobe. Jefferson, (2004) supports this hypothesis, by discussing oral colonisation by aerobes creating an environment suitable for anaerobic bacteria. Hibbling *et al.*, (2010) confirmed that biofilms can select the best variants to colonise the niche created by the biofilm.

In nature, monospecies biofilms are rarely found (Burmølle *et al.*, 2014), the experiments carried out in this study allowed for the quantification of dual-species biofilm of *F. necrophorum* grown with *S. aureus*, thus allowing the determination of the effect of antibiotic resistance with biofilm formed in dual-species biofilms. Polymicrobial cultures are able to create mutually beneficial communities within a biofilm. *S. aureus* is a self-limited biofilm producer, with self-produced D-amino acids, which mediate the release of protein components of the matrix, preventing the formation of fully formed biofilm by *S. aureus*. Nutrient depletion and waste product accumulation, which leads to subsequent disassembly of biofilm, may be some of the reasons for reduced biofilm formation by ARU 01 and *S. aureus* co-culture (Hochbaum *et al.*, 2011). The biofilm assays were performed several times for individual species and co-cultures, but the data obtained were inconsistent. The wash stages for the crystal violet staining may have contributed to the inconsistency in the data obtained. *F. necrophorum* is thought to die when exposed to air for a short period. The handling of the culture during preparation of the biofilm assay can significantly reduce the viability of the organism. Mineral

oil has been demonstrated in various studies to provide a relatively anaerobic environment (Ahn and Burne, 2007; Ahn *et al.*, 2009; Liu and Burne, 2011) and was used in this study. As well as mineral oil, anaerobic conditions can be improved by incubation of the microtitre plates in an anaerobic jar, but this can lead to *F. necrophorum* thriving and dominating both *S. aureus* and *E. coli* in the co-culture, generating results that are not representative. It has been reported that *E. coli*, when grown on its own does not produce stable biofilm, but co-culture with *P. aeruginosa* facilitated biofilm production (Burmølle *et al.*, 2014). Their studies also demonstrated how bacteria can alter the physicochemical surroundings, thus changing the pH and oxygen concentration (Burmølle *et al.*, 2014).

Biofilm had increased resistance to wide range of antibiotics compared to planktonic cells. The challenges of antibiotics resistance and difficulty of eradicating biofilms has prompted novel approaches to preventing or delaying biofilm growth. The objectives of these studies included investigating the effect of different antibiotics on *F. necrophorum* biofilms in anaerobic condition. Biofilm assays were set up in the presence of antibiotics including, penicillin (PEN), metronidazole (MET), kanamycin (KAN) and ciprofloxacin (CIP), each with different modes of action against bacteria. The higher concentration of PEN and KAN at 512 µg/ml was observed to be the most effective for ARU 01 with antibiotic efficacy of 70 % and 60 % respectively. PEN and KAN also had significant effect on inhibition of biofilm growth than MET for strain JCM 3718, with 65 % and 60 % efficacy of antibiotic respectively. *F. necrophorum* is known to have high susceptibility to beta-lactams which include penicillin (Chukwu *et al.*, 2013). Penicillin is known to target cell walls of Gram-positive bacteria and its mechanism of activity involves targeting the cross-linker polymer, peptidoglycan, which maintains integrity and shape of bacteria. The binding of penicillin to penicillin binding protein irreversibly, results in the disruption of peptidoglycan synthesis, which subsequently decreases the enzyme activity, interrupting cell wall development and resulting in cell death (Scheffers and Pinho, 2005; Lange *et al.*, 2007). Penicillin, although widely used to treat infections caused by *F. necrophorum*, though resistance has been noted; a study reported 2 % of 100 *F. necrophorum* isolates were resistant to penicillin (Brazier *et al.*, 2002).

Metronidazole was shown to be the least effective in inhibiting *F. necrophorum* biofilm formation. All single-species produced biofilms in the presence of metronidazole, with JCM 3724 shown to produce the most biofilms. The result observed is conflicting, since metronidazole is the common antibiotic of choice for anaerobic infections (Brazier, 2006; Brazier *et al.*, 2006; Lofmark *et al.*, 2010).

Examination of single-species biofilms showed that ARU 01 had reduced growth in the presence of antibiotics compared to no antibiotics. Strains JCM 3718 and JCM 3724 in contrast had increased biofilm formation in the presence of antibiotics. It was postulated by Vlamakis *et al.*, (2008) that antibiotics may not be able to penetrate deep inside the biofilm, thus protecting its inhabitants. They also stated that antibiotics diffusion are hindered by the slimy residue of the biofilms. In their study, they used mathematical models to predict that biofilm infections would not be cleared if the rate of antibiotic diffusion through biofilm was slower than the rate of antibiotic activation (Vlamakis *et al.*, 2008). This study confirms that with the exception of ARU 01, single-species biofilms do protect the bacteria, but planktonic cells are susceptible to a range of antibiotics. Biofilm formation for dual-species in the presence of antibiotics was the most striking in this study. Biofilms resistant to antibiotics have not been fully elucidated, however, there are a number of factors that may be contributing to this resistance. Several reasons for this increased antibiotic resistance in the biofilm communities include one suggested by Hall-Stoodley *et al.*, (2004) that some cells within biofilms are in the stationary phase, creating areas of dormancy within the biofilm. For antibiotics to have an effect on bacteria, there should be a display of some cellular activity (Hall-Stoodley *et al.*, 2004; Hall-Stoodley and Stoodley, 2009). Kirby *et al.*, (2012) support that biofilms unyielding to antibiotics are likely to be a result of metabolic state rather than environmental conditions. The efficacy of antibiotic is dependent on active cell division and metabolism, but the activity of antibiotics may be influenced by low metabolic rate of bacteria forming biofilm (Cramton *et al.*, 2001). Thus, there is the possibility that increase in biofilm formation from the dual-species assays could be due to the antibiotics not being able to kill the bacteria, as the cells may be dormant. The development of gradients within biofilm clusters are shown to create anoxic, acidic and nutrient-depleted areas, which can activate

dormancy states, where no growth or death are observed (Walters *et al.*, 2003; Stoodley *et al.*, 2008). The idea of dormant cells lead to the hypothesis that persister cells occur within biofilm communities. Persister cells are sub-population of bacteria produced during stationary growth phase that display tolerance to antimicrobial killing, and survival not shown by the other cells. They have the ability to re-grow as planktonic cells and are responsible for repopulating and carrying on with biofilm infections through dispersal and colonisation of new niches (Lewis, 2001; Lewis, 2007); Keren *et al.*, 2004; Keren *et al.*, 2012; Zhang, 2014). Persister cells, which make up about 0.1-1 % of the biofilm communities are thought to be responsible for the tolerance to potent, high concentration antibiotic, which are unable to inhibit or eradicate biofilms (Lewis, 2001; Lewis, 2007). The combination of species within multispecies biofilms are unaffected by the introduction of antibiotics. Burmølle *et al.*, (2014), hypothesised that resistant species might be providing synergism with their neighbours. The mechanism underlying the formation of persister cells is still unknown, although it is known that the highest rate of persister cell formation is at the stationary phase of growth and is independent of quorum sensing (Lewis, 2007).

Quorum sensing (QS), also known as bacterial communication, is a phenomenon where bacteria produce, release, detect and respond to extracellular chemical signal molecules known as autoinducers (AI) that increase in concentration as a function of cell density, when it reaches an optimum level. The bacteria community undergoes phenotypic changes at this point (Davies *et al.*, 1998; Miller & Bassler, 2001; Schachter, 2003b; Schachter, 2003; Parsek and Greenberg, 2005; Ng and Bassler, 2009). Several bacteria species have evolved the ability to take advantage of this communication system. Well studied systems include: N-acyl homoserine lactone (AHL), the first to be described for *Vibrio fischeri*, an aquatic bacterium (Moons *et al.*, 2006), and the autoinducing peptide signalling system in Gram-positive species (Bassler, 2002; Bassler & Losick, 2006). A response regulator binds the signal once the “quorum” has been reached, and this modulates gene expression. A loss in this signalling pathway will stop the formation of biofilm (Moons *et al.*, 2006). The third system is autoinducer-2 QS system, first described in *Vibrio harveyi*. This system facilitates interspecies communication and was found to be produced by a large number of

Gram-negative and Gram-positive species, this signal stimulated the aggregation required for bioluminescence (DeKeersmaecker and Vanderleyden, 2003; Schachter, 2003; Bassler & Losick, 2006). The expression of efflux systems has been implicated in quorum sensing regulation, and QS is known to control the expression of several virulence factors and differentiation of biofilm. It was shown by Chan and Chua (2005) that QS controlled biofilm formation were dependent on BpeAB-OprB efflux pump function in *Burkholderia pseudomallei*. *P. aeruginosa* presents several putative multidrug resistance (MDR) efflux pumps, which play an important role in antibiotic resistance of planktonic *P. aeruginosa*. *S. aureus* has been reported to have six efflux pumps for mechanisms of resistance to antimicrobial agents, and in relation to biofilm, they found a polymicrobial-biofilm-associated multidrug isolate of *S. aureus*, which may have the MDR gene cluster and the macrolides efflux pump *msrA*. The expression of biofilm efflux pumps in *E. coli* may be the reason why their biofilms are more resistant to antibiotics than their planktonic cells (Soto, 2013). QS and efflux pumps may have contributed to the increase observed in the biofilm of dual-species with antibiotics in this study. Indeed, the effect of QS molecules on the mono and dual species biofilms is an area worthy of future investigation.

The EPS limits antibiotic diffusivity within the biofilm through chemical reaction with antimicrobial agents or by restricting their rate of transport. Expression of resistance genes, low growth rates which reduce the rate of antibiotic uptake into the cells and the conditions presented in the surrounding environment of cells forming biofilm may collectively contribute to resistance (Cramton *et al.*, 2001). The incubation step of the conventional MTP assay is undefined and subject to modification based on the growth requirement of the organism being investigated; slow- or fast-growing, aerobes or anaerobes. Rigorous and careful washing steps are involved in the MTP assay where the 96-well plate is submerged in a bowl of water (Merritt *et al.*, 2011). The inconsistencies in the absorbance values of the crystal violet stained biofilm may be due to factors such as the washing steps as some biofilms may be washed off the unbound cells after incubation of the MTP plates (Merritt *et al.*, 2011; Pye *et al.*, 2013). Therefore, bacterial isolates, which were classified either as weak, moderate or strong biofilm producers using the MTP assay may be inaccurate. These variations suggest that the MTP assay may

be unreliable for accurate estimation and subsequent classification of bacterial isolates as biofilm producers.

Some of the modifications made during this study to the MTP assay outlined in section 2.2.8.1 included fixation of the biofilm produced with 4 % formaldehyde before the initial washing step. The rigorous washing step in a bowl of water was modified, by carefully aspirating the unbound, planktonic cells using a multi-pipette, and the 96-wells were washed with 1X PBS buffer using a pipette. The final modification to the assay was the solubilising agent used, 33 % acetic acid instead of the 95 % ethanol, 80 % ethanol/20 % acetone or 100 % dimethyl sulfoxide; the choice is dependent on the type of strains producing the biofilm (Merritt *et al.*, 2011).

The Live/Dead BacLight assay was used to measure the viability of biofilms formed by each of the *F. necrophorum* strain at each condition tested. Low pH (4) and high pH (10) were shown to have increased viable cells in the biofilm. The BacLight biofilm assay generated interesting results, under the different temperatures studied. At low temperature of 26 °C there was a decrease in the amount of viable cells of the biofilm and an increase in the amount of viable cells at high temperature of 42 °C. The interesting findings with decrease in nutrient concentration was that the viability of cells remained very high in the biofilm. A possible explanation of these results might be that at extreme pH, high temperature and limiting nutrient, biofilm is more rigid where the EPS can protect the cells in the biofilm more efficiently.

All the cultures were incubated anaerobically, but as manipulation was done outside an anaerobic cabinet, the observed results may be due to oxygen exposure during manipulation. Studies by Cox *et al.*, (1997), showed that manipulating anaerobic bacteria in air can compromise optimal results; their studies compared uses of anaerobic chamber versus anaerobic jars. They were able to show that plates inoculated and incubated in anaerobic chambers yielded 100 % viability. Certain anaerobes such as *F. necrophorum* and *C. perfringens* passed the air inoculation-chamber incubation quality control test at 100 %, but *F. nucleatum* had a 19.2 % failure under these conditions. The air-chamber procedure had lower percentage failures when compared to jar procedures, due

to shorter exposure in the air-chamber procedure. Optimal growth was obtained under complete anaerobic conditions during all the manipulation and incubation steps (Cox *et al.*, 1997).

Problems encountered in this study included the inconsistency in the growth of the broth culture of the *F. necrophorum* strains and the biofilm assays, which were not carried out in an anaerobic chamber due to financial constraints, and loss of collaborators. This could have resulted in these obligate anaerobes being unable to produce the level of biofilm that might have resulted under strict anaerobic conditions. The production of biofilm formed increased towards the latter part of the studies, but this could be due to improved techniques and not as a direct result of the conditions being tested or the environment in which the study was performed. *In vitro* biofilm studies do not resemble that of *in vivo* infections since biofilm in infections form before antibiotics are prescribed. An experiment that would best represent the *in vivo* state would be to grow and mature the biofilms and then add the antibiotics to assess the resistance (Jefferson, 2004).

Another issue that may have affected the results was the difficulty in growing *F. necrophorum* in BHI to the correct OD, and in trying to avoid introducing oxygen into the culture when taking samples for OD readings; the growth was hence sometimes estimated visually in the liquid culture. As the organism sometimes did not grow to the required OD of 0.6-0.7, the dilutions used for the biofilm assays were 1:10 instead of 1:100. It was not possible to remove the atmospheric oxygen from the BHI media before use and air bubbles may have been introduced into the broth media when mixing the cultures; growth of *F. necrophorum* in the broth media could have been hindered by the presence of oxygen. All the issues mentioned could have contributed to the inconsistencies in results between the repeated experiments.

Differences in starting material may be an intrinsic problem with *F. necrophorum*, as it is an obligate anaerobe, exposure time to air should be minimum. The time taken in preparing the dilutions, aliquoting into the 96-well plates and overlaying with mineral oil varied between 10-30 minutes and sometimes longer and this could mean that some of the organisms might already be dead before incubation for growth of the assay. Therefore, the results obtained may not be accurate. This may explain the variation in results of *F. necrophorum* biofilm formed for each replicate when compared to *S. aureus* (positive control organism), which being a

facultative anaerobe formed firm and uniform biofilm. Mohammed *et al.*, (2013) studied biofilm formation of two anaerobes: *F. nucleatum* and *Porphyromonas gingivalis* using the MTP assay under anaerobic conditions. They were able to show that *F. nucleatum* can grow in a non-strictly anaerobic environment using a flow cell biofilm model, but this was not the case for *P. gingivalis*. It indicates that *F. nucleatum* might be protecting *P. gingivalis* from oxidative stress, thus biofilm formation is synergistically enhanced when these two organisms are grown together even in a partially oxygenated condition. Others have also reported this in their studies (Mohammed *et al.*, 2013).

BacLight assay results were inconclusive; the percentage of Live/Dead cell ratios were estimated, as it was not possible to count individual cells. It was observed that examination of the results immediately after staining was better with improved accuracy of interpretation when viewed under the microscope; photo-degradation occurred when the slides were stored for long periods of time. Due to problems with the imaging software, most of the photomicrograph imaging was delayed and this may have affected the estimation of Live/Dead percentages.

The biofilm study was successfully validated by sequencing the DNA extracted directly from planktonic and biofilms of all three strains; these were confirmed to be *F. necrophorum*. Cell cultures were set up for biofilm formation using the microtitre plate method described in section 2.4.1. DNA was then extracted from planktonic cells and biofilm separately. This proved that the biofilms formed in this study were indeed produced by *F. necrophorum* isolates and not by other organisms, which might have contaminated the assay. The strains were not identified to subspecies level.

Chapter 5

5 Cell surface sugars and the Galactose-binding protein of *F. necrophorum*.

5.1 Introduction

5.1.1 Glycan-lectin interactions

Glycan-lectin binding plays a role in biofilm formation with for example, lectins on organisms binding to host glycans, lectins on the host binding bacterial glycans and lectin-glycan binding between organisms of the same or different species. The results of the investigation of the mechanisms of biofilm formation in *F. necrophorum* infection could lead to the development of biofilm inhibitors and potential therapeutic strategies based on glycan and biofilm formation (Lesman-Movshovich *et al.*, 2003; Ofek *et al.*, 2003; Wu *et al.*, 2007; Rachmaninov *et al.*, 2012). The inhibition of glycan-lectin interactions and quorum sensing have been considered as alternative strategies to antibiotic treatment that can be useful in the treatment of chronic infections through the prevention and disruption of biofilm formation (Brackman *et al.*, 2011). An understanding of these interactions requires knowledge of the glycans and lectins present on the bacteria.

Studies on the structures of Gram-negative anaerobes have focused on adhesins (lectins) that are involved in the interactions responsible for biofilm formation and for internalisation of bacteria into the host cells (Nobbs *et al.*, 2009). *F. nucleatum* is the most widely studied of the *Fusobacterium* species, due to its association with periodontitis. In 1989, Mangan and co-workers showed that the attachment of *F. nucleatum* to human neutrophils was lectin-like and could be inhibited by N-acetyl-D-galactosamine (GalNac), galactose (Gal), lactose (Gal β 1,4Glc), but not mannose (Man), glucose (Glc) or N-acetyl-D-glucosamine (GlcNac) (Mangan *et al.*, 1989). Shanitzki *et al.*, (1997) demonstrated that exogenous galactose prevented the action of four different monoclonal antibodies that inhibited coaggregation of *F. nucleatum* with *P. gingivalis*. The study suggested that a 30 kDa outer polypeptide of *F. nucleatum* helped in coaggregation with other Gram-negative strains (Shanitzki *et al.*, 1997). Rosen and Sela (2006) reported that purified capsular polysaccharide (CPS) and lipopolysaccharide (LPS) of *P. gingivalis* could bind to *F. nucleatum* cells and inhibited its binding to *P. gingivalis* serotype K5. Sugar binding studies showed that D-galactose was the sugar

involved in the interactions, and the authors concluded that galactose-binding determinants in *F. nucleatum* played a crucial role in biofilm (plaque) formation. More recent studies, (Copenhagen-Glazer *et al.*, 2015) demonstrated that the attachment of *F. nucleatum* to mammalian cells and the ability to coaggregate with the major periodontal pathogen *Porphyromonas gingivalis* and at least nine other oral bacterial species were also inhibited by D-galactose.

The current study utilised lectin-based detection of cell surface and intracellular sugars and analysis, and characterisation to elucidate the role of the Galactose-binding protein.

The aims of this study were to:

1. identify sugars on *F. necrophorum* cells using labelled lectins
2. investigate the Galactose binding lectin and determine its likely function.

5.2 Methods

Lectin based assays, DNA extraction, primer design, PCR and sequencing were performed as described in the methods sections 2.3.3.3, 2.6.1, 2.6.2.4, 2.6.2.5 and 2.6.5 (see chapter 2).

5.2.1 Determination of specificity of the Galactose-binding protein

To determine the likely glycan specificity of the Galactose-binding protein, three tests were carried out;

a) Analysis of the agglutination of Human blood group A, B and O erythrocytes; these carry the glycans shown in Figure 5.1.

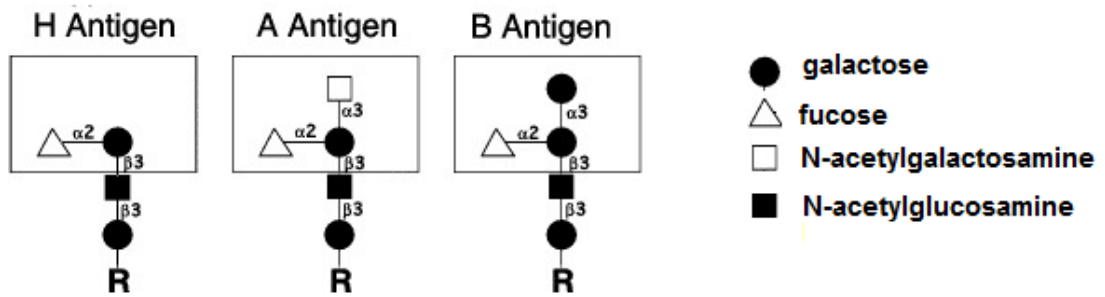


Figure 5.1 Glycan structures of the Human A, B and H antigens.
(Gunnarsson *et al.*, 1984).

b) Analysis of the agglutination of sheep red blood cells that carry the terminal galactose containing glycans shown in Figure 5.2.

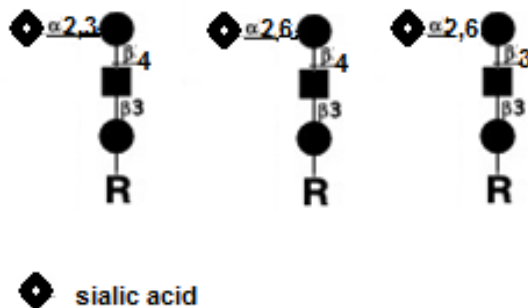


Figure 5.2 Glycan structures of sheep;
 α 2,3 sialyllacto-N-biose 1 (left), α 2,6 sialyllacto-N-biose 1 (centre) and α 2,6 sialyllactosamine (right) (Gunnarsson *et al.*, 1984).

It is interesting to note that the Gal α 1,3 Gal epitopes (both sialylated and unsialylated) (Tan *et al.*, 2010), that are commonly expressed on red cells of mammals other than humans and higher apes, have not been detected on sheep red cells; however, these epitopes are present on other ovine tissues (Macher & Galili, 2008).

c) Bead based analysis using Sepharose and agarose beads carrying specific sugars.

Methods are described in section 2.5.2.4 and 2.5.2.5.

5.2.2 Protein modelling

The Uniprot Knowledgebase was used to obtain the FUS007_00675 D-Galactose-binding protein sequence. The target sequence was loaded into the SWISS-MODEL (<http://swissmodel.expasy.org>) protein structure modelling server, and SwissDock (<http://www.swissdock.ch/docking>) was used to investigate ligand binding. Models were visualised using DeepView Swiss pdb viewer (<https://spdbv.vital-it.ch/>).

5.3 Results

5.3.1 Cell surface glycans; ELISA lectin binding assay

In cell surface analyses using fluorescent labelled lectins, Con A (glucose and mannose specific) demonstrated very weak binding for the 3 reference strains JCM 3718, JCM 3724, ARU 01 and 4/11 of the clinical isolates (F21, F30, F39 and F41); *S. aureus* and clinical isolate 40 demonstrated weak binding. WGA (N-acetylglucosamine/N-acetylneuraminic acid specific) bound very weakly to ARU 01 and JCM 3718; PNA (Gal β 1, 3GalNAc specific) bound weakly to ARU 01 and clinical strains F39 and F42 and weakly to JCM 3724 and clinical isolate F62. The SNA lectin (N-acetylglucosamine/N-acetylneuraminic acid specific) bound weakly to JCM 3718 and clinical sample F11 and weakly to clinical isolate F12. SBA (N-acetylgalactosamine specific) bound very weakly to clinical isolates F21 and F52. Auto-fluorescence and patchy distribution of binding provided issues reading the fluorescence-based assay (Table 5.1). Experiments using biotinylated lectins were very difficult to read and hence an ELLA assay was set up to detect sugars on the solubilise cell extracts of the bacteria.

Table 5.1 Results of lectin histochemistry using fluorescent-labelled lectins for *F. necrophorum* and *S. aureus*.

Sample ID						Predicted sugars
	Con A	WGA	PNA	SNA	SBA	
ARU 01	±	±	+	-	-	Glu/mann, GlcNAc/NANA, Galβ1,3GalNAc
JCM 3718	±	±	-	±	-	Glu/mann, GlcNAc/NANA, α2,6 NANA /GlcNAc
JCM 3724	±	-	±	-	-	Glu/mann, Galβ1,3GalNAc
F1	-	-	-	-	-	
F11	-	-	-	±	-	α2,6 NANA /GlcNAc
F21	±	-	-	+	±	Glu/mann, α2,6 NANA /GlcNAc, GalNAc
F24	-	-	-	-	-	
F30	±	-	-	-	-	Glu/mann,
F39	±	-	+	-	-	Glu/mann, Gal
F40	+	-	-	-	-	Glu/mann,
F41	±	-	-	-	-	Glu/mann,
F42	-	-	+	-	-	Galβ1,3GalNAc
F52	-	-	-	-	±	GalNAc
F62	-	-	±	-	-	Galβ1,3GalNAc
<i>S. aureus</i>	+	±	-	-	-	Glu/mann, GlcNAc/NANA

Key: +: Positive, ±: very weak, +: weakly positive and -: negative. Glu= glucose, Gal = galactose, mann = mannose, GlcNAc = N-acetylglucosamine, GalNAc = N-acetylgalactosamine, NANA= N-acetylneuraminic acid (sialic acid).

5.3.2 Glycans present in whole cell extracts; ELLA assay

To determine the glycans present in the solubilised fraction of the bacterial isolates, an adaptation of the ELISA procedure, ELLA, was used. This assay would detect a mixture of intracellular and cellular glycoconjugates. Assays were performed in duplicate using the reference strains, and 6 clinical isolates.

Table 5.2 ELLA lectin assay for *F. necrophorum*

Sample ID	Lectin					Predicted sugars
	ConA Abs	WGA Abs	PNA Abs	SNA Abs	SBA Abs	
ARU 01	3.4	0.01	3.4	1.8	0	Glu/mann, GlcNAc/NANA, Gal β 1,3GalNAc, 2,6 NANA/GlcNAc
JCM 3718	0.22	0	0	0.054	0	Glu/mann, 2,6 NANA/GlcNAc
JCM 3724	0.28	0	0	0.44	0	Glu/mann, 2,6 NANA/GlcNAc
F1	1.6	0.48	0.027	1.09	0	Glu/mann, GlcNAc/NANA, Gal β 1,3GalNAc, 2,6 NANA/GlcNAc
F11	0.03	0.016	0.15	0.21	0	Glu/mann, GlcNAc/NANA, Gal β 1,3GalNAc, 2,6 NANA /GlcNAc
F21	0.08	0.3	0.069	0.052	0	Glu/mann, GlcNAc/NANA, Gal β 1,3GalNAc, 2,6 NANA /GlcNAc
F30	1.1	0.024	0	0.83	0	Glu/mann, GlcNAc/NANA, 2,6 NANA /GlcNAc
F42	0.59	0.04	0	0.65	0	Glu/mann, GlcNAc/NANA, 2,6 NANA /GlcNAc
F52	0.62	0.016	0	0.61	0	Glu/mann, GlcNAc/NANA, 2,6 NANA /GlcNAc

Solubilised proteins were probed with respective biotinylated lectins and absorbance was read at 405 nm. Key: Glu=glucose, gal=galactose, mann=mannose, GlcNAc=N-acetylglucosamine, GalNAc= N-acetylgalactosamine, NANA= N-acetylneuraminic acid (sialic acid).

All reference and clinical isolates gave positive results with Con A suggesting that glucose and /or mannose was present: the highest values were obtained for ARU 01 and clinical strains F1, F30, F42 and F52. WGA that detects N-acetylglucosamine and/or sialic acid (α 2,3, α 2,6 and α 2,8 linkages) bound less well and the highest results were seen with clinical isolates F1 and F21; neither of the two animal derived reference strains, JCM 3718 and JCM 3724, were detected. PNA that preferentially binds to Gal β 1, 3GalNAc detected ARU 01 and showed low levels of reactivity with F1, F11 and F21; all other isolates gave negative results. SNA, that binds to α 2,6 sialic acid and to a much lesser extent

α 2,3 sialic acid, was detected in all strains; the highest binding was seen with ARU 01, JCM 3724 and clinical isolates F1, F11, F30, F42 and F52. No binding was recorded for the lectin SBA that binds to α - or β -linked N-acetylgalactosamine, and to a lesser extent, galactose residues (Table 5.2). The results clearly demonstrated cell surface and intracellular glycans of *F. necrophorum* and suggest differences between different strains/isolates. The potential presence of sialic acid (neuraminic acid) is important as it is implicated in pathogenicity of other bacterial species. Hence, further studies were carried out to investigate the pathways of biosynthesis (see chapter 8).

5.3.3 The *galactose-binding protein* gene; PCR based analysis

The *galactose-binding* protein gene (FUSO07_00675) was amplified using the designed primers with DNA from the reference and clinical strains of *F. necrophorum*. All the amplicons were analysed on 1 % agarose gel, the bands generated were of the expected size of 209 base pairs (Figure 5.3). All other clinical samples produced amplicons with the *galactose-binding* primers (images not included).

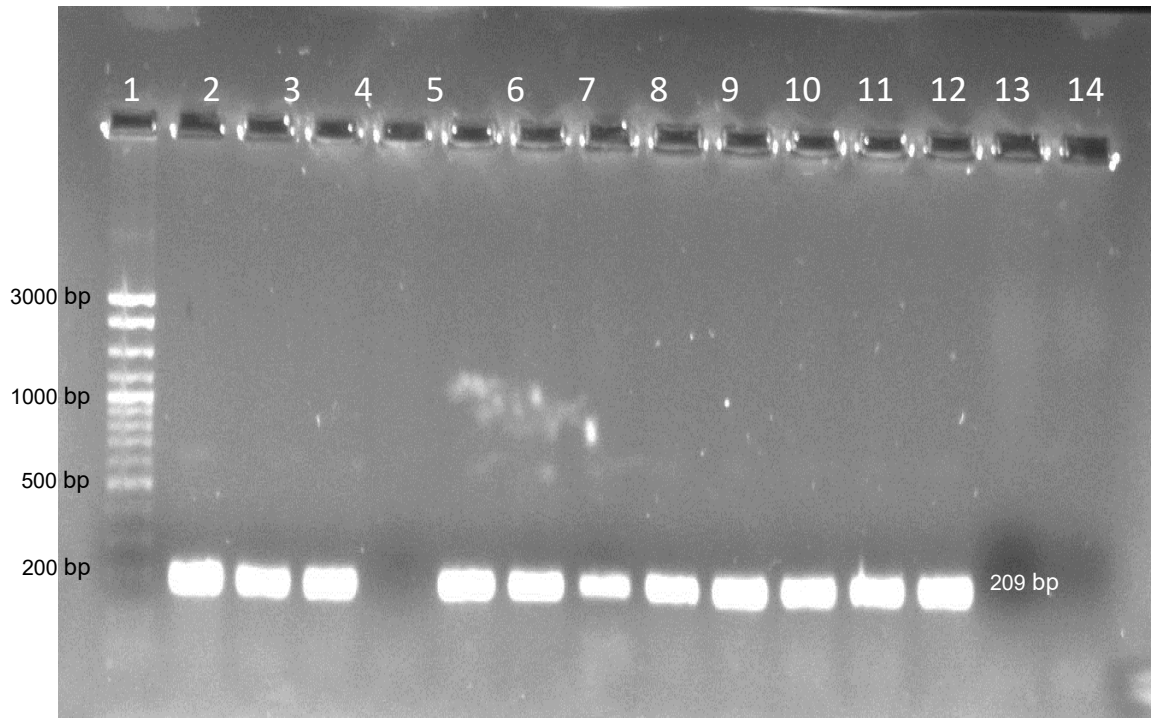


Figure 5.3 Gel electrophoresis of amplicons of *F. necrophorum* clinical Lemierre's strain ARU 01 and reference strains JCM 3718, JCM 3724 and clinical samples F1, F5, F11, F21, F24, F30, F39, F40, F41 & F42, amplified with *F. necrophorum* Gal-binding primers.

No template controls were also included. Lane 1 – DNA ladder, Lane 2 – ARU 01, Lane 3 – JCM 3718, Lane 4 – JCM 3724, Lane 6 – F5, Lane 7 – F11, Lane 8 – F21, Lane 9 – F24, Lane 10 – F30, Lane 11 – F39, Lane 12 – F40, Lane 13 – F41, Lane 14 – 42 and Lane 15 – Negative (no template) control.

5.3.4 Rt qPCR analysis

Table 5.3 qPCR results showing CT values and melting temperature analysis of *F. necrophorum* cDNA with the Gal binding primers.

Sample ID	CT values		Melt values	
	Gal 1 primer	Gal 2 primer	Gal 1 primer	Gal 2 primer
ARU 01	9.69	8.46	78.5	78.3
JCM3718	15.66	17.52	77.5	77.3
JCM3724	16.06	22.28	78.5	78
F1	22.35	20.29	79.2	78.7
F5	9.17	11.8	78.5	78
F11	8.97	9.74	78.2	78
F21	20.92	18.6	78.5	78.5
F24	11.75	8.87	79	78.8
F30	10.85	9.33	79	78.5
F39	15.57	13	78.7	79.2
F40	15.63	12.61	78.5	79.3
F41	8.17	10.48	78.3	77.8
F42	19.79	25.49	80.5	78.7

All isolates tested expressed mRNA encoding the Galactose binding protein as shown by the CT values and melting temperatures. Negative controls gave CT values of 30 or more. With the Gal1 primers, the highest expression was shown in ARU 01, F5, F11, F24, F30 and F41 the lowest expression was shown in F1, F21 and F42. For the Gal 2 primers similar trends were seen.

5.3.5 DNA sequencing

The chromatographs were checked for high quality reads and misreads using Chromas software. All the sequences were retrieved and saved as 'FASTA' files and these were submitted to NCBI BLAST for further analysis. Misread sequences were trimmed by removal of all misread bases prior to use. The BLAST results identified the presence of the *galactose-binding* gene in the *F. necrophorum* DNA samples submitted. The results showed that nucleotide sequences had 98 – 100% similarity to the *galactose-binding* gene of *F. necrophorum* in the NCBI database (See Appendix III for sequence data and BLAST query results). The similarity between the *F. necrophorum* and other

Fusobacteria sp. was greater than 65%. Galactose/glucose binding proteins from other bacteria such as *Aeromonas* sp, *Serratia* sp, *Yersinia* sp, *Tatumella* sp, *Citrobacter* sp. and *E. coli* shared 60% or greater similarity to that from *F. necrophorum*.

5.3.6 Haemagglutination assays

No haemagglutination was detected between any of the *F. necrophorum* samples and red cells of Human blood groups A, B, O or AB, (see Appendix IV, Table I). This implies that the Galactose-binding protein did not recognise α 1, 3 galactose linked to an α 1, 2 fucosylated β -galactose. As there was no agglutination with blood group O cells, the protein did not bind to α 1, 2 fucosylated β -galactose either. By comparison, agglutination assays of *F. necrophorum* with neuraminidase treated sheep erythrocytes showed some positive reactions. ARU 01-mediated haemagglutination of the neuraminidase treated sheep erythrocytes was observed as grape-like clusters of cells. Haemagglutination was also noted with JCM 3718 and JCM 3724; the results with JCM 3724 were weaker than those observed with JCM 3718. As removal of the sialic acid residue at the N-terminus of α 2,3 or 2,6 sialyllacto-N-biose1 or 2,6 sialylated N-acetyllactosamine exposed β galactose linked β 1,3 or β 1,4 respectively to N-acetylglucosamine (or, in glycolipids, linked to glucose), these results suggested the Galactose-binding protein of *F. necrophorum* bound to unsubstituted β -galactose residues. There was no evidence that the *F. necrophorum* cells self-agglutinated.

The bacterial cells used for the haemagglutination assay were stained with BacLight Live/Dead staining ([Live/Dead[®]BacLight[™] kit L7012]. Life technologies, NY, USA & Molecular Probes, USA), and the results (not shown) showed that the majority were viable.

5.3.7 Bead based lectin assay

Using beads with different sugars attached is one of the simplest ways of examining the attachment of bacteria to glycans; however, the concentration of sugars are significantly lower than that found on cells. The results were not easy to interpret (see Appendix IV, Figure III and IV) as the beads were distorted and their size made it difficult to examine microscopically; it was difficult to determine

whether bacteria were specifically binding to the beads. Results were interpreted by comparison of the test results with those of the unsubstituted Sepharose controls. There was no compelling evidence that any specific binding had occurred.

5.3.8 Protein modelling

The sequence for FUSO07_00675 D-Galactose-binding protein of *F. necrophorum* was downloaded from the Uniprot Knowledgebase (Figure 5.4). The target sequence was then used to create a three-dimensional protein structure using the SWISS-MODEL server.

```
MKKMGIVLGALVLAAGLVGCGEKKEAAAPAEAVRMGLTYKFDDNFIALFRQAFQAEADAVGD
QVALQMVD SQNDAAKQNEQLDVLLEKIGIDTLAINLVDPAGVDVVLEKIKAKELPVVFYNRKPS
EEALASYDKAYYVGIDPNAQGV AQGKVEKAWQAPALDLNGDGVIFAMLKGE PGHPDAEART
VYSIKTLNEDGIKTEELHLD TAMWDTAQAKDKMDAWLSG PADKIEVVICNDGMALGAIESMKA
FGKSLPVFGVDALPEA I TLIEKGEMAGTVL NDAKGQAKATQVAMN LGEGKEATEGTDIQMEN
KIVLVPSIGIDKENVAEYK
```

Figure 5.4 Protein sequence of the Galactose-binding protein of *F. necrophorum*.

Figure 5.5 shows the list of suggested template sequences generated by Swiss-Model; all those with identity greater than 50 % were Galactose-binding proteins from a variety of bacteria. Most (<75 %) homologues bound both galactose and glucose. The structure selected (automatically) to generate the model was from *Yersinia pestis*. The GMQE of 0.78 and QMean of 0.74 (Figure 5.6) rated the models as very good.

	Name	Title	Coverage	GMQE	QSQE	Identity	Method	Oligo State	Ligands
<input checked="" type="checkbox"/>	5kws.1.A	Galactose-binding protein		0.79	-	63.42	X-ray, 1.3Å	monomer ✓	1 x CA _β , 1 x BGC
<input type="checkbox"/>	2ipn.1.A	D-galactose-binding periplasmic protein		0.78	-	62.08	X-ray, 1.1Å	monomer ✓	1 x CA _β , 1 x BGC
<input type="checkbox"/>	3gbp.1.A	GALACTOSE-BINDING PROTEIN		0.78	-	62.42	X-ray, 2.4Å	monomer ✓	1 x CA _β , 1 x BGC
<input type="checkbox"/>	2ipm.1.A	D-galactose-binding periplasmic protein		0.78	-	61.74	X-ray, 1.1Å	monomer ✓	1 x CA _β , 1 x BGC
<input type="checkbox"/>	2ipl.1.A	D-galactose-binding periplasmic protein		0.78	-	61.74	X-ray, 1.2Å	monomer ✓	1 x CA _β , 1 x BGC
<input type="checkbox"/>	2hph.1.A	D-galactose-binding periplasmic protein		0.77	-	62.42	X-ray, 1.3Å	monomer ✓	1 x CA _β , 1 x BGC
<input type="checkbox"/>	3ga5.1.A	D-galactose-binding periplasmic protein		0.77	-	62.42	X-ray, 1.9Å	monomer ✓	1 x CA _β , 1 x RGG
<input type="checkbox"/>	1glg.1.A	GALACTOSE/GLUCOSE-BINDING PROTEIN		0.77	-	62.42	X-ray, 2.0Å	monomer ✓	1 x CA _β , 1 x GAL
<input type="checkbox"/>	2qw1.1.A	D-galactose-binding periplasmic protein		0.77	-	62.42	X-ray, 1.7Å	monomer ✓	1 x 3MG _β , 1 x CA
<input type="checkbox"/>	2fvy.1.A	D-galactose-binding periplasmic protein		0.77	-	62.42	X-ray, 0.9Å	monomer ✓	1 x CA _β , 1 x BGC 1 x CO2 _β
<input type="checkbox"/>	4z0n.1.A	Periplasmic binding protein/LacI transcriptional regulator		0.77	-	59.33	X-ray, 1.3Å	monomer ✓	1 x CA _β , 1 x GAL
<input type="checkbox"/>	5kws.1.A	Galactose-binding protein		0.74	-	61.79	X-ray, 1.3Å	monomer ✓	1 x CA _β , 1 x BGC
<input type="checkbox"/>	3gbp.1.A	GALACTOSE-BINDING PROTEIN		0.73	-	60.54	X-ray, 2.4Å	monomer ✓	1 x CA _β , 1 x BGC
<input type="checkbox"/>	3ga5.1.A	D-galactose-binding periplasmic protein		0.72	-	60.54	X-ray, 1.9Å	monomer ✓	1 x CA _β , 1 x RGG
<input type="checkbox"/>	1glg.1.A	GALACTOSE/GLUCOSE-BINDING PROTEIN		0.72	-	60.54	X-ray, 2.0Å	monomer ✓	1 x CA _β , 1 x GAL

Figure 5.5 Suggested templates for modelling the Galactose-binding protein (Swiss-Model)

5kws.1 Crystal Structure of Galactose Binding Protein from *Yersinia pestis* in the Complex with beta D Glucose.

3gbp.1 Structure of the periplasmic glucose/galactose receptor of *Salmonella typhimurium*.

Model Results

Order by: GMQE

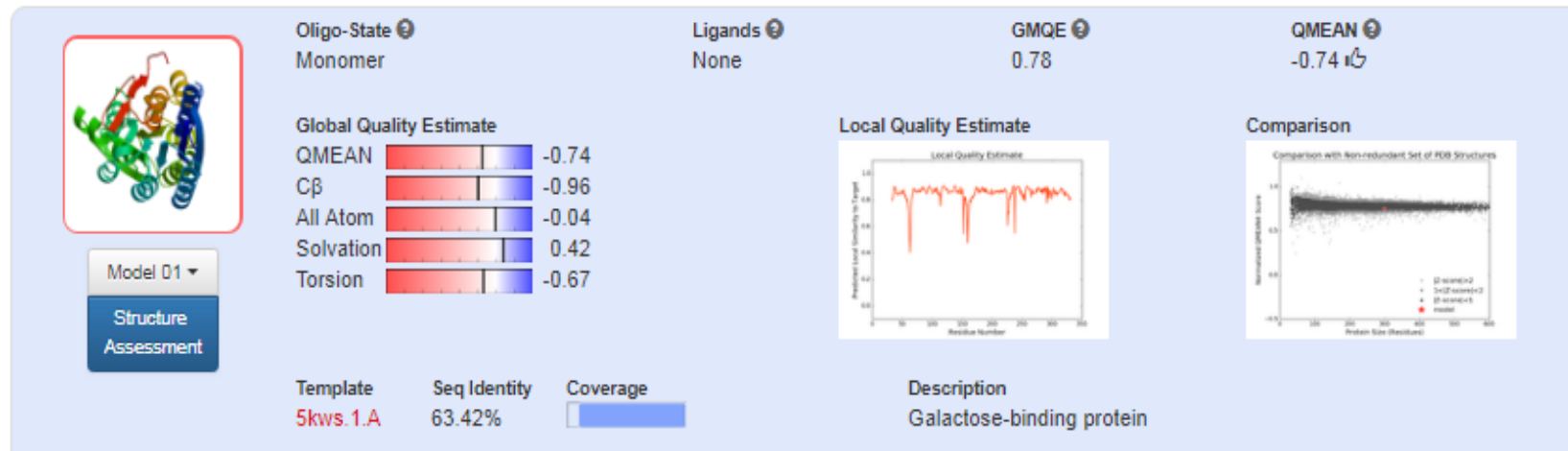


Figure 5.6 Results of modelling the Galactose-binding protein of *F. necrophorum*

The pdb file of the Galactose-binding protein was loaded into SwissDock and the structure was interrogated with ligands of glucose, galactose, N-acetyllactosamine (Gal β 1, 4 GlcNAc) and lacto-N-biose1 (Gal β 1, 3Glc). Based solely on the estimated ΔG (kcal/mol), the energy required to maintain the docked structure, the disaccharides N-acetyllactosamine and lacto-N-biose1 were bound more tightly - $\Delta G = -7.66$ and -7.87 kcal/mol respectively, than glucose or galactose $\Delta G = -6.20$ and -6.55 kcal/mol respectively. All of the sugars bound to 2 major sites on the protein, however, the galactose and glucose also bound weakly to other areas of the molecule (Figures 5.7, 5.8 and 5.9).

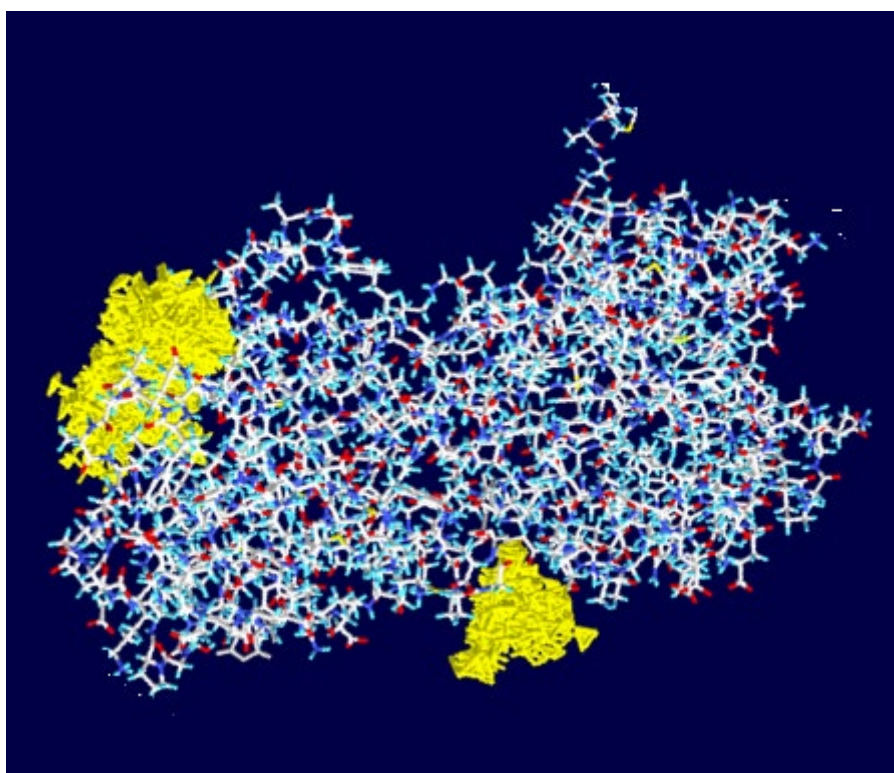


Figure 5.7 N-acetyllactosamine (yellow) binding to the Galactose-binding protein.

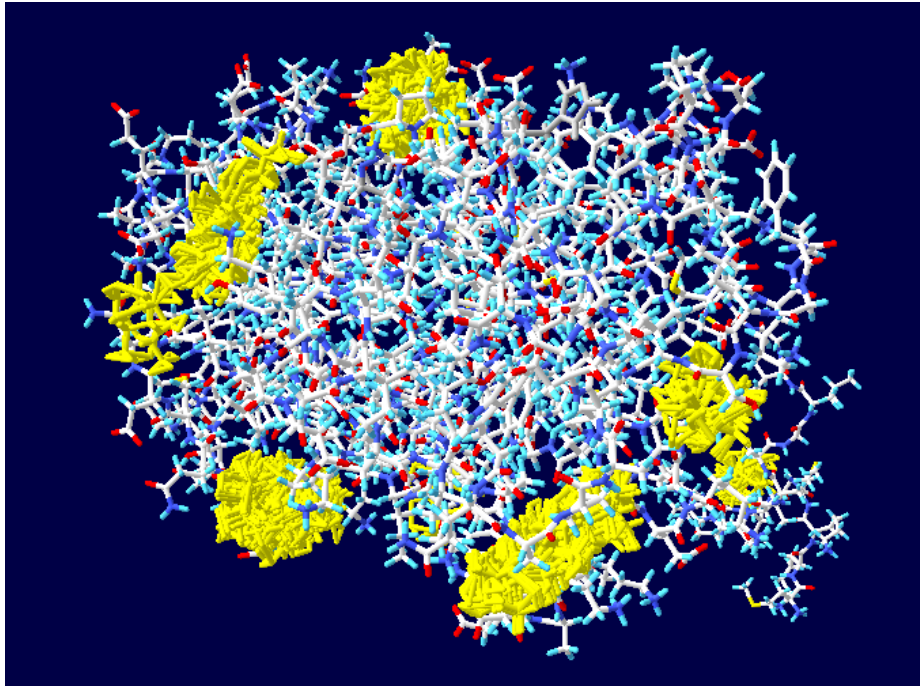


Figure 5.8 Galactose binding (yellow) binding to the Galactose-binding protein.

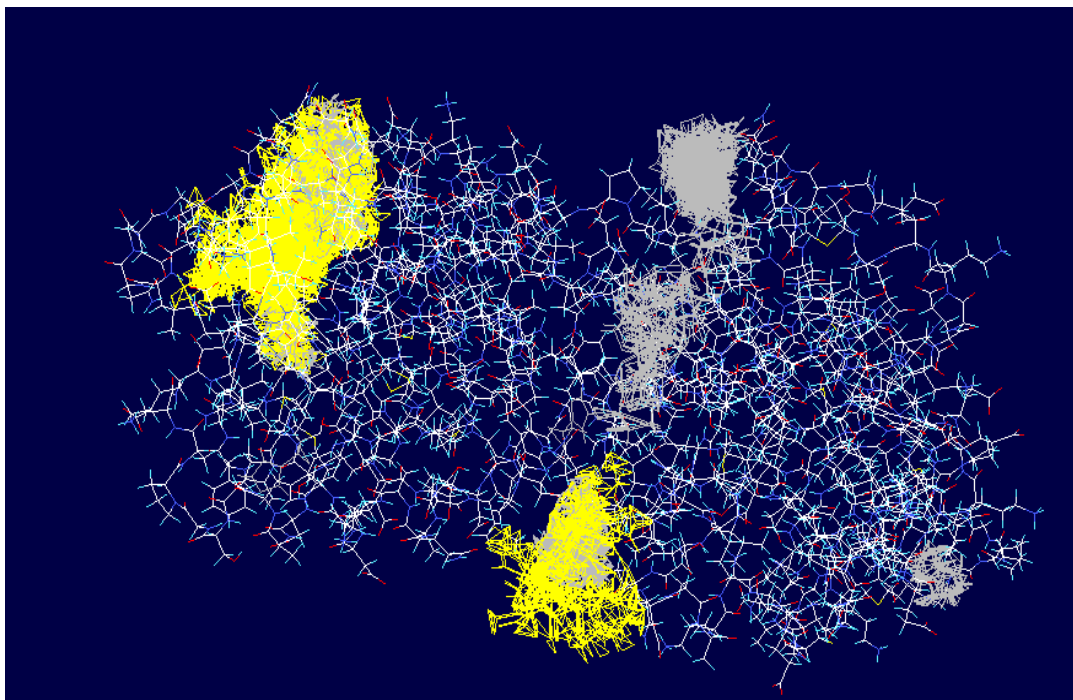


Figure 5.9 Overlay of galactose (white) and N-acetyllactosamine (yellow) predictive binding to the Galactose-binding protein.

Two of the binding sites for galactose are co-incident with the binding sites for N-acetyllactosamine. The results for glucose and lacto-N-biose binding were similar to those for galactose and N-acetyllactosamine respectively.

5.4 Discussion

Cell surface glycans and bacterial lectins are important in interactions of bacterial cells and the formation of biofilms and in the binding of bacterial cells to host cells and tissues. Hence, the identification of cell surface and intracellular glycans, and bacterial lectins is important for the future development of novel therapies.

Preliminary work using fluorescent and biotinylated lectins to detect cell surface molecules gave results that were difficult to interpret; this was due to autofluorescence (fluorescence assays) and difficulties in discriminating the chromophores (biotin assays). Therefore, bacterial cells were solubilised to free the intracellular content that was then bound to ELISA plates and probed with biotinylated lectins. The results were semi-quantitative but represented interaction of lectins with glycans from the whole cells. The results showed variations in the glycans present in different isolates, nevertheless, Glu/mann, GlcNAc/NANA, Gal β 1, 3GalNAc, α 2, 6 NANA /GlcNAc were detected in most isolates and there was no evidence of terminal GalNAc. However, the “control” strains, JCM 3718 and JCM 3724 that were both isolated from animals, lacked GlcNAc/NANA and Gal β 1, 3GalNAc and the clinical isolates F30, F42 and F52 lacked Gal β 1, 3GalNAc. F1 and F21 were the only 2 isolates to show strong expression of GlcNAc/NANA. There were also significant differences in the amounts of glycans detected with the lectins used.

The implications of these differences are difficult to interpret in the absence of clinical data. To further understand the results and determine cell surface expression, biosensors, such as those marketed by Attana, Sweden, could be utilised either by binding cells to inert supports, interrogating these with unlabelled lectins and detection using quartz balance technology or by immobilising lectins and evaluating bacterial binding (reviewed by Wang and Anzai, 2015). Given the interplay between cell surface sugars carried by bacteria and the lectins present on bacterial and host cells, this is an area that requires further work. Glycosylation is a complex process; a multidisciplinary approach, involving chemical, biochemical, molecular and genomic/proteomic technologies will be needed to unravel the mechanisms.

Compared to the difficulties encountered in the detection of surface sugars, the elucidation of the Galactose-binding protein of *F. necrophorum* was relatively straightforward. The BioCyc genome database was used to identify the nucleotide sequence encoding the Galactose-binding protein of *F. necrophorum*. Primers specific for the *galactose-binding* gene produced amplicons of the expected size with all the *F. necrophorum* strains (ARU 01, JCM 3718, JCM 3724 and the available clinical strains) studied. DNA sequencing of the amplicons from the *F. necrophorum* strains and analysis using bioinformatics tools such as BLASTN enabled species-specific identification of the PCR amplicons. The search results showed 99 – 100 % similarity with *F. necrophorum* BTFR-2 contig0006 and 98 % similarity to *F. necrophorum* BTFR-2 contig0032 whole genome shotgun sequence. The encoded protein was well conserved in all *Fusobacteria* species (greater than 65 % similarity) and shared 60 % or greater similarity to Galactose-binding proteins of *Aeromonas* sp, *Serratia* sp, *Yersinia* sp, *Tatumella* sp, *Citrobacter* sp. and *E. coli*.

Shaniztki *et al.*, (1997) demonstrated that the Galactose-binding protein of *F. nucleatum* was involved in mediating galactose-sensitive binding to galactose derivatives on bacterial and mammalian cells. Given the recorded absence of both sialylated and unsialylated Gal α 1,3 Gal epitopes on sheep red blood cells, the results of the haemagglutination assays undertaken in the current study suggested that the Galactose-binding protein of *F. necrophorum* bound to the terminal unsubstituted β -galactose of cell surface glycans such as those described by Gunnarsson *et al.*, (1984). The lack of haemagglutination with Human blood group O cells or untreated sheep red blood cells was probably due to steric hindrance caused by the presence of fucose and sialic acid molecules respectively on the terminal β -galactose; once the sialic acid residues were removed with neuraminidase the bacterial cells were able to agglutinate the sheep red blood cells. This suggested that the required epitope for binding had a terminal non-reducing unsubstituted β -galactose residue. The lack of “self-agglutination” suggested that the Galactose-binding protein did not bind to galactose residues carried by the organism itself.

The important role of Galactose-binding proteins in the interaction between bacteria and host cells has been demonstrated in a study of *Vibrio cholera* (Sasmal *et al.*, 1999), an organism whose Galactose-binding protein had greater than 60 % similarity to that of *F. necrophorum* and whose structure was used as the template for protein modelling. The Galactose binding protein of *V. cholera* selectively recognised host cell epitopes and was shown to facilitate intragenic coaggregation between *V. cholera* and *P. aeruginosa* resulting a chronic lung infections in patients who were immunocompromised (Ma *et al.*, 2007). Murray *et al.*, (1988) demonstrated that the Galactose-binding proteins expressed on cell surfaces of *F. nucleatum* facilitated attachment of the pathogen to cell surfaces of the oral epithelial layer. Weiss *et al.*, (2000), reinforced these findings in their study and also demonstrated that the Galactose-binding protein resulted in coaggregation of *F. nucleatum* with *Porphyromonas gingivitis*, a pathogenic periodontal bacterium and Rosen *et al.*, (2003) were able to show that the Galactose-binding protein of *F. nucleatum* played an indispensable role in formation of biofilm. Yoneda *et al.*, (2011) reported that *F. nucleatum*, a strict and invasive anaerobe contributed to polymicrobial anaerobic infections, which arose due to interaction of Galactose-binding proteins present on the oral surfaces allowing coaggregation with several anaerobes. Hence, the discovery of a Galactose-binding protein in *F. necrophorum* suggests mechanisms for inter-bacterial aggregation, production of biofilm and adhesion to host cells and opens an exciting area of future research.

The inability to detect binding of the Galactose binding protein on *F. necrophorum* to glycans on agarose beads could have been due to 1) preferential binding to longer chain glycans, 2) the low density of glycans on the beads or 3) steric hindrance due to the size of the beads. Using molecular modelling and ligand docking, there was an obvious binding preference of the Galactose-binding protein; the disaccharides used bound more tightly than did the monosaccharides supporting the first explanation. Interestingly, both glucose and galactose were predicted to bind to the protein; this supports the reported activities of related Galactose-binding proteins, all of which had been identified as binding both galactose and glucose. There were two common areas of predicted glycan binding for the 4 glycans investigated (galactose, glucose, N-acetylglucosamine

and lacto-N-biose 1); galactose and glucose showed potential binding to 4 other areas of the protein. The disaccharides bound more strongly than did the monosaccharides but there was no difference in binding between N-acetyllactosamine (Gal β 1, 4 GlcNAc) and lacto-N-biose1 (Gal β 1, 3 Glc). This would indicate that neither the positional linkage (1, 3 versus 1, 4) nor the nature of the second sugar (GlcNAc versus Glc) was important for binding. This in turn would suggest potential for binding to the β -galactosyl residues carried on both glycoproteins (GlcNAc) and glycolipids (Glc). The SWISS-MODEL also revealed that the Galactose-binding protein contained a bound calcium ion; further studies should be undertaken to determine its role and importance.

Novel therapeutic interventions have been investigated recently using glycan analogues to prevent the interactions of bacteria via Galactose binding proteins. Anti-adhesive therapeutics which use lactose [Gal β 1-4 Glc] and D-galactose derivatives were effective in early preclinical trials, as they interrupted the interaction between *F. nucleatum* *Porphyromonas gingivalis* in the oral microbiome (Kawsar *et al.*, 2009). However, sugar derivatives are inhibitory only in the micromolar range, are expensive and have the potential to be metabolised *in vivo*; this has prompted investigations into mimetics that could have clinical utility, though much of the work involves adhesins binding α 1-4Gal rather than those binding to β -Gal, the principles are the same. Ohlsson *et al.*, (2005) investigated Gal α 1-4Gal (galabiose) derivatives as inhibitors of two galactose binding proteins; PapG class II adhesin of uropathogenic *E. coli* and of the P (N) and P (O) adhesins of *Streptococcus suis* strains. They determined that methoxyphenyl O-galabiosides were potent inhibitors of the PapG adhesion, whereas phenylurea derivatives and methoxymethylated galabiose inhibited the *S. suis* strains type P (N) adhesin with affinities of 30 and 50 nM, respectively. Bergmann *et al.*, (2016) developed inhibitors with chloroacetylated dendrimer cores and digalactosylated dendritic arms to the Galactose specific lectin LecA that mediates the formation of antibiotic resistant biofilms by *Pseudomonas aeruginosa*. In 2018, Huang, *et al.*, developed LecA inhibitors based on bivalent galactosides supported on polyproline peptide scaffolds. Haataja *et al.*, (2018) designed chemically modified glycodendrimers that inhibited the *adhesin* SadP, a galactosyl- α 1-4-Galactose binding protein, of *Streptococcus suis* at picomolar

concentrations. They chemically modified ligands and constructed multivalent dendrimers; using a phenylurea-modified galabiose-containing trisaccharide in a tetravalent dendrimeric scaffold, these inhibited binding at a low picomolar levels. Although these derivatives showed promise as therapeutic agents, care would need to be taken when using them in humans. There are a number of Galactose binding proteins in the human proteome, for example galactosyltransferases, galectin and C-type lectins, whose inhibition could be detrimental to the host and hence any agents delivered systemically would need to be bacteria specific; those delivered topically would provide less risk.

Chapter 6

6 LPS and lipid A biosynthesis

6.1 Introduction

Lipopolysaccharide (LPS) is the major component of the outer membrane of Gram-negative bacteria where it contributes to the structural integrity of the bacteria. LPS is a large molecule comprising of lipid A, a core oligosaccharide and the polysaccharide O-antigen. LPS also increases the negative charge of the cell membrane and helps stabilise the overall membrane structure. Lipopolysaccharide (LPS) is important for the growth and survival of Gram-negative bacteria and helps to anchor the outer membrane, protects from chemical attack and promotes cell adhesion to different surfaces (Emiola *et al.*, 2015; Christie, 2018; Cuny, 2009). It is a potent endotoxin, which is able to trigger the life-threatening condition: septic shock. The LPS layer forms the outer membrane that provides an effective barrier at the environmental interface, resisting antimicrobials and preventing harmful toxins and antibiotics, including those of clinical value from entering the cells. This impermeability is due mainly to the asymmetrical outer membrane, with the LPS molecules surrounding the outer leaflet and glycerophospholipids in the inner leaflet.

Kirchheiner (1940) first reported the presence of a toxic lipopolysaccharide (LPS) in extracts of *F. necrophorum* cells. In 1972, Sonnenwirth *et al.* reported endotoxins isolated from *Bacteroidaceae*, including clinical isolates of *F. necrophorum*. Garcia *et al.*, (1975) prepared endotoxic lipopolysaccharide from *F. necrophorum* and reported that on acid hydrolysis, hexosamines (7.0%), neutral and reducing sugars (50.5%), heptose (6.4%), 2-keto-3-deoxyoctonate (0.8%), lipid A (21.0%), and phosphorus (1.7%) were detected. The endotoxin produced both localised and generalised Shwartzman reactions and biphasic pyrogenic responses in animal models. A mouse LD₅₀ value of 584 µg/Kg was obtained for this endotoxin; a parallel test using *Escherichia coli* O111:B4 LPS (Difco) produced an LD₅₀ of 555 µg/Kg. The authors suggested that their results established that a classical and potent endotoxin was present in *F. necrophorum* providing support to their suggestion that cell wall-associated components contributed significantly to the pathogenicity of *F. necrophorum*.

Extracellular products such as lipopolysaccharide (LPS) endotoxins confer the pathogenicity of *Fusobacteria*. The LPS is released after lysis and is recognized by LPS-binding protein (LBP) circulating in the blood. This complex triggers the production of cytokines, which are responsible of inflammatory response, activation of complement pathways and the coagulation pathway. This mechanism is essential to overcome the infection, but severe systemic infections can induce excessive cytokine production harming the body. Massive Gram-negative infection can advance to high fever, breathing difficulties, tissue destruction, hypotension, disseminated intravascular coagulation (DIC), multisystem organ failure (MSOF), shock and death.

Though lipid A is a hydrophobic glycolipid with a conserved biosynthetic pathway, there are variations downstream of lipid A biosynthesis by way of enzyme modification and adaptation of lipid A species to particular functions, which increase bacterial fitness. Resistance to certain types of antibiotics are provided by these modifying enzymes, and this may alter the permeability of the outer membrane (Powers and Trent, 2018). These features highlight the importance of the study of LPS in the fields of bacteriology, immunology and drug discovery (Dong *et al.*, 2014; Emiola *et al.*, 2015; Christie, 2018). The outer membrane of Gram-negative bacteria, the most important feature distinguishing them from Gram-positive bacteria, provided a significant challenge to the discovery of antibacterial drugs because of its ability to prevent access of small molecules to the periplasmic space (Tomaras *et al.*, 2014).

Their amphipathic nature and strong tendency to aggregate by hydrophobic bonding or through cross-linking via ionic species, hindered earlier attempts to determine lipid A and lipopolysaccharide structures. Improved extraction methods and cleavage of the lipid component from the rest of the molecule by hydrolysis has resolved the detailed structures. Analyses have been made possible by modern mass spectrometric methods such as matrix-assisted laser desorption/ionisation (MALDI) and electrospray ionisation (Christie, 2018).

LPS is a complex molecule of about 30 kDa known to consist of three regions: lipid A anchor, core oligosaccharide, and O-antigen (see Figure 6.1). Lipid A, the endotoxin component includes six hydrophobic acyl chains located in the outer leaflet of the outer membrane of the bacteria, linked together by a glucosamine and phosphate head group (Emiola *et al.*, 2015). Lipid A is a unique and distinctive

phosphoglycolipid, with a highly conserved structure among species and considered essential for survival of Gram-negative bacteria.

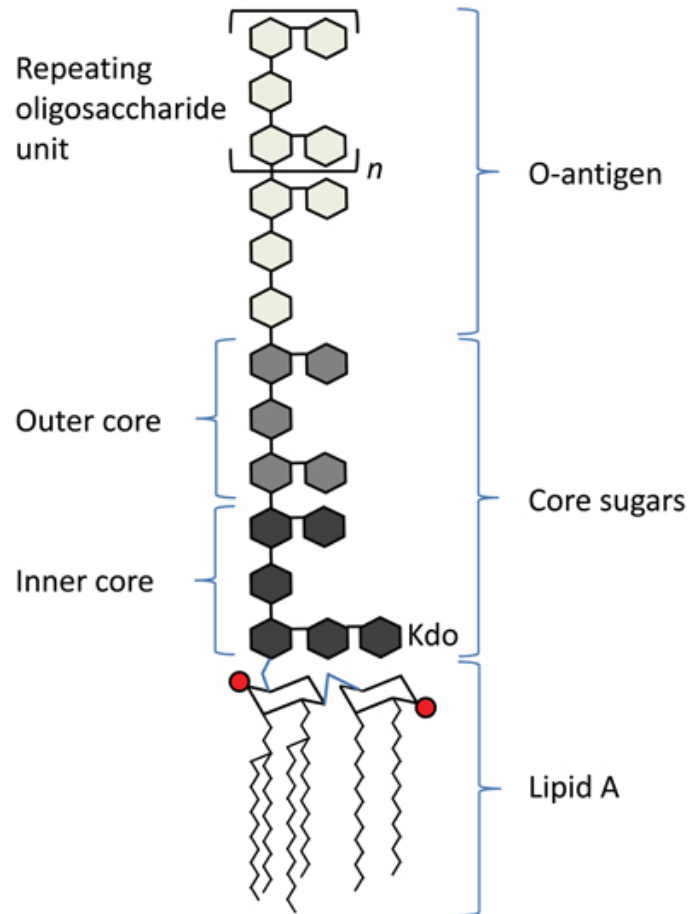


Figure 6.1 Schematic of the basic structure of lipopolysaccharide.

LPS consists of three regions: from the bottom, lipid A (chair structure indicates di-glucosamine head group, red circles indicate phosphate groups, squiggly lines indicate acyl chains), core sugars, and O-antigen, which consists of repeating units (denoted in brackets, with an “n”) of oligosaccharides (Maeshima and Fernandez, 2013).

The O-antigen that is bound to the core oligosaccharide is the most heterogeneous part of the LPS, consisting of many sugar unit repeats. This is the outer part of the LPS and the first target of the host immune system and is important in serological classification of bacteria strains (Atlas, 1997). The core part of the LPS is the hetero-oligosaccharide consisting of sugars, such as: 2-

keto-3-deoxyoctulosonate (KDO), L-glycerol-D-manno-heptose, D-galactose and D-glucose. This connects the O-antigen repeats with lipid A (Henderson, 2001). The lipid A moiety is of interest because it is highly conserved and is important for cell viability, thus making its biosynthetic pathway attractive for the targeting of new antibiotics (Emiola *et al.*, 2015). Studies in *E. coli* have shown involvement of a number of enzymes and genes in the biosynthesis of lipid A, many of which are shared by Gram-negative bacteria (Wang *et al.*, 2010).

Research into the biochemical structure and synthesis of LPS began in the 1960s, and the general outline of LPS synthesis and its assembly was completed in the early 1970s. Christian Raetz determined the biochemical pathway for lipid A synthesis; the enzymes in the pathway were discovered by groups led by Raetz, who identified the deacetylase enzyme, UDP-3-O(R-3-hydroxymyristol)-N-acetylglucosamine deacetylase, which is now known as LpxC. This is a cytosolic zinc-based enzyme that catalyses the first committed step in the synthesis of lipid A (Cuny, 2009; Zhang *et al.*, 2017). Although the whole biosynthetic pathway has been elucidated for *E. coli*, little research has been carried out on anaerobes such as *F. necrophorum*. Since the initial reports, there has been some debate on the composition of the LPS in *F. necrophorum*. Inoue *et al.*, (1985) stated that the organism had been shown to contain lipopolysaccharide, comprising Kdo (3-deoxy-D-manno-octulosonic acid), and heptose, as well as neutral and amino sugars including D-mannosamine. This work was supported in 1988 when Okahashi and co-workers demonstrated the major sugars of the *F. necrophorum* LPS were glucose and heptose. However, Garcia and co-workers (1999) suggested that LPS from *F. necrophorum* contained neither heptose nor Kdo.

The aims of this study were to:

1. identify the presence and expression of the genes of the lipid A pathway in different subspecies of *F. necrophorum* (subsp. *necrophorum*, and subsp. *funduliforme*).
2. utilise bioinformatics to understand the lipid A pathway in *F. necrophorum*.

6.2 Methods

DNA extraction, PCR, RNA extraction, cDNA synthesis, qRT-PCR and sequencing were performed as described in methods sections 2.2.2.4, 2.2.2.6 and 2.2.2.8.

6.2.1 Bacterial strains

The clinical strain of *F. necrophorum*, ARU 01, two reference strains JCM 3718 and JCM 3724 and clinical strains (from UCLH, London, UK) were used in this study. *S. aureus* was used as positive control. All the microorganisms were grown as detailed in the general method section 2.3.2.1 and 2.3.3.2 (see chapter 2).

6.2.2 Bioinformatics

The nucleotide sequences of the enzymes implicated in the biosynthetic pathways of *F. necrophorum* were obtained from the BioCyc database (<http://www.biocyc.org>) or from Uniprot (www.uniprot.org). Clustal Omega was used to identify highly conserved amino acids within and between strains.

Primers for the genes (in the lipid A pathway) were designed using 'Primer 3' and the sequences were confirmed by BLAST (The Basic Local Alignment Search Tool). The primers are shown in Table 2.6.

All primers were synthesized by MWG - Eurofins Genomics, Ebersberg, Germany.

6.2.3 PCR and Sequencing

These were carried out as described in the method section 2.6.2.

6.2.4 Sequence analysis

The sequences obtained were compared with sequences in the NCBI (www.ncbi.nlm.nih.gov/Blast.cgi) GenBank database using BLAST. CLUSTALW (www.ebi.ac.uk/Tools/msa/clustalw2/) was used to align the sequences from the different strains of *F. necrophorum*. DNA to protein translation was performed using ExPASy translate tool (<https://www.expasy.org/genomics>) to confirm any

changes of the primary amino acids structure due to nucleotide sequence differences. RaptorX server (<http://raptorx.uchicago.edu/>) was used to predict 3D structure of the enzyme of lipid A biosynthesis.

6.3 Results

6.3.1 LPS and lipid IVA pathway of *F. necrophorum*

The original work on the lipid IVA pathway was based on information on the lipid IVA pathway of *E. coli* (Fig. 6.2) and sequences available at BioCyc. There was no sequence information for the *lpxH* gene in *F. necrophorum* hence it was reported as absent. Preliminary work focussed on the *lpxA*, *lpxB*, *lpxC* and *lpxD* genes.

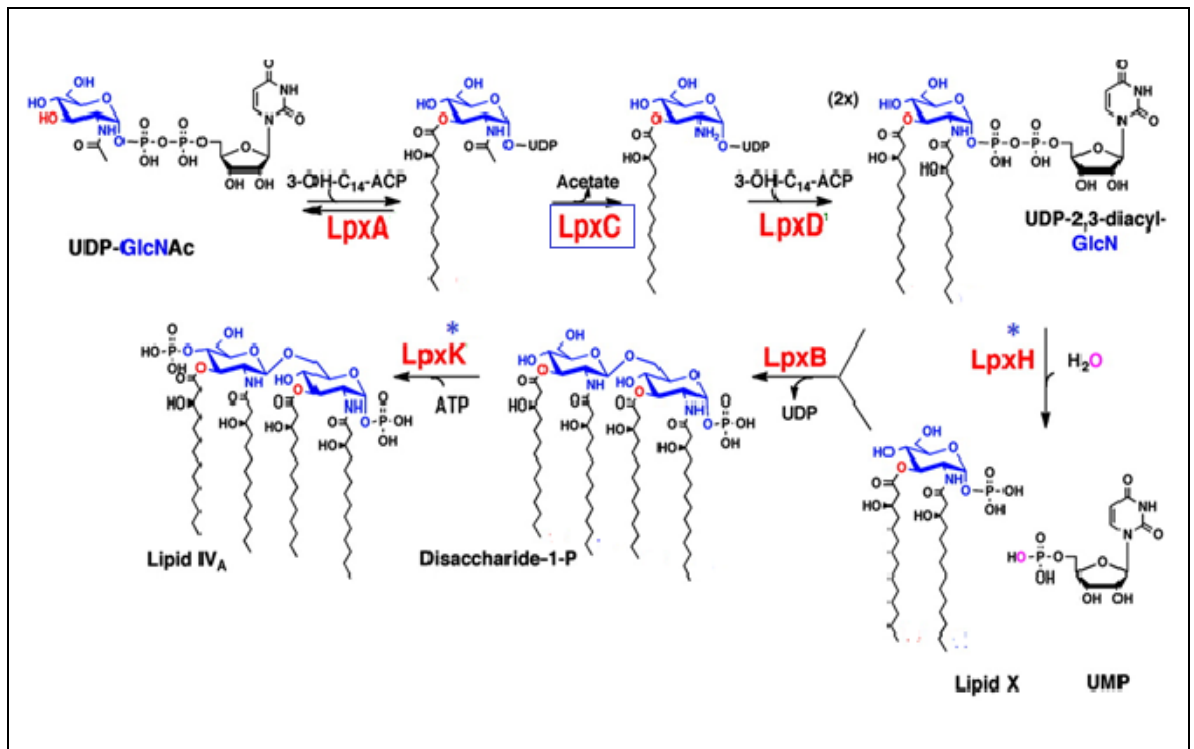


Figure 6.2 Biosynthetic pathway of lipid A in *E. coli*.

Each reaction is catalyzed by enzymes shown in red. The second reaction catalyzed by LpxC (deacetylation) is the committed step of lipid A biosynthesis representing an excellent target to develop new antibiotics. LpxH* is reported to be absent in lipid A pathway of *Fusobacterium necrophorum*.

PCR was performed using gene-specific primers designed from sequences available at BioCyc. The DNA from *F. necrophorum* isolates used in this study generated PCR products of the expected size (base pairs) for target sequences of all four genes implicated in the lipid A pathway: *lpxA*: UDP-N-acetylglucosamine-O-acyltransferase, *lpxC*: UDP-3-O-[hydroxymyristoyl]-N-acetylglucosamine deacetylase; *lpxD*: UDP-3-O-[3-hydroxymyristoyl] glucosamine -N- acetyltransferase and *lpxB*: lipid-A-disaccharide synthetase (Figures 6.3 and 6.4).

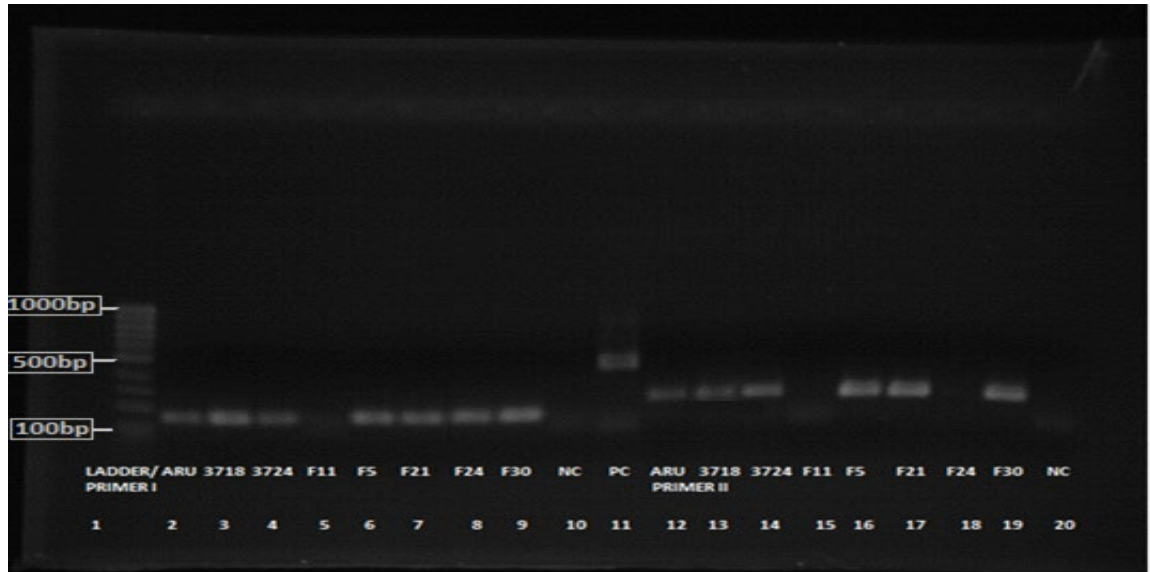


Figure 6.3 Analysis of amplicons of *F. necrophorum* using *lpxA* and *lpxC* primer sets run on 1% agarose gel.

DNA bands were observed in all *Fusobacteria* samples: ARU 01, JCM 3718, JCM 3724, F5, F21, F24 and F30 indicating successful amplification of the target genes implicated in the lipid IVA pathway. DNA ladder (Lane 1), Positive Control (PC) Lane 11) and Negative Controls (NC) lanes 10 and 20) are also shown on the gel image.

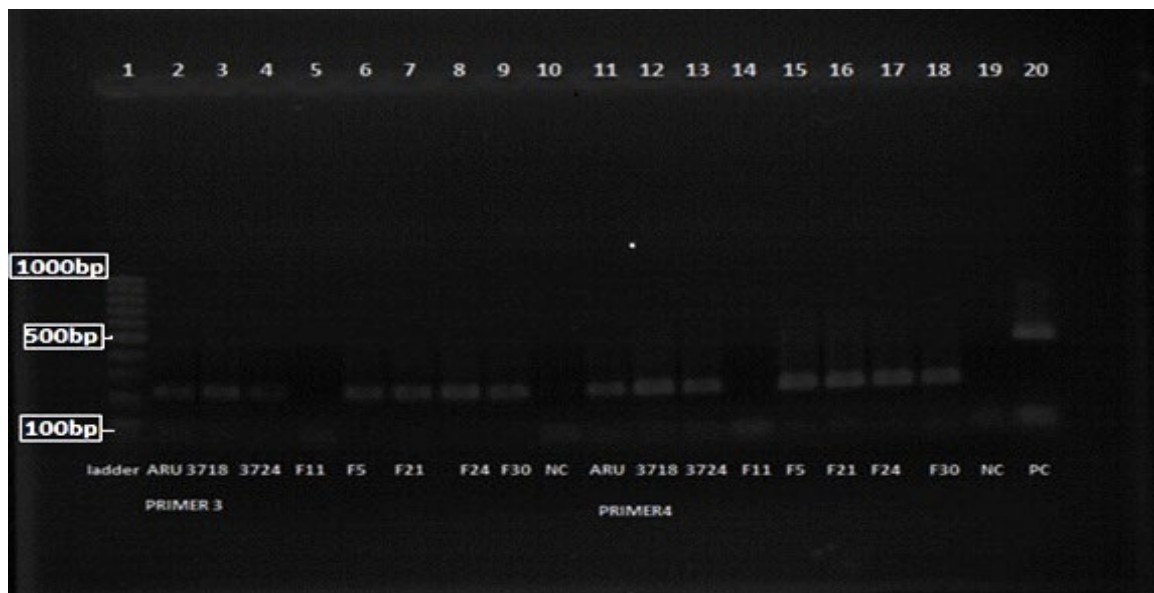


Figure 6.4 Analysis of amplicons of *F. necrophorum* with the *lpxD* and *lpxB* primers.

The sequences target for the *lpxD* and *lpxB* genes implicated in the lipid IV A pathway were amplified in all the following samples ARU 01, JCM 3718, JCM 3724, F5, F21, F24 and F30. DNA ladder (Lane 1), Positive Control (PC) and Negative Control (NC) are shown on the gel image.

The amplicons were sequenced and ClustalW (<https://www.ebi.ac.uk/Tools/msa/clustalw2/>) was used to compare the sequences generated, by different isolates, for each of the enzymes involved in the lipid A pathway. The multiple alignment shows greater similarity between JCM 3724 (less virulent subspecies, *funduliforme*) and the clinical strain ARU 01, compared with JCM 3718 (more virulent subspecies, *necrophorum*), especially for *lpxC*. The portions shown in red (Figures 6.5, 6.6 and 6.7) show the overall identity among target sequences. Mismatches at the beginning and end region of the target sequences may be due to errors during sequencing; in these regions the chromatogram showed ambiguity. Analysis of the impact of single base changes in *lpxA*, *lpxB*, *lpxC* and *lpxD* on the encoded sequences were carried out.



Figure 6.5 Multiple Alignment of the target sequence of *lpxA* of lipid A pathway for all samples.

```

F24 16622653.seq -----TGT-AGTATTTCGAGAAATTTGTAGAAGTCGGAAGAGAATGTATTTTCAAT 50
F5 16622776.seq -----GT-AGTATTTCGAGAA--TTTGTAGAAGTCGGAAGAGAATGTATTTTCAAT 48
F21 16622239.seq -----TATTTCGAGAA--TTTGTGA--AAGTCGGAAGAGAATGTATTTTCA-T 42
F30 16621891.seq -TGTATTCATGT-AGTATTTCGAGAAATTTGTAGAAGTCGGAAGAGAATGTATTTTCAAT 58
ARU 16618855.seq -----CATGT-AGTATTTCGAGAA--TTTGTAGAAGTCGGAAGAGAATGTATTTTCAAT 51
3724 16621882.seq TCCTGTTTCATGT-AGTATTTCGAGA--TTTGTGA--AAGTCGGAAGAGA-TGTATTTTCAAT 55
3718 16627663.seq -----CATGTTAGTATTTCGAGAA--TTTGTAAAAGTCGGGAAAGGATGTATTTTCAAT 52
***** * * * *

F24 16622653.seq CGGGAGCGGTCATAGGCTCTGACGGATTCCGGTTTTGTCAAAGTACAGGGAAATAATATGA 110
F5 16622776.seq CGGGAGCGGTCATAGGCTCTGACGGATTCCGGTTTTGTCAAAGTACAGGGAAATAATATGA 108
F21 16622239.seq CGGGAGCGGTCATAGGCTCTGACGGATTCCGGTTTTGTCAAAGTACAGGGAAATAATATGA 102
F30 16621891.seq CGGGAGCGGTCATAGGCTCTGACGGATTCCGGTTTTGTCAAAGTACAGGGAAATAATATGA 118
ARU 16618855.seq CGGGAGCGGTCATAGGCTCTGACGGATTCCGGTTTTGTCAAAGTACAGGGAAATAATATGA 111
3724 16621882.seq CGGGAGCGGTCATAGGCTCTGACGGATTCCGGTTTTGTCAAAGTACAGGGAAATAATATGA 115
3718 16627663.seq CGGGAGCGGTCATAGGCTCTGATGGATTTGGCTTTGTCAAAGTACAGGGAAATAATATGA 112
***** * * * *

F24 16622653.seq AAATTGAGCAAATCGGTTCTGTGGTGATAGAAGATTTTGTAGAAATCGGGCAAATACGA 170
F5 16622776.seq AAATTGAGCAAATCGGTTCTGTGGTGATAGAAGATTTTGTAGAAATCGGGCAAATACGA 168
F21 16622239.seq AAATTGAGCAAATCGGTTCTGTGGTGATAGAAGATTTTGTAGAAATCGGGCAAATACGA 162
F30 16621891.seq AAATTGAGCAAATCGGTTCTGTGGTGATAGAAGATTTTGTAGAAATCGGGCAAATACGA 178
ARU 16618855.seq AAATTGAGCAAATCGGTTCTGTGGTGATAGAAGATTTTGTAGAAATCGGGCAAATACGA 171
3724 16621882.seq AAATTGAGCAAATCGGTTCTGTGGTGATAGAAGATTTTGTAGAAATCGGGCAAATACGA 175
3718 16627663.seq AAATTGAGCAAATCGGTTCTGTGGTGATAGAAGATTTTGTAGAAATCGGGCAAATACGA 172
***** * * * *

F24 16622653.seq CTGTAAAA----- 178
F5 16622776.seq CTGTA----- 173
F21 16622239.seq CTGTAAAACTATTC--- 177
F30 16621891.seq CTGTAATTTTCTTTAT 196
ARU 16618855.seq CTGTA----- 176
3724 16621882.seq CTGTAAA----- 182
3718 16627663.seq CTGAA----- 177
***

```

Figure 6.6 Multiple Alignment of the target sequence of *lpxD* of lipid A pathway for all samples.



Figure 6.7 Multiple Alignment of the target sequence of *lpxB* of lipid A pathway for all samples.

It appeared from the analysis of the amplicons from the *lpxC* gene that there were deleted areas of the sequence in JCM 3718 compared to the other sequences generated (Figure 6.8). Interestingly, 5 out of 7 of these deletions were in areas where there was nucleotide repetition; *AAAGACCCGA*, *CTGGG*, *AAAGC*, *GAACAT* and *TTTA*. Translation of the amplicons showed that 9 amino acids were changed after which the sequence was restored (Figure 6.9). However, on analysis of the *LpxC* these differences were not located in regions involved in catalytic activity and hence would probably not affect the enzyme activity (Figure 6.10).

```

3724 16622758.seq  -----TTGTAAGAACCAGATATATCTTTCTCTGGGTGATAAACATATCATAGCTCTA 52
F5    16618549.seq  -----TTGTAAGAACCAGATATATCTTTCTCTGGGTGATAAACATATCATAGCTCTA 52
F30   16618510.seq  -----TATTGTAAGAACCAGATATATCTTTCTCTGGGTGATAAACATATCATAGCTCTA 54
F21   16618402.seq  -----TTATTGTAAGAACCAGATATATCTTTCTCTGGGTGATAAACATATCATAGCTCTA 55
F24   16621879.seq  -----TTATTGTAAGAACCAGATATATCTTTCTCTGGGTGATAAACATATCATAGCTCTA 55
ARU   16622194.seq  CCAGTATATTGTAAGAACCAGATATATCTTTCTCTGGGTGATAAACATATCATAGCTCTA 60
3718  16627843.seq  -----TTATT-----CATAACTTCAT-----TATTAGA---ATCACTCGTTTT 35
                * * * * * * * * * * * * * * * * * * * * * * * * * * * * * *

3724 16622758.seq  CCCTATGACGGAAAAAAGCTTACTTACAGTATTCGATTTGAACATAGTTTTTTAAAAATCG 112
F5    16618549.seq  CCCTATGACGGAAAAAAGCTTACTTACAGTATTCGATTTGAACATAGTTTTTTAAAAATCG 112
F30   16618510.seq  CCCTATGACGGAAAAAAGCTTACTTACAGTATTCGATTTGAACATAGTTTTTTAAAAATCG 114
F21   16618402.seq  CCCTATGACGGAAAAAAGCTTACTTACAGTATTCGATTTGAACATAGTTTTTTAAAAATCG 115
F24   16621879.seq  CCCTATGACGGAAAAAAGCTTACTTACAGTATTCGATTTGAACATAGTTTTTTAAAAATCG 115
ARU   16622194.seq  CCCTATGACGGAAAAAAGCTTACTTACAGTATTCGATTTGAACATAGTTTTTTAAAAATCG 120
3718  16627843.seq  TTCTATTA-GGATA-----TTGTTTCTGCAAGAACCTT-----CGGCTT---AAATCG 80
                * * * * * * * * * * * * * * * * * * * * * * * * * * * * * *

3724 16622758.seq  CAAATGGCGGAGTTTGTATTGGATTATGATACTTACCGAAAGGAAATTGCTCCTGCAAGA 172
F5    16618549.seq  CAAATGGCGGAGTTTGTATTGGATTATGATACTTACCGAAAGGAAATTGCTCCTGCAAGA 172
F30   16618510.seq  CAAATGGCGGAGTTTGTATTGGATTATGATACTTACCGAAAGGAAATTGCTCCTGCAAGA 174
F21   16618402.seq  CAAATGGCGGAGTTTGTATTGGATTATGATACTTACCGAAAGGAAATTGCTCCTGCAAGA 175
F24   16621879.seq  CAAATGGCGGAGTTTGTATTGGATTATGATACTTACCGAAAGGAAATTGCTCCTGCAAGA 175
ARU   16622194.seq  CAAATGGCGGAGTTTGTATTGGATTATGATACTTACCGAAAGGAAATTGCTCCTGCAAGA 180
3718  16627843.seq  CAAATGGCAGAGTTTGTATTGGATTATGATACTTACCGAAAGGAAATTGCTCCTGCAAGA 140
                *****

3724 16622758.seq  ACTTTCGGCTTA- 184
F5    16618549.seq  ACTTTCGGCTTA- 184
F30   16618510.seq  ACTTTCGGCTTA- 186
F21   16618402.seq  ACTTTCGGCTTA- 187
F24   16621879.seq  ACTTTCGGCTTA- 187
ARU   16622194.seq  ACTTTCGGCTTAA 193
3718  16627843.seq  ACTTTCGGCTTA- 152
                *****

```

Figure 6.8 Multiple Alignment of the target sequence of *lpxC* of lipid A pathway for all samples.

```

ARU      YSIRFEHSFLKSQ MAEFVLDYD TYRKEIAPARTFGL

3718     DIVSCKNFR LKSQ MAEFVLDYD TYRKEIAPARTFGL

3724     YSIRFEHSFLKSQ MAEFVLDYD TYRKEIAPARTFGL

F5       YSIRFEHSFLKSQ MAEFVLDYD TYRKEIAPARTFGL

F21     YSIRFEHSFLKSQ MAEFVLDYD TYRKEIAPARTFGL

F24     YSIRFEHSFLKSQ MAEFVLDYD TYRKEIAPARTFGL

F30     YSIRFEHSFLKSQ MAEFVLDYD TYRKEIAPARTFGL

```

Figure 6.9 Impact of nucleotide deletions in *lpxC* on derived protein sequence.

A pairwise alignment of the LpxC protein showed that the amplified area contained none of the enzyme active sites.

LpxA

ARU EKKVYRIIFRRGLPLKEALAEAEQ

3718 LKKVYRIIFRKGLPLKEALAKAEQ

3724 FKKVYRIIFRRGLPLKEALAEAEQ

F5 FKKVYRIIFRRGLPLKEALAEAEQ

F21 LKKVYRIIFRRGLPLKEALAEAEQ

F24 FKKVYRIIFRRGLPLKEALAEAEQ

F30 FKKVYRIIFRRGLPLKEALAEAEQ

Figure 6.11 Protein sequence analysis of the amino acid for the enzyme LpxA.

LpxD

ARU GAVIGSDGFGFVKVQGNN **Met**KIEQIGSVVIEDFVEIGANT
TV

3718 GAVIGSDGFGFVKVQGNN **Met**KIEQIGSVVIEDFVEIGANT
TE

3724 GAVIGSDGFGFVKVQGNN **Met**KIEQIGSVVIEDFVEIGANT
TV

F5 GAVIGSDGFGFVKVQGNN **Met**KIEQIGSVVIEDFVEIGANT
TV

F21 GAVIGSDGFGFVKVQGNN **Met**KIEQIGSVVIEDFVEIGANT
TV

F24 GAVIGSDGFGFVKVQGNN **Met**KIEQIGSVVIEDFVEIGANT
TV

F30 GAVIGSDGFGFVKVQGNN **Met**KIEQIGSVVIEDFVEIGANT
TV

Figure 6.12 Protein sequence analysis of the amino acid for the enzyme LpxD.

LpxB	
ARU	S L E E E V F P E L I Q K D C N V V N I E N S L Q E I E N K P E L
3718	S L E E E V F P E L I Q K D C N V V N I E N S L Q E I E N K P E L
3724	S L E E E V F P E L I Q K D C N V V N I E N S L Q E I E N K P E L
F5	Q L R E E V F P E L I Q K D C N V V N I E N S L Q E I E N K P E L
F21	S L E E E V F P E L I Q K D C N V V N I E N S L Q E I E N K P E L
F24	S L E E E V F P E L I Q K D C N V V N I E N S L Q E I E N K P E L
F30	S L E E E V F P E L I Q K D C N V V N I E N S L Q E I E N K P E L

Figure 6.13 Protein sequence analysis of the amino acid for the enzyme LpxB.

The impact of the nucleotide substitutions in the amplicons from *lpxA*, *lpxB* and *lpxD* was determined by translating each DNA sequence. The translation (<http://web.expasy.org/translate/>) of the amplified sequences detected a single amino acid change in the LpxA protein (Figure 6.11); 2 alternative sequences were seen: LKKVYR in JCM 3718, and clinical isolate F21 and FKKVYR in the other isolates (Figure 6.11). There is no significant difference in the amino acids leucine and phenylalanine; both are non-polar and hydrophobic, hence there is unlikely to be any impact on protein function. A pairwise alignment of the genes in *E. coli* and *F. necrophorum* (Figure 6.14) demonstrated that the active sites were found outside the amplified area.

6.3.2 Identification of the *lpxI* gene in *Fusobacterium necrophorum*

A bioinformatics analysis using BLASTN and BLASTP revealed no homology between the *lpxH* gene (or encoded protein) from a range of organisms (including *Haemophilus influenzae*, *Escherichia coli*, *Pseudomonas aeruginosa* and *Enterobacter cloacae*) with any genes / proteins in *Fusobacteria* species (data not shown). However, an alternative gene must exist as these organisms produce the metabolic end-product, lipid A. Based on the fact that many Gram-negative organisms, including all α -proteobacteria, lack LpxH even though they produce lipid A Metzger & Raetz (2010), put forward an alternative pathway. They identified a novel *lpxI* gene in *Caulobacter crescentus*, this was a conserved structural gene located between *lpxA* and *lpxB*; the site where the *lpxH* gene is found in other organisms. *LpxI* had no homology with *lpxH* at either the DNA or protein sequence level but the authors synthesised a recombinant form of the protein that demonstrated the same biological/enzymatic function, converting UDP-2,3-bis[O-(3R)-3-hydroxymyristoyl]- α -D-glucosamine to 2,3-bis[(3R)-3-hydroxymyristoyl]- α -D-glucosaminyl 1-phosphate. This led to the conclusion that this *lpxI* gene was a functional replacement for the *lpxH* gene.

Therefore, in this current study the operon containing *lpx A*, *B* and *C* in the *F. necrophorum* (ATCC 51357) genome was accessed using BioCyc and analysed for the possible presence of a *lpxI* homolog. The encoded protein sequences of an unannotated gene (HMPREF1049_1173; G11D6-1165 [Fnec1095747Cyc]) that lay between the *lpxA* and *B* genes was analysed by multiple sequence alignment with the sequences identified as LpxI by Metzger *et al.*, (2010). Only two wild-type protein sequences for LpxI were available in the Uniprot database, one from *Rhizobium galegae* and one from *Caulobacter crescentus* (strain NA1000/ CB15N), these two protein sequences were used in a multiple sequence alignment with the candidate LpxI protein (HMPREF1049_1173) from *F. necrophorum*. Although the overall similarity between these three proteins was low (28-42 %), it is clear from Figure 6.15 that all the key amino acids identified in LpxI by Metzger *et al.*, (2010) as important in the functioning of the enzyme (where they were believed to play a role in substrate binding, catalysis and dimerization) were also present in the *F. necrophorum* candidate protein.

```

F.necrophorum   NGIRVLSQNYLLSSCMVEEKCYTEKIPKEEDDRSIQLGIEAAKILTRLDIGQTVIVKEEA
Rhizobium       MGCEVLGAHDIVPGLLAKTGPIGANTPSDDDDRRDIDSASEAAKRLGELDIGQGAVSVGGR
Caulobacter     EGFEIEGAHEVMGEMTLPRGRLGKVSPEPEHMADIDKALDVAREIGRLDIGOGAVVCEGL
                * .: . . : :                * :. .*: . .*: : .***** .:

F.necrophorum   VVALEGIEGTDQAILRAGELA-----GKNCCIIVKMARPKQDMRVDIPTVG VETIRRA
Rhizobium       VVALEGVEGTDRLMLERV TALRAEGR-ISARRKGVLVKLC KPQQDMRADLPTIGPSTVENV
Caulobacter     VLAVEAQEGTDAMLR RVADLPEAIRGRAERRLGV LAKAPKPIQETRV D LPTIGVATI HRA
                *:*:* . **** * : * . *                : : : . * : * : .:*:* * : :...

```

Figure 6.15 Multiple sequence alignment of the LpxI proteins of *F. necrophorum*, *Caulobacter crescentus* and *Rhizobium galegae*.

The residues highlighted by coloured boxes are absolutely conserved polar residues within the LpxI sequence. Those residues thought to be involved in substrate binding and/or catalysis are coloured in red and those thought to be involved in dimerization are shown in green.

In a multiple sequence alignment of candidate LpxI homologues from all available *Fusobacteria* species, the residues highlighted in Figure 6.16 were also found to be conserved; the sequence identity between the homologues varied between 53 and 97 % (results not shown).

The 3D structure of the candidate LpxI protein was predicted using Swiss-Model (<https://swissmodel.expasy.org/>) using 4ggm (www.pdb.org), the known LpxI protein from *C. crescentus*, whose sequence identity with the *Fusobacterium* species was 28.4 %, as template. This template sequence also contained a bound ligand LPX (also termed LP5), derived from *E. coli* during preparation of the recombinant protein; LP5 is a lipid A precursor. The resultant model generated was rated as poor based on a GMQE score of 0.68 and a QMEAN4 of - 6.63 (<https://swissmodel.expasy.org/docs/help>). Thus, to achieve a better model Raptor X, which utilises a different algorithm was used (Källberg *et al.*, 2012). The models generated were subjected to structural alignment using the Dali server (Holm and Rosenstrom, 2010). The results had very high structural homology and the key conserved amino acids (see Figure 6.16) all lay in areas where there was no conflict in the predicted structures.

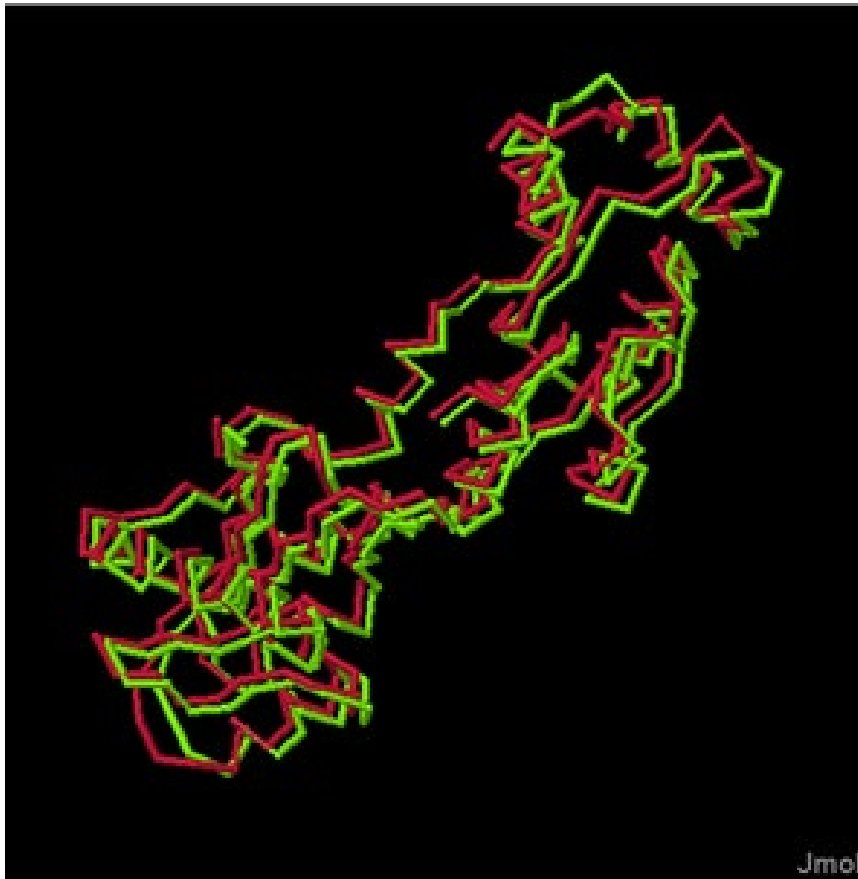


Figure 6.16 Structural alignment of models of LpxI from *F. necrophorum* generated using Swiss-Model (green) and RaptorX (red) using the Dali server.

The “Select neighbours” function of Dali was used to find any potential structural homologues of the *F. necrophorum* candidate LpxI protein in the PDB; retrieved structures with the highest Z-scores (Holm and Rosenström, 2010). ‘Significant similarities’ have a Z-score above 2; they usually correspond to similar folds. ‘Strong matches’ have sequence identity above 20% or a Z-score above a cut-off that is empirically set to $n/10 - 4$, where n is the number of residues in the query structure; in this case the value would be 23. Each neighbour has links to a pairwise structural alignment with the query structure, to pre-computed structural neighbours in the Dali Database, and to the PDB format coordinate file where the neighbour is superimposed onto the query structure. The three top “hits” from this analysis that were “Strong matches” with Z-scores of 39.8 (rmsd 0.6), 26.0 (rmsd 5.7) and 25.7 (rmsd 5.6) (Table 6.1) were 4ggm, 4j6e and 4ggi (now re-submitted as 4j6e) respectively: all three structures correspond to LpxI, UDP-2,3-diacylglucosamine pyrophosphatase, from *Caulobacter vibrioides* (previously known as *Caulobacter crescentus* str. CB15) whose structure was first reported

by Metzler *et al.*, (2012). The results show that a higher Z score and much lower RMSD was obtained when comparing the *Fusobacterium* structure to 4ggm than to the 4j6e structure (Table 6.1).

Table 6.1 Output of the “Select neighbours” function of the Dali server

No:	Chain	Z	rmsd	lali	nres	%id	PDB	Description
<input type="checkbox"/>	1: 4ggm-X	39.8	0.6	265	277	28	PDB	MOLECULE: UDP-2,3-DIACYLGLUCOSAMINE PYROPHOSPHATASE LPXI;
<input type="checkbox"/>	2: 4j6e-A	26.0	5.7	172	273	26	PDB	MOLECULE: UDP-2,3-DIACYLGLUCOSAMINE PYROPHOSPHATASE LPXI;
<input type="checkbox"/>	3: 4ggi-A	25.7	5.6	175	273	26	PDB	MOLECULE: UDP-2,3-DIACYLGLUCOSAMINE PYROPHOSPHATASE LPXI;
<input type="checkbox"/>	4: 2b1g-A	13.8	10.4	141	590	19	PDB	MOLECULE: BIFUNCTIONAL PURINE BIOSYNTHESIS PROTEIN PURH;
<input type="checkbox"/>	5: 2b1i-A	13.8	14.7	163	590	15	PDB	MOLECULE: BIFUNCTIONAL PURINE BIOSYNTHESIS PROTEIN PURH;
<input type="checkbox"/>	6: 2b1g-D	13.8	14.9	161	590	14	PDB	MOLECULE: BIFUNCTIONAL PURINE BIOSYNTHESIS PROTEIN PURH;
<input type="checkbox"/>	7: 1m9n-A	13.7	18.0	168	589	15	PDB	MOLECULE: AICAR TRANSFORMYLASE-IMP CYCLOHYDROLASE;
<input type="checkbox"/>	8: 1thz-B	13.7	16.2	164	590	16	PDB	MOLECULE: BIFUNCTIONAL PURINE BIOSYNTHESIS PROTEIN PURH;
<input type="checkbox"/>	9: 2b1g-C	13.7	14.9	153	590	15	PDB	MOLECULE: BIFUNCTIONAL PURINE BIOSYNTHESIS PROTEIN PURH;

The related models are sorted by Z-score. 4j6e and 4ggi are now recognised to represent the same protein; now named 4j6e.

Visualisation of the 4ggm and 4j6e structures showed that these molecules, though differing only by 1 key catalytic amino acid (D225), differ very significantly in their crystal structure presumably as a consequence of a conformational change when the ligands bound; 4ggm is reported to have spontaneously co-crystallised with lipid X (LP5) a lipid A precursor whereas 4j6e is the structure of LPXI D225A mutant with the bound nucleotide sugar substrate, UDP-2,3-diacylglucosamine. Metzger *et al.*, (2012) described that “The domains of the CcLpxl-D225A (4j6e) - substrate complex swing open on forming the CcLpxl-product complex”, however, the authors also acknowledged that they could not exclude the fact that the conformational changes were artefacts of crystal packing.

A structural alignment of the three structures: 4ggm, 4je6 and the candidate Lpxl from *F. necrophorum* is shown in Figure 6.17. 4ggmX is shown in red (with the ligand LP5 bound) and 4j6e is shown in grey (with UDP-2,3, -diacylglucosamine bound at the potential interface of the dimeric active structure) and the putative Lpxl protein from *Fusobacterium* is shown in green. It is clear that there is a high degree of structural homology between the *Fusobacterium* Lpxl candidate protein and 4ggm (Lpxl from *C. crescentus*) particularly surrounding the substrate-binding sites.

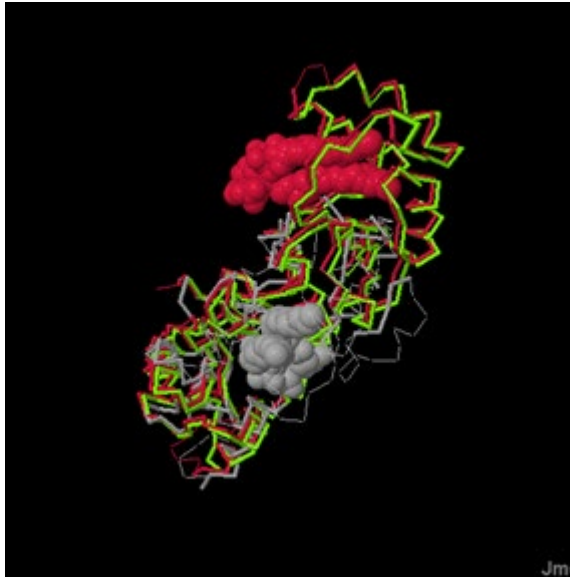


Figure 6.18: Structural alignment of the *F. necrophorum* LpxI with models of the LpxI from *Caulobacter crescentus* str. CB15 (previously *Caulobacter vibrioides*).

4ggm (*Caulobacter crescentus*) is shown in red with the bound ligand, LP5, shown as red spheres; 4j6e (*Caulobacter crescentus*) is shown in grey with UDP-2, 3, -diacetylglucosamine shown as grey spheres at the potential interface of the dimeric active structure. The candidate LpxI protein from *Fusobacteria* is shown in green. All proteins are shown as monomers.

Table 6.2 (A and B) illustrates the amino acid residues of *C. crescentus* predicted by Poseview and Raptor X to be important in ligand binding. The Poseview prediction (<http://www.rcsb.org/structure/4GGM>) showed the acyl chains of lipid 5 (part of the substrate for LpxI) interacting with F71, V75, V111 on one side of the binding site, and I51, P78, L107, L108 on the other side. Raptor X predicted additional amino acids binding the acyl groups but, in both cases, these interacting amino acids were hydrophobic and aliphatic.

All amino acids predicted by Poseview to be involved in binding of LP5 in *C. crescentus* were also predicted by RaptorX. Of these 9 amino acids, 7 had been reported in the Metzger *et al.*, (2012) paper as being highly conserved. Six of these 9 amino acids were also predicted by RaptorX to be involved in LP5 binding in *F. necrophorum*; at V111, *F. necrophorum* has M110, a change from polar neutral to hydrophobic aliphatic; at F54 there is a change to L55, both are hydrophobic aliphatic amino acids. RaptorX predicted binding at D104 for *C. crescentus*; in *F. necrophorum* where there is a change to N103, no binding was predicted. Both amino acids are polar and hydrophilic; D is negatively charged

whereas N has no charge. Of the 19 amino acids identified by Raptor for *C. crescentus*, 10 were completely conserved in *F. necrophorum*, 6 were partially conserved and 3 resulted in changes in properties.

In the case of UDG binding, of the 12 amino acids identified by Poseview, 2 (P78 and D88) were not identified by RaptorX. For *F. necrophorum*, of the 10 identified by both programs, 8 were also completely conserved between the two bacteria; the other 2 were strongly conserved. A comparison of the binding of UDG as predicted by Raptor X showed of 35 amino acids involved 20 were completely conserved, of the remaining 15, 9 were strongly conserved, 4 were not conserved and one (D104) was identified in *C. crescentus* whilst another (F50) was only identified in *F. necrophorum*.

The results obtained from both programs strongly supported the hypothesis that the candidate protein in *F. necrophorum* was indeed LpxI.

Table 6.2 Amino acids implicated by Raptor X in substrate binding

A-Binding of LP5

Raptor X prediction of amino acids involved in binding		Poseview prediction	Amino acid characteristics
<i>Fusobacterium</i>	<i>Caulobacter crescentus</i>	<i>Caulobacter crescentus</i>	
F50	-		Hydrophobic no charge
H51*	G50		Basic charged to Hydrophobic no charge
I52***	I51	I51	Hydrophobic aliphatic
G53***	G52		Hydrophobic no charge
H54*	E53		Basic charged to acidic charged
L55**	F54	F54	Hydrophobic aliphatic
I58***	I57	I57	Hydrophobic aliphatic
L72**	F71	F71	Hydrophobic aliphatic
L73**	A72		Hydrophobic aliphatic
G74***	G73		Hydrophobic no charge
V76***	V75	V75	Hydrophobic aliphatic
E77*	S76		Charged acidic to polar neutral
K78**	R77		Basic charged
L85***	L83		Hydrophobic aliphatic
L98***	L96		Hydrophobic aliphatic
-(N103)	D104	D104	Hydrophilic polar negative to uncharged
L106***	L107	L107	Hydrophobic aliphatic
L107**	L108	L108	Hydrophobic aliphatic
M110**	V111	V111	Polar neutral to hydrophobic aliphatic
F114***	F115		Hydrophobic

B-Binding of UDG

Raptor X prediction of amino acids involved in binding		Poseview prediction	Amino acid characteristics
<i>Fusobacterium</i>	<i>Caulobacter crescentus</i>	<i>Caulobacter crescentus</i>	
F50	-(V49)		Hydrophobic no charge
H51*	G50		Basic charged to Hydrophobic no charge
I52***	I51	I51	Hydrophobic aliphatic
G53***	G52		Hydrophobic no charge
H54*	E53		Basic charged to acidic charged
L55**	F54		Hydrophobic aliphatic
I58***	I57		Hydrophobic aliphatic
L72**	F71	F71	Hydrophobic aliphatic
L73**	A72		Hydrophobic aliphatic
G74***	G73		Hydrophobic no charge
V76***	V75	V75	Hydrophobic aliphatic
E77*	S76		Charged acidic to polar neutral
K78**	R77		Basic charged
-(S79)	-(P78)	P78	Non-polar; Hydrophobic to polar hydrophilic
L85***	L83		Hydrophobic aliphatic
-(D87)	-(D88)	D88	Negatively charged, polar, hydrophilic
L98***	L96		Hydrophobic aliphatic
-(N103)	D104		Hydrophilic negative
L106***	L107	L107	Hydrophobic aliphatic
L107**	L108	L108	Hydrophobic aliphatic
M110**	V111	V111	Polar neutral to hydrophobic aliphatic
F114***	F115		Hydrophobic
Q168***	Q169 #		Polar neutral
T186***	T187	T187	Polar neutral
D187***	D188#		Charged acidic
K205***	K214 #	K214	Basic charged
D216***	D225 #		Charged acidic

I217**	L226		Hydrophobic aliphatic
P218***	P227		Hydrophobic no charge
T219***	T228	T228	Polar neutral
V220**	I229		Hydrophobic aliphatic
G221***	G230		Hydrophobic no charge
V222***	V231		Hydrophobic aliphatic
E223*	A232		Charged acidic to hydrophobic aliphatic
T224***	T233	T233	Polar neutral
L246**	V255		Hydrophobic aliphatic

Key red= conserved in Metzger *et al.*, (2012), *** conserved, ** similar properties, * dissimilar properties; - indicates no amino acid highlighted at this position by RaptorX. # active site amino acids. Poseview was developed by Center for Bioinformatics Hamburg. LP5 =R - (2R,3S,4R,5R,6R)-3-Hydroxy-2-(hydroxymethyl)-5- (R)-3-hydroxytetradecanamido)-6-(phosphonoxy) tetrahydro-2H-pyran-4-yl) 3-hydroxytetradecanoate. UDG= (2R,3R,4R,5S,6R)-2-[[[S)-[[[2R,3S,4R,5R)-5-(2,4-dioxo-3,4-dihydropyrimidin-1(2H)-yl)-3,4-dihydroxytetrahydrofuran-2-yl]methoxy](hydroxy)phosphoryl]oxy](hydroxy)phosphoryl]oxy]-5-hydroxy-6-(hydroxymethyl)-3-[[[3R)-3-hydroxytetradecanoyl]amino]tetrahydro-2H-pyran-4-yl (3R)-3-hydroxytetradecanoate.

The table shows a comparison of the amino acids predicted to be involved in binding LPS and UDG substrates, and the impact of changes/differences.

Although experimental biochemical work was not performed, due to issues of availability of substrates and equipment required, the work presented and the published research showing that *Fusobacteria* do produce lipid A strongly support the hypothesis that LpxI acts as a replacement of LpxH in this organism.

6.4 Discussion

This study was undertaken to elucidate the lipid A pathway in the two subspecies of *F. necrophorum*. The presence of *lpxA*, *B*, *C* and *D* amplicons implies that all isolates tested had the genes encoding the first four enzymes of the lipid A pathway. In the multiple alignment of the target sequences, greater similarity was seen between JCM 3724 (subsp. *funduliforme*) and the clinical strains than between JCM 3718 (subsp. *necrophorum*) and the clinical strains. This supports the fact that the subsp. *funduliforme* is involved in human infection rather than subsp. *necrophorum*, which is more common as pathogen in animals (Riordan, 2007).

The pathogenic mechanism of *F. necrophorum* is complex and not well defined; it is unclear why *F. necrophorum* subsp. *necrophorum* is more virulent than the subsp. *funduliforme*. Among the several toxins expressed by these organisms, leukotoxin, endotoxin and lipid A are considered as major virulence factors. Recent studies have identified additional enzymes responsible for the modification of lipid A, which are closely related to the virulence. Two of these enzymes LpxE and LpxF are implicated in removing, or modification, of phosphate; in position '1' and '4' of lipid A, respectively; there is scope for further study.

Some differences and similarities were noted from the comparative studies between *F. necrophorum* D12 and *E. coli* K12. There were differences in the number of enzymes involved in the lipid A pathway between these two microorganisms. Studies on the evolution of the lipid A in bacteria revealed that the number of enzymes in Gram-negative organisms are different, but all the organisms shared the first four enzymes in the pathway. Opiyo *et al.*, (2010) observed that more enzymes could be generated by duplicated genes which allowed functional specialisation and pathway optimisation, giving greater adaptability as in the highly adapted *E. coli* with vertebrate enteric habitats. Their studies showed that gene duplication as well as the partial or complete loss of genes encoding the enzymes has happened independently several times during the bacterial evolution. Each group of bacteria has taken advantage of such evolutionary events to optimise the pathway and adapt to their specialised life style (Opiyo *et al.*, 2010).

The first four genes of the lipid IVA pathway were investigated in *F. necrophorum*; all four genes, *lpxA*, *lpxB*, *lpxC* and *lpxD* had been annotated and sequences were available in the BioCyc database. PCR and sequencing of the amplicons demonstrated single base pair changes that either did not change the properties of the encoded amino acid or did not affect the active site of the enzymes. Q-RT-PCR suggested that all enzymes were well-expressed in the strains/isolates examined. Alignment of the amino acid sequences (for the LpxA and LpxC enzymes of the lipid A pathway) of *F. necrophorum* D12 and *E. coli* K12 (for the LpxA and LpxC enzymes of the lipid A pathway) showed 57 % and 40 % identity respectively. The sites involved in the binding and catalytic activity in both enzymes were highly conserved. The enzymes, especially LpxC, are of interest in helping to develop new antibiotics by targeting the conserved domains to treat

Gram-negative bacterial infections. LpxC is a metalloenzyme that requires bound zinc for activity; thus, it is an essential gene. Mutations in this gene compromise cell division, reduce expression of LPS increasing the permeability to antibacterial agents. LpxC does not have sequence homology to other deacetylases or eukaryotic proteins; therefore, it is a target for the design of new antibiotics specific for Gram-negative bacteria. The advantage of using LpxC as a target for novel antibiotics is that it allows specific inhibition, reducing undesirable effects and the high conservation of the protein in bacteria allows a wide spectrum of action. Recent studies identified LpxC inhibitors containing hydroxamate group as targeting the catalytic zinc ion (Barb and Zhou, 2008). CHIR-090 is particularly interesting among the LpxC inhibitors; this is an antibiotic, which controls the growth of *E. coli* and *P. aeruginosa* with an efficacy comparable to that of ciprofloxacin. The success of this antibiotic suggests that potent LpxC-targeting antibiotics may be developed which can control a broad range of Gram-negative bacteria (Barb and Zhou, 2008).

In the lipid IVA pathway, *lpxH* that belongs to the metallophosphoesterase superfamily, and in *E. coli* and many other bacteria, it catalyses the hydrolysis of pyrophosphate bond of UDP-2, 3-diacylglucosamine, was absent from all *Fusobacteria* sp. The current study demonstrated that the *lpxI* gene that catalyses UDP-2, 3-diacylglucosamine hydrolysis by a different mechanism that had been fully characterised in *Caulobacteria* (Metzger *et al.*, 2012), was utilised instead of *lpxH* not only by *F. necrophorum*, but also by all other *Fusobacteria* sp. These findings may enable research into specific inhibitors that could be used in the future as therapeutic agents.

Chapter 7

7 Genome Analysis of *F. necrophorum* reference strains and clinical isolates using NGS

7.1 Introduction

To date, much of the focus of genomic studies of *Fusobacteria* sp. has centred on *F. nucleatum*. DNA sequence analysis of *F. nucleatum* subspecies *nucleatum* (ATCC 25586) and *vincentii* (ATCC 49256) shows clear differences in genetic content between the strains. Some of the open reading frames (ORFs) from these strains were not present in the other strains of *F. nucleatum* (*polymorphum*, *fusiforme*, and *animalis*) and there was evidence of rearrangements in the ORFs present in both strains. There was phenotypic heterogeneity among the *F. nucleatum* strains giving rise to the idea that it is a “species complex” (Karpathy *et al.*, 2007). From the taxonomic studies, researchers confirmed that subspecies *polymorphum* ATCC 10953 represents a separate phylogenetic branch that included significant human pathogens compared to the other previously sequenced strains of *F. nucleatum*. Phenotypic studies of *polymorphum* ATCC 10953 have characterised some of its functions, such as its uptake and metabolism of amino acids, simple sugars and peptides and how it interacts with epithelial, host immune cells and connective tissues and its modulation of host immune cells to induce apoptosis and enhance survival of strict anaerobes in both planktonic and biofilm multispecies cultures. They also characterised how it acts synergistically with other oral pathogens, enhancing virulence in animal model systems. The taxonomic status, phenotypic analysis and genetic transformability of *F. nucleatum* subsp. *polymorphum* (FNP) ATCC 10953 indicated that genomic analysis would be of benefit for future studies of this species. Further studies and analysis of the FNP genome, led to the observation that 25 % of the genes identified were not represented in genomes of the previously sequenced *Fusobacteria*, which suggested that evolution of this strain was due to contribution of horizontal gene transfer (HGT) (Karpathy *et al.*, 2007).

Availability of the complete genome sequence from *F. necrophorum* should give some insight into the relatedness of the mechanisms resulting in disease progression to Lemierre's syndrome.

The aims of this study were to:

1. understand the genetic, metabolic and pathogenic features by analyzing the genomes sequences of *F. necrophorum* reference strains and clinical isolates.
2. determine the impact of nucleotide substitutions on amino acid sequence.

7.2 Methods

7.2.1 Retrieval of whole genome sequences from public databases and microbesNG.

Whole genome sequence data for 20 *Fusobacterium necrophorum* isolates were generated by microbesNG (Table 7.1) and whole-genome nucleotide sequences for 31 *Fusobacterium necrophorum* isolates and 32 representative isolates of related species were downloaded from NCBI and NCTC 3000 on 18 June 2018 (Table 7.1).

(<https://www.phe-culturecollections.org.uk/products/bacteria/nctc-3000-strains-d-f.aspx>)

7.2.2 Preliminary phylogenetic analyses.

Prokka 1.13 (Seemann, 2014) software was used to predict genes encoded within the genomes listed in Table 7.1. All protein sequences were analysed with PhyloPhlAn 0.99, to determine the placement of the whole-genome within the *Fusobacterium* genus (Segata *et al.*, 2013). The resulting multiple-sequence alignment was imported into R and phangorn v.2.3.1 (Schliep, 2011) was used to construct a neighbour-joining tree. FigTree v1.4.2 (<http://tree.bio.ed.ac.uk/software/figtree/>) was used to visualize the phylogenetic tree and it was annotated using Adobe Illustrator.

7.2.3 16S rRNA gene sequence analysis of strain F88.

Using RNAmmer 1.2 (Lagesen *et al.*, 2007) the 16S rRNA gene sequence of strain F88 was predicted, with a partial (1229 nt) sequence recovered that was extended to 1514 nt by comparison with other *Fusobacterium* spp. Accession numbers for 16S rRNA gene sequences of type strains of the genus *Fusobacterium* were obtained from the List of Prokaryotic Names With Standing In Nomenclature (<http://www.bacterio.net/fusobacterium.html>) and De Witte *et al.*, (2017). The sequences were imported into Geneious 8.1.4. A multiple-sequence alignment was created using CLUSTAL W, and this used to create a neighbour-joining tree (Jukes Cantor); bootstrap values were generated from 1000 replicates.

7.2.4 Quality control checks on genome sequence data.

For all *Fusobacterium necrophorum* genomes listed in Table 7.1, the size of genome, number of CDS and number of scaffolds were examined. Potential contaminants within genomes were identified by running any questionable *Fusobacterium necrophorum* assemblies against the nt (NCBI non-redundant nucleotide) database (created 3 March 2018) of Centrifuge 1.0.3 (Kim *et al.*, 2016).

7.2.5 Determination of average nucleotide identity (ANI).

This was determined between pairs of genomes using OrhtoANI implemented in OAT 0.93 (≤ 10 sequences to compare) or OAT_cmd 1.30 (Lee *et al.*, 2016); outputs were imported into R to generate a heatmap (heatmap.2 function in package gplots).

7.2.6 Comparative and pangenome analyses of *Fusobacterium necrophorum* strains.

The 49 whole-genome sequences identified as *Fusobacterium necrophorum* were subject to further analyses. ANI was determined for the 49 genome sequences and other *Fusobacterium* species using OAT_cmd 1.3.0. A pangenome analysis

was carried out on the 49 *Fusobacterium necrophorum* strains using Roary (Page *et al.*, 2015).

Using Roary, coding sequences (CDSs) were extracted from the input files and translated to protein sequences, filtered to remove partial sequences and iteratively pre-clustered using CD-HIT (Fu *et al.*, 2012). This resulted in a substantially smaller dataset of protein sequences, which were then clustered with TRIBE-MCL (Enright *et al.*, 2002). Finally, results from CD-HIT and TRIBE-MCL were merged together and used to make a core gene alignment with MAFFT (Kato *et al.*, 2002); the output was a core cluster alignment file. A maximum-likelihood tree (GTR model) was created using FastTree with the core alignment file. The phylogenetic tree was visualised using FigTree v1.4.2, phandango (Hadfield *et al.*, 2017) was used to visualise pangenome data. Single nucleotide polymorphism (SNP) sites in the core cluster alignment file generated by Roary were identified using *SNP-sites* (Page *et al.*, 2016). Principal component analysis (PCA) of the presence/absence of accessory genes within *Fusobacterium necrophorum* subsp. *funduliforme* genomes was performed using the R package FactoMineR (Lê *et al.*, 2008). Representative sequences of the 6819 genes detected in the Roary analysis were submitted to eggNOG-mapper v4.5.1 (<http://eggnogdb.embl.de/#/app/home>); (Huerta-Cepas *et al.*, 2016) to obtain additional functional information. ProgressiveMauve (Darling *et al.*, 2010) was used to visualize genome arrangements, using the .gbk files produced by Prokka.

7.2.7 Impact of nucleotide changes on amino acid sequence.

A large number of single nucleotide polymorphisms were noted in the genomic studies and research was undertaken to determine their impact on the encoded amino acids in a small number of proteins. The protein sequences were downloaded from the annotated sequence data supplied by microbesNG. Clustal Omega was used to align the encoded protein sequences.

LpxI encodes an enzyme in the lipid A pathway (see chapter 6) and Galactose binding periplasmic protein enables binding of the organism to cell surface unsubstituted β -galactose residues (see chapter 5). Pyruvate synthase (*nifJ_1*)

is a member of the pyruvate ferredoxin flavodoxin oxidoreductase family involved in the electron transport chain. DNA polymerase III Tau (*dnaX_1*) is a nucleotidyltransferase (<https://www.uniprot.org/uniparc/?query=A0A2X3M9F5>). Leukotoxin (*lktA*) (from amino acid 121-419) is a potent virulence factor toxic to human white blood cells (<https://www.uniprot.org/uniprot/Q2NLH6>). Threonine--tRNA ligase 2 (*thrS*) catalyzes the attachment of threonine to tRNA (Thr) (<https://www.uniprot.org/uniprot/A0A017H6B3>). The Elongation factor Tu (*tuf*) protein promotes the GTP-dependent binding of aminoacyl-tRNA to the A-site of ribosomes during protein biosynthesis (<https://www.uniprot.org/uniprot/J5VR20>).

Table 7.1 Information for NCBI, NCTC and microbesNG genome assemblies used in preliminary phylogenetic analyses

Summary statistics (i.e. size, scaffolds, CDS) were generated using Prokka 1.13. GC % information as supplied by NCBI, NCTC and microbesNG.

Strain	Identified in this study as:	WGS	Size(Mb)	GC%	Scaffolds	CDS	Source	Genome reference
F59	<i>Fusobacterium necrophorum</i> subsp. <i>funduliforme</i>		2.08	35.1	70	1979	Human, recurrent and persistent sort throat (HRPSR)	This study
F62	<i>Fusobacterium necrophorum</i> subsp. <i>funduliforme</i>		2.22	34.5	45	2110	HRPSR	This study
F70	<i>Fusobacterium necrophorum</i> subsp. <i>funduliforme</i>		2.14	35.1	114	2001	HRPSR	This study
F80	Contaminated*		4.02	37.6	316	3758	HRPSR	This study
F86	<i>Fusobacterium necrophorum</i> subsp. <i>funduliforme</i>		2.19	35.0	67	2149	HRPSR	This study
F87	<i>Fusobacterium necrophorum</i> subsp. <i>funduliforme</i>		2.35	35.0	73	2321	HRPSR	This study
F88	<i>Fusobacterium nucleatum</i> / <i>Fusobacterium simiae</i> †		2.49	27.1	140	2248	HRPSR	This study
F1	<i>Fusobacterium necrophorum</i> subsp. <i>funduliforme</i>		2.16	35.0	66	2044	HRPSR	This study
F5	<i>Fusobacterium necrophorum</i> subsp. <i>funduliforme</i>		2.14	35.1	69	2043	HRPSR	This study
F11	<i>Fusobacterium necrophorum</i> subsp. <i>funduliforme</i>		2.06	35.1	48	1929	HRPSR	This study
F21	<i>Fusobacterium necrophorum</i> subsp. <i>funduliforme</i>		2.26	34.9	36	2211	HRPSR	This study
F24	<i>Fusobacterium necrophorum</i> subsp. <i>funduliforme</i>		2.24	35.0	66	2162	HRPSR	This study
F30	<i>Fusobacterium necrophorum</i> subsp. <i>funduliforme</i>		2.16	35.0	60	2070	HRPSR	This study
F39	<i>Fusobacterium necrophorum</i> subsp. <i>funduliforme</i>		2.21	34.9	78	2080	HRPSR	This study

Strain	Identified in this study as:	WGS	Size(Mb)	GC%	Scaffolds	CDS	Source	Genome reference
F40	<i>Fusobacterium necrophorum</i> subsp. <i>funduliforme</i>		2.16	35.0	71	2039	HRPSR	This study
F42	<i>Fusobacterium necrophorum</i> subsp. <i>funduliforme</i>		2.21	35.0	74	2159	HRPSR	This study
F52	<i>Fusobacterium necrophorum</i> subsp. <i>funduliforme</i>		2.48	34.9	61	2075	HRPSR	This study
Aru 01	<i>Fusobacterium necrophorum</i> subsp. <i>funduliforme</i>		2.15	35.1	54	2068	Patient with Lemierre's disease, Cardiff	This study
JCM 3718 ^T	<i>Fusobacterium necrophorum</i> subsp. <i>necrophorum</i>		2.60	34.0	189	2268	Bovine liver abscess	This study
JCM 3724 ^T	<i>Fusobacterium necrophorum</i> subsp. <i>funduliforme</i>		2.13	34.9	42	2025	Bovine liver abscess	This study
HUN048	<i>Fusobacterium necrophorum</i> subsp. <i>funduliforme</i> ‡	GCA_000622045.1	2.03	35.1	17	1872	Cow rumen, NZ	Seshadri et al. (2018)
BL	<i>Fusobacterium necrophorum</i> subsp. <i>necrophorum</i> ‡	GCA_000691645.1	2.46	34.1	235	2164	Bovine liver	–
DJ-1	<i>Fusobacterium necrophorum</i> subsp. <i>necrophorum</i> ‡	GCA_000691665.1	2.46	34.0	370	2176	Deer tongue, jaw	–
BFTR-1	<i>Fusobacterium necrophorum</i> subsp. <i>necrophorum</i> ‡	GCA_000691685.1	2.53	33.9	304	2234	Bovine foot rot	–
DAB	<i>Fusobacterium necrophorum</i> subsp. <i>necrophorum</i> ‡	GCA_000691705.1	2.52	34.0	254	2225	Deer jaw abscess	–
BFTR-2	<i>Fusobacterium necrophorum</i> subsp. <i>necrophorum</i> ‡	GCA_000691725.1	2.61	33.8	389	2380	Bovine foot rot	–
DJ-2	<i>Fusobacterium necrophorum</i> subsp. <i>necrophorum</i> ‡	GCA_000691745.1	2.52	34.0	226	2235	Deer jaw	–
LS_1260	<i>Fusobacterium necrophorum</i> subsp. <i>funduliforme</i>	GCA_001596475.1	2.24	35.1	62	2207	Human blood, Denmark	–
LS_1264	<i>Fusobacterium necrophorum</i> subsp. <i>funduliforme</i>	GCA_001596485.1	2.33	34.4	117	2249	Human blood, Denmark	–
LS_1197	<i>Fusobacterium necrophorum</i> subsp. <i>funduliforme</i>	GCA_001596495.1	1.98	35.2	38	1811	Human blood, Denmark	–

Strain	Identified in this study as:	WGS	Size(Mb)	GC%	Scaffolds	CDS	Source	Genome reference
LS_1195	<i>Fusobacterium necrophorum</i> subsp. <i>funduliforme</i>	GCA_001597305.1	2.23	35.3	36	2135	Human blood, Denmark	–
LS_1266	<i>Fusobacterium necrophorum</i> subsp. <i>funduliforme</i>	GCA_001597315.1	2.10	35.1	83	2013	Human blood, Denmark	–
LS_1280	<i>Fusobacterium necrophorum</i> subsp. <i>funduliforme</i>	GCA_001597325.1	2.10	35.1	56	1978	Human blood, Denmark	–
LS_1272	<i>Fusobacterium necrophorum</i> subsp. <i>funduliforme</i>	GCA_001597335.1	2.14	35.2	32	1984	Human blood, Denmark	–
LS_1291	<i>Fusobacterium necrophorum</i> subsp. <i>funduliforme</i>	GCA_001597385.1	2.10	35.1	37	1988	Human blood, Denmark	–
F1248	<i>Fusobacterium necrophorum</i> subsp. <i>funduliforme</i>	GCA_001597395.1	2.24	34.8	49	2208	Human throat swab, Denmark	–
F1285	<i>Fusobacterium necrophorum</i> subsp. <i>funduliforme</i>	GCA_001597405.1	2.34	35.0	70	2306	Human throat swab, Denmark	–
F1250	<i>Fusobacterium necrophorum</i> subsp. <i>funduliforme</i>	GCA_001597445.1	2.42	34.9	46	2452	Human throat swab, Denmark	–
F1267	<i>Fusobacterium necrophorum</i> subsp. <i>funduliforme</i>	GCA_001597465.1	2.29	35.1	71	2204	Human throat swab, Denmark	–
F1309	<i>Fusobacterium necrophorum</i> subsp. <i>funduliforme</i>	GCA_001597475.1	2.14	35.2	51	2051	Human throat swab, Denmark	–
F1314	<i>Fusobacterium necrophorum</i> subsp. <i>funduliforme</i>	GCA_001597485.1	2.08	35.1	105	1937	Human throat swab, Denmark	–
F1353	<i>Fusobacterium necrophorum</i> subsp. <i>funduliforme</i>	GCA_001597525.1	2.11	35.1	45	2013	Human throat swab, Denmark	–
F1330	<i>Fusobacterium necrophorum</i> subsp. <i>funduliforme</i>	GCA_001597545.1	2.11	35.2	72	1979	Human throat swab, Denmark	–
F1365	<i>Fusobacterium necrophorum</i> subsp. <i>funduliforme</i>	GCA_001597565.1	2.17	35.1	47	2102	Human throat swab, Denmark	–
F1351	<i>Fusobacterium necrophorum</i> subsp. <i>funduliforme</i>	GCA_001597575.1	2.20	35.0	56	2184	Human throat swab, Denmark	–
P1_CP	<i>Fusobacterium necrophorum</i> subsp. <i>funduliforme</i>	GCA_002761995.1	2.10	35.2	34	1977	Human colorectal primary tumour, Spain	–

Strain	Identified in this study as:	WGS	Size(Mb)	GC%	Scaffolds	CDS	Source	Genome reference
P1_LM	<i>Fusobacterium necrophorum</i> subsp. <i>funduliforme</i>	GCA_002762025.1	2.09	35.2	35	1976	Human liver metastasis, Spain	–
D12	<i>Fusobacterium necrophorum</i> subsp. <i>funduliforme</i> †	GCA_000158295.2	1.96	35.2	17	1919	Human gastrointestinal tract, ulcerative colitis	Human microbiome project
B35	<i>Fusobacterium necrophorum</i> subsp. <i>funduliforme</i>	GCA_000814775.1	2.05	35.0	42	2320	Bovine liver abscess	Calcultt et al. (2014)
1_1_36S	<i>Fusobacterium necrophorum</i> subsp. <i>funduliforme</i>	GCA_003019715.1	2.28	34.7	1	2119	Human terminal ileum	Sanders et al. (2018)
Fnf 1007	<i>Fusobacterium necrophorum</i> subsp. <i>funduliforme</i>	GCA_000292975.1	2.17	35.1	87	2090	Unknown	Human microbiome project
CMW8396	<i>Fusobacterium equinum</i>	GCA_001546395.1	1.80	32.5	77	1748	Human vagina	Human microbiome project
ATCC 25563 ^T	<i>Fusobacterium gonidiaformans</i>	GCA_003019695.1	1.68	32.7	1	1610	Human tonsil	Sanders et al. (2018)
ChDC F128	<i>Fusobacterium hwasookii</i> [†]	GCA_000292935.1	2.36	27.0	30	2210	Human upper jaw tissue with sinusitis, South Korea	Park et al. (2012a)
Marseille-P2749	<i>Fusobacterium massiliense</i> [†]	GCA_900095705.1	1.81	27.3	6	1649	Human duodenum sample	Mailhe et al. (2016)
ATCC 9817	<i>Fusobacterium mortiferum</i>	GCA_003019315.1	2.72	29.3	1	2631	Human peri-renal abscess	Sanders et al. (2018)
ATCC 25832 ^T	<i>Fusobacterium naviforme</i>	GCA_003014445.1	2.40	52.8	23	2184	Human, exudate from head lesion	–
NCTC 10723 ^T	<i>Fusobacterium necrogenes</i>	ERS956170	2.02	29.2	5	1802	Duck caecum	NCTC 3000
ATCC 51190 ^T	<i>Fusobacterium nucleatum</i> subsp. <i>fusiforme</i>	GCA_000279975.1	1.84	27.2	198	1718	Human sinusitis in upper jaw	Park et al. (2012b)
ATCC 25586 ^T	<i>Fusobacterium nucleatum</i> subsp. <i>nucleatum</i>	GCA_000007325.1	2.17	27.2	1	2016	Human cervico-facial lesion	Kapatral et al. (2002)
NCTC 10562 ^T	<i>Fusobacterium nucleatum</i> subsp. <i>polymorphum</i>	NZ_LN831027 (chr.), NZ_LN831028 (plasmid)	2.46	27.0	2	2330	Human inflamed gingiva	NCTC 3000

Strain	Identified in this study as:	WGS	Size(Mb)	GC%	Scaffolds	CDS	Source	Genome reference
ATCC 49256 ^T	<i>Fusobacterium nucleatum</i> subsp. <i>vincentii</i>	GCA_000182945.1	2.12	27.3	302	2240	Human periodontal pocket	Kapatral et al. (2003)
ATCC 29250 ^T	<i>Fusobacterium perfoetens</i>	GCA_000622245.1	2.10	26.0	25	1934	Piglet faeces	–
ATCC 33693 ^T	<i>Fusobacterium periodonticum</i>	GCA_000160475.1	2.62	27.7	53	2454	Human periodontitis	–
ATCC 25533 ^T	<i>Fusobacterium russii</i>	GCA_000381725.1	1.94	28.7	41	1714	Infection in a cat	–
clos_1_1	<i>Fusobacterium</i> sp.	GCA_900015295.1	2.04	28.9	8	1852	Soil	–
CAG:649	<i>Fusobacterium</i> sp.	GCA_000433695.1	2.16	26.7	172	2121	Human gut metagenome	–
CAG:815	<i>Fusobacterium</i> sp.	GCA_000437775.1	1.84	32.2	32	1825	Human gut metagenome	–
CAG:439	<i>Fusobacterium</i> sp.	GCA_000438175.1	2.19	34.7	90	2333	Human gut metagenome	–
CM1	<i>Fusobacterium</i> sp.	GCA_000524215.1	2.44	26.7	155	2288	Unknown	Human microbiome project
CM21	<i>Fusobacterium</i> sp.	GCA_000517705.1	2.36	27.7	471	2058	Unknown	Human microbiome project
CM22	<i>Fusobacterium</i> sp.	GCA_000524395.1	2.44	26.7	87	2362	Unknown	Human microbiome project
HMSC064B11	<i>Fusobacterium</i> sp.	GCA_001815715.1	2.40	26.8	119	2258	Human blood, central line	–
HMSC064B12	<i>Fusobacterium</i> sp.	GCA_001810995.1	2.12	26.9	56	1950	Human breast wound	–
HMSC065F01	<i>Fusobacterium</i> sp.	GCA_001813745.1	2.13	26.8	56	1939	Human gastric wound	–
HMSC073F01	<i>Fusobacterium</i> sp.	GCA_001810475.1	3.50	29.3	221	3132	Human abdominal fluid	–
OBRC1	<i>Fusobacterium</i> sp.	GCA_000524235.1	2.50	26.8	87	2428	Unknown	Human microbiome project
W7671	<i>Fusobacterium</i> sp. oral taxon 203	GCA_002243405.1	2.13	27.5	1	1973	Human, curette	–

Strain	Identified in this study as:	WGS	Size(Mb)	GC%	Scaffolds	CDS	Source	Genome reference
F0437	<i>Fusobacterium</i> sp. oral taxon 370	GCA_000235465.1	2.09	27.6	133	2141	Unknown	Human microbiome project
ATCC 49185 ^T	<i>Fusobacterium ulcerans</i>	GCA_003019675.1	3.54	30.5	1	3230	Human skin ulcer, Gambia	Sanders et al. (2018)
ATCC 27725	<i>Fusobacterium varium</i>	GCA_003019655.1	3.35	29.3	2	3053	Unknown	Sanders et al. (2018)
ATCC 700028 ^T	<i>Cetobacterium ceti</i>	GCA_900167275.1	2.58	28.3	61	2500	Sea mammal	–
DSM 19335 ^T	<i>Psychrilyobacter atlanticus</i>	GCA_000426625.1	3.54	31.9	3	3302	Marine sediment	–

*Contaminated sequence; see text and Figure 7.1 and Figure 7.2 for explanation.

†Misclassified, should be *Fusobacterium nucleatum*/*Fusobacterium simiae*. See text and Figure 7.1 and Figure 7.3 for explanation.

‡Deposited in NCBI as *Fusobacterium necrophorum*.

7.3 RESULTS

7.3.1 Preliminary sequence analyses

The 20 genome sequences generated in this study and other, publicly available *Fusobacterium necrophorum* strains within the family *Fusobacteriaceae*, a total of 83 whole genome sequences, were included in a preliminary phylogenetic analysis (Figure 7.1). Original whole genome nucleotide assemblies were used (from NCBI, NCTC or microbesNG) as raw reads were not available for the majority of publicly available genomes, preventing assembly of all sequence data using the same assembler. However, proteins in all genomes were predicted using Prokka 1.13; this analysis predicted 2119 genes for the complete genome sequence of *Fusobacterium necrophorum* subsp. *funduliforme* 1_1_36S, whereas Sanders *et al.*, (2018) predicted 2125 using a combination of Prodigal, RAST, Barrnap and CRISPRone.

Of the 20 whole genome sequences generated by microbesNG for this study, F80 and F88 were problematical (Figure 7.1). The microbesNG-generated genome of F80 was much larger than those of other *Fusobacterium necrophorum* isolates and encoded far more proteins (Table 7.1); microbesNG had also reported the genome sequence might represent a mixed culture as numerous sequence reads mapped to *Streptococcus* spp. Together, these results suggested F80 either represented a novel species or its genome was contaminated. Searching the assembled contigs against the non-redundant NCBI nucleotide database via Centrifuge 1.0.3 (Kim *et al.*, 2016) revealed the genome of F80 was contaminated with a large number of *Streptococcus*-associated reads (Figure 7.2). Given that the genome of F80 was contaminated, it was removed from the dataset.

Strain F88 fell within a clade containing proteome data from *Fusobacterium hwasookii*, the four subspecies of *Fusobacterium nucleatum*, *Fusobacterium periodonticum*, '*Fusobacterium massiliense*' and *Fusobacterium russii*; no issues with the genome of F88 had been reported by microbesNG. An ANI analysis of F88 against the species in its clade and the genome sequence of *Fusobacterium necrophorum* subsp. *necrophorum* JCM 3718 revealed it to be most closely related to *Fusobacterium nucleatum* subsp. *fusiforme* ATCC 51190 (89.5 % ANI)

and only distantly related to *Fusobacterium necrophorum* subsp. *necrophorum* JCM 3718 (70.3 % ANI) (Figure 7.3a); the ANI threshold range for species affiliation is ≥ 95 % (Goris *et al.*, 2007; Richter & Rosselló -Móra, 2009; Chun *et al.*, 2018), confirming F88 belonged to neither *Fusobacterium necrophorum* nor *Fusobacterium nucleatum*. 16S rRNA gene sequence analysis confirmed F88 was closely related to *Fusobacterium nucleatum* subspecies (97.0–99.1 % sequence similarity; *Fusobacterium nucleatum* subsp. *nucleatum*, 99.1 %). However, it shared 99.3 % sequence similarity (1458 nt) with *Fusobacterium simiae*, with this association supported at 100 % by bootstrap analysis (Figure 7.3b). Comparison with the (currently unavailable) whole genome sequence of *Fusobacterium simiae* would be required to accurately determine the species affiliation of F88. As the focus of this study was *Fusobacterium necrophorum*, strain F88 was removed from the datasets.

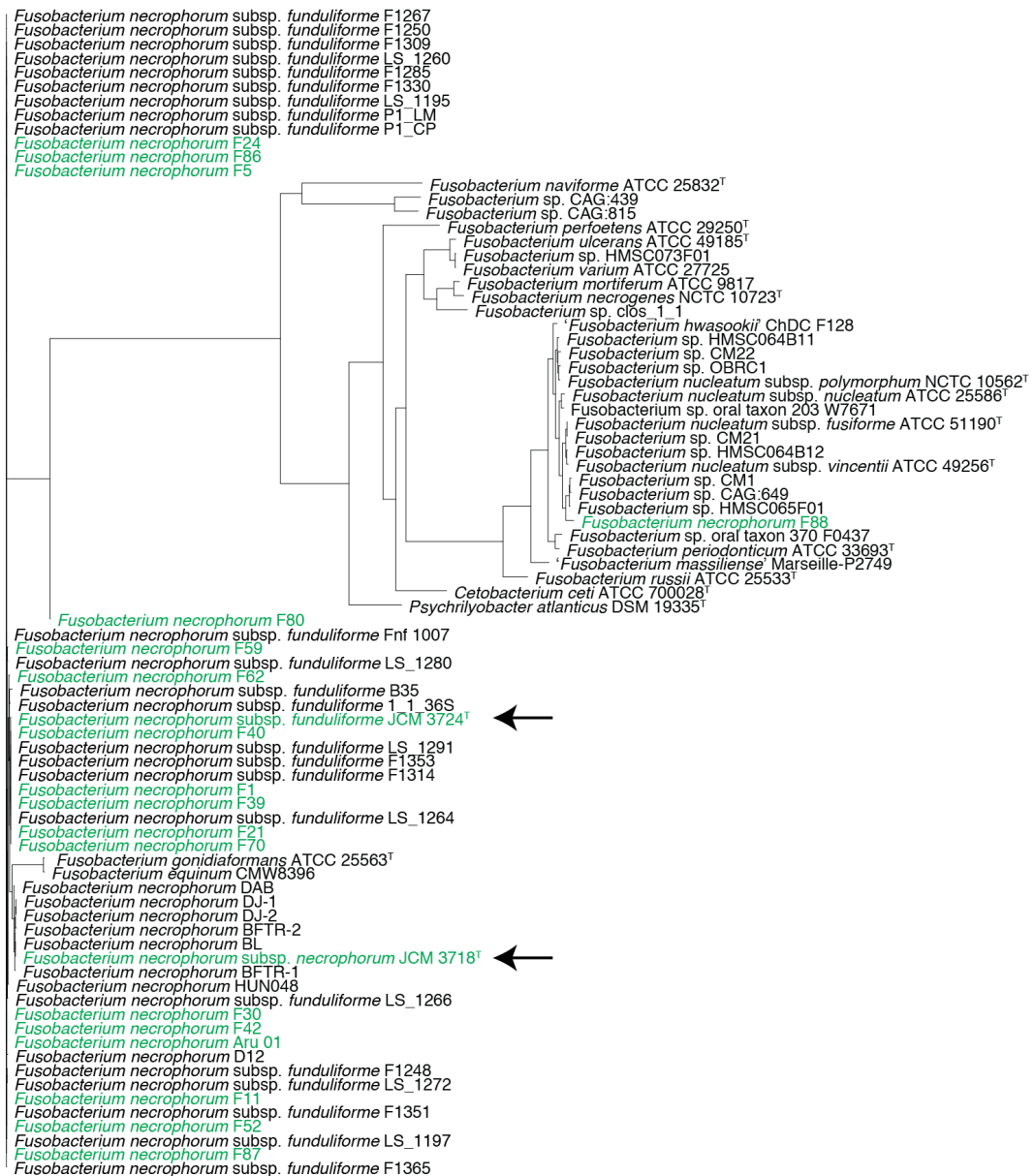


Figure 7.1 Phylogenetic (neighbour-joining) tree showing taxonomic placement of strains included in this study within the family Fusobacteriaceae.

The tree was generated using an alignment of 374 concatenated proteins selected from the whole-genome sequences by PhyloPhlAn 0.99. Arrows point to type strains of *Fusobacterium necrophorum* subsp. *necrophorum* and *Fusobacterium necrophorum* subsp. *funduliforme*. Green text = isolates sequenced for this study. Designations for all other genomes are as given in the relevant NCBI genome records. Bootstrap values are not shown at the nodes as this tree was intended to quickly highlight any potential issues with genome assignments, not to provide an authoritative phylogeny.

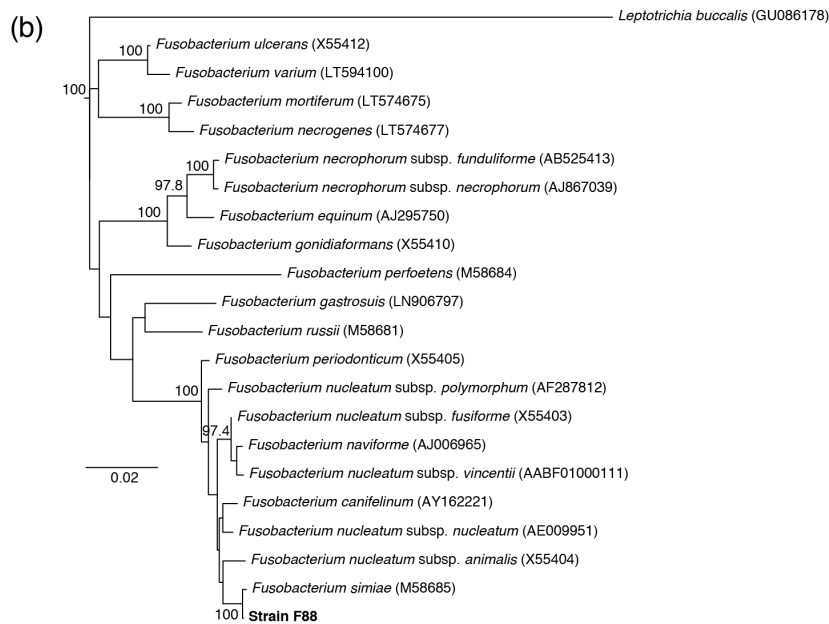
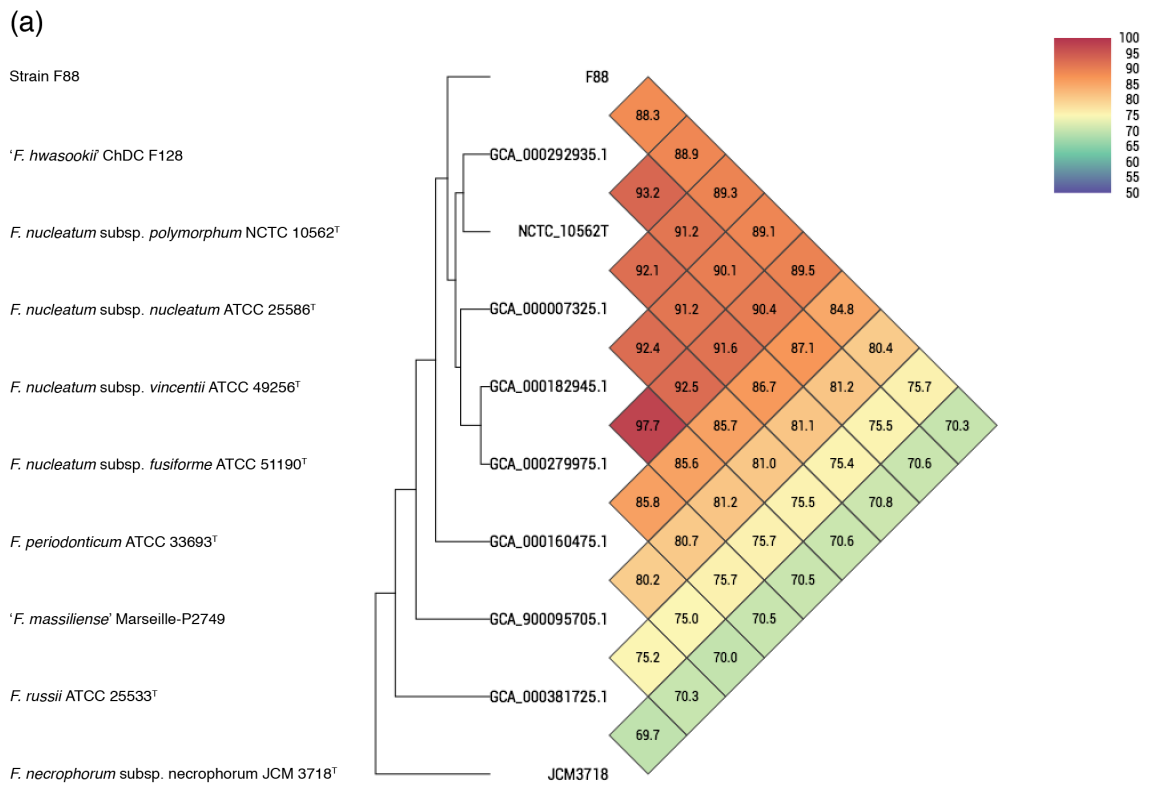


Figure 7.3 Species assignment of F88.

(a) The whole-genome nucleotide sequence of F88 was compared with that of its closest relatives to generate ANI values (OAT 0.93 output shown). (b) The *16S rRNA* gene sequence of F88 was extracted from its whole-genome sequence and included in a phylogenetic analysis with the *16S rRNA* gene sequences of the type strains of its closest relatives. Neighbour-joining tree shown. Values at nodes are bootstrap values displayed as a percentage of 1000 replicates; only values >80 % are shown.

7.3.2 ANI comparisons of *Fusobacterium necrophorum* genomes with other *Fusobacteria*

The type strains of *Fusobacterium necrophorum* subsp. *necrophorum* (JCM 3718) and *Fusobacterium necrophorum* subsp. *funduliforme* (JCM 3724) shared less than 82.7 % and 82.6 % ANI, respectively, with the type strains of other *Fusobacterium* species (Figure 7.4). JCM 3718 shared 97.1 % ANI with JCM 3724 and formed a cluster with six other strains (BFTR-1, BFTR-2, BL, DAB, DJ-1, DJ-2) that shared 98.5–99.6 % ANI with JCM 3718 and 97.2–97.4 % ANI with JCM 3724. All other *Fusobacterium necrophorum* strains shared 98.2–99.8 % ANI with JCM 3724. As all *Fusobacterium necrophorum* strains shared ≥ 95 % ANI, it could be confirmed they were authentic members of the species (Goris *et al.*, 2007; Richter and Rosselló-Móra, 2009; Chun *et al.*, 2018).

7.3.3 *Fusobacterium necrophorum* pangenome analysis

The 49 authentic *Fusobacterium necrophorum* genomes were submitted to Roary (minimum identity for BLAST of 95 %). The analysis showed there to be 1053 core genes (present in ≥ 99 % – 100 % of strains), 276 soft core genes (present in ≥ 95 % – < 99 % of strains), 1359 shell genes (i.e. genes present in ≥ 15 % – < 95 % of strains) and 4131 cloud genes (i.e. genes present in 0 – < 15 % of strains). In total, 6819 genes were detected in the analysis. Within the core genes, 37436 SNPs were detected. The strains fell into two groups, with the majority of strains clustering with the type strain of *Fusobacterium necrophorum* subsp. *funduliforme* (Figure 7.5). Strains DAB, BFTR-1, BFTR-2, DJ-1, DJ-2 and BL clustered with the type strain of *Fusobacterium necrophorum* subsp. *necrophorum*, in agreement with the results from the ANI analysis (Figure 7.4).

The seven *Fusobacterium necrophorum* subsp. *necrophorum* strains shared 1540 core genes (present in all strains) and 1794 accessory genes (present in one or more strains). The 42 *Fusobacterium necrophorum* subsp. *funduliforme* strains shared 1253 core genes and 4412 accessory genes. Of the 6819 genes detected in both subspecies by Roary, 1154 were unique to *Fusobacterium necrophorum* subsp. *necrophorum* and 3485 were unique to *Fusobacterium necrophorum*

subsp. *funduliforme* at BLASTp cut-off of 95 %. PCA of accessory genes present in 5–95 % of the strains confirmed separation of the two subspecies (Figure 7.6a). Although *Fusobacterium necrophorum* subsp. *funduliforme* strains clustered on the left-hand side of the PCA plot, it appeared there were at least two separate clusters within the subspecies that warranted further attention (Figure 7.6b).

PCA of only the accessory genes of *Fusobacterium necrophorum* subsp. *funduliforme* revealed there to be three clusters within the subspecies. Cluster A contained the type strain of *Fusobacterium necrophorum* subsp. *funduliforme* (JCM 3724) and strains F1, F21, F39, F40, F70, F1314, LS_1291, F1353 and LS_1264, while Cluster B contained F24, F87, Fnf 1007, LS_1195, F1267, F1285, F1250, LS_1260, F1330, F1365, F1309, P1_LM and P1_CP (Figure 7.7a). Cluster A can clearly be seen in the ANI heatmap in Figure 7.4, while clusters A and B are seen in the pangenome analysis in Figure 7.5. Cluster C was more diffuse (Figure 7.7a, b). Inclusion of additional *Fusobacterium necrophorum* subsp. *funduliforme* genomes in the analysis may allow separation of Cluster C into additional clusters. The three *Fusobacterium necrophorum* subsp. *funduliforme* clusters shared 790 core genes, but each cluster had its own unique genes (Figure 7.8).

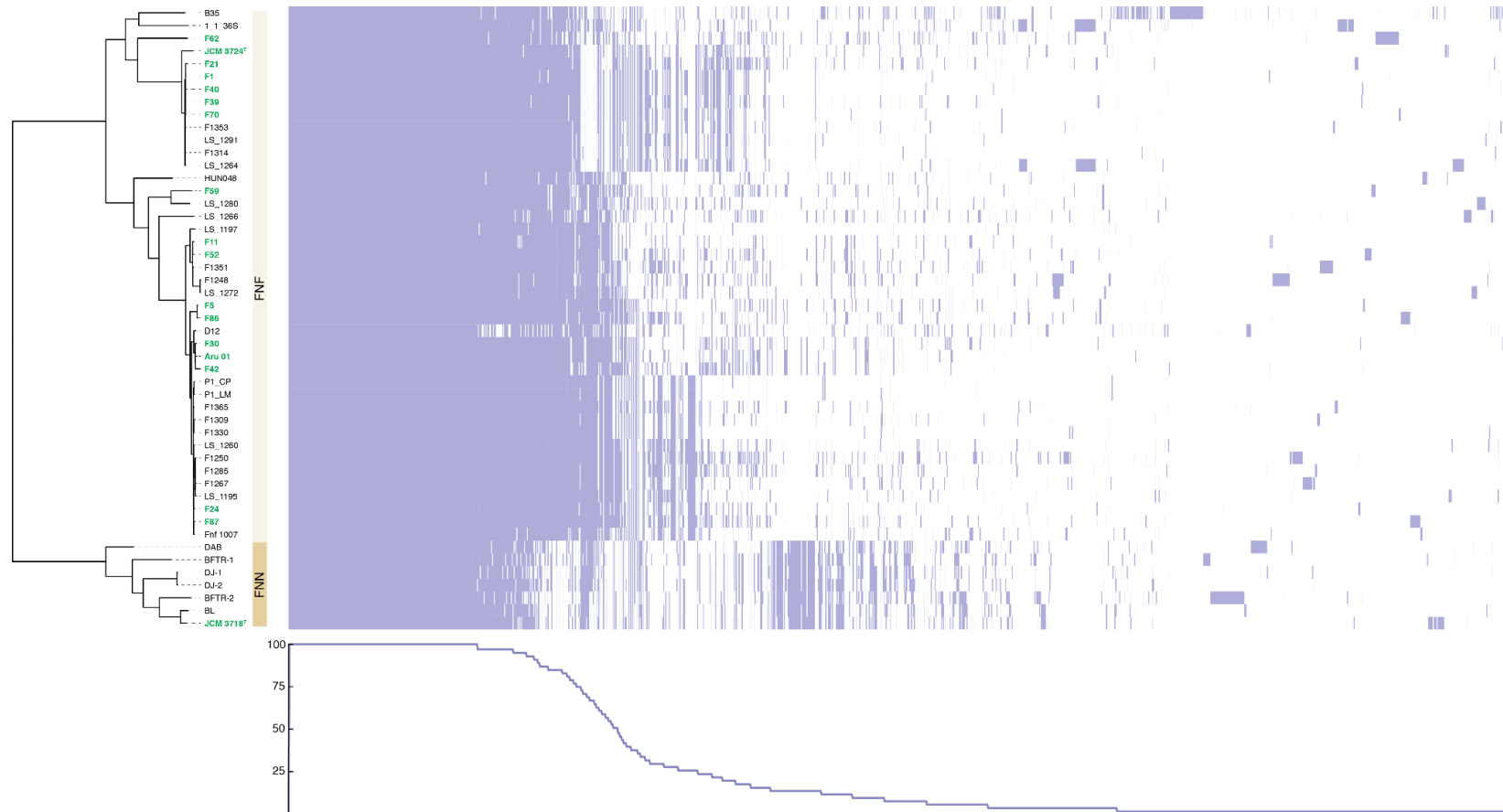


Figure 7.5 Pangenome analysis of *Fusobacterium necrophorum* subsp. *necrophorum* (FNN) and *Fusobacterium necrophorum* subsp. *funduliforme* (FNF).

The dendrogram was generated from the core alignment produced by Roary using FastTree (Price *et al.*, 2009). Image generated using phandango (Hadfield *et al.*, 2017) and edited in Illustrator. Green text, genome sequences generated for this study.

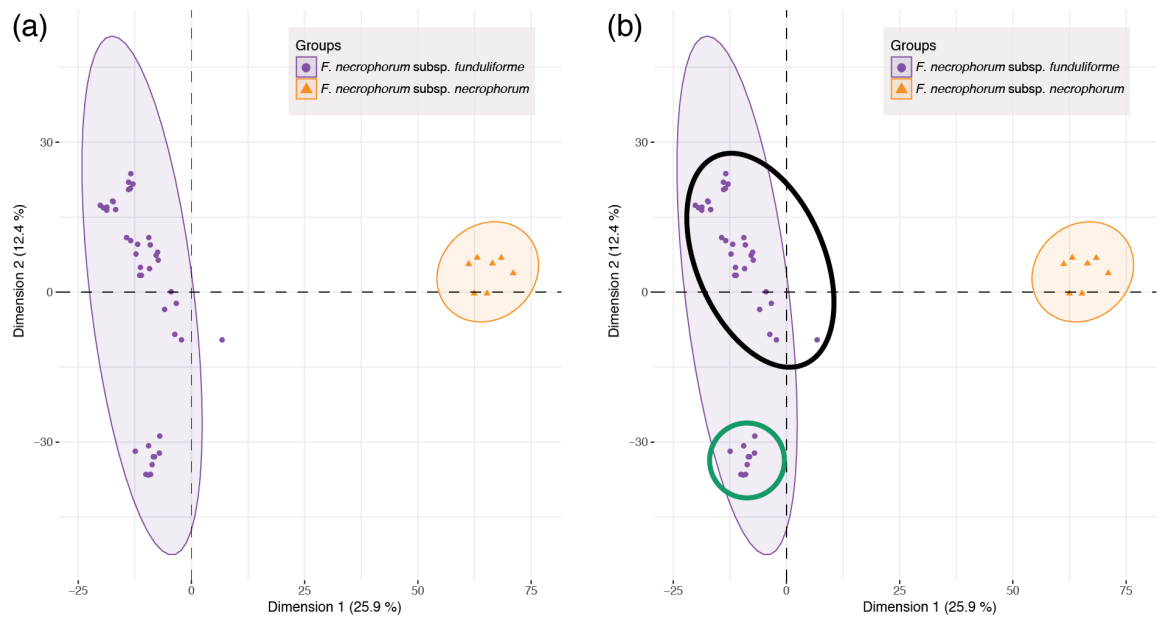


Figure 7.6 PCA of accessory genes (present in 5 – 95 % of strains) for *Fusobacterium necrophorum* subsp. *necrophorum* and *Fusobacterium necrophorum* subsp. *funduliforme*.

(a) PCA plot showing separation of data into the two subspecies based on the first principal component. (b) The *F. necrophorum* subsp. *funduliforme* strains appeared to form two distinct clusters (marked by thick black and green lines). The cluster outlined in green contains the type strain (JCM 3724) of the subspecies.

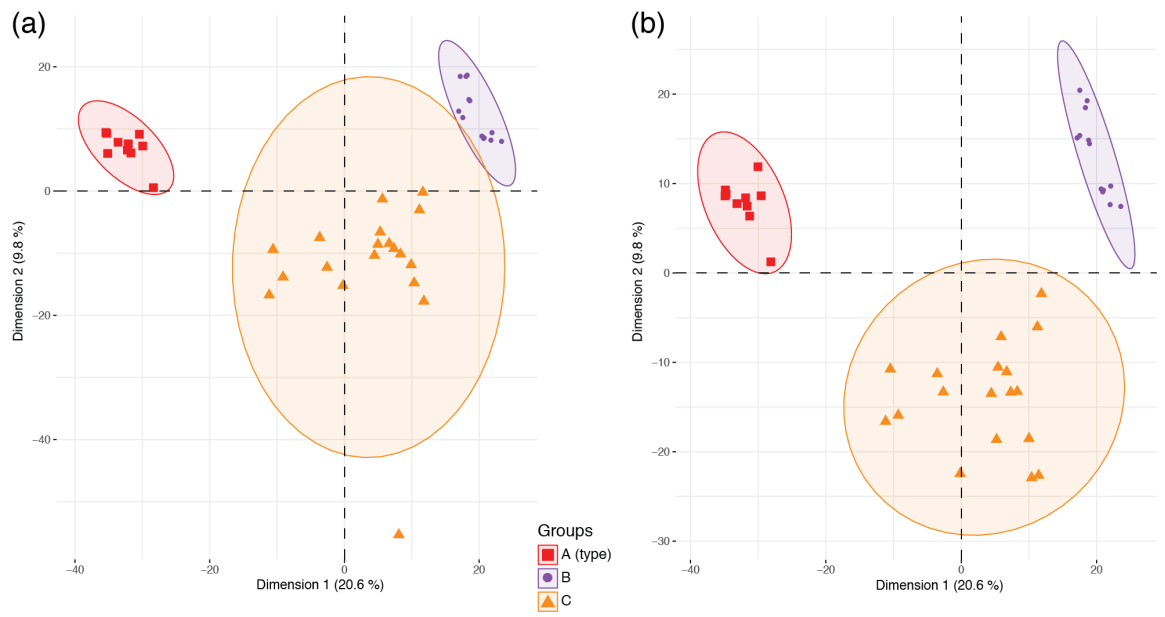


Figure 7.7 PCA of accessory genes (present in 5 – 95 % of strains) for *Fusobacterium necrophorum* subsp. *funduliforme*.

(a) PCA including an outlier strain, D12. (b) PCA with outlier D12 removed.

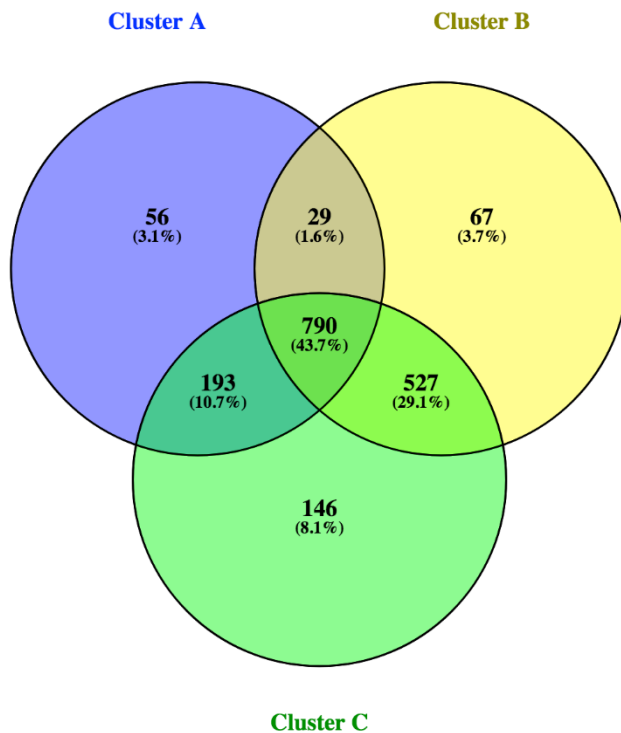


Figure 7.8 Venn diagram showing numbers of core and accessory genes shared by the three *Fusobacterium necrophorum* subsp. *funduliforme* clusters identified from PCA of accessory genes.

Image produced using Venny 2.1.0 (<http://bioinfogp.cnb.csic.es/tools/venny/>).

7.3.4 Impact of nucleotide changes on amino acid sequence.

The results of the Clustal Omega alignment of the protein sequences of the LpxI protein (described in chapter 6) in 24 isolates are shown in Figure 7.9 and Table 7.2. In this case 13 amino acid differences, the products of non-synonymous SNPs, were noted in the 24 sequences analysed. Five of these were close to the amino acids identified as important for catalytic activity (see chapter 6). Of the three SNPs that were predicted to cause structural changes in the protein, one was close to the active site of the protein and requires further analysis to determine impact on enzyme activity and LPS production.

Table 7.2 Impact of non-synonymous SNPs on LpxI.

Alternative amino acids	Amino acid properties	Impact	Incidences
Asparagine (N) or Aspartic acid (D)	Amide Acidic	Not close to active site	1
Methionine (M) or Isoleucine(I)	Hydrophobic Hydrophobic	None	5
Cysteine (C) or Tyrosine (Y)	Aromatic Nucleophilic	Not close to active site	1
Lysine (K) or Glutamic acid (E)	Basic Acidic	Both can form salt bridges	1
Leucine (L) or Phenylalanine (F)	Hydrophobic Aromatic	Both hydrophobic	1
Serine(S) or Arginine (R)	Nucleophilic Basic	Likely: close to active site	1
Arginine (R) or Glutamine (Q)	Basic Polar	Unlikely	1
Isoleucine (I) or Valine (V)	Hydrophobic Hydrophobic	None	1
Leucine (L) or Isoleucine (I)	Hydrophobic Hydrophobic	None	1

Interestingly, the alignment (Figure 7.9) showed 3 distinct clusters of isolates; based on analysis of 10 polymorphisms, the subsp. *funduliforme* isolates F1, F21, F39, F40, F62, F70, 05310, B35, JCM 3724 and WP1(ATCC 51357) formed one cluster (A), the subsp. *funduliforme* F5, F11, F24, F30, F42, F52, ARU 01, F59, F80, F86, F87, WP2 the second (B + C) and the subsp. *necrophorum* isolates JCM 3718 and WP3 (DAB, BFTR-1, DJ-1, BFTR-2, DJ-2) the third. JCM 3718 and WP3 had a pattern similar to cluster B+C at 8 of 10 sites, but for two sites they resembled cluster A. One polymorphism was noted in JCM 3724 and WP1; a change from L to F, that was not present in other isolates and two polymorphisms D to N, M to I and I to L were seen only in JCM 3718 and WP3. The two subsp. *funduliforme* clusters were identical to the two main clusters (A and B+C) seen in the genomic study.

F1	HFSFYGVKKLILLGKVEKSILFQNLDDLDDYQGQEILKMLPDRKDETLFAMISFLKLNIGIR	120
F21	HFSFYGVKKLILLGKVEKSILFQNLDDLDDYQGQEILKMLPDRKDETLFAMISFLKLNIGIR	120
F39	HFSFYGVKKLILLGKVEKSILFQNLDDLDDYQGQEILKMLPDRKDETLFAMISFLKLNIGIR	120
F40	HFSFYGVKKLILLGKVEKSILFQNLDDLDDYQGQEILKMLPDRKDETLFAMISFLKLNIGIR	120
F62	HFSFYGVKKLILLGKVEKSILFQNLDDLDDYQGQEILKMLPDRKDETLFAMISFLKLNIGIR	120
F70	HFSFYGVKKLILLGKVEKSILFQNLDDLDDYQGQEILKMLPDRKDETLFAMISFLKLNIGIR	120
05310	HFSFYGVKKLILLGKVEKSILFQNLDDLDDYQGQEILKMLPDRKDETLFAMISFLKLNIGIR	120
B35	HFSFYGVKKLILLGKVEKSILFQNLDDLDDYQGQEILKMLPDRKDETLFAMISFLKLNIGIR	120
JCM 3724	HFSFYGVKKLILLGKVEKSILFQNLDDLDDYQGQEILKMLPDRKDETLFAMISF F KLNIGIR	120
WP1	HFSFYGVKKLILLGKVEKSILFQNLDDLDDYQGQEILKMLPDRKDETLFAMISF F KLNIGIR	120
F5	YFSFYGVKKLILLGKVEKSILFQNLDDLDDYQGQEILKMLPDRKDETLF AI SFLKLNIGIR	120
F11	YFSFYGVKKLILLGKVEKSILFQNLDDLDDYQGQEILKMLPDRKDETLF AI SFLKLNIGIR	120
F24	YFSFYGVKKLILLGKVEKSILFQNLDDLDDYQGQEILKMLPDRKDETLF AI SFLKLNIGIR	76
F30	YFSFYGVKKLILLGKVEKSILFQNLDDLDDYQGQEILKMLPDRKDETLF AI SFLKLNIGIR	120
F42	YFSFYGVKKLILLGKVEKSILFQNLDDLDDYQGQEILKMLPDRKDETLF AI SFLKLNIGIR	120
F52	YFSFYGVKKLILLGKVEKSILFQNLDDLDDYQGQEILKMLPDRKDETLF AI SFLKLNIGIR	120
ARU 01	YFSFYGVKKLILLGKVEKSILFQNLDDLDDYQGQEILKMLPDRKDETLF AI SFLKLNIGIR	120
F59	YFSFYGVKKLILLGKVEKSILFQNLDDLDDYQGQEILKMLPDRKDETLF AI SFLKLNIGIR	120
F80	YFSFYGVKKLILLGKVEKSILFQNLDDLDDYQGQEILKMLPDRKDETLF AI SFLKLNIGIR	120
F86	YFSFYGVKKLILLGKVEKSILFQNLDDLDDYQGQEILKMLPDRKDETLF AI SFLKLNIGIR	120
F87	YFSFYGVKKLILLGKVEKSILFQNLDDLDDYQGQEILKMLPDRKDETLF AI SFLKLNIGIR	120
WP2	-----LFQNLDDLDDYQGQEILKMLPDRKDETLF AI SFLKLNIGIR	40
JCM 3718	YFSFYGVKKLILLGKVEKSILFQNLDDLDDYQGQEILKML P NRKDETLF AI SFLKLNIGIR	120
WP3	YFSFYGVKKLILLGKVEKSILFQNLDDLDDYQGQEILKML P NRKDETLF AI SFLKLNIGIR	120
	*****:*****:***:*****	
F1	VLSQNYLLSSCMVEEKCYTEKIPKEEDDRSIQLGIEAAKILTRLDIGQTVIVKEEAVVAL	180
F21	VLSQNYLLSSCMVEEKCYTEKIPKEEDDRSIQLGIEAAKILTRLDIGQTVIVKEEAVVAL	180
F39	VLSQNYLLSSCMVEEKCYTEKIPKEEDDRSIQLGIEAAKILTRLDIGQTVIVKEEAVVAL	180
F40	VLSQNYLLSSCMVEEKCYTEKIPKEEDDRSIQLGIEAAKILTRLDIGQTVIVKEEAVVAL	180
F62	VLSQNYLLSSCMVEEKCYTEKIPKEEDDRSIQLGIEAAKILTRLDIGQTVIVKEEAVVAL	180
F70	VLSQNYLLSSCMVEEKCYTEKIPKEEDDRSIQLGIEAAKILTRLDIGQTVIVKEEAVVAL	180
05310	VLSQNYLLSSCMVEEKCYTEKIPKEEDDRSIQLGIEAAKILTRLDIGQTVIVKEEAVVAL	180
B35	VLSQNYLLSSCMVEEKCYTEKIPKEEDDRSIQLGIEAAKILTRLDIGQTVIVKEEAVVAL	180
JCM 3724	VLSQNYLLSSCMVEEKCYTEKIPKEEDDRSIQLGIEAAKILTRLDIGQTVIVKEEAVVAL	180
WP1	VLSQNYLLSSCMVEEKCYTEKIPKEEDDRSIQLGIEAAKILTRLDIGQTVIVKEEAVVAL	180
F5	VLSQNYLLSSYMVEEKCYTEEMPKEEDDRSIQLGMEAAKMLTSLDIGQTVIVKEEAVVAL	180
F11	VLSQNYLLSSYMVEEKCYTEEMPKEEDDRSIQLGMEAAKMLTSLDIGQTVIVKEEAVVAL	180
F24	VLSQNYLLSSYMVEEKCYTEEMPKEEDDRSIQLGMEAAKMLTSLDIGQTVIVKEEAVVAL	136
F30	VLSQNYLLSSYMVEEKCYTEEMPKEEDDRSIQLGMEAAKMLTSLDIGQTVIVKEEAVVAL	180
F42	VLSQNYLLSSYMVEEKCYTEEMPKEEDDRSIQLGMEAAKMLTSLDIGQTVIVKEEAVVAL	180
F52	VLSQNYLLSSYMVEEKCYTEEMPKEEDDRSIQLGMEAAKMLTSLDIGQTVIVKEEAVVAL	180
ARU 01	VLSQNYLLSSYMVEEKCYTEEMPKEEDDRSIQLGMEAAKMLTSLDIGQTVIVKEEAVVAL	180
F59	VLSQNYLLSSYMVEEKCYTEEMPKEEDDRSIQLGMEAAKMLTSLDIGQTVIVKEEAVVAL	180
F80	VLSQNYLLSSYMVEEKCYTEEMPKEEDDRSIQLGMEAAKMLTSLDIGQTVIVKEEAVVAL	180
F86	VLSQNYLLSSYMVEEKCYTEEMPKEEDDRSIQLGMEAAKMLTSLDIGQTVIVKEEAVVAL	180
F87	VLSQNYLLSSYMVEEKCYTEEMPKEEDDRSIQLGMEAAKMLTSLDIGQTVIVKEEAVVAL	180
WP2	VLSQNYLLSSYMVEEKCYTEEMPKEEDDRSIQLGMEAAKMLTSLDIGQTVIVKEEAVVAL	100
JCM 3718	VLSQNYLLSSYMVEEKCYTEEMPKEEDDRSIQLG I EAAKMLTSLDIGQTVIVKEEAVVAL	180
WP3	VLSQNYLLSSYMVEEKCYTEEMPKEEDDRSIQLG I EAAKMLTSLDIGQTVIVKEEAVVAL	180
	***** *****:***:*****:***:*** *****	

F1	EGIEGTDQAILRAGELAGKNCIIVKMARPKQDMRVDIPTVGVETIRRAIEIGAKGIVMEA	240
F21	EGIEGTDQAILRAGELAGKNCIIVKMARPKQDMRVDIPTVGVETIRRAIEIGAKGIVMEA	240
F39	EGIEGTDQAILRAGELAGKNCIIVKMARPKQDMRVDIPTVGVETIRRAIEIGAKGIVMEA	240
F40	EGIEGTDQAILRAGELAGKNCIIVKMARPKQDMRVDIPTVGVETIRRAIEIGAKGIVMEA	240
F62	EGIEGTDQAILRAGELAGKNCIIVKMARPKQDMRVDIPTVGVETIRRAIEIGAKGIVMEA	240
F70	EGIEGTDQAILRAGELAGKNCIIVKMARPKQDMRVDIPTVGVETIRRAIEIGAKGIVMEA	240
05310	EGIEGTDQAILRAGELAGKNCIIVKMARPKQDMRVDIPTVGVETIRRAIEIGAKGIVMEA	240
B35	EGIEGTDQAILRAGELAGKNCIIVKMARPKQDMRVDIPTVGVETIRRAIEIGAKGIVMEA	240
JCM 3724	EGIEGTDQAILRAGELAGKNCIIVKMARPKQDMRVDIPTVGVETIRRAIEIGAKGIVMEA	240
WP1	EGIEGTDQAILRAGELAGKNCIIVKMARPKQDMRVDIPTVGVETIRRAIEIGAKGIVMEA	240
F5	EGMEGTDRAILRAGELAGKNCIIKMARPKQDMRVDIPTVGVETIRRAIEIGAKGIVMEA	240
F11	EGMEGTDRAILRAGELAGKNCIIKMARPKQDMRVDIPTVGVETIRRAIEIGAKGIVMEA	240
F24	EGMEGTDRAILRAGELAGKNCIIKMARPKQDMRVDIPTVGVETIRRAIEIGAKGIVMEA	196
F30	EGMEGTDRAILRAGELAGKNCIIKMARPKQDMRVDIPTVGVETIRRAIEIGAKGIVMEA	240
F42	EGMEGTDRAILRAGELAGKNCIIKMARPKQDMRVDIPTVGVETIRRAIEIGAKGIVMEA	240
F52	EGMEGTDRAILRAGELAGKNCIIKMARPKQDMRVDIPTVGVETIRRAIEIGAKGIVMEA	240
ARU 01	EGMEGTDRAILRAGELAGKNCIIKMARPKQDMRVDIPTVGVETIRRAIEIGAKGIVMEA	240
F59	EGMEGTDRAILRAGELAGKNCIIKMARPKQDMRVDIPTVGVETIRRAIEIGAKGIVMEA	240
F80	EGMEGTDRAILRAGELAGKNCIIKMARPKQDMRVDIPTVGVETIRRAIEIGAKGIVMEA	240
F86	EGMEGTDRAILRAGELAGKNCIIKMARPKQDMRVDIPTVGVETIRRAIEIGAKGIVMEA	240
F87	EGMEGTDRAILRAGELAGKNCIIKMARPKQDMRVDIPTVGVETIRRAIEIGAKGIVMEA	240
WP2	EGMEGTDRAILRAGELAGKNCIIKMARPKQDMRVDIPTVGVETIRRAIEIGAKGIVMEA	160
JCM 3718	EGMEGTDRAILRAGELAGKNCIIKMARPKQDMRVDIPTVGVETLRRRAIEIGAKGIVMEA	240
WP3	EGMEGTDRAILRAGELAGKNCIIKMARPKQDMRVDIPTVGVETLRRRAIEIGAKGIVMEA	240
	__:***:*****:*****:*****:*****:*****	

Figure 7.9 Clustal Omega analysis of the LpxI protein.

Amino acids 1-60 and 241-267 were identical and are not included. WP1= WP_005958282.1; ATCC 51357, WP2 = WP_005964136.1, WP3 = WP_035902054.1; DAB, BFTR-1, DJ-1, BFTR-2, DJ-2. * = active site. An * (asterisk) indicates positions which have a single, fully conserved residue. A : (colon) indicates conservation between amino acids with strongly similar properties (conservative replacements). A . (full stop) indicates conservation between amino acids with weakly similar properties. A gap indicates non-conserved amino acids. Two clusters were noted, highlighted in green and black, and other individual amino acid changes are highlighted in red.

Having noted the clustering of isolates with respect to the amino acid sequence of LpxI, similar analyses were completed on a number of other proteins. Figure 7.10 shows the Clustal Omega alignment of the Galactose periplasmic binding protein (see chapter 5, Fig. 5.4); in 5 representative isolates, only 6 amino acid changes and one deletion were noted. Four amino acid differences were seen between JCM 3718 and the other isolates, ARU 01 and isolate F5 had a single amino acid deletion, and ARU 01 had an amino acid different to all other isolates. One difference was noted where isolate F5 and JCM 3718 differed from the other isolates; hence the changes in this protein did not demonstrate the same clustering as LpxI and the protein was similar in both subspecies. All changes

were conservative replacements and hence unlikely to cause significant changes in protein structure or function.

A small section of the Leukotoxin protein was analysed in 13 isolates; it was clear that JCM 3718, the only subsp. *necrophorum* analysed was significantly different at 34 sites from the other isolates (highlighted in red in Figure 7.10). Conservative, semi-conservative and non-conservative replacements were seen. The sequence from JCM 3718 was used as the interrogator in a BLASTp analysis and matched with more than 98 % identity 6 uncharacterised *F. necrophorum* isolates, 2 subsp. *necrophorum* isolates, BTFR-1 and BTFR-2 suggesting these changes were likely to be subsp. *necrophorum* specific. Polymorphisms, conservative, semi-conservative and non-conservative, were seen at 65 locations in the other isolates differentiating two clusters F1, F21, F39, F40 and JCM 3724 from F5, F11, F24, F30, F42, F52 and ARU 01; these results define clusters identical to those obtained for LpxI.

Analysis of the Elongation factor Tu in 5 representative isolates was highly conserved. There was only one amino acid change (R to K; a conservative replacement) in JCM 3718 and a difference in the isolate F5 that appeared to produce a shorter protein: this was at the start of the protein and may represent a sequencing, assembly or annotation issue, although one similarly shortened sequence was found in the NCBI database following a BLASTp analysis.

Aru01_00496	MKKMGIIILGALVLAAGLVGCGEKKEA-APAENAVRMGLTAYKFDDNFIALFRQAFQAEAD	59
F5_01730	MKKMGIIILGALVLAAGLVGCGEKKEA-APAENAVRMGLTAYKFDDNFIALFRQAFQAEAD	59
JCM3718_01896	MKKMGIVLGLALVLAAGLVGCGEKKEAAAPAENAVRMGLTAYKFDDNFIALFRQAFQAEAD	60
F1_00295	MKKMGIIILGALVLAAGLVGCGEKKEAAAPAENAVRMGLTAYKFDDNFIALFRQAFQAEAD	60
JCM3724_01150	MKKMGIIILGALVLAAGLVGCGEKKEAAAPAENAVRMGLTAYKFDDNFIALFRQAFQAEAD	60
	*****:*****	
Aru01_00496	AVGNQVALQMVDSQNDAAKQNE <u>N</u> LDVLLLEKGIDTLAINLVDPAGVDVVLEKIKAKELPVV	119
F5_01730	AVG <u>D</u> QVALQMVDSQNDAAKQNEQLDVLLLEKGIDTLAINLVDPAGVDVVLEKIKAKELPVV	119
JCM3718_01896	AVG <u>D</u> QVALQMVDSQNDAAKQNEQLDVLLLEKGIDTLAINLVDPAGVDVVLEKIKAKELPVV	120
F1_00295	AVGNQVALQMVDSQNDAAKQNEQLDVLLLEKGIDTLAINLVDPAGVDVVLEKIKAKELPVV	120
JCM3724_01150	AVGNQVALQMVDSQNDAAKQNEQLDVLLLEKGIDTLAINLVDPAGVDVVLEKIKAKELPVV	120
	:**:*****	
Aru01_00496	FYNRKPSDEALASYDKAYYVVGIDPNAQGIAQGK L IEKAWQANPALDLNGDGVIQFAM L KG	179
F5_01730	FYNRKPS E EALASYDKAYYVVGIDPNAQGIAQGK L IEKAWQANPALDLNGDGVIQFAM L KG	179
JCM3718_01896	FYNRKPS E EALASYDKAYYVVGIDPNAQGV A QGK L IEKAWQANPALDLNGDGVIQFAM L KG	180
F1_00295	FYNRKPSDEALASYDKAYYVVGIDPNAQGIAQGK L IEKAWQANPALDLNGDGVIQFAM L KG	180
JCM3724_01150	FYNRKPS E EALASYDKAYYVVGIDPNAQGIAQGK L IEKAWQANPALDLNGDGVIQFAM L KG	180
	*****:*****:*****	
Aru01_00496	EPGHPDAEARTVYSIKTLNEDGIKTEELHLD T AMWD T AQAKDKMDAWLSGPNADKIEVVI	239
F5_01730	EPGHPDAEARTVYSIKTLNEDGIKTEELHLD T AMWD T AQAKDKMDAWLSGPNADKIEVVI	239
JCM3718_01896	EPGHPDAEARTVYSIKTLNEDGIKTEELHLD T AMWD T AQAKDKMDAWLSGPNADKIEVVI	240
F1_00295	EPGHPDAEARTVYSIKTLNEDGIKTEELHLD T AMWD T AQAKDKMDAWLSGPNADKIEVVI	240
JCM3724_01150	EPGHPDAEARTVYSIKTLNEDGIKTEELHLD T AMWD T AQAKDKMDAWLSGPNADKIEVVI	240
	*****:*****:*****	

```

Aru01_00496      CNNDGMALGAIESMKAFGKSLPVFGVDALPEAITLIEKGEMAGTVLNDAKGQAKATFQVA      299
F5_01730        CNNDGMALGAIESMKAFGKSLPVFGVDALPEAITLIEKGEMAGTVLNDAKGQAKATFQVA      299
JCM3718_01896   CNNDGMALGAIESMKAFGKSLPVFGVDALPEAITLIEKGEMAGTVLNDAKGQAKATFQVA      300
F1_00295        CNNDGMALGAIESMKAFGKSLPVFGVDALPEAITLIEKGEMAGTVLNDAKGQAKATFQVA      300
JCM3724_01150   CNNDGMALGAIESMKAFGKSLPVFGVDALPEAITLIEKGEMAGTVLNDAKGQAKATFQVA      300
*****

Aru01_00496      MNLGQGKEATEGTDIQMENKIVLVPSIGIDKENVAEYK      337
F5_01730        MNLGQGKEATEGTDIQMENKIVLVPSIGIDKENVAEYK      337
JCM3718_01896   MNLGEGKEATEGTDIQMENKIVLVPSIGIDKENVAEYK      338
F1_00295        MNLGQGKEATEGTDIQMENKIVLVPSIGIDKENVAEYK      338
JCM3724_01150   MNLGQGKEATEGTDIQMENKIVLVPSIGIDKENVAEYK      338
****:*****

```

Figure 7.10 Clustal Omega analysis of the Galactose binding periplasmic protein.

Five strains were examined; ARU 01 (Aru01), F1, F5, JCM 3718, JCM 3724. Amino acid changes are highlighted in red. Conservative replacements are indicated by a colon (:), a dash (-) in the sequence denotes a deletion.

F5_02091	-----MLSDLGLAQKVDKIDVAPEERERG	26
Aru01_00001	MAKEKYERSKPHVNIGTIGHVDHGKTTTTAAISKVLSDLGLAQKVDKIDVAPEERERG	60
F1_00113	MAKEKYERSKPHVNIGTIGHVDHGKTTTTAAISKVLSDLGLAQKVDKIDVAPEERERG	60
JCM3724_02077	MAKEKYERSKPHVNIGTIGHVDHGKTTTTAAISKVLSDLGLAQKVDKIDVAPEERERG	60
JCM3718_01095	MAKEKYERSKPHVNIGTIGHVDHGKTTTTAAISKVLSDLGLAQKVDKIDVAPEEK <u>ER</u> G	60
	:*****:	
F5_02091	ITINTAHIEYETEARHYAHVDCPGHADVKNMITGAAQMDGAILVVSADGMPQTREHI	86
Aru01_00001	ITINTAHIEYETEARHYAHVDCPGHADVKNMITGAAQMDGAILVVSADGMPQTREHI	120
F1_00113	ITINTAHIEYETEARHYAHVDCPGHADVKNMITGAAQMDGAILVVSADGMPQTREHI	120
JCM3724_02077	ITINTAHIEYETEARHYAHVDCPGHADVKNMITGAAQMDGAILVVSADGMPQTREHI	120
JCM3718_01095	ITINTAHIEYETEARHYAHVDCPGHADVKNMITGAAQMDGAILVVSADGMPQTREHI	120

F5_02091	LLSRQVGVPIYIVVYLNKADMVEDEELLELVEMEVRELLSEYGFPGEIPIVTGSSLGALN	146
Aru01_00001	LLSRQVGVPIYIVVYLNKADMVEDEELLELVEMEVRELLSEYGFPGEIPIVTGSSLGALN	180
F1_00113	LLSRQVGVPIYIVVYLNKADMVEDEELLELVEMEVRELLSEYGFPGEIPIVTGSSLGALN	180
JCM3724_02077	LLSRQVGVPIYIVVYLNKADMVEDEELLELVEMEVRELLSEYGFPGEIPIVTGSSLGALN	180
JCM3718_01095	LLSRQVGVPIYIVVYLNKADMVEDEELLELVEMEVRELLSEYGFPGEIPIVTGSSLGALN	180

F5_02091	GEQKWVDKIMELMKAVDEYIPTPERAVDQPFLMPIEDVFTITGRGTVVVTGRVERGVVKG	206
Aru01_00001	GEQKWVDKIMELMKAVDEYIPTPERAVDQPFLMPIEDVFTITGRGTVVVTGRVERGVVKG	240
F1_00113	GEQKWVDKIMELMKAVDEYIPTPERAVDQPFLMPIEDVFTITGRGTVVVTGRVERGVVKG	240
JCM3724_02077	GEQKWVDKIMELMKAVDEYIPTPERAVDQPFLMPIEDVFTITGRGTVVVTGRVERGVVKG	240
JCM3718_01095	GEQKWVDKIMELMKAVDEYIPTPERAVDQPFLMPIEDVFTITGRGTVVVTGRVERGVVKG	240

F5_02091	EEVEIVGIKATTKTTCTGVEMFRKLLDQGQAGDNIGALLRGTKKEEVERGQVLAKPGSIH	266
Aru01_00001	EEVEIVGIKATTKTTCTGVEMFRKLLDQGQAGDNIGALLRGTKKEEVERGQVLAKPGSIH	300
F1_00113	EEVEIVGIKATTKTTCTGVEMFRKLLDQGQAGDNIGALLRGTKKEEVERGQVLAKPGSIH	300
JCM3724_02077	EEVEIVGIKATTKTTCTGVEMFRKLLDQGQAGDNIGALLRGTKKEEVERGQVLAKPGSIH	300
JCM3718_01095	EEVEIVGIKATTKTTCTGVEMFRKLLDQGQAGDNIGALLRGTKKEEVERGQVLAKPGSIH	300

F5_02091	PHTNFSGEVYVLTKEEGGRHTPFFTGYRPPQFYFRITDITGAVTLPEGVEMVMPGDNITMT	326
Aru01_00001	PHTNFSGEVYVLTKEEGGRHTPFFTGYRPPQFYFRITDITGAVTLPEGVEMVMPGDNITMT	360
F1_00113	PHTNFSGEVYVLTKEEGGRHTPFFTGYRPPQFYFRITDITGAVTLPEGVEMVMPGDNITMT	360
JCM3724_02077	PHTNFSGEVYVLTKEEGGRHTPFFTGYRPPQFYFRITDITGAVTLPEGVEMVMPGDNITMT	360
JCM3718_01095	PHTNFSGEVYVLTKEEGGRHTPFFTGYRPPQFYFRITDITGAVTLPEGVEMVMPGDNITMT	360

F5_02091	VELIHPIAMETGLRFAIREGGRTVASGVVSEITK	360
Aru01_00001	VELIHPIAMETGLRFAIREGGRTVASGVVSEITK	394
F1_00113	VELIHPIAMETGLRFAIREGGRTVASGVVSEITK	394
JCM3724_02077	VELIHPIAMETGLRFAIREGGRTVASGVVSEITK	394
JCM3718_01095	VELIHPIAMETGLRFAIREGGRTVASGVVSEITK	394

Figure 7.12 Clustal Omega analysis of the Elongation factor Tu.
 Five isolates were studied: ARU 01 (Aru01), F1, F5, JCM 3718 and JCM 3724.

JCM3718_01643	DVT <u>A</u> H <u>M</u> <u>A</u> E <u>I</u> S <u>K</u> <u>V</u> TGRDYKPF <u>N</u> YYGAADA <u>E</u> RIIVAMGSVC <u>E</u> AAEEV <u>I</u> D <u>Y</u> L <u>N</u> A <u>K</u> G <u>E</u> K <u>V</u> G <u>M</u> <u>V</u>	300
F1_00215	DIAA <u>Y</u> M <u>E</u> E <u>I</u> S <u>K</u> E <u>T</u> G <u>R</u> E <u>Y</u> K <u>P</u> F <u>K</u> Y <u>R</u> G <u>A</u> A <u>D</u> A <u>T</u> R <u>I</u> L <u>I</u> A <u>M</u> G <u>S</u> I <u>C</u> P <u>A</u> A <u>E</u> E <u>T</u> V <u>D</u> Y <u>L</u> V <u>E</u> K <u>G</u> E <u>K</u> V <u>G</u> L <u>L</u>	297
Aru01_00063	D <u>V</u> A <u>A</u> Y <u>M</u> E <u>E</u> I <u>S</u> K <u>E</u> T <u>G</u> R <u>E</u> Y <u>K</u> P <u>F</u> K <u>Y</u> R <u>G</u> A <u>A</u> D <u>A</u> T <u>R</u> I <u>L</u> I <u>A</u> M <u>G</u> S <u>I</u> C <u>P</u> A <u>A</u> E <u>E</u> T <u>V</u> D <u>Y</u> L <u>V</u> E <u>K</u> G <u>E</u> K <u>V</u> G <u>L</u> L	300
F5_00952	D <u>V</u> A <u>A</u> Y <u>M</u> E <u>E</u> I <u>S</u> K <u>E</u> T <u>G</u> R <u>E</u> Y <u>K</u> P <u>F</u> K <u>Y</u> R <u>G</u> A <u>A</u> D <u>A</u> T <u>R</u> I <u>L</u> I <u>A</u> M <u>G</u> S <u>I</u> C <u>P</u> A <u>A</u> E <u>E</u> T <u>V</u> D <u>Y</u> L <u>V</u> E <u>K</u> G <u>E</u> K <u>V</u> G <u>L</u> L	300
JCM3724_00851	DIAA <u>Y</u> M <u>E</u> E <u>I</u> S <u>K</u> E <u>T</u> G <u>R</u> E <u>Y</u> K <u>P</u> F <u>K</u> Y <u>R</u> G <u>A</u> A <u>D</u> A <u>T</u> R <u>I</u> L <u>I</u> A <u>M</u> G <u>S</u> I <u>C</u> P <u>A</u> A <u>E</u> E <u>T</u> V <u>D</u> Y <u>L</u> V <u>E</u> K <u>G</u> E <u>K</u> V <u>G</u> L <u>L</u>	300
	.::* ** * **:*:*:* * **:*:*:* * **:*:*:* * **:*:*:* * **:*:*:* * **:*:*:* * **:*:*:*	
JCM3718_01643	<u>K</u> V <u>H</u> L <u>R</u> P <u>F</u> S <u>E</u> K <u>Y</u> F <u>F</u> D <u>V</u> F <u>P</u> K <u>S</u> V <u>K</u> R <u>I</u> A <u>V</u> L <u>D</u> R <u>T</u> K <u>E</u> P <u>G</u> S <u>L</u> G <u>E</u> P <u>L</u> L <u>L</u> D <u>V</u> K <u>S</u> L <u>F</u> Y <u>G</u> K <u>E</u> N <u>A</u> P <u>L</u> I <u>V</u> G <u>G</u>	360
F1_00215	T <u>V</u> H <u>L</u> R <u>P</u> F <u>S</u> E <u>K</u> Y <u>F</u> F <u>A</u> V <u>L</u> P <u>K</u> T <u>V</u> E <u>K</u> I <u>A</u> V <u>L</u> E <u>R</u> T <u>K</u> E <u>P</u> G <u>A</u> P <u>G</u> E <u>P</u> L <u>L</u> L <u>D</u> V <u>K</u> G <u>L</u> F <u>Y</u> G <u>K</u> D <u>R</u> A <u>P</u> I <u>I</u> V <u>G</u> G	357
Aru01_00063	T <u>V</u> H <u>L</u> R <u>P</u> F <u>S</u> E <u>K</u> Y <u>F</u> F <u>A</u> V <u>L</u> P <u>K</u> T <u>V</u> E <u>K</u> I <u>A</u> V <u>L</u> E <u>R</u> T <u>K</u> E <u>P</u> G <u>A</u> P <u>G</u> E <u>P</u> L <u>L</u> L <u>D</u> V <u>K</u> G <u>L</u> F <u>Y</u> G <u>K</u> D <u>R</u> A <u>P</u> I <u>I</u> V <u>G</u> G	360
F5_00952	T <u>V</u> H <u>L</u> R <u>P</u> F <u>S</u> E <u>K</u> Y <u>F</u> F <u>A</u> V <u>L</u> P <u>K</u> T <u>V</u> E <u>K</u> I <u>A</u> V <u>L</u> E <u>R</u> T <u>K</u> E <u>P</u> G <u>A</u> P <u>G</u> E <u>P</u> L <u>L</u> L <u>D</u> V <u>K</u> G <u>L</u> F <u>Y</u> G <u>K</u> D <u>R</u> A <u>P</u> I <u>I</u> V <u>G</u> G	360
JCM3724_00851	T <u>V</u> H <u>L</u> R <u>P</u> F <u>S</u> E <u>K</u> Y <u>F</u> F <u>A</u> V <u>L</u> P <u>K</u> T <u>V</u> E <u>K</u> I <u>A</u> V <u>L</u> E <u>R</u> T <u>K</u> E <u>P</u> G <u>A</u> P <u>G</u> E <u>P</u> L <u>L</u> L <u>D</u> V <u>K</u> G <u>L</u> F <u>Y</u> G <u>K</u> D <u>R</u> A <u>P</u> I <u>I</u> V <u>G</u> G	360
	.***** *.:*:*:* *.:*:*:* *.:*:*:* *.:*:*:* *.:*:*:* *.:*:*:* *.:*:*:* *.:*:*:*	
JCM3718_01643	RYGLSSKDTTPAQI <u>V</u> A <u>V</u> F <u>D</u> N <u>L</u> K <u>A</u> E <u>Q</u> P <u>K</u> <u>D</u> L <u>F</u> T <u>V</u> G <u>I</u> <u>V</u> DDVTFTSLEVG <u>A</u> P <u>V</u> V <u>S</u> D <u>P</u> S <u>T</u> K <u>A</u> C <u>L</u>	420
F1_00215	RYGLSSKDTTPAQI <u>K</u> A <u>A</u> L <u>D</u> N <u>L</u> K <u>L</u> E <u>H</u> P <u>K</u> T <u>N</u> F <u>T</u> I <u>G</u> I <u>I</u> D <u>D</u> V <u>T</u> F <u>T</u> S <u>L</u> E <u>V</u> G <u>E</u> R <u>L</u> M <u>V</u> S <u>D</u> P <u>S</u> T <u>K</u> A <u>C</u> L	417
Aru01_00063	RYGLSSKDTTPAQI <u>K</u> A <u>V</u> L <u>D</u> N <u>L</u> K <u>L</u> E <u>H</u> P <u>K</u> T <u>N</u> F <u>T</u> I <u>G</u> I <u>I</u> D <u>D</u> V <u>T</u> F <u>T</u> S <u>L</u> E <u>V</u> G <u>E</u> R <u>L</u> M <u>V</u> S <u>D</u> P <u>S</u> T <u>K</u> A <u>C</u> L	420
F5_00952	RYGLSSKDTTPAQI <u>K</u> A <u>V</u> L <u>D</u> N <u>L</u> K <u>L</u> E <u>H</u> P <u>K</u> T <u>N</u> F <u>T</u> I <u>G</u> I <u>I</u> D <u>D</u> V <u>T</u> F <u>T</u> S <u>L</u> E <u>V</u> G <u>E</u> R <u>L</u> M <u>V</u> S <u>D</u> P <u>S</u> T <u>K</u> A <u>C</u> L	420
JCM3724_00851	RYGLSSKDTTPAQI <u>K</u> A <u>A</u> L <u>D</u> N <u>L</u> K <u>L</u> E <u>H</u> P <u>K</u> T <u>N</u> F <u>T</u> I <u>G</u> I <u>I</u> D <u>D</u> V <u>T</u> F <u>T</u> S <u>L</u> E <u>V</u> G <u>E</u> R <u>L</u> M <u>V</u> S <u>D</u> P <u>S</u> T <u>K</u> A <u>C</u> L	420
	***** *.:*:* *.:*:* *.:*:* *.:*:* *.:*:* *.:*:* *.:*:* *.:*:* *.:*:*	
JCM3718_01643	FYGLGADGT <u>V</u> G <u>A</u> N <u>K</u> S <u>I</u> K <u>I</u> I <u>G</u> D <u>K</u> T <u>D</u> L <u>Y</u> A <u>Q</u> G <u>Y</u> F <u>A</u> D <u>S</u> K <u>S</u> G <u>G</u> V <u>T</u> R <u>S</u> H <u>L</u> R <u>F</u> G <u>K</u> N <u>P</u> I <u>K</u> S <u>T</u> Y <u>L</u> V	480
F1_00215	FYGLGADGT <u>V</u> G <u>A</u> N <u>K</u> S <u>I</u> K <u>I</u> I <u>G</u> D <u>K</u> T <u>D</u> L <u>Y</u> A <u>Q</u> G <u>Y</u> F <u>A</u> D <u>S</u> K <u>S</u> G <u>G</u> V <u>T</u> R <u>S</u> H <u>L</u> R <u>F</u> G <u>K</u> N <u>P</u> I <u>K</u> S <u>T</u> Y <u>L</u> V	477
Aru01_00063	FYGLGADGT <u>V</u> G <u>A</u> N <u>K</u> S <u>I</u> K <u>I</u> I <u>G</u> D <u>K</u> T <u>D</u> L <u>Y</u> A <u>Q</u> G <u>Y</u> F <u>A</u> D <u>S</u> K <u>S</u> G <u>G</u> V <u>T</u> R <u>S</u> H <u>L</u> R <u>F</u> G <u>K</u> N <u>P</u> I <u>K</u> S <u>T</u> Y <u>L</u> V	480
F5_00952	FYGLGADGT <u>V</u> G <u>A</u> N <u>K</u> S <u>I</u> K <u>I</u> I <u>G</u> D <u>K</u> T <u>D</u> L <u>Y</u> A <u>Q</u> G <u>Y</u> F <u>A</u> D <u>S</u> K <u>S</u> G <u>G</u> V <u>T</u> R <u>S</u> H <u>L</u> R <u>F</u> G <u>K</u> N <u>P</u> I <u>K</u> S <u>T</u> Y <u>L</u> V	480
JCM3724_00851	FYGLGADGT <u>V</u> G <u>A</u> N <u>K</u> S <u>I</u> K <u>I</u> I <u>G</u> D <u>K</u> T <u>D</u> L <u>Y</u> A <u>Q</u> G <u>Y</u> F <u>A</u> D <u>S</u> K <u>S</u> G <u>G</u> V <u>T</u> R <u>S</u> H <u>L</u> R <u>F</u> G <u>K</u> N <u>P</u> I <u>K</u> S <u>T</u> Y <u>L</u> V	480

JCM3718_01643	STPNFVACSVPAYLNQYDMTSGLR EGGK FLLNCVWDKEEALQRIPNNV KRDIAR ANGKLY	540
F1_00215	SSPSFVACSVPAYLNQYDMTSGLKEGGK FLLNCVWDKEEALQRIPNNIKRDLAKANGKLY	537
Aru01_00063	SSPSFVACSVPAYLNQYDMTSGLKEGGK FLLNCVWDKEEALQRIPNNIKRDLAKANGKLY	540
F5_00952	SSPSFVACSVPAYLNQYDMTSGLKEGGK FLLNCVWDKEEALQRIPNNIKRDLAKANGKLY	540
JCM3724_00851	SSPSFVACSVPAYLNQYDMTSGLKEGGK FLLNCVWDKEEALQRIPNNIKRDLAKANGKLY	540
	:.*****:*****:***:*	
JCM3718_01643	IINATKLA HD I GLG QRTNTIMQ S AFFKLA EI IPFED AA Q Q YMKDYA K KS Y A AK GDDIVQLN	600
F1_00215	IINATKLAQEIGL G QRTNTIMQAAFFKLA EI IPFEEA Q Q Q YMKDYAYKSYGKKGDDIVQLN	597
Aru01_00063	IINATKLAQEIGL G QRTNTIMQAAFFKLA EI IPFEEA Q Q Q YMKDYAYKSYGKKGDDIVQLN	600
F5_00952	IINATKLAQEIGL G QRTNTIMQAAFFKLA EI IPFEEA Q Q Q YMKDYAYKSYGKKGDDIVQLN	600
JCM3724_00851	IINATKLAQEIGL G QRTNTIMQAAFFKLA EI IPFEEA Q Q Q YMKDYAYKSYGKKGDDIVQLN	600
	*****:*****:*****:***** ***.*****	
JCM3718_01643	Y Q AID I GASGLVE I EVDP PAWKDLEVE TK V EEA AKDCSCSSC DCSAVEK FV ER I AK P V N AI K	660
F1_00215	YRAIDV GASGLVE LEVDP PAWKDLEV VDSIKEEKENDTCNCKT TS SLKTFVQKIVEPINAIR	657
Aru01_00063	YRAIDV GASGLVE LEVDP PAWKDLEV VDSIKEEKENDTCNCKT TS SLKTFVQKIVEPINAIR	660
F5_00952	YRAIDV GASGLVE LEVDP PAWKDLEV VDSIKEEKENDTCNCKT TS SLKTFVQKIVEPINAIR	660
JCM3724_00851	YRAIDV GASGLVE LEVDP PAWKDLEV VDSIKEEKENDTCNCKT TS SLKTFVQKIVEPINAIR	660
	*:***:*****:***** .::* *: . .*. ::::***:*.::***:	
JCM3718_01643	GYDLPVSAF NGY EDGTFENGTS A FEKRGVAV D VP L W D STKCIQCNQCSYVCPHAA V IRPFL	720
F1_00215	GYDLPVSAFMGREDGTFENGTS A FEKRGVAVEVPEWIADNCIQCNQCSYVCPHAAIRPFL	717
Aru01_00063	GYDLPVSAFMGREDGTFENGTS A FEKRGVAVEVPEWIADNCIQCNQCSYVCPHAAIRPFL	720
F5_00952	GYDLPVSAFMGREDGTFENGTS A FEKRGVAVEVPEWIADNCIQCNQCSYVCPHAAIRPFL	720
JCM3724_00851	GYDLPVSAFMGREDGTFENGTS A FEKRGVAVEVPEWIADNCIQCNQCSYVCPHAAIRPFL	720
	***** * *****:*****.* * : :*****.*****	

JCM3718_01643	<u>V</u> SEEEK <u>A</u> ASPV <u>A</u> <u>F</u> <u>D</u> <u>T</u> L <u>K</u> <u>A</u> <u>M</u> <u>G</u> <u>K</u> <u>G</u> <u>L</u> <u>D</u> <u>G</u> <u>L</u> <u>T</u> YRIQV <u>S</u> PLDCVGCSCVNVCPAPGKA <u>I</u> TMQPIA	780
F1_00215	ITEEEKKASPVEFVTKKAVGKGL <u>E</u> DV <u>N</u> YRIQVTPLDCVGCSCVNVCPAPGKALIMKPIA	777
Aru01_00063	ITEEEKKASPVEFVTKKAVGKGL <u>E</u> DVSYRIQVTPLDCVGCSCVNVCPAPGKALIMKPIA	780
F5_00952	ITEEEKKASPVEFVTKKAVGKGL <u>E</u> DVSYRIQVTPLDCVGCSCVNVCPAPGKALIMKPIA	780
JCM3724_00851	ITEEEKKASPVEFVTKKAVGKGL <u>E</u> DVSYRIQVTPLDCVGCSCVNVCPAPGKALIMKPIA	780
	:**** * * * * *:****:..*****:*****:*****:*****:****	
JCM3718_01643	<u>M</u> SMDA <u>E</u> EDKKA <u>D</u> Y <u>L</u> <u>F</u> <u>N</u> <u>K</u> <u>V</u> <u>E</u> <u>Y</u> <u>R</u> <u>S</u> <u>N</u> <u>L</u> <u>M</u> <u>S</u> <u>I</u> <u>D</u> TVKGSQF <u>A</u> QPLFE <u>F</u> <u>H</u> GACPGCGETPYLK <u>A</u> I <u>T</u> <u>Q</u>	840
F1_00215	ESLDLEEDKKASYLYTSVPYRSDRMPSTSTVKGSQFSQPLFEFNGACPGCGETPYLKVISQ	837
Aru01_00063	ESLDLEEDKKASYLYTSVPYRSDRMPSTSTVKGSQFSQPLFEFNGACPGCGETPYLKVISQ	840
F5_00952	ESLDLEEDKKASYLYTSVPYRSDRMPSTSTVKGSQFSQPLFEFNGACPGCGETPYLKVISQ	840
JCM3724_00851	ESLDLEEDKKASYLYTSVPYRSDRMPSTSTVKGSQFSQPLFEFNGACPGCGETPYLKVISQ	840
	*: * ***** .*: ..* ***: * .*****:*****:*****:*****.*:*	
JCM3718_01643	<u>L</u> FGDRMM <u>I</u> ANA <u>T</u> GCSS <u>I</u> YSGSAP <u>A</u> TPYTTN <u>S</u> CGE <u>G</u> <u>P</u> <u>S</u> WASSLFEDNAE <u>F</u> <u>G</u> <u>M</u> <u>G</u> <u>M</u> <u>H</u> <u>V</u> A <u>V</u> EAL	900
F1_00215	MFGDRMMVSNASGCSSVYSGSAPSTPYTKNCHGEGPAWASSLFEDNAEYGFGMHIGVEAL	897
Aru01_00063	MFGDRMMVSNASGCSSVYSGSAPSTPYTKNCHGEGPAWASSLFEDNAEYGFGMHIGVEAL	900
F5_00952	MFGDRMMVSNASGCSSVYSGSAPSTPYTKNCHGEGPAWASSLFEDNAEYGFGMHIGVEAL	900
JCM3724_00851	MFGDRMMVSNASGCSSVYSGSAPSTPYTKNCHGEGPAWASSLFEDNAEYGFGMHIGVEAL	900
	:*****:***:****:*****:****.*. *****:*****:***:***:****	

Figure 7.13 Clustal Omega analysis of the Pyruvate synthase.

Five isolates were studied: ARU 01 (Aru01), F1, F5, JCM 3718 and JCM 3724. The changes seen in JCM 3718 are underscored in red. An * (asterisk) indicates positions which have a single, fully conserved residue. A : (colon) indicates conservation between amino acids with strongly similar properties (conservative replacements). A . (full stop) indicates conservation between amino acids with weakly similar properties. A gap indicates non-conserved amino acids.

The results of the analysis of the Pyruvate synthase of 5 representative isolates showed that whilst 4 isolates, ARU 01, F1, F5 and JCM 3724 shared greater than 99.75 % identity, JCM 3718 shared only 80 % identity with the other strains. This is highlighted in Figure 7.12 where all but 2 of the 139 amino acid differences, which were a mixture of conservative, semi-conservative and non-conservative replacements) were seen only in JCM 3718. One unique change was seen in the isolate F1. One polymorphism (V or I) was seen to differentiate JCM 3718, ARU 01 and isolate F5 from isolate F1 and JCM 3724: potentially discrimination clusters A and B+C. A BLASTp search using the sequence from JCM 3718 as the interrogator, identified 5 subsp. *necrophorum* strains; BTFR-1, BTFR-2, ATTC 51357, DJ-2 and B35 with 100 % coverage and more than 98.5 % identity. This strongly suggests a significant difference in protein sequence between the two subspecies with respect to this protein.

Figure 7.13 illustrates the Clustal Omega analysis of the DNA polymerase III subunit tau from 5 representative isolates. In this case fifteen amino acid differences were noted, all but one of which were unique to JCM 3718; these were a mixture of conservative, semi-conservative and non-conservative replacements. A BLAST search using the sequence from JCM 3718 as interrogator identified 6 subsp. *necrophorum* strains: BTFR-1, BTFR-2, DJ1, DJ2, DAB and B35 with 100 % identity, implying the differences were subspecies specific. One polymorphism (N or D) resulting in a conservative replacement differentiated JCM 3718, JCM 3724 and F1 from ARU 01 and F5; again, discriminating cluster A from B+C.


```

JCM3718_01085    PCERKDFARLFHYCLLQDRYQGKIE EKLLLSKMLNFPINNKVLFANLFLK    290
Aru01_00178     PCERKDFARLFHYCLLQARYQGKME EKLLLSKMLNFPINNKVLFANLFLK    290
F5_01504        PCERKDFARLFHYCLLQARYQGKME EKLLLSKMLNFPINNKVLFANLFLK    290
F1_00103        PCERKDFARLFHYCLLQARYQGKME EKLLLSKMLNFPINNKVLFANLFLK    290
JCM3724_01536   PCERKDFARLFHYCLLQARYQGKME EKLLLSKMLNFPINNKVLFANLFLK    290
*****:*****

```

Figure 7.14 Clustal Omega analysis of the DNA polymerase III subunit tau.

Five isolates were analysed, ARU 01 (Aru01), F1, F5, JCM 3718 and JCM 3724. An * (asterisk) indicates positions which have a single, fully conserved residue. A : (colon) indicates conservation between amino acids with strongly similar properties (conservative replacements). A . (full stop) indicates conservation between amino acids with weakly similar properties. A gap indicates non-conserved amino acids. Individual amino acid changes are highlighted in red.

```

JCM3718_00247    MKIEFLDGNVQEFQEACNMFVIAKSI SNLAKKAVAAKIDGELYDMSYILDHDAKVEFIM    60
Aru01_01113     MKIEFLDGNVQEFQEACNMFVIAKSI SNLAKKAVAAKIDGELYDMSYILDHDAKVEFIM    60
F5_00354        MKIEFLDGNVQEFQEACNMFVIAKSI SNLAKKAVAAKIDGELYDMSYILDHDAKVEFIM    60
F1_01307        MKIEFLDGNVQEFQEACNMFVIAKSI SNLAKKAVAAKIDGELYDMSYILDHDAKVEFIM    60
JCM3724_01407   MKIEFLDGNVQEFQEACNMFVIAKSI SNLAKKAVAAKIDGELYDMSYILDHDAKVEFIM    60
*****

JCM3718_00247    PESEEGVEVIRHSA AHLMAQAVIRLFPGTKVTIGPSIENGFYYDFDPKEQFTEEDLLKIE    120
Aru01_01113     PESEEGVEVIRHSA AHLMAQAVIRLFPGTKVTIGPSIENGFYYDFDPKEQFTEEDLLKIE    120
F5_00354        PESEEGVEVIRHSA AHLMAQAVIRLFPGTKVTIGPSIENGFYYDFDPKEQFTEEDLLKIE    120
F1_01307        PESEEGVEVIRHSA AHLMAQAVIRLFPGTKVTIGPSIENGFYYDFDPKEQFTEEDLLKIE    120
JCM3724_01407   PESEEGVEVIRHSA AHLMAQAVIRLFPGTKVTIGPSIENGFYYDFDPKEQFTEEDLLKIE    120
*****

```

JCM3718_00247	EEMKRLSKEDIKVERFMSREEAIEYFEKLGEHYKVEIIKDIAKGEQLSFYRQGEFVDLC	180
Aru01_01113	EEMKRLSKEDIKVERFMSREEAIEYFEKLGEHYKVEIIKDIAKGEQLSFYRQGEFVDLC	180
F5_00354	EEMKRLSKEDIKVERFMSREEAIEYFEKLGEHYKVEIIKDIAKGEQLSFYRQGEFVDLC	180
F1_01307	EEMKRLSKEDIKVERFMSREEAIEYFEKLGEHYKVEIIKDIAKGEQLSFYRQGEFVDLC	180
JCM3724_01407	EEMKRLSKEDIKVERFMSREEAIEYFEKLGEHYKVEIIKDIAKGEQLSFYRQGEFVDLC ****:*****	180
JCM3718_00247	RGPHVPSTGHIIKAIKLKSVAGAYWRGDSKNKMLQRIYGYAFATEKDLKDFLQLMEEAEKR	240
Aru01_01113	RGPHVPSTGHIIKAIKLKSVAGAYWRGDSKNKMLQRIYGYAFATEKDLKDFLQLMEEAEKR	240
F5_00354	RGPHVPSTGHIIKAIKLKSVAGAYWRGDSKNKMLQRIYGYAFATEKDLKDFLQLMEEAEKR	240
F1_01307	RGPHVPSTGHIIKAIKLKSVAGAYWRGDSKNKMLQRIYGYAFATEKDLKDFLQLMEEAEKR	240
JCM3724_01407	RGPHVPSTGHIIKAIKLKSVAGAYWRGDSKNKMLQRIYGYAFATEKDLKDFLQLMEEAEKR *****:*****	240
JCM3718_00247	DHRKLGKELELFFLSEYGPFPFFLPKGMVLRNTLIDLWRAEHEKAGYVQIDTPIMLNRE	300
Aru01_01113	DHRKLGKELELFFLSEYGPFPFFLPKGMVLRNTLIDLWRAEHEKAGYVQIDTPIMLNRE	300
F5_00354	DHRKLGKELELFFLSEYGPFPFFLPKGMVLRNTLIDLWRAEHEKAGYVQIDTPIMLNRE	300
F1_01307	DHRKLGKELELFFLSEYGPFPFFLPKGMVLRNTLIDLWRAEHEKAGYVQIDTPIMLNRE	300
JCM3724_01407	DHRKLGKELELFFLSEYGPFPFFLPKGMVLRNTLIDLWRAEHEKAGYVQIDTPIMLNRE *****	300
JCM3718_00247	LWEISGHWFNYRENMYTSSIDDVDFAIKPMNCPGGVLAFKYQQHSYRDLPARVAELGKVH	360
Aru01_01113	LWEISGHWFNYRENMYTSSIDDVDFAIKPMNCPGGVLAFKYQQHSYRDLPARVAELGKVH	360
F5_00354	LWEISGHWFNYRENMYTSSIDDVDFAIKPMNCPGGVLAFKYQQHSYRDLPARVAELGKVH	360
F1_01307	LWEISGHWFNYRENMYTSSIDDVDFAIKPMNCPGGVLAFKYQQHSYRDLPARVAELGKVH	360
JCM3724_01407	LWEISGHWFNYRENMYTSSIDDVDFAIKPMNCPGGVLAFKYQQHSYRDLPARVAELGKVH *****	360

JCM3718_00247	RHEFSGALHGLFRVRAFTQDDSHIFMTEEQIESEIIGVVNLIDKFYSKLFQYSIELST	420
Aru01_01113	RHEFSGALHGLFRVRAFTQDDSHIFMTEEQIESEIIGVVNLIDKFYSKLFQYSIELST	420
F5_00354	RHEFSGALHGLFRVRAFTQDDSHIFMTEEQIESEIIGVVNLIDKFYSKLFQYSIELST	420
F1_01307	RHEFSGALHGLFRVRAFTQDDSHIFMTEEQIESEIIGVVNLIDKFYSKLFQYSIELST	420
JCM3724_01407	RHEFSGALHGLFRVRAFTQDDSHIFMTEEQIESEIIGVVNLIDKFYSKLFQYSIELST	420

JCM3718_00247	RPEKSIGTDEIWEKAEAAALAGALHHLGREFKINEGDGAFYGPKLDFKIKDAIGRTWQCGT	480
Aru01_01113	RPEKSIGTDEIWEKAEAAALAGALHHLGREFKINEGDGAFYGPKLDFKIKDAIGRTWQCGT	480
F5_00354	RPEKSIGTDEIWEKAEAAALAGALHHLGREFKINEGDGAFYGPKLDFKIKDAIGRTWQCGT	480
F1_01307	RPEKSIGTDEIWEKAEAAALAGALHHLGREFKINEGDGAFYGPKLDFKIKDAIGRTWQCGT	480
JCM3724_01407	RPEKSIGTDEIWEKAEAAALAGALHHLGREFKINEGDGAFYGPKLDFKIKDAIGRTWQCGT	480

JCM3718_00247	IQLDFNLPERFDVTYVGEDGEGKHRPVMHRVIYGSIERFIGILIEHYAGAFPMWLAPVQI	540
Aru01_01113	IQLDFNLPERFDVTYVGEDGEGKHRPVMHRVIYGSIERFIGILIEHYAGAFPMWLAPVQI	540
F5_00354	IQLDFNLPERFDVTYVGEDGEGKHRPVMHRVIYGSIERFIGILIEHYAGAFPMWLAPVQI	540
F1_01307	IQLDFNLPERFDVTYVGEDGEGKHRPVMHRVIYGSIERFIGILIEHYAGAFPMWLAPVQI	540
JCM3724_01407	IQLDFNLPERFDVTYVGEDGEGKHRPVMHRVIYGSIERFIGILIEHYAGAFPMWLAPVQI	540

JCM3718_00247	KVLTINDDCVSYAKEVVEALKGQGIRAELDDRSESIGYKIREANGRYKIPMQVIIGKNEI	600
Aru01_01113	KVLTINDDCVSYAKEIVEKLKEQGIRAELDDRSESIGYKIREANGRYKIPMQVIIGKNEI	600
F5_00354	KVLTINDDCVSYAKEIVEKLKEQGIRAELDDRSESIGYKIREANGRYKIPMQVIIGKNEI	600
F1_01307	KVLTINDDCVSYAKEIVEKLKEQGIRAELDDRSESIGYKIREANGRYKIPMQVIIGKNEI	600
JCM3724_01407	KVLTINDDCVSYAKEIVEKLKEQGIRAELDDRSESIGYKIREANGRYKIPMQVIIGKNEI	600

*****: ** ** *****

The analysis of the Threonine--tRNA ligase 2 (Figure 7.14) showed that ARU 01 and F5 shared 100 % identity, likewise, JCM 3724 shared 100 % identity with F1 and greater than 99.6 % identity with ARU 01 and F5; JCM 3718 shared about 98.5 % identity with each of the other isolates. JCM 3718 had 8 unique amino acid changes, 3 of which were non-conservative, and one polymorphism (K or Q) was noted to differentiate ARU 01 and F5 from JCM 3724 and F1, potentially discriminating cluster A from B+C; at the same site JCM 3718 had a different amino acid (R). The sequence of JCM 3718 was used in a BLASTp search as interrogator and detected 6 isolates with 100 % identity; the subsp. *necrophorum* strains BL. BTFR-1, 2 with no recorded speciation and 2 subsp. *necrophorum* suggesting the differences seen were likely to be subspecies specific.

7.4 Discussion

Whole genome sequencing (WGS) was not an original aim, but during the project the cost of WGS significantly dropped to the point at which it was more cost effective to sequence whole genomes than to sequence individual genes. Hence, whole genome sequencing was performed on the type culture strains JCM 3718, JCM 3724, ARU 01 and 17 clinical isolates. The data was combined with all data available in databases (this included *F. necrophorum*, *Fusobacteria* sp. (not speciated) and other authenticated Fusobacterial species) and analysed by Dr Lesley Hoyles (see acknowledgment).

One of the clinical isolates in this study, F88, was shown to resemble *Fusobacterium hwasookii*, the four subspecies of *Fusobacterium nucleatum*, *Fusobacterium periodonticum*, *Fusobacterium massiliens* and *Fusobacterium russii* rather than *F. necrophorum*. Although it shared 99.3 % sequence similarity (1458 nt) with *Fusobacterium simiae*, further analysis was hampered by the lack of whole genome sequence data for a reference strain. This issue had not been detected in biochemical tests or by microbesNG; the isolate was removed from the dataset. This highlights the value of WGS in speciation. Within the genomes, contaminants were identified, for example in isolate F80, by analysis of the *Fusobacterium necrophorum* assemblies against the nt (NCBI non-redundant

nucleotide) database (created 3 March 2018) of Centrifuge 1.0.3. Any potentially contaminated data was removed from the dataset. In this way, all the data generated in the current project and that harvested from databases was authenticated prior to further analyses.

The analyses of the selected, authenticated 49 genomes of *F. necrophorum* demonstrated the presence of 1053 core genes (present in $\geq 99\%$ – 100% of strains), 276 soft core genes (present in $\geq 95\%$ – $< 99\%$ of strains), 1359 shell genes (present in $\geq 15\%$ – $< 95\%$ of strains) and 4131 cloud genes (present in 0% – $< 15\%$ of strains); a total of 6819 genes were detected. An analysis of the core genes detected 37436 SNPs. As expected, based on sub-speciation analysis, most of the strains clustered with the type strain of *Fusobacterium necrophorum* subsp. *funduliforme*; these shared 1253 core genes and 4412 accessory genes. The clinical isolates sequenced as part of this project, with the exception of F88 and F80 were authenticated as *Fusobacterium necrophorum* subsp. *funduliforme*. Strains DAB, BFTR-1, BFTR-2, DJ-1, DJ-2 and BL clustered with JCM 3718, the type strain of *Fusobacterium necrophorum* subsp. *necrophorum*; these shared 1540 core genes and 1794 accessory genes. The sub-speciation was confirmed by PCA of accessory genes present. Interestingly, PCA of the accessory genes of *Fusobacterium necrophorum* subsp. *funduliforme* revealed there to be three clusters, A, B and C, within the subspecies. Cluster A contained the type strain of *Fusobacterium necrophorum* subsp. *funduliforme* (JCM 3724) and isolates F1, F21, F39, F40, F70, F1314, LS_1291, F1353 and LS_1264, while Cluster B contained isolates F24, F87, Fnf 1007, LS_1195, F1267, F1285, F1250, LS_1260, F1330, F1365, F1309, P1_LM and P1_CP; cluster C was more diffuse. Each cluster had its own unique genes whilst all three shared 790 core genes.

The relevance of these clusters to pathogenicity, clinical profile, ecological/environmental niche or geographical location has yet to be explored. One of the preliminary aims was to define differences between the Lemierre's strain and less pathogenic isolates. From the genomic data presented thus far, ARU 01 clustered with 5 clinical isolates F11, F30, F42, F52 and F87 whilst at the protein level, it was found in cluster B+C along with the majority of clinical isolates. At the start of 2019, the whole genome sequences of two further Lemierre's isolates became available; a limited analysis (data not shown) showed one

belonged to cluster A whilst the other belonged to cluster B+C (Lyster *et al.*, 2019); this suggested that Lemierre's disease was not simply a product of a distinct, more virulent strain. The availability of the two new Lemierre's strains should enable a more in-depth comparative analysis that may reveal new insights.

For the clinical isolates collected in this study no clinical data was available; except that these were from throat swabs of patients with persistent sore throats. Similarly, many of the sequences lodged in databases do not have further available information. Clearly at the genomic level there is scope for more in-depth research; this was outside the timescale of the current project. It was obvious that there were significant differences between subsp. *necrophorum* and *funduliforme* that could be used to develop a new, robust assay for identification of the two sub-species. The relevance of the 3 clusters of *F. necrophorum* subsp. *funduliforme* is yet to be determined, but it would be profitable to review these for the presence/absence of known or potential virulence genes. Although the three *Fusobacterium necrophorum* subsp. *funduliforme* clusters (A, B and C) shared 790 core genes, each cluster had its own unique genes (Figure 7.8); this would enable targeted assays to be developed. However, in a clinical environment, techniques reliant on the presence/absence of genes may be prone to misinterpretation whilst those based on sequence variations within a gene, or a number of genes would be more reliable.

A small study of the outcome of non-synonymous SNPs, on protein sequences, was undertaken to understand the impact on protein structure and, potentially, function. The alignment of LpxI sequences showed 3 distinct clusters of isolates; based on analysis of 10 polymorphic sites, *F. necrophorum* subsp. *funduliforme* isolates F1, F21, F39, F40, F62, F 70, 05310, B35. JCM 3724, WP1(ATCC 51357) formed one cluster defined at the genomic level as cluster A: F5, F11, F24, F30, F42, F52, ARU 01, F59, F80, F86, F87, WP2 the second cluster defined as clusters B+C at the genomic level and a cluster of the *F. necrophorum* subsp. *necrophorum* isolates JCM 3718 and WP3 (DAB, BFTR-1, DJ-1, BFTR-2, DJ-2). The subsp. *necrophorum* cluster had two unique changes and then shared 8 of 10 sites with the cluster B+C and 2 with cluster A. From the data, clusters B and C could not be separated. Only one of the polymorphisms caused a change that

could affect the active site of the enzyme; further *in silico* and biochemical studies need to be performed to assess the effect.

In contrast, in an analysis of a small portion of the Leukotoxin protein, the amino acid sequence of JCM 3718 and other subsp. *necrophorum* isolates were significantly different from the subsp. *funduliforme* isolates. These differences included non-conservative amino acid changes that could affect both protein structure and function. Two clusters, A [F1, F21, F39, F40 and JCM 3724], and B+C [F5, F11, F24, F30, F42, F52 and ARU 01] that were differentiated based on the analysis of 65 non-synonymous SNPs were noted; identical to those obtained for LpxI. These results suggest that the two subsp. *funduliforme* clusters (A and B+C) split and diverged and that all strains/isolates represented today are derived from 2 original variants. The amino acid differences included non-conservative amino acid changes that could affect both protein structure and function. Further studies are required to determine the likely impact of these polymorphisms on the function of this known virulence factor. The conservation of 65 polymorphisms in the two subsp. *funduliforme* clusters is suggestive of 2 evolutionary distinct strains.

In the 900 amino acids of Pyruvate kinase 139 amino acid polymorphisms were seen; of these, all but 2 were unique to subspecies *necrophorum* re-iterating the differences between the two subspecies. These were a mixture of conservative, semi-conservative and non-conservative amino acid replacements. The subsp. *funduliforme* isolates shared 99.75 % identity and only one polymorphism (V or I; a conservative replacement) was seen to differentiate JCM 3718, ARU 01 and isolate F5 (cluster B+C) from isolate F1 and JCM 3724 (cluster A). By contrast, analysis of the Galactose binding periplasmic protein highlighted only 6 amino acid differences, all conservative replacements, of which 4 were unique to the subsp. *necrophorum*. The Elongation factor Tu was also highly conserved with only one conservative amino acid change (R to K) in JCM 3718.

Due to the degenerate nature of the genetic code, many genetic polymorphisms do not result in a change in the encoded amino acid: synonymous SNPs. Amino acid conservation may be of greater importance in those proteins whose presence is vital to the functioning of the organism, however, care should be taken to determine their likely impact; changes that impact on protein structure or affect the

active site/binding site of a protein are more likely to be deleterious. Most of the non-synonymous changes that differentiated the subsp. *funduliforme* isolates involved amino acids of similar properties unlikely to impact structure or function. However, those differentiating the two subspecies, *funduliforme* and *necrophorum* were a mixture of conservative, semi-conservative and non-conservative replacements.

The similarity between the encoded proteins in JCM 3724 and the clinical isolates F1, F21, F39, F40 is of interest as the type strain was originally isolated from a bovine liver abscess in 1985 (https://www.jcm.riken.jp/cgi-bin/jcm/jcm_number?JCM=3724) whereas the clinical samples were collected from patients with recurrent sore throats within the last decade. The conservation of 65 non-synonymous SNPs in the portion of the Leukotoxin protein suggests a strong relationship between these strains: further research could reveal the dynamics of their evolution.

Of course, there are many more changes seen at the genomic than at the protein level as synonymous SNPs, including those involving the third nucleotide of a codon that do not change the encoded amino acid, are not represented in the protein studies. Organisms also have a codon bias and hence a change from a codon to one not, or rarely used by the organism could result in either a reduction in transcription or no transcription at all leading to lower levels of proteins or fore-shortened proteins (Sharp and Li, 1987). Although from a functional standpoint the impact of non-synonymous SNPs on amino acid sequence has been thought to be key, synonymous SNPs may change mRNA structure and stability (Kudla *et al.*, 2009; Goodman *et al.*, 2013; Firnberg *et al.*, 2014), alter protein or nucleic acid binding sites (Li *et al.*, 2012), increase or decrease the rate of translation (Sørensen and Pedersen, 1991) and impact protein folding and solubility (Rosano and Ceccarelli, 2009; Zhang *et al.*, 2009). Indeed, Agashe *et al.*, (2016) were able to demonstrate that synonymous SNPs in the *fae* gene of *Methylobacterium extorquens* decreased both enzyme production and organism fitness. Genetic engineering of point mutations in the N-terminal region of the gene (including four synonymous mutations) impacted transcription levels, enzyme production, and/or enzyme activity.

There is much future work required to determine the impact of both the synonymous and non-synonymous SNPs on the functioning of *F. necrophorum*. Clearly the genomic data is a valuable resource for future work. In chapter 8, analysis of the data generated was used to unravel the biochemical pathways involved in sialic acid uptake/metabolism/catabolism/cell surface expression, in *F. necrophorum*.

Acknowledgements

Genomic analyses described herein were performed by Lesley Hoyles, an MRC Intermediate Research Fellow in Data Science (MR/L01632X/1, UK MED-BIO). This work used the computing resources of the UK MEDical BIOinformatics partnership – aggregation, integration, visualisation and analysis of large, complex data (UK MED-BIO), which is supported by the Medical Research Council (grant number MR/L01632X/1).

Chapter 8

8 Sialylation pathways in *F. necrophorum*; the utility of *in silico* analysis of WGS data

8.1 Introduction

The processes involved in sialic acid utilisation can be broken down into uptake, *de novo* synthesis, polysialic acid (PSA) capsule biosynthesis and export, O-acetylation, LPS sialylation, surface expression and catabolism (Figure 8.1); organisms may possess none, some or all of these processes. Sialic acid metabolism and surface expression is complex with some organisms able to scavenge sialic acid from the host: in human blood the concentration of free sialic acid is 16 mg/L (Uslu *et al.*, 2003). In biofilms, production of sialidases by one partner frees sialic acids from host glycoconjugates that can be utilised by other partners. Swords *et al.*, (2004) demonstrated that *Haemophilus influenzae* scavenged sialic acids from the environment that it then was able to use to sialylate lipooligosaccharides (LOS). Growth in a sialic acid free medium resulted in significant reduction of cell surface expression of sialic acid and a decrease in biofilm formation. The data supported the hypothesis that sialylated LOS glycoforms promote biofilm formation and persistence *in vivo*.

In 2014, Yoneda *et al.*, demonstrated that *F. nucleatum* could both catabolise and synthesise sialic acid. They concluded that surface sialylation was a general ability of *F. nucleatum* and *F. periodonticum*, the two major fusobacterial species in the oral cavity whereas sialic acid catabolism was probably minimal. They reported that the FN1470 – FN1476 operon encoded the *nan* operon: this comprised specific TRAP transporters (FN1472 and FN1473), the catabolic enzymes NanA, K, and E (FN1474– FN1476), an operon transcription regulator (FN1471) and a sialic acid mutarotase NanM (FN1470) that facilitated the transport of exogenous sialic acid.

Although the *nan* operon responded to the addition of exogenous sialic acid, the authors suggested that sialic acid probably did not play a major role in energy generation. Consistent with evidence of cell surface sialylation, albeit patchy in nature, the authors identified the FN1682 – FN1686 operon as the *neu* operon responsible for *de novo* sialic acid synthesis; this contained genes with roles in lipopolysaccharide (LPS) synthesis/modification. The *neu* operon contained a candidate *neuB* orthologue (FN1684), a gene encoding a protein with both NeuA

and NeuB domains (FN1686) and at least two other genes with predicted roles in LPS or cell surface modification. There was no candidate for *neuC* in this operon; this suggests that *de novo* sialic acid synthesis in *F. nucleatum* would require either an alternative source of N-acetylmannosamine (ManNAc) or a novel UDP-N-acetylglucosamine 2-epimerase with little homology to NeuC orthologs. Nevertheless, this work did suggest that, *F. nucleatum* subsp. *nucleatum* was capable of both sialic acid catabolism and synthesis.

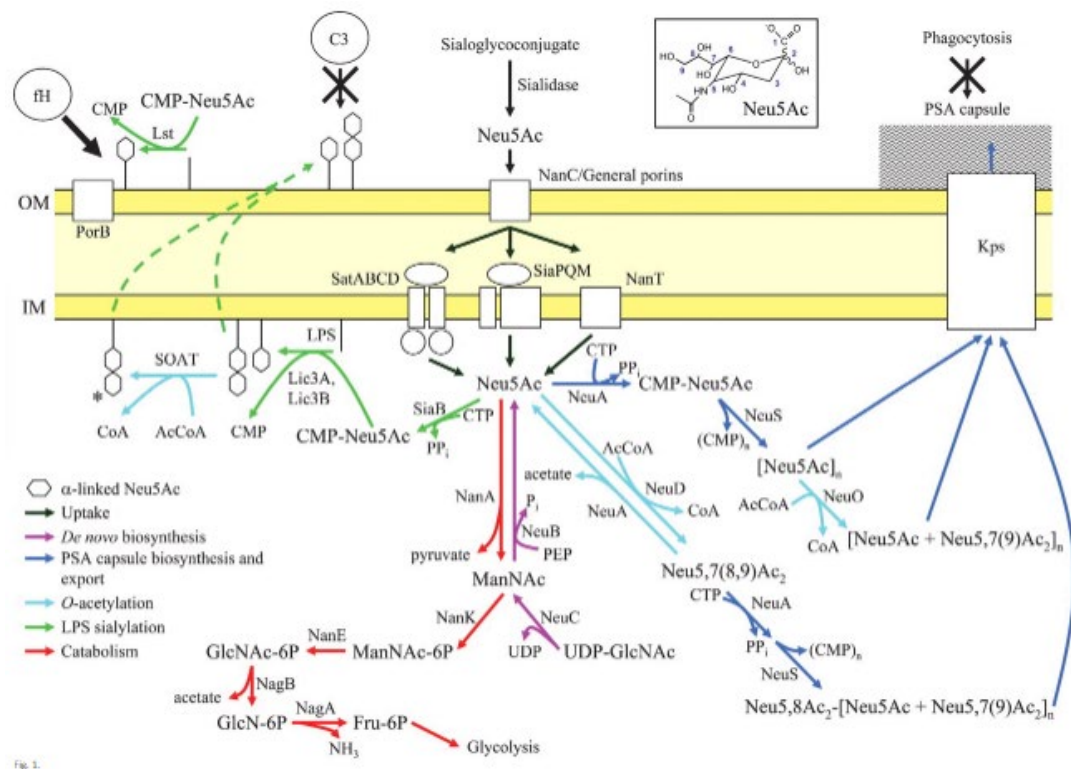


Figure 8.1 Overview of the major pathways for sialic acid utilization in bacterial pathogens.

This figure summarizes the major pathways and mechanisms discussed in <https://mic.microbiologyresearch.org/content/journal/micro/10.1099/mic.0.2007/009480-0#tab2> (see text for a description of each pathway) Sialic acid is shown as Neu5Ac. The light-green dotted line represents the pathways (mostly not defined) by which the LPS is exposed on the outer membrane. **Abbreviations:** IM, inner membrane; OM, outer membrane; Neu5Ac, N-acetylneuraminic or sialic acid; ManNAc, N-acetylmannosamine; GlcNAc, N-acetylglucosamine; GlcN, glucosamine; Fru, fructose; PSA, polysialic acid; PEP, phosphoenolpyruvate; Lst, *Neisseria* LPS sialyltransferase; NanC, Neu5Ac-specific porin; Kps, *E. coli* PSA capsule export system; SatABCD, *H. ducreyi* Neu5Ac ABC (ATP-binding cassette) transporter; SiaPQM, Neu5Ac TRAP (tripartite ATP-independent periplasmic) transporter; NanT, Neu5Ac transporter; SiaB and NeuA, respectively CMP-Neu5Ac synthetases /deacetylase; Lic3A, Lic3B sialyltransferases; SOAT, Neu5Ac O-acetyltransferase; NeuC, UDP-GlcNAc 2-epimerase; NeuB, Neu5Ac synthase; NeuS, polysialyltransferase; NeuO, PSA O-acetyltransferase; NeuD, Neu5Ac O-acetyltransferase; NanA, Neu5Ac aldolase; NanK, ManNAc kinase; NanE, ManNAc-6P epimerase; NagB, GlcNAc-6P deacetylase; NagA, GlcN-6P deaminase.

In 2016, Lewis and colleagues performed bioinformatics analysis on 31 genomes to determine whether *de novo* sialic acid synthesis was conserved amongst all four subspecies of *F. nucleatum* (*animalis*, *nucleatum*, *vincentii* and *polymorphum*). NeuA, NeuB and NeuC amino acid sequences from strain *F. nucleatum* subsp. *polymorphum* ATCC10953 and relevant sequences from *E. coli* were used to interrogate the translated proteins encoded by fusobacterial genomes using BLASTP. Two of four strains of subsp. *polymorphum* possessed all three enzymes needed for *de novo* sialic acid synthesis (encoded by *neuA*, *neuB* and *neuC*). Two of the six strains ssp *vincentii* encoded genes required for *de novo* sialic acid synthesis that were nearly identical to those found in the ssp *polymorphum* strains. Of the remaining strains, several encoded one or more putative homologues of these enzymes; their amino acid sequences shared limited identity to those of *F. nucleatum* ATCC10953 or *E. coli* UTI89 pathways. However, in a number of sequenced strains there was no evidence that a complete sialic acid pathway existed. High performance liquid chromatography (HPLC) and mass spectrometry demonstrated that high levels of Neu5Ac were produced by *F. nucleatum* subsp. *polymorphum* ATCC10953. The authors hypothesised that sialic acids were used by *F. nucleatum* to evade the immune system and could aid dissemination through the host bloodstream.

In 2017, Vinogradov *et al.*, isolated lipopolysaccharide from *F. nucleatum* strain 10953 and identified a trisaccharide repeating unit of the O-antigen with the following structure:



where Ac indicates 4-N-acetylation of ~30% FucNAc4N residues.

Additionally, they showed, using a chemical stain-based methodology that, in a bacterial smear, some but not all the *F. nucleatum* cells expressed cell surface sialic acid.

The aims of this study were to:

1. determine, using bioinformatics the likely biosynthetic pathways for sialic catabolism, sialylation and *de novo* synthesis in *F. necrophorum* and a range of other *Fusobacterium* sp.
2. investigate any polymorphisms that could be associated with virulence/pathogenicity.

As little was known about sialic acids in *F. necrophorum*, research was undertaken to understand the metabolic pathways concerned. Although no information was available on sialic acid catabolism or *de novo* synthesis in *F. necrophorum*, the work presented in chapter 5 suggested that sialic acid was present both on the cell surface and intracellularly. A comparative study of sialic acid pathways was undertaken using sequences derived in the current study (chapter 7, section 7.2.1) and those lodged in available databases.

8.2 Methods

To identify candidate proteins, amino acid sequences were downloaded from Uniprot; identification was by gene or protein name. BLASTP searches were performed to verify protein identity. Genomic data was generated as described in chapter 7, section 7.2.1. Searches of the translated protein sequences were performed manually using search terms such as gene name, protein name and/or conserved amino acid sequences.

For the generation of Table 8.2, annotated amino acid sequence data (from microbesNG) were interrogated using gene names, enzyme names or short segments of conserved sequences (see table for details).

8.3 Results

8.3.1 Interrogation of the Uniprot database

The Uniprot database (www.uniprot.org) for *Fusobacterium necrophorum* was interrogated using gene and enzyme names and/or conserved amino acid motifs and candidate proteins were subjected to BLASTP analysis to check identity. Whilst *nanA*, *nanE*, *nanK*, *nanT*, *nagA*, *nagB*, *neuA*, *siaA*, *siaP*, *siaT* and *MurJ* were identified; *neuB*, *neuC*, *neuD* and *neuS* were absent (Table 8.1).

Table 8.1 Candidate proteins for sialic acid pathways of *F. necrophorum*

Gene	<i>F. necrophorum</i> candidate	Enzyme specificity
<i>nanA</i>	A0A017H2Y7	N-acetylneuraminate lyase
<i>nanE</i>	A0A017H4J6	N-acetylmannosamine-6-phosphate 2-epimerase
<i>nanK</i>	A0A162IIB5	N-acetylmannosamine kinase
<i>nanM</i>	A0A2X3KQ65	N-acetylneuraminate epimerase
<i>nanT</i>	No candidate	Sialic acid transporter
<i>nagA</i>	J5TYX7	N-acetylglucosamine-6-phosphate deacetylase
<i>nagB</i>	A0A017H7C7	Glucosamine-6-phosphate deaminase
<i>neuA</i>	A0A2X3MEE5	N-acetylneuraminate cytidyltransferase
<i>neuB</i>	No candidate	N-acetyl neuramic acid synthetase
<i>neuC</i>	No candidate	UDP-N-acetyl-D-glucosamine 2-epimerase
<i>neuS</i>	No candidate	Poly-alpha-2,8 sialosyl sialyltransferase
<i>siaA</i>	A0A017H790	Lipooligosaccharide sialyltransferase
<i>SiaP</i>	J5W387	Sialic acid-binding periplasmic protein
<i>SiaT</i>	J5U0J4	Sialic acid TRAP transporter, permease protein
<i>murJ(mviN)</i>	J5W1X4	Lipid II flippase

Lewis *et al.*, (2016) had demonstrated probable *de novo* synthesis of sialic acids in some isolates of *F. nucleatum*, the information in that paper was used to highlight genes utilised by *F. nucleatum* to synthesise sialic acid. Each protein sequence was retrieved from Uniprot, subjected to BLASTP to verify identity and was then used to interrogate the *F. necrophorum* proteome. Potential homologues were then subjected to BLASTP to verify identity. The results (Table 8.1) showed that two key enzymes for *de novo* synthesis, NeuB and NeuC, were not present in the *F. necrophorum* sequences available on Uniprot. In the case of NeuB, BLASTP identified as the closest match a hypothetical protein with 27 % identity with only 12 % coverage. This protein had homologues (30 %) only in

Fusobacterium sp. In the case of NeuC, UDP-N-acetyl-D-glucosamine 2-epimerase, the only match detected was to an unrelated enzyme, nucleotidyl transferase, with 34 % identity 13 % coverage. This nucleotidyl transferase was similar (40 %) to nucleotidyl transferases in other bacteria. Thus, there was no compelling evidence for *de novo* sialic acid synthesis. However, based on the bioinformatics data collected from Uniprot, *F. necrophorum* possessed the genes required for scavenging and catabolising sialic acid, LPS sialylation and expression on the cell surface; Figure 8.2 shows the proposed pathway for sialic acid utilisation in *F. necrophorum*.

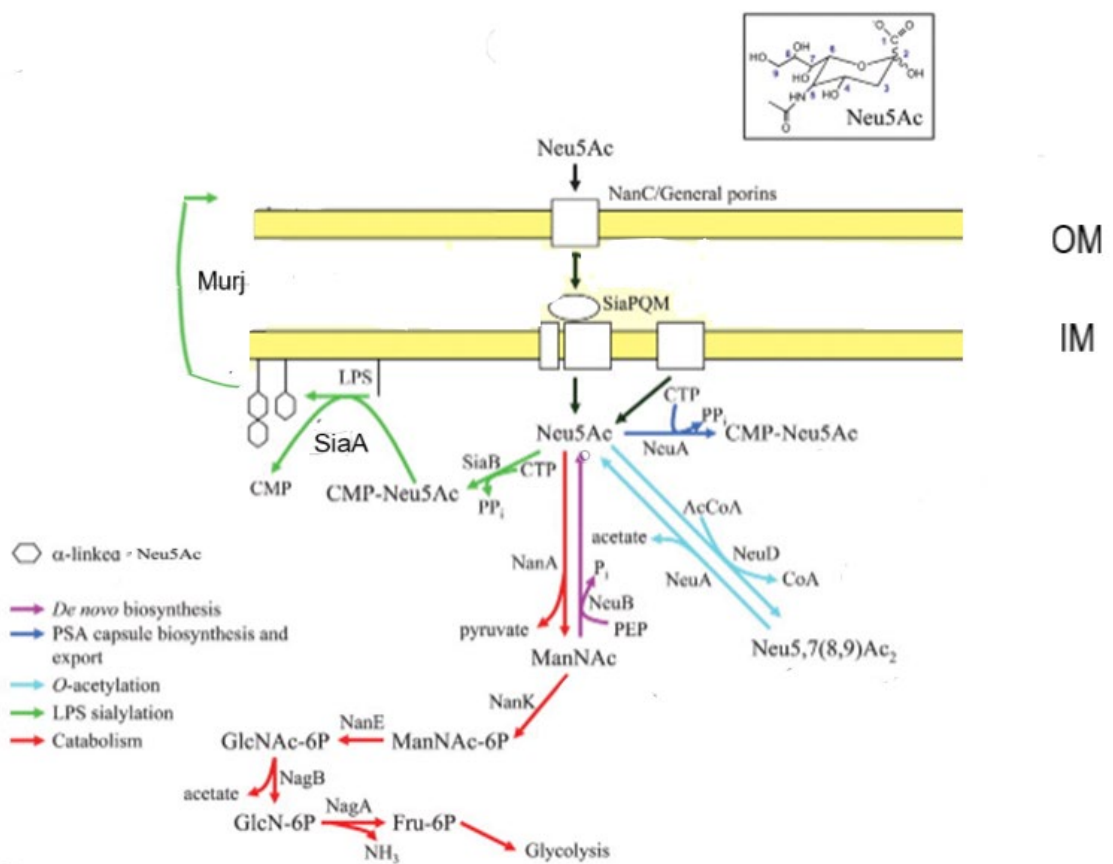


Figure 8.2 Proposed major pathways for sialic acid utilization in *F. necrophorum*.

Subsequent to this primary study, novel genome data was generated from a range of clinical and type strains of *F. necrophorum* (see Chapter 7 section 7.2.7), this was combined with available data on *Fusobacterium* sp. The translated gene products were interrogated for the presence/absence of enzymes/proteins required for sialic acid uptake, catabolism, metabolism, sialylation of LPS and transfer to the cell surface. The data was interrogated, by keywords or sequence,

for the presence/absence of *SiaA* (lipo-oligosaccharide sialyltransferase), *NagA* (N-acetylglucosamine-6-phosphate deacetylase), *NagB* (glucosamine-6 phosphate deaminase), *NeuA* (N-acetylneuraminic acid cytidyltransferase), *NeuB* (N-acetyl neuramic acid synthetase), *NeuC* (UDP-N-acetyl-D-glucosamine 2-epimerase), *NanA* (N-acetylneuraminic acid lyase), *NanE* (N-acetylmannosamine-6-phosphate 2-epimerase), *NanK* (N-acetylmannosamine kinase (annotated as glucoside kinase in the data)), *NanM* (N-acetylneuraminic acid epimerase), *NanT* (Sialic acid transporter), *NeuO* (Polysialic acid O-acetyltransferase), *NeuS* (Poly- α -2,8 sialosyl sialyltransferase), *SiaM* (sialic acid TRAP transporter large permease protein), *SiaQ* (sialic acid TRAP transporter small permease protein), *SiaT* (sialic acid TRAP transporter permease protein), *SiaP* (sialic acid-binding periplasmic protein) (Table 8.1).

Analysis of the data from *F. necrophorum* subsp. *funduliforme* (41 isolates) showed that all isolates possessed the *murJ*, *nagA*, *neuA*, *nanA*, *nanE*, *nanK*, *nanM*, *siaT* and *siaP* genes. Almost all possessed *nagB* (40/41). In most isolates 2-4 copies of *siaP* and *siaT* were found within the genome; one copy of each gene was found within the operon shown in Figure 8.3. There was no evidence for the presence of *neuB*, *neuC*, *nanT*, *neuO*, *neuS* in any of the *F. necrophorum* subsp. *funduliforme* isolates; most also lacked *siaM* (40/41) and *siaQ* (39/41). The most obvious variation was in the presence/absence of *siaA*; 14 of the 41 isolates possessed the *siaA* gene. This gene encodes an enzyme that is key in the sialylation of lipooligosaccharides prior to cell surface expression. Of the two control strains, ARU 01 did not have the gene whilst JCM 3724 was shown to possess it. Of the clinical strains sequenced in the current study (see chapter 8), 6 had the gene whilst 8 did not. By comparison, in the *F. necrophorum* subsp. *necrophorum* isolates there were some significant differences. All isolates (7) had the *murJ*, *nagA*, *nagB*, *nanA*, *nanE*, *siaP* and *siaT* genes and lacked *neuB*, *neuC*, *nanT*, *neuO*, *neuS* and *siaM*. Only 4/7 isolates had the *neuA* gene, 2/7 lacked *nanK*, and 6/7 possessed the *siaQ* genes. With respect to *siaA*, 3/7 isolates were positive for this gene. This data suggests that lipooligosaccharide sialylation, and hence the potential for surface expression of sialic acid in subsp. *funduliforme* and subsp. *necrophorum* is different, but there are also differences in some strains within each subspecies. Whether there are links between virulence and sialic acid expression is as yet unclear. It would have been predicted that ARU 01, the isolate

from the Lemierre's case would be more virulent than those isolates from clinical samples from patients with persistent sore throat. Since ARU 01 lacked *siaA* and the gene was polymorphic within the clinical isolates, 6/14 possessed the gene, sialic acid expression does not seem to be directly involved in virulence.

An analysis (Table 8.2) of a limited range of other *Fusobacterium* species, *F. equinum*, *F. gonidiaformans*, *F. hwasookii*, *F. mortiferum*, *F. naviforme*, *F. necrogenes*, *F. nucleatum* (4 isolates), *F. perfoetens*, *F. periodonticum*, *F. russii*, *F. ulcerans*, and *F. varium*, showed that none possessed *siaA*, *neuB* or *nanT*. Only *F. naviforme* lacked *murJ*, *F. naviforme* and *F. periodonticum* lacked *nagA*, 3 strains lacked *nagB* (*F. naviforme*, *F. periodonticum* and *F. nucleatum* (2 isolates)). Seven strains lacked *neuA*, two of the four *F. nucleatum* isolates had *neuC*, three strains (*F. naviforme*, *F. periodonticum* and one *F. nucleatum* isolates) lacked *nanA*. *NanE* was absent from 2 strains (*F. equinum* and *F. periodonticum*), five strains lacked *nanK* (*F. naviforme*, *F. perfoetens*, *F. periodonticum*, *F. ulcerans*, and *F. varium*), *nanM* was absent from 3 strains (*F. naviforme*, one isolate of *F. nucleatum* and *F. periodonticum*). *Neu O* was present in 3 strains (*F. hwasookii*, one isolate of *F. nucleatum* and *F. ulcerans*), *neuS* was present in *F. hwasookii*, 2 isolates of *F. nucleatum*, *F. perfoetens*, *F. periodonticum*, and *F. ulcerans*. *siaM* was present in *F. naviforme* and *F. perfoetens* and *siaQ* was found in *F. mortiferum*, *F. russii*, *F. ulcerans*, and *F. varium*, *siaT* was absent from *F. necrogenes* and *siaP* was absent from *F. necrogenes* and one isolate of *F. nucleatum*. The data imply that sialic acid pathways are both complex and different in different strains, subspecies and even isolates from a single subspecies.

Table 8.2 Analysis of gene encoded proteins in sialic acid pathways

<i>F.necrophorum funduliforme</i>																			
ID	strain	Sia A	Mur J	Nag A	Nag B	Neu A	Neu B	Neu C	Nan A	Nan E	Nan K	Nan M	Nan T	Neu O	Neu S	Sia M	Sia Q	Sia T	Sia P
Aru	fund	No	yes	yes	yes	yes	no	no	yes	yes	yes	yes	no	no	no	no	no	yes	yes
B35	fund	yes	yes	yes	yes	yes	no	no	yes	yes	yes	yes	no	no	no	no	yes	yes	yes
F1	fund	yes	yes	yes	yes	yes	no	no	no	yes	yes	yes	no	no	no	no	no	yes	yes
F1-1-36	fund	yes	yes	yes	yes	yes	no	no	yes	yes	yes	yes	no	no	no	no	no	yes	yes
F5	fund	No	yes	yes	yes	yes	no	no	yes	yes	yes	yes	no	no	no	no	no	yes	yes
F11	fund	No	yes	yes	yes	yes	no	no	yes	yes	yes	yes	no	no	no	no	no	yes	yes
F21	fund	yes	yes	yes	yes	yes	no	no	yes	yes	yes	yes	no	no	no	no	no	yes	yes
F24	fund	No	yes	yes	yes	yes	no	no	yes	yes	yes	yes	no	no	no	no	no	yes	yes
F30	fund	No	yes	yes	yes	yes	no	no	yes	yes	yes	yes	no	no	no	no	no	yes	yes
F39	fund	yes	yes	yes	yes	yes	no	no	yes	yes	yes	yes	no	no	no	no	no	yes	yes
F40	fund	yes	Yes	yes	yes	yes	no	no	yes	yes	yes	yes	no	no	no	no	no	yes	yes
F42	fund	No	Yes	yes	yes	yes	no	no	yes	yes	yes	yes	no	no	no	no	no	yes	yes
F52	fund	No	Yes	yes	yes	yes	no	no	yes	yes	yes	yes	no	no	no	no	no	yes	yes
F59	fund	yes	Yes	yes	yes	yes	no	no	yes	yes	yes	yes	no	no	no	no	no	yes	yes
F62	fund	No	Yes	yes	yes	yes	no	no	yes	yes	yes	yes	no	no	no	no	no	yes	yes
F70	fund	yes	Yes	yes	yes	yes	no	no	yes	yes	yes	yes	no	no	no	no	no	yes	yes
F80	fund	No	yes	yes	yes	yes	no	no	yes	yes	yes	yes	no	no	no	yes	no	yes	yes
F0437	fund	No	yes	yes	no	yes	no	no	yes	yes	yes	yes	no	no	no	no	no	yes	yes
F1248	fund	No	yes	yes	yes	yes	no	no	yes	yes	yes	yes	no	no	no	no	no	yes	yes
F1250	fund	No	Yes	yes	yes	yes	no	no	yes	yes	yes	yes	no	no	no	no	no	yes	yes
F1267	fund	No	Yes	yes	yes	yes	no	no	yes	yes	yes	yes	no	no	no	no	no	yes	yes
F1285	fund	No	yes	yes	yes	yes	no	no	yes	yes	yes	yes	no	no	no	no	no	yes	yes
F1309	fund	No	Yes	yes	yes	yes	no	no	yes	yes	yes	yes	no	no	no	no	no	yes	yes
F1314	fund	yes	Yes	yes	yes	yes	no	no	yes	yes	yes	yes	no	no	no	no	no	yes	yes
F1330	fund	No	Yes	yes	yes	yes	no	no	yes	yes	yes	yes	no	no	no	no	no	yes	yes
F1351	fund	No	Yes	yes	yes	yes	no	no	yes	yes	yes	yes	no	no	no	no	no	yes	yes
F1353	fund	yes	Yes	yes	yes	yes	no	no	yes	yes	yes	yes	no	no	no	no	no	yes	yes
F1365	fund	No	Yes	yes	yes	yes	no	no	yes	yes	yes	yes	no	no	no	no	no	yes	yes
Fnf1007	fund	No	yes	yes	yes	yes	no	no	yes	yes	yes	yes	no	no	no	no	no	yes	yes
HUND48	fund	No	yes	yes	yes	yes	no	no	yes	yes	yes	yes	no	no	no	no	yes	yes	yes
JCM3724	fund	yes	yes	yes	yes	yes	no	no	yes	yes	yes	yes	no	no	no	no	no	yes	yes
LS1195	fund	no	Yes	yes	yes	yes	no	no	yes	yes	yes	yes	no	no	no	no	no	yes	yes
LS1197	fund	no	Yes	yes	yes	yes	no	no	yes	yes	yes	yes	no	no	no	no	no	yes	yes
LS1260	fund	no	Yes	yes	yes	yes	no	no	yes	yes	yes	yes	no	no	no	no	no	yes	yes
LS1264	fund	yes	Yes	yes	yes	yes	no	no	yes	yes	yes	yes	no	no	no	no	no	yes	yes
LS1266	fund	no	Yes	yes	yes	yes	no	no	yes	yes	yes	yes	no	no	no	no	no	yes	yes
LS1272	fund	no	Yes	yes	yes	yes	no	no	yes	yes	yes	yes	no	no	no	no	no	yes	yes
LS1280	fund	yes	Yes	yes	yes	yes	no	no	yes	yes	yes	yes	no	no	no	no	no	yes	yes
LS1291	fund	yes	Yes	yes	yes	yes	no	no	yes	yes	yes	yes	no	no	no	no	no	yes	yes
PICP	fund	no	Yes	yes	yes	yes	no	no	yes	yes	yes	yes	no	no	no	no	no	yes	yes
PICM	fund	no	yes	yes	yes	yes	no	no	yes	yes	yes	yes	no	no	no	no	no	yes	yes
negative		27	0	0	1	0	41	41	0	0	0	0	41	41	41	40	39	0	0
<i>F.necrophorum necrophorum</i> isolates																			
Bftr-1	neccr	yes	yes	yes	yes	yes	no	no	yes	yes	yes	yes	no	no	no	no	yes	yes	yes
Bftr-2	neccr	no	yes	yes	yes	yes	no	no	yes	yes	yes	yes	no	no	no	no	no	yes	yes
BL	neccr	no	yes	yes	yes	no	no	no	yes	yes	yes	yes	no	no	no	no	yes	yes	yes
DAB	neccr	yes	yes	yes	yes	yes	no	no	yes	yes	yes	yes	no	no	no	no	yes	yes	yes
DJ-1	neccr	no	yes	yes	yes	no	no	no	yes	yes	no	yes	no	no	no	no	yes	yes	yes
DJ2	neccr	yes	yes	yes	yes	yes	no	no	yes	yes	no	yes	no	no	no	no	yes	yes	yes
JCM3718	neccr	no	yes	yes	yes	yes	no	no	yes	yes	yes	yes	no	no	no	no	no	yes	yes
negative		4	0	0	0	3	7	7	0	0	2	0	7	7	7	7	1	0	0
<i>Fusobacterium</i> sp.																			
CMW8396	equi	no	yes	yes	yes	yes	no	no	yes	yes	yes	yes	no	no	no	no	no	yes	yes
ATTC25563	gana	no	yes	yes	yes	yes	no	no	yes	yes	yes	yes	no	no	no	no	no	yes	yes
CHDCF128	hwags	No	yes	yes	yes	no	no	no	yes	yes	yes	yes	no	yes	yes	no	no	yes	yes
ATTC9817	morti	no	yes	yes	yes	no	no	no	yes	yes	yes	yes	no	no	no	no	no	yes	yes
ATTC25832	navif	no	yes	no	yes	yes													
NCTC10723	nec	no	yes	yes	yes	yes	no	no	yes	yes	yes	yes	no						
ATTC25586	nucl	no	yes	yes	yes	no	no	no	yes	yes	yes	yes	no	no	no	no	no	yes	yes
ATTC49256	nucl	No	yes	yes	no	yes	no	yes	yes	yes	yes	yes	no	no	yes	no	no	yes	yes

ATTC51190	<i>nucl</i>	no	yes	yes	no	no	no	no	yes	yes	yes	yes	no	no	no	no	no	yes	yes
NCTC10562	<i>nucl</i>	No	yes	yes	yes	yes	no	yes	no	yes	yes	no	no	no	yes	no	no	yes	no
ATTC29250	<i>perfo</i>	No	yes	yes	yes	yes	no	no	yes	yes	no	yes	no	yes	yes	yes	no	yes	yes
ATTC33693	<i>perid</i>	No	yes	no	no	no	no	no	no	no	no	no	no	no	yes	no	no	yes	yes
ATTC25533	<i>russi</i>	no	yes	yes	yes	yes	no	no	yes	yes	yes	yes	no	no	no	no	yes	yes	yes
ATTC49185	<i>ulcer</i>	No	yes	yes	yes	yes	no	no	yes	yes	no	yes	no	yes	yes	no	yes	yes	yes
ATTC27725	<i>variu</i>	no	yes	yes	yes	no	no	no	yes	yes	no	yes	no	no	no	no	yes	yes	yes
negative		15	1	2	4	7	15	13	3	2	5	3	15	12	9	13	11	1	2

(Continued from page 192.)

Key: fund = *funduliforme*, necr = *necrophorum*, equi = *equinum*, gona = *gonidiaformans*, hwas = *hwasookii*, morti = *mortiferum*, navif = *naviforme*, nec = *necrogenes*. Nucl = *nucleatum*, perfo = *perfoetens*, perid = *periodonticum*, russi = *russii*, ulcer = *ulcerans*, variu = *varium*.

Red=absent, green= present

SiaA- glycosyltransferase 52 (sialyltransferase) was searched by key word and with conserved sequences "MKKEYIC" and "QDHMLLSYI". NanK was searched with conserved sequences "FQKKIEEELQ" and "GGGII" and key words mannosamine kinase and glucoside kinase. All other genes were searched by gene and protein name.

An analysis of the gene organisation (Figure 8.3), demonstrated similar organisation, *nanM*- *catabolite control protein A/exuR* -*siaP*-*siaT*-*nanK*-*nanA*-*nanE*, in *F. necrophorum* (subsp. *funduliforme* and subsp. *necrophorum*), *F. hwasookii*, *F. nucleatum*, *F. equinum* and *F. gonidiaformans*. The structure was similar in *F. russii* except that the *tabA* gene, found just outside the cluster in the preceding organisms, had been relocated between the *nanK* and *nanA* genes. *F. ulcerans* had the first four genes (*nanM*-*catabolite control protein A/exuR* -*siaP*-*siaT*) in a cluster whereas *F. varium* had the genes, *cephalosporin-C deacetylase-glucokinase*- *tabA* between *siaT* and *nanA*.

Gene cluster organisation;

F. necrophorum (subsp. *funduliforme* and subsp. *necrophorum*) *F. hwasookii*,
F. nucleatum, *F. equinum*, *F. gonidiaformans*;

nanM- catabolite control protein A/ *exuR* -*siaP*-*siaT*-*nanK*-*nanA*- *nanE*;

F. russii;

NanM-catabolite control protein A/*exuR* -*siaP*-*siaT*, *nanK*, *tabA*, *nanA*, *nanE*;

F. ulcerans;

nanM-catabolite control protein A/*exuR* -*siaP*-*siaT*

F. varium;

nanM-catabolite control protein A/*exuR* -*siaP*-*siaT*- cephalosporin-C
deacetylase- glucokinase- *tabA*-*nanA*-*nanE*

F. mortiferum, *F. naviforme*, *F. necrogenes*, *F. perfoetens*, *F. periodonticum*;

no obvious structure.

Figure 8.3 Comparison of the gene order in *Fusobacteria* sp.

exuR = HTH-type transcriptional repressor; *tabA* Toxin-antitoxin biofilm protein; in other species this is found just outside the operon.

During the study, it was noted that N, N'-diacetyllegionaminic acid synthase, was present in one of the *F. necrophorum* subsp. *funduliforme* isolate, 3 of 4 of the *F. nucleatum* isolates, *F. varium* and *F. ulcerans*. This enzyme, that was originally isolated from *Legionella pneumophila* and *Campylobacter jejuni*, is involved in the biosynthesis of a sialic acid-like derivative legionaminic acid that is incorporated into virulence-associated cell surface glycoconjugates such as lipopolysaccharide (LPS), capsular polysaccharide, pili and flagella. Clearly, this requires further investigation.

8.4 Discussion

Initial work using lectins (see section 5.3.2 (Table 5.2)) suggested that sialic acid was present in *F. necrophorum*. However, the organism does not possess a gene for sialidase and hence cannot cleave sialic acid from glyconjugates in the environment (from the host or other bacteria). An in-depth bioinformatics study showed that the organism possessed *nanM* that encodes N-acetylneuraminase epimerase which converts α -N-acetylneuraminic acid (Neu5Ac) to the beta-

anomer; this has been reported to enable those bacteria that lack sialidase activity to compete for and take up the extracellular Neu5Ac present in the host (Severi *et al.* 2008). There was evidence for the presence of the genes required uptake, catabolism and O-acetylation of sialic acids in almost all *F. necrophorum funduliforme* isolates tested: indeed, the pattern of presence/absence of genes was highly conserved. The pattern was significantly different in *F. necrophorum* subsp. *necrophorum*; 6/7 of which had the *siaQ* gene that was absent in subsp. *funduliforme*, 3/7 lacked *neuA* that subsp. *funduliforme* possessed and 2/7 lacked *nank* that was present in subsp. *funduliforme*. Interestingly, the gene (*siaA*) required for sialylation of lipooligosaccharides was present in only 14/41 isolates of *F. necrophorum* subsp. *funduliforme* and 3/7 of the subsp. *necrophorum* isolates. These results imply that the ability to express surface sialic acid is variable in isolates of *Fusobacterium necrophorum*; there was no obvious correlation between known pathogenicity, host specificity or subspecies. A study of a limited number of genomes of other *Fusobacterium* sp. showed a much more diverse pattern; none had *siaA* whilst 9/15 possessed the *neuS* gene that encodes a polysialic acid O-acetyltransferase capable of sialylating LPS. Two of the four *F. nucleatum* isolates had the *neuC* gene that would enable *de novo* sialic acid synthesis as described by Yoneda *et al.*, (2014). Clearly more work is required to unravel the complexity of sialylation, sialic acid synthesis, metabolism and catabolism in *Fusobacterium* sp.

The importance of sialylation has been reported for a number of organisms, though some of the findings seem contradictory. Vogel *et al.*, (1999) showed, using an infant rat model system of meningococcal disease that LPS sialylation was only of minor importance for resistance of serogroup B and C to attack by complement. Jones *et al.*, (2003) investigated the recognition of meningococcal sialylated LPS by sialic acid binding lectins, siglecs, expressed on myeloid cells. Using a mouse model, they showed that bacteria with sialylated LPS were recognized and phagocytosed by two siglecs, Sn and siglec-5. This suggested that sialylation was detrimental to the organism in meningococcal disease.

However, in 2003, Bouchet *et al.*, reported that in capsule deficient strains of *Haemophilus influenzae*, sialylation of LPS was a significant virulence factor in development of *otitis media* in a chinchilla model. Sialylation of LPS of *H. influenzae* was required to enable the organism to evade the innate immune response of the host; mutant strains with non-sialylated LPS were more sensitive

to killing by human serum than the sialylated strains (Severi *et al.*, 2005). Sialylation of LPS of non-capsular *H. influenzae* has a role in biofilm formation and has been suggested to be important to both commensal behaviour and virulence (Jurcisek *et al.*, 2005; Swords *et al.*, 2004; Greiner *et al.*, 2004). This data implies a positive impact of sialylation.

The presence of terminal NeuAc (sialic acid) in the O-antigen units of LPS produces a structure that is similar to those found in human glycosphingolipids and protects the bacteria from host response through molecular mimicry (Heikema *et al.*, 2013; Spinola *et al.*, 2012; Bax *et al.*, 2011; Pawlak *et al.*, 2017). Bugla-Ploskonska *et al.*, (2010) hypothesised that sialic acid (NeuAc)-containing lipopolysaccharides (LPS) of *Salmonella* O48 strains could camouflage the bacterial surface from the immunological response of the host resulting in down-regulation of complement activation. However, their experimental results indicated that the presence of sialic acid in LPS did not play a major role in determining resistance to the bactericidal activity of complement or block the activation of the alternative pathway of complement; this work questioned the role of sialic acid in virulence.

Zaric *et al.*, (2017) demonstrated that highly sialylated LPS from *Porphyromonas gingivalis* had significantly lower inflammatory potential than a less sialylated form but that a reduction in endotoxicity was not mediated by sialic acid carried on LPS. They also suggested that interactions of sialylated LPS with the CD33 receptor were inhibited by endogenously expressed sialic acid of the host. Further proof of the role of host, free sialic acid in bacterial: host interactions was demonstrated by Hsu *et al.*, (2016) who showed that pre-treatment of rats with free sialic acid reduced the detrimental effects -induced by LPS on systemic and renal haemodynamics, renal ROS production and renal function, and LPS-activated TLR4/gp91/Caspase3 mediated apoptosis signalling. This implies that LPS plays a crucial role in renal infection. For organisms such as *F. necrophorum* that are reliant on host endogenous sialic acid or sialic acid liberated by bacterial sialidases to provide the building blocks for sialylation, the free sialic acid available would also inhibit adverse interactions of the sialylated bacteria with host lectins. Of course, the surface sialylation of bacteria may play an important role in bacteria: bacteria interaction, specifically in biofilm formation. In a study of *H. influenzae* in Chinchilla otitis, Jurcisek *et al.*, (2005) suggested that lipooligosaccharide sialylation was indispensable in biofilm formation. Future

metagenomic analyses of biofilms and subsequent pathway analyses may improve our understanding of the role of sialic acid.

Given the reported role of sialic acids in pathogenicity, it was surprising that the results of the current study did not show significant differences between the ARU 01 control strain that was originally isolated from a patient with Lemierre's disease and the clinical isolates (from London). However, a polymorphism was seen in lipooligosaccharide sialylation; ARU 01 and eight of the clinical isolates lacked *siaA* that encodes the sialyltransferase that sialylates LPS whilst the six other clinical isolates possessed this gene. Analysis of the *siaA* of two newly reported isolates from the blood of Lemierre's patients (Lyster *et al.*, 2019) demonstrated that one isolate had the *siaA* whereas the other did not. This polymorphism was seen not only in subsp. *funduliforme* but also subsp. *necrophorum*. There were also differences between the two type cultures, (JCM 3724 and JCM 3718); sialylation was seen in JCM 3724 subsp. *funduliforme* whilst JCM 3718 subsp. *necrophorum* lacked the gene. It is as yet unclear why sialylation of LPS is polymorphic in *Fusobacterium* sp., or whether it plays any role in pathogenesis and/or biofilm formation. Given that it was impossible to identify Lemierre's isolates based on the analyses performed, there was no obvious link to pathogenicity; however, it is possible that sialylation could play a role in tissue specific adhesion/homing. It would be important to collect and analyse new isolates and correlate the results with in-depth information on the isolate pathogenicity, location of the organism and presence co-infecting organisms using metagenomics. The impact of host free sialic acid on the binding between sialic acid containing LPS and lectins/adhesins of the host requires further research. Bioinformatics does not provide proof of expression of genes and hence results should be couched in terms of "potential to express"; all work should be backed up by biochemical analyses.

An intriguing finding of the analyses was that the *F. necrophorum* could be split into 2 clusters based on the presence or absence of *siaA*; these corresponded to the two major clusters seen in the WGS and protein analyses in chapter 7 (section 7.3.3). This supports the idea that there are at least 2 evolutionary distinct types of subsp. *funduliforme*.

Chapter 9

9 General Discussion

9.1 Discussion

The original aims of the project were to investigate biofilm formation and, to ensure strict growth conditions and reproducibility, this work relied heavily on the availability of an anaerobic cabinet in the laboratory of our collaborators. However, within 20 months, changes within the NHS brought about closure of that facility and work continued in less than ideal conditions, all work presented in the thesis used gas jars and mineral oil overlay to establish anaerobic growth conditions. Nevertheless, interesting results were obtained for the biofilm studies; *F. necrophorum* was shown to form mono and dual species biofilm and in dual culture the organism showed enhanced resistance to the antibiotics penicillin and ciprofloxacin. Whilst *F. necrophorum* is considered to be easy to treat, formation of biofilm could lead to resistance that would endanger the patient. In the related organism *F. nucleatum*, biofilm production is recognised to play an important role not only in dental plaque formation but also, in rare cases, in cardiac disease and colorectal cancer (reviewed by Kolenbrander, 2011; Persson and Imfeld, 2008; Cordero and Varela-Calviño, 2018; Brennan and Garrett, 2019). As glycans have been implicated in cell adhesion between different microbes and between microbial and eukaryotic cells, the research was re-focused to investigate the potential role of glycans and lectins in biofilm formation (reviewed by Cross and Ruhl, 2018; Moran *et al.*, 2011; Szymanski and Wren, 2005). This study involved biochemical and molecular studies that did not require the strict growth conditions needed to continue the physiological biofilm work.

A study undertaken to investigate one bacterial adhesion, the Galactose binding protein, showed that this protein did not bind to human red blood cells but did bind to desialylated sheep red blood cells. This suggested that the specificity was to unsubstituted beta galactosyl residues found on many bacterial cells and supports a role for this lectin in biofilm formation. This glycan is found on some types of eukaryotic cells, though the galactose is usually substituted with fucose or sialic acid residues that would preclude binding. The lectin-based studies of the cell surface and cell extracts showed the presence of glucose, galactose and N-

acetylglucosamine; although there were difficulties in visualising cell surface binding no significant differences were noted between the subspecies *funduliforme* and *necrophorum* or between the clinical isolates and the Lemierre's strain ARU 01. The results with *Sambucus nigra*, the lectin that detected sialic acid, were difficult to interpret; however, such issues had been noted with similar studies in *F. nucleatum* where "patchy and variable expression" was noted (Vinogradov, 2017). Further work was then undertaken to examine key pathways for lipid A biosynthesis and sialic acid cell surface expression.

Although lipidA had been described in the organism one gene, *lpxH*, was absent; all other key genes/enzymes required for lipid A synthesis were detected and characterised using bioinformatics. Data mining, protein studies and molecular modelling were used to identify and characterise an alternative enzyme LpxI that had been shown to replace LpxH in *Caulobacter crescentus* (Metzger *et al.*, 2012). However, biochemical studies were not carried out as the substrates had been synthesised by the authors of the paper and were not available to purchase. Nevertheless, it is clear that all *Fusobacterium* sp. utilise LpxI to complete the lipid A pathway.

During the 7 years of this project, there were dramatic changes in molecular technologies and the accessibility and affordability of genome sequencing technology. Hence, for studies of the sialic acid pathway, it was decided to sequence the whole genomes of the strains and isolates under study rather than using PCR and Sanger sequencing to investigate the genes of interest. At the time of the study it was estimated that each PCR assay (with replicates) and subsequent gene sequencing cost £10 whereas genome sequencing cost £50 per genome; hence whole genome sequencing was cost-effective if more than 5 genes were to be studied. The genome sequencing generated far more data than was required, and limited genome analysis was carried out (with the help of Dr Lesley Hoyles). The results highlighted significant differences between the two subspecies that will be used in future work to develop a simple PCR based identification. More interestingly, gene analysis of the subsp. *funduliforme*, from data generated in this study and that available in databases worldwide, determined that the subspecies comprised 3 clusters (A, B and C): A was distinct from B and C which showed a close relationship to each other. A number of clinical strains from the current study were found in each cluster.

This work was then extended to investigate the presence and impact of non-synonymous snps on a small range of encoded proteins. For some proteins, for example the Elongation factor Tu, few amino acid replacements were seen, and these were conservative or semi-conservative changes unlikely to affect protein structure and function. However, in other proteins there were numerous replacements: 65 in the case of a small part of Leukotoxin. Based on the sequence data, the isolates and strains of subsp. *funduliforme* could be split into 2 clusters; one corresponded to cluster A seen in the genome study whilst the other corresponded to clusters B and C which could not be differentiated. Analysis of the alignments of the subsp. *necrophorum* demonstrated more changes, some similar to cluster A, some to cluster B+C and other unique changes, many of which were non-conservative. The data that was compiled from the current study and from data available worldwide suggested 2 major ancestral lines leading to the distinct clusters noted. Future studies are required to determine whether there is any correlation between these clusters and bacterial pathogenesis; current studies suggest that the Lemierre's strains were not differentiated from the other clinical isolates based on this clustering. The recent submission of 2 new Lemierre's strains to available databases will enable more in-depth studies into any differences between these and the clinical isolates sequenced. It should be noted that a preliminary study suggested that one of the new strains was cluster A whilst the other was cluster B+C based on protein analysis.

The analysis of sialic acid pathway genes in *F. necrophorum* demonstrated that all isolates and strains lacked the genes required for *de novo* synthesis of sialic acid; in agreement with the literature, these genes were found in some but not all *F. nucleatum* strains (Lewis *et al.*, 2016). There were also differences that characterised the subsp. *necrophorum* strains, for example 6/7 had *siaQ* that was absent in subsp. *funduliforme* and 3/7 lacked *neuA*. Interestingly, the key gene required for surface expression of sialic acid, *siaA* was present in some but not all strains and isolates of both subspecies of *F. necrophorum*, but absent from other Fusobacteria that possessed an alternative gene for surface sialylation. In subsp. *funduliforme*, the presence/absence of *siaA* defined the same 2 clusters (A and B+C) noted in chapter 7. This supports the suggestion that at least 2 distinct lineages of subsp. *funduliforme* are present worldwide and that these could be differentiated based on the ability to express of sialic acid on their surfaces. The correlation between surface sialic acid and pathogenicity in bacteria is currently

controversial and this area is worthy of further investigation. However, as these bacteria are reliant on uptake of available sialic acid from the environment, great care should be taken in the research methodology to standardise the free sialic acid present. Additionally, to understand the *in vivo* role of sialic acid expression would require an understanding of “local” environmental levels. It is clear that the organism can only sialylate in the presence of free sialic acid in the host; this would preclude the detection of the bacterial sialic acid by the immune system whose receptors would be blocked by the endogenous sialic acid present.

9.2 Future Work

Utilise the genome sequencing information to suggest genes suitable for inclusion in a PCR based sub-speciation/ group differentiation assay. Are the sub-groups noted in the genomic studies associated with specific/different clinical presentation/ patient profile?

Analyse the two new strains from Lemierre’s patients that have been lodged in public databases: is there any evidence of unique genes/snps differentiating Lemierre’s strains from those causing sore throats?

Provide strain F88 to collaborators to review the phenotypic characteristics of this strain that has been identified as *F. siminae* by genomic analysis.

Further investigate the large numbers of snps seen in the Leucotoxin gene; increase the analysis from a fragment of the gene to the whole gene. Does the distribution of snps reveal information about the potential toxicity of the molecule? Extend the study of specific metabolic pathways to understand the glycosylation potential of these organisms.

Investigate the expression of mRNA encoding genes of interest and the impact of environmental conditions on gene expression.

9.3 Conclusion

Much of the work presented is based on bioinformatics and the results and their implications must be verified by cell biology and/or biochemistry. Nevertheless, the results do demonstrate the potential, or lack of potential, of the organism to

express certain proteins. A number of novel discoveries have been made during this work:

- 1- *F. necrophorum* produces mono and dual species biofilms the formation of which affects antibiotic sensitivity.
- 2- The Galactose binding protein is specific for unsubstituted terminal beta galactosyl residues.
- 3- LpxI is used as an alternative to LpxH in the lipid A pathway.
- 4- There are many differences between the genomes of subsp. *necrophorum* and *funduliforme* that could be used to set up a PCR based species specific test.
- 5- Three clusters (A, B and C) in the subsp. *funduliforme* were identified using genome sequencing, assembly and analysis.
- 6- Two clusters (A and B+C) in the subsp. *funduliforme* were identified by proteomic analysis.
- 7- Detailed analysis of the sialic acid pathways highlighted difference between species and subspecies and the differentiation of the subsp. *funduliforme* into 2 clusters (A, and B+C) based on the presence/absence of *siaA*.
- 8- Genome sequences of type culture strains, ARU 01 and 17 clinical strains have been deposited into public databases to enable further research.

Appendices

Appendix I: Biochemical tests

These tests include Gram staining and tests for catalase, oxidase, indole and lipase.

i-1 Gram stain and Microscopic appearance

Gram staining was carried out using the method of Halebain *et al.*, (1981), with slight modifications. A colony was smeared onto a drop of distilled water on a glass slide. The smear was left to air-dry at room temperature, after which it was heat fixed by passing through a blue flame several times. The slide was then covered with crystal violet solution for 30-60 seconds, this was followed by adding iodine solution to the slide and incubating for 30-60 seconds. The slide was rinsed briefly with tap water, until the water was clear. The slide was quickly rinsed with decolouriser solution (approximately 10 seconds), and then rinsed with tap water. The slide was covered with safranin solution for 30 seconds, and then rinsed under tap water until the water was clear. The slide was gently blotted dry and the sample examined under a light microscope. *F. necrophorum* should appear as a Gram-negative pleomorphic rod, sometimes with long, tapered filaments present.

i-2 Catalase test

The catalase test is used to show the presence or absence of the enzyme catalase, an important enzyme which protects cells from oxidative damage by reactive oxygen species (ROS), which catalyses the release of oxygen from hydrogen peroxide (H₂O₂).

Using a clean dry glass slide, a small amount of a bacterial colony was transferred onto the slide using a sterile toothpick. A drop of 3 % hydrogen peroxide (H₂O₂) (Sigma Aldrich Ltd, Dorset, UK) was placed onto the slide and mixed. A positive result was a rapid production of oxygen within 5 -10 seconds, seen as bubbles, and a negative result was recorded when only a few scattered bubbles, or no bubbles were produced. *F. necrophorum* strains are catalase negative.

i-3 Oxidase test

This test is to identify bacteria that produce cytochrome c oxidase, an enzyme involved in the bacterial electron transport chain. When this enzyme is present, it oxidises the reagent (tetramethyl-*p*-phenylenediamine dihydrochloride) to a purple (indophenol) colour end product. The reagent remains reduced and colourless when the enzyme is not present.

A filter paper was placed in a petri-dish and soaked with 1 % (w/v) solution of oxidase reagent (N, N, N', N'- tetramethyl-*p*-phenylenediamine dihydrochloride (TMPD) (Sigma, Gillingham, UK), made up with sterile distilled water. Using a sterile toothpick, a small amount of bacterial colony to be tested was smeared onto the filter paper. The inoculated area was observed for colour change to dark blue or purple within 10 - 30 seconds. Purple colonies were positive for cytochrome oxidase, or negative if no colour change was observed. *F. necrophorum* strains are oxidase negative.

i-4 Spot Indole test

This test is used to determine the ability of an organism to split the amino acid tryptophan to generate the compound indole. A number of different intracellular enzymes known as tryptophanase are involved in the conversion that produces three end products, one of which is indole. The indole released then reacts with cinnamaldehyde to produce a blue-green compound, the absence of the enzyme shows no colour production.

A piece of filter paper in a petri-dish was saturated with reagent (1 % para-dimethylamino cinnamaldehyde) from a vial of Bactodrop Spot Indole test (Remel™; Thermo Scientific, DE, USA). A toothpick was used to take a small portion of the bacterial colony from an agar plate and smeared onto the filter paper. A development of a blue-green colour within 30 seconds indicated a positive result for indole production from tryptophan. Pink or no colour change was seen if negative. *F. necrophorum* strains are indole positive.

i-5 Lipase test

The lipase test is used to identify organisms that are capable of producing the exoenzyme lipase. The presence of lipase activity is detected by distinct halo zone around the colony (with the help of a lamp).

11.175 grams of L.D. Egg Yolk agar base (HiMedia, Mumbai, India) was suspended in 250 ml of sterile distilled water, this was heated to boiling to dissolve completely and then sterilised by autoclaving at 121 °C for 15 minutes. This was then allowed to cool to 50 °C and about 25 ml of sterile Egg Yolk emulsion (LabM, Lancashire, UK) was added aseptically, mixed well and poured into sterile Petri-dishes. The set agar was streaked with *F. necrophorum* isolates and incubated anaerobically in an anaerobic jar with AnaeroGen™ sachet (Oxoid Ltd., Basingstoke, UK) for 48 hours at 37 °C, as described in the methods section (see chapter 2). The agar plates were then examined for lipase production. Plates with isolates negative for lipase were kept for up to 7 days to confirm presumptive identification, since lipase reaction may be delayed. Lipase breaks down free fats present in the egg yolks, resulting an iridescent, “oil on water” sheen on the surface of the colonies. Some of the *F. necrophorum* tested were positive and some negative for lipase.

Appendix II: DNA Sequence [16S rRNA]

ii-1 ARU planktonic

tgGGCgtAagCGCgtCtagGCGGCAAGGAAAGTCTGATGTGAAAATGCGGgagctCaacT
 CCGTATGGCGttgGAAACTGCCTTACTAGAGTACTGGAGagGTAGGCGGAACTAC
 AAgtGTAGAGGTGAAATTCGTaGaTATTTGTAGGAATGCCGATGGGGAAAGCCAGC
 CTA CTGGACAGATACTGACGCTAAAGCGCGAAAGCGTGGGTAGCAAACAGGATT
 AGATACCCTggtaGTCCACGCTGTA AACGATGATTActaggTGTTGGGGGTCAAACC
 TCAGCGCCCAAGCTAACGCGATAAGTAATCCGCCTGGGGagTACGTACGCAAGT
 ATGAAACTCAAAGGAATTGACGGGGGCCCGCACAAAGa

	Description	Max score	Total score	Query cover	E value	Ident	Accession
<input type="checkbox"/>	Fusobacterium necrophorum strain JCM 3718 16S ribosomal RNA gene, partial sequence	657	657	99%	0.0	99%	NR_114400.1
<input type="checkbox"/>	Fusobacterium necrophorum subsp. funduliforme strain P30B 16S ribosomal RNA gene, partial se	657	657	99%	0.0	99%	KC407936.1
<input type="checkbox"/>	Fusobacterium necrophorum subsp. funduliforme strain Fn524 16S ribosomal RNA gene, partial s	657	657	99%	0.0	99%	NR_104683.1
<input type="checkbox"/>	Fusobacterium necrophorum 16S ribosomal RNA gene, partial sequence	657	657	99%	0.0	99%	DQ486127.1
<input type="checkbox"/>	Fusobacterium necrophorum strain RMA16505 16S ribosomal RNA gene, partial sequence	657	657	99%	0.0	99%	EF447427.1
<input type="checkbox"/>	Fusobacterium necrophorum subsp. funduliforme strain B35 16S ribosomal RNA gene, partial seg	657	657	99%	0.0	99%	EF447425.1
<input type="checkbox"/>	Fusobacterium necrophorum strain Ulm E 16S ribosomal RNA gene, partial sequence	657	657	99%	0.0	99%	EF153310.1
<input type="checkbox"/>	Fusobacterium necrophorum strain Ulm 1 16S ribosomal RNA gene, partial sequence	657	657	99%	0.0	99%	DQ440550.1
<input type="checkbox"/>	Fusobacterium necrophorum strain ATCC 25286 16S ribosomal RNA gene, complete sequence	657	657	99%	0.0	99%	NR_042365.1
<input type="checkbox"/>	Fusobacterium necrophorum 16S ribosomal RNA gene, complete sequence	657	657	99%	0.0	99%	AF044948.1
<input type="checkbox"/>	Fusobacterium necrophorum subsp. funduliforme strain P27B 16S ribosomal RNA gene, partial se	654	654	99%	0.0	99%	KC407934.1
<input type="checkbox"/>	Fusobacterium necrophorum subsp. funduliforme strain P20B 16S ribosomal RNA gene, partial se	654	654	99%	0.0	99%	KC407923.1
<input type="checkbox"/>	Fusobacterium necrophorum subsp. funduliforme strain P18B 16S ribosomal RNA gene, partial se	654	654	99%	0.0	99%	KC407922.1
<input type="checkbox"/>	Fusobacterium necrophorum strain 2008-10-864 16S ribosomal RNA gene, partial sequence	654	654	99%	0.0	99%	FJ984622.1
<input type="checkbox"/>	Fusobacterium necrophorum strain Ulm 6 16S ribosomal RNA gene, partial sequence	654	654	99%	0.0	99%	DQ440555.1
<input type="checkbox"/>	Fusobacterium necrophorum subsp. necrophorum gene for 16S ribosomal RNA, partial sequence	652	652	99%	0.0	99%	AB971800.1

ii-2 3718 planktonic

acTaGGtntGGGGTCcatTcnnngggttcCgtgCcntanna

	Description	Max score	Total score	Query cover	E value	Ident	Accession
<input type="checkbox"/>	Fusobacterium necrophorum subsp. necrophorum gene for 16S ribosomal RNA, partial sequence	16.4	30.7	35%	64	100%	AB971800.1
<input type="checkbox"/>	Fusobacterium necrophorum strain JCM 3718 16S ribosomal RNA gene, partial sequence	16.4	30.7	35%	64	100%	NR_114400.1
<input type="checkbox"/>	Fusobacterium necrophorum subsp. funduliforme strain SIRD 333 16S ribosomal RNA gene, partial sequence	16.4	16.4	19%	64	100%	JX103157.1
<input type="checkbox"/>	Fusobacterium necrophorum subsp. necrophorum strain F4 outer membrane protein gene, partial cds	16.4	45.1	35%	64	100%	JQ846351.1
<input type="checkbox"/>	Fusobacterium necrophorum outer membrane protein gene, partial cds	16.4	45.1	35%	64	100%	JQ740822.1
<input type="checkbox"/>	Fusobacterium necrophorum canine oral taxon 190 clone QD026 16S ribosomal RNA gene, partial sequence	16.4	30.7	35%	64	100%	JN713357.1
<input type="checkbox"/>	Fusobacterium necrophorum canine oral taxon 190 clone ZM126 16S ribosomal RNA gene, partial sequence	16.4	16.4	19%	64	100%	JQ299277.1
<input type="checkbox"/>	Fusobacterium necrophorum canine oral taxon 190 clone ZM116 16S ribosomal RNA gene, partial sequence	16.4	16.4	19%	64	100%	JQ299267.1
<input type="checkbox"/>	Fusobacterium necrophorum canine oral taxon 190 clone ZM041 16S ribosomal RNA gene, partial sequence	16.4	16.4	19%	64	100%	JQ299240.1
<input type="checkbox"/>	Fusobacterium necrophorum canine oral taxon 190 clone ZM031 16S ribosomal RNA gene, partial sequence	16.4	16.4	19%	64	100%	JQ299230.1
<input type="checkbox"/>	Fusobacterium necrophorum canine oral taxon 190 clone ZM003 16S ribosomal RNA gene, partial sequence	16.4	16.4	19%	64	100%	JQ299206.1
<input type="checkbox"/>	Fusobacterium necrophorum canine oral taxon 190 clone QD026 16S ribosomal RNA gene, partial sequence	16.4	16.4	19%	64	100%	JQ298662.1
<input type="checkbox"/>	Fusobacterium necrophorum subsp. funduliforme strain Fn524 16S ribosomal RNA gene, partial sequence	16.4	30.7	35%	64	100%	NR_104683.1
<input type="checkbox"/>	Fusobacterium necrophorum strain 2008-10-864 16S ribosomal RNA gene, partial sequence	16.4	30.7	35%	64	100%	FJ984622.1
<input type="checkbox"/>	Fusobacterium necrophorum subsp. funduliforme strain DSM 19678 16S ribosomal RNA gene, partial sequence	16.4	30.7	35%	64	100%	NR_115077.1
<input type="checkbox"/>	Fusobacterium necrophorum 16S ribosomal RNA gene, partial sequence	16.4	30.7	35%	64	100%	DQ486127.1

ii-3 3724 planktonic

cGCGcgTAgGCGGtTTTTTaAgTCTGATGTGAaanccacgGcTCanccgnGgagG
gtcaTTGnannctg

	Description	Max score	Total score	Query cover	E value	Ident	Accession
<input type="checkbox"/>	F.necrophorum (FnS-1) gene for 16S rRNA	30.1	30.1	48%	0.008	79%	X74407.1
<input type="checkbox"/>	Fusobacterium necrophorum subsp. necrophorum gene for 16S ribosomal RNA, partial sequence	28.3	28.3	21%	0.027	100%	AB971800.1
<input type="checkbox"/>	Fusobacterium necrophorum strain JCM 3718 16S ribosomal RNA gene, partial sequence	28.3	28.3	21%	0.027	100%	NR_114400.1
<input type="checkbox"/>	Fusobacterium necrophorum subsp. funduliforme strain P30B 16S ribosomal RNA gene, partial sequence	28.3	28.3	21%	0.027	100%	KC407936.1
<input type="checkbox"/>	Fusobacterium necrophorum subsp. necrophorum strain P26A 16S ribosomal RNA gene, partial sequence	28.3	28.3	21%	0.027	100%	KC407928.1
<input type="checkbox"/>	Fusobacterium necrophorum subsp. funduliforme strain P20B 16S ribosomal RNA gene, partial sequence	28.3	28.3	21%	0.027	100%	KC407923.1
<input type="checkbox"/>	Fusobacterium necrophorum subsp. funduliforme strain P18B 16S ribosomal RNA gene, partial sequence	28.3	28.3	21%	0.027	100%	KC407922.1
<input type="checkbox"/>	Fusobacterium necrophorum subsp. funduliforme strain SIRD 333 16S ribosomal RNA gene, partial sequence	28.3	28.3	21%	0.027	100%	JX103157.1
<input type="checkbox"/>	Fusobacterium necrophorum canine oral taxon 190 clone QD026 16S ribosomal RNA gene, partial sequence	28.3	28.3	21%	0.027	100%	JN713357.1
<input type="checkbox"/>	Fusobacterium necrophorum subsp. funduliforme strain Fn524 16S ribosomal RNA gene, partial sequence	28.3	28.3	21%	0.027	100%	NR_104683.1
<input type="checkbox"/>	Fusobacterium necrophorum strain 2008-10-864 16S ribosomal RNA gene, partial sequence	28.3	28.3	21%	0.027	100%	FJ984622.1
<input type="checkbox"/>	Fusobacterium necrophorum subsp. funduliforme strain DSM 19678 16S ribosomal RNA gene, partial sequence	28.3	28.3	21%	0.027	100%	NR_115077.1
<input type="checkbox"/>	Fusobacterium necrophorum 16S ribosomal RNA gene, partial sequence	28.3	28.3	21%	0.027	100%	DQ486127.1
<input type="checkbox"/>	Fusobacterium necrophorum strain RMA16505 16S ribosomal RNA gene, partial sequence	28.3	28.3	21%	0.027	100%	EF447427.1
<input type="checkbox"/>	Fusobacterium necrophorum strain RMA10682 16S ribosomal RNA gene, partial sequence	28.3	28.3	21%	0.027	100%	EF447426.1
<input type="checkbox"/>	Fusobacterium necrophorum subsp. funduliforme strain B35 16S ribosomal RNA gene, partial sequence	28.3	28.3	21%	0.027	100%	EF447425.1

ii-4 ARU biofilm

CntaTCGganTtatTGGgCGTaAGCGCGTCTAGGCGGCAAGGAAAGTCTGAT
 GTGAAAATGCGGAGCTCAACTCCGTATGGCGTTGGAAACTGCCTTACTAG
 AGTACTGGAGAGGTAGGCGGAACTACAAGTGTAGAGGTGAAATTCGTAG
 ATATTTGTAGGAATGCCGATGGGGAAGCCAGCCTACTGGACAGATACTG
 ACGCTAAAGCGCGAAAGCGTGGGTAGCAAACAGGATTAGATACCCTGGT
 AGTCCACGCTGTAAACGATGATTACTAGGTGTTGGGGGTCAAACCTCAGC
 GCCCAAGCTAACGCGATAAGTAATCCGCCTGGGGAGTACGTACGCAAGT
 ATGAAACTCAAAGGAATTGACGGGGGCCCGCACAAgaa

	Description	Max score	Total score	Query cover	E value	Ident	Accession
<input type="checkbox"/>	Fusobacterium necrophorum strain JCM 3718 16S ribosomal RNA gene, partial sequence	670	670	98%	0.0	99%	NR_114400.1
<input type="checkbox"/>	Fusobacterium necrophorum subsp. funduliforme strain P30B 16S ribosomal RNA gene, partial se	670	670	98%	0.0	99%	KC407936.1
<input type="checkbox"/>	Fusobacterium necrophorum subsp. funduliforme strain Fn524 16S ribosomal RNA gene, partial s	670	670	98%	0.0	99%	NR_104683.1
<input type="checkbox"/>	Fusobacterium necrophorum 16S ribosomal RNA gene, partial sequence	670	670	98%	0.0	99%	DQ486127.1
<input type="checkbox"/>	Fusobacterium necrophorum strain RMA16505 16S ribosomal RNA gene, partial sequence	670	670	98%	0.0	99%	EF447427.1
<input type="checkbox"/>	Fusobacterium necrophorum subsp. funduliforme strain B35 16S ribosomal RNA gene, partial seq	670	670	98%	0.0	99%	EF447425.1
<input type="checkbox"/>	Fusobacterium necrophorum strain Ulm E 16S ribosomal RNA gene, partial sequence	670	670	98%	0.0	99%	EF153310.1
<input type="checkbox"/>	Fusobacterium necrophorum strain Ulm 1 16S ribosomal RNA gene, partial sequence	670	670	98%	0.0	99%	DQ440550.1
<input type="checkbox"/>	Fusobacterium necrophorum strain ATCC 25286 16S ribosomal RNA gene, complete sequence	670	670	98%	0.0	99%	NR_042365.1
<input type="checkbox"/>	Fusobacterium necrophorum 16S ribosomal RNA gene, complete sequence	670	670	98%	0.0	99%	AF044948.1
<input type="checkbox"/>	Fusobacterium necrophorum subsp. funduliforme strain P27B 16S ribosomal RNA gene, partial se	666	666	98%	0.0	99%	KC407934.1
<input type="checkbox"/>	Fusobacterium necrophorum subsp. funduliforme strain P18B 16S ribosomal RNA gene, partial se	666	666	98%	0.0	99%	KC407922.1
<input type="checkbox"/>	Fusobacterium necrophorum strain 2008-10-864 16S ribosomal RNA gene, partial sequence	666	666	98%	0.0	99%	FJ984622.1
<input type="checkbox"/>	Fusobacterium necrophorum strain Ulm 6 16S ribosomal RNA gene, partial sequence	666	666	98%	0.0	99%	DQ440555.1
<input type="checkbox"/>	Fusobacterium necrophorum subsp. necrophorum gene for 16S ribosomal RNA, partial sequence	664	664	98%	0.0	99%	AB971800.1
<input type="checkbox"/>	Fusobacterium necrophorum canine oral taxon 190 clone QD026 16S ribosomal RNA gene, partie	664	664	98%	0.0	99%	JN713357.1

ii-5 3718 Biofilm

tTaTTcGGattatTGGgCGTAaGCGCGCGTtagGCGGTTTTTtaAGTCTGATGTG
AAAGCCCACGGCTCAACCGTGGAGGGTCATTGGAAACTGGAAAACCTTGA
GTGCAGAAGAGGAAAGTGAATTCCATGTGTAGCGGTGAAATGCGCAGA
GATATGGAGGAACACCAGTGGCGAAGGCGACTTTCTGGTCTGTAACCTGA
CGCTGATGTGCGAAAGCGTGGGGATCAAACAGGATTAGATACCCTGGTA
GTCCACGCCGTAAACGATGAGTGCTAAGTGTTAGGGGGTTTCCGCCCT
TAGTGCTGCAGCTAACGCATTAAGCACTCCGCCTGGGGAGTACGACCGC
AAGGTTGAAACTCAAAGGAATTGACGGGGGCCCGCACAAgaa

<input type="checkbox"/>	Fusobacterium necrophorum canine oral taxon QD026 16S ribosomal RNA gene, part	286	286	99%	4e-79	77%	JN713357.1
<input type="checkbox"/>	Fusobacterium necrophorum strain Ulm 2 16S ribosomal RNA gene, partial sequence	286	286	99%	4e-79	77%	DQ440551.1
<input type="checkbox"/>	Fusobacterium necrophorum subsp. necrophorum strain P26A 16S ribosomal RNA gene, partial s	284	284	99%	2e-78	77%	KC407928.1
<input type="checkbox"/>	Fusobacterium necrophorum subsp. funduliforme strain P20B 16S ribosomal RNA gene, partial se	284	284	99%	2e-78	77%	KC407923.1
<input type="checkbox"/>	Fusobacterium necrophorum rRNA small subunit	284	284	99%	2e-78	77%	X55411.1
<input type="checkbox"/>	Fusobacterium necrophorum subsp. funduliforme strain DSM 19678 16S ribosomal RNA gene, pa	282	282	99%	5e-78	77%	NR_11507.1
<input type="checkbox"/>	Fusobacterium necrophorum strain RMA10682 16S ribosomal RNA gene, partial sequence	282	282	99%	5e-78	77%	EF447426.1
<input type="checkbox"/>	Fusobacterium necrophorum subsp. necrophorum strain P38A 16S ribosomal RNA gene, partial s	280	280	99%	2e-77	77%	KC407942.1
<input type="checkbox"/>	Fusobacterium necrophorum strain Ulm 5 16S ribosomal RNA gene, partial sequence	279	279	99%	7e-77	77%	DQ440554.1
<input type="checkbox"/>	F.necrophorum (FnS-40) gene for 16S rRNA	255	255	99%	7e-70	76%	X74408.1
<input type="checkbox"/>	Fusobacterium necrophorum strain Ulm 17 16S ribosomal RNA gene, partial sequence	251	251	88%	9e-69	77%	EF153313.1
<input type="checkbox"/>	F.necrophorum (FnS-1) gene for 16S rRNA	251	251	99%	9e-69	76%	X74407.1
<input type="checkbox"/>	Fusobacterium necrophorum strain Ulm 16 16S ribosomal RNA gene, partial sequence	242	242	71%	5e-66	80%	EF153312.1
<input type="checkbox"/>	Fusobacterium necrophorum strain JB2 16S ribosomal RNA gene, partial sequence	228	228	98%	1e-61	75%	AY661810.1
<input type="checkbox"/>	Fusobacterium necrophorum strain JB7 16S ribosomal RNA gene, partial sequence	208	208	77%	1e-55	77%	AY661809.1
<input type="checkbox"/>	Fusobacterium necrophorum subsp. funduliforme strain SIRD 333 16S ribosomal RNA gene, parti	91.5	91.5	42%	2e-20	73%	JX103157.1
<input type="checkbox"/>	Fusobacterium necrophorum subsp. necrophorum strain NCTC10576 16S ribosomal RNA gene, r	22.9	22.9	3%	8.0	100%	AF410970.1

ii-6 3724 Biofilm

cgGgatntTGGgcgTAaGCGCgnntagGCGgnnnntaaGTCTGATGTGaaatgcnnag
CTCAAActc

	Description	Max score	Total score	Query cover	E value	Ident	Accession
<input type="checkbox"/>	Fusobacterium necrophorum subsp. necrophorum gene for 16S ribosomal RNA, partial sequence	55.4	55.4	89%	2e-10	81%	AB971800.1
<input type="checkbox"/>	Fusobacterium necrophorum strain JCM 3718 16S ribosomal RNA gene, partial sequence	55.4	55.4	89%	2e-10	81%	NR_114400.1
<input type="checkbox"/>	Fusobacterium necrophorum subsp. funduliforme strain P30B 16S ribosomal RNA gene, partial sequence	55.4	55.4	89%	2e-10	81%	KC407936.1
<input type="checkbox"/>	Fusobacterium necrophorum subsp. necrophorum strain P26A 16S ribosomal RNA gene, partial sequence	55.4	55.4	89%	2e-10	82%	KC407928.1
<input type="checkbox"/>	Fusobacterium necrophorum subsp. funduliforme strain P20B 16S ribosomal RNA gene, partial sequence	55.4	55.4	89%	2e-10	81%	KC407923.1
<input type="checkbox"/>	Fusobacterium necrophorum subsp. funduliforme strain P18B 16S ribosomal RNA gene, partial sequence	55.4	55.4	89%	2e-10	81%	KC407922.1
<input type="checkbox"/>	Fusobacterium necrophorum subsp. funduliforme strain SIRD 333 16S ribosomal RNA gene, partial sequence	55.4	55.4	89%	2e-10	81%	JX103157.1
<input type="checkbox"/>	Fusobacterium necrophorum canine oral taxon 190 clone QD026 16S ribosomal RNA gene, partial sequence	55.4	55.4	89%	2e-10	81%	JN713357.1
<input type="checkbox"/>	Fusobacterium necrophorum subsp. funduliforme strain Fn524 16S ribosomal RNA gene, partial sequence	55.4	55.4	89%	2e-10	81%	NR_104683.1
<input type="checkbox"/>	Fusobacterium necrophorum strain 2008-10-864 16S ribosomal RNA gene, partial sequence	55.4	55.4	89%	2e-10	81%	FJ984622.1
<input type="checkbox"/>	Fusobacterium necrophorum subsp. funduliforme strain DSM 19678 16S ribosomal RNA gene, partial sequence	55.4	55.4	89%	2e-10	81%	NR_115077.1
<input type="checkbox"/>	Fusobacterium necrophorum 16S ribosomal RNA gene, partial sequence	55.4	55.4	89%	2e-10	81%	DQ486127.1
<input type="checkbox"/>	Fusobacterium necrophorum strain RMA16505 16S ribosomal RNA gene, partial sequence	55.4	55.4	89%	2e-10	81%	EF447427.1
<input type="checkbox"/>	Fusobacterium necrophorum strain RMA10682 16S ribosomal RNA gene, partial sequence	55.4	55.4	89%	2e-10	81%	EF447426.1
<input type="checkbox"/>	Fusobacterium necrophorum subsp. funduliforme strain B35 16S ribosomal RNA gene, partial sequence	55.4	55.4	89%	2e-10	81%	EF447425.1
<input type="checkbox"/>	Fusobacterium necrophorum strain Ulm E 16S ribosomal RNA gene, partial sequence	55.4	55.4	89%	2e-10	81%	EF153310.1

ii-7 Positive control

tCCatGTGTAnngGTGAAATgcgtaGATAttggaGGAacgcCgntggggaaancgGCC

	Description	Max score	Total score	Query cover	E value	Ident	Accession
<input type="checkbox"/>	Fusobacterium necrophorum subsp. necrophorum gene for 16S ribosomal RNA, partial sequence	62.6	62.6	84%	1e-12	86%	AB971800.1
<input type="checkbox"/>	Fusobacterium necrophorum strain JCM 3718 16S ribosomal RNA gene, partial sequence	62.6	62.6	84%	1e-12	86%	NR_114400.1
<input type="checkbox"/>	Fusobacterium necrophorum subsp. funduliforme strain P30B 16S ribosomal RNA gene, partial sequence	62.6	62.6	84%	1e-12	86%	KC407936.1
<input type="checkbox"/>	Fusobacterium necrophorum subsp. funduliforme strain P27B 16S ribosomal RNA gene, partial sequence	62.6	62.6	84%	1e-12	86%	KC407934.1
<input type="checkbox"/>	Fusobacterium necrophorum subsp. funduliforme strain Fn524 16S ribosomal RNA gene, partial sequence	62.6	62.6	84%	1e-12	86%	NR_104683.1
<input type="checkbox"/>	Fusobacterium necrophorum strain 2008-10-864 16S ribosomal RNA gene, partial sequence	62.6	62.6	84%	1e-12	86%	FJ984622.1
<input type="checkbox"/>	Fusobacterium necrophorum subsp. funduliforme strain DSM 19678 16S ribosomal RNA gene, partial sequence	62.6	62.6	84%	1e-12	86%	NR_115077.1
<input type="checkbox"/>	Fusobacterium necrophorum 16S ribosomal RNA gene, partial sequence	62.6	62.6	84%	1e-12	86%	DQ486127.1
<input type="checkbox"/>	Fusobacterium necrophorum strain RMA16505 16S ribosomal RNA gene, partial sequence	62.6	62.6	84%	1e-12	86%	EF447427.1
<input type="checkbox"/>	Fusobacterium necrophorum strain RMA10682 16S ribosomal RNA gene, partial sequence	62.6	62.6	84%	1e-12	86%	EF447426.1
<input type="checkbox"/>	Fusobacterium necrophorum subsp. funduliforme strain B35 16S ribosomal RNA gene, partial sequence	62.6	62.6	84%	1e-12	86%	EF447425.1
<input type="checkbox"/>	Fusobacterium necrophorum strain Ulm 17 16S ribosomal RNA gene, partial sequence	62.6	62.6	84%	1e-12	86%	EF153313.1
<input type="checkbox"/>	Fusobacterium necrophorum strain Ulm 16 16S ribosomal RNA gene, partial sequence	62.6	62.6	84%	1e-12	86%	EF153312.1
<input type="checkbox"/>	Fusobacterium necrophorum strain Ulm E 16S ribosomal RNA gene, partial sequence	62.6	62.6	84%	1e-12	86%	EF153310.1
<input type="checkbox"/>	Fusobacterium necrophorum strain Ulm 6 16S ribosomal RNA gene, partial sequence	62.6	62.6	84%	1e-12	86%	DQ440555.1
<input type="checkbox"/>	Fusobacterium necrophorum strain Ulm 5 16S ribosomal RNA gene, partial sequence	62.6	62.6	84%	1e-12	86%	DQ440554.1

nlm.nih.gov/Blast.cgi#alnHdr_451806384

Figure I. BLAST search results of sequenced purified PCR products of planktonic cells and biofilms compared to those in the GenBank database. These revealed all the strains as *F. necrophorum*. Strains tested were: ARU 01, JCM 3718 and JCM 3724.

Appendix III: BLAST data analysis for *galactose binding* primers with *F. necrophorum* DNA samples.

iii-1 ARU 01-*gal binding* primer:

TATTCGCATATTGGGGCTGTATGGAGTGGAGAAAAAAGAAGCAGCTCCCGCTGAAAATGC
AGTAAGAATGGGATTAACCGCTTATAAATTCGATGACAACCTCATTGCATTGTTTCAGACA
AGCTTTTCAAGCAGAAGCGGATGCCGTGGGAAATCAAGTTGCCTTACAAATGGTTGACTC
TCAAAATGATGCAGCAAAACAAAATGAAAACCTGGATGTATTATTAGAAAAAGGAATCGA
CACCTTGGCAATCAATTTGGTTGACCCGGCCGGTGTGATGTCGTATTGGAAAAAATCAA
AGCAAAAGAATTGCCGGTTGTTTTCTATAATAGAAAACCTTCGGATGAAGCATTGGCTTC
TTATGATAAAGCTTACTATGTAGGAATTGACCCAAATGCACAGGGAATTGCTCAAGGAAA
ATTGATTGAAAAAGCATGGCAAGCAAATCCTGCTTTGGATTAAACGGAGATGGAGTGAT
TCAATTCGCTATGTTGAAAGGAGAACCGGGACATCCGGATGCAGAAGCAAGAACCGTTTA
TTCCATTA AAACTTTAAATGAAGATGGAATAAAAAACAGAAGAATTACACTTAGATACAGC
TATGTGGGATACTGCACAAGCAAAAGACAAAATGGATGCATGGTTGTCAGGACCGAATGC
GGATAAAATTGAAGTGGTTATCTGTAATAACGACGGAATGGCTTTAGGAGCTATCGAATC
TATGAAAGCCTTCGGAAAATCATTACCGGTATTTGGAGTGGATGCTTTACCGGAAGCAAT
CACTTTGATTGAAAAGGGAGAAATGGCAGGAACCGTTTTAAATGATGCAAAAGGTCAAGC
AAAAGCAACTTTCCAAGTAGCTATGAACTTAGGGCAAGGAAAAGAAGCAACAGAAGGAAC
AGATATTCAAATGGAAAATAAAATTGTATTGGTGCCTTAGTATCGGGACCCAAGTGGGCA
ATACTTCGGTTATCCTTAAATCCAAATATTTCTAGATCTCCTTATCAACCATTTATTC
TATTC

iii-2 JCM 3718 – gal binding primer:

AAGATCACAGGTAGACTAGATAGCTCGCATAATGCGCGGGGAGAAGAAAGAGCAGCAGCT
CCCGCTGAAAATGCAGTAAGAATGGGATTAAGTCTTATAAATTTGATGATAACTTCATT
GCATTGTTGAGACAAGCTTTTCAAGCAGAAGCGGATGCTGTAGGAGATCAAGTTGCTCTA
CAAATGGTTGACTCTCAAATGATGCAGCAAAACAAAATGAACAATTGGATGTGTTATTA
GAAAAAGGAATTGACACCTTAGCAATCAATTTGGTTGACCCGGCCGGTGTTCGATGTTGTA
TTGGAAAAAATCAAAGCAAAAAAATTGCCAGTTGTTTTCTATAATCGAAAACCTTCAGAG
GAAGCGTTGGCTTCTTATGACAAAGCTTACTATGTAGGAATTGATCCAAATGCACAAGGA
GTTGCTCAAGGAAAATTAATTGAAAAAGCATGGCAAGCAAATCCTGCTTTGGATTTAAAC
GGAGACGGAGTGATTCAATTCGCTATGTTAAAAGGAGAACCCGGACATCCAGATGCAGAA
GCAAGAACTGTTTACTCCATTAATACTTGAATGAAGATGGAATTTAACAGAAAATTACAT
TTAATACAGCTATGTGGGATACTGCATAAGCAAAGGATAAATGGATGCATGGTGTTCAGGA
CCGAATGCCGATAAATTTAATTGATATCTGTATAATGACGGATTTCTTTAGGACTATTG

iii-3 JCM 3724 – gal binding primer:

AATTTTCATGTGCGGCTAGTAGCGATGTGGAGAAGAAGAAGCGGCAGCTCCTGCTGAAAAT
GCAGTAAGAATGGGATTAACCGCTTATAAATTCGATGACAACCTTCATTGCATTGTTTCAGA
CAAGCTTTTCAAGCAGAAGCGGATGCCGTGGGAAATCAAGTTGCCTTACAAATGGTTGAC
TCTCAAAATGATGCAGCAAAACAAAATGAACAATTGGATGTGTTATTAGAAAAAGGAATT
GACACCTTGGCAATCAATTTGGTTGACCCGGCCGGTGTTCGATGTTGTATTGGAAAAAATC
AAAGCAAAGAATTGCCGGTTGTTTTCTATAATCGAAAACCTTCAGAGGAAGCATTGGCT
TCTTATGACAAAGCTTACTATGTAGGAATTGACCCAAATGCACAAGGAATTGCTCAAGGA
AAATTGATTGAAAAAGCATGGCAAGCAAATCCTGCTTTGGATTTAAACGGAGATGGAGTG
ATTCAATTCGCTATGTTGAAAGGAGAACCGGGACATCCGGATGCGGAAGCAAGAACCGTT
TACTCCATTA AAACTTTAAATGAAGATGGAATAAAAACAGAAGAATTACACTTAGATACA
GCTATGTGGGATACCGCACAAAGCAAAGGATAAAATGGATGCATGGTTGTCAGGACCGAAT
GCGGATAAAATTGAAGTGGTTATCTGTAATAACGACGGAATGGCTTTAGGAGCTATCGAA
TCTATGAGAGCCTTCGGAAAATCATTACCGGTATTTGGAGTGGATGCTTTACCGGAAGCA
ATCACTTTGATTGAAAAGGGAGAAATGGCGGGAACCGTTTTAAATGATGCAAAGGTCAA
GCAAAGCAACTTTCCAAGTAGCTATGAACTTAGGGCAAGGAAAGAAGCACGGAAGGAAC
AGATATTCAAATGGAGAATAAATTGTATTGTGCCCTAGTATCGGCCCAA

Figure II. Nucleotide sequences of purified *F. necrophorum* samples with *gal binding* primer used for identification of the presence of *galactose binding* gene in *F. necrophorum* species.

Appendix IV: Haemagglutination Assays

iv-1 Haemagglutination assay of human blood cells with commercial anti-sera.

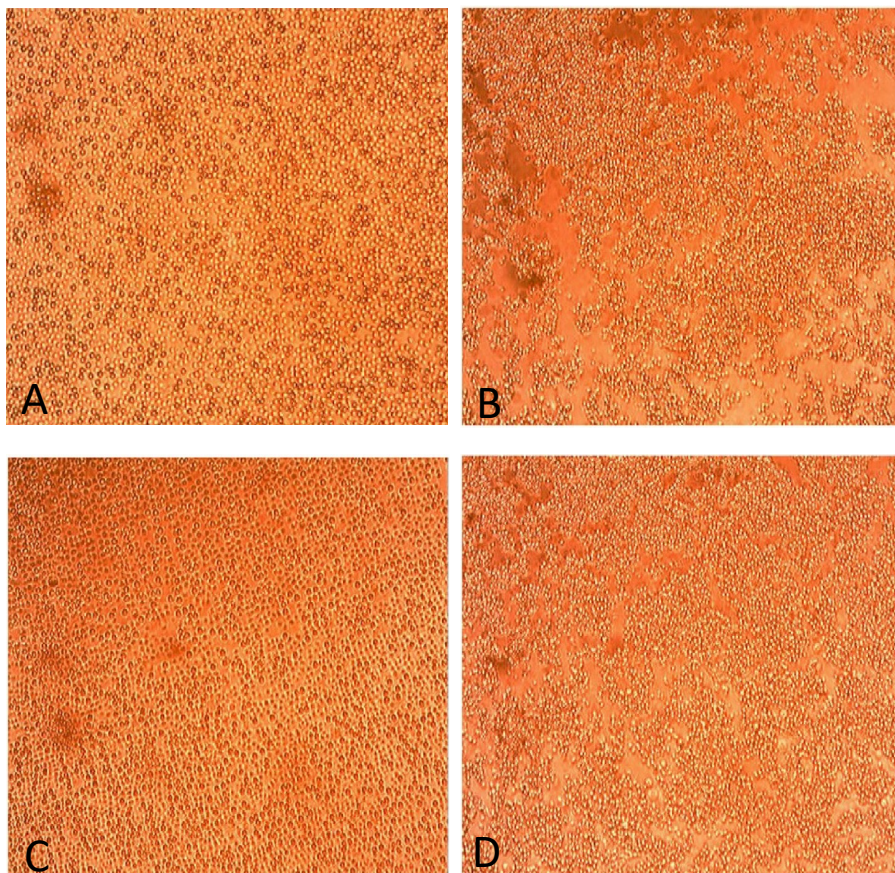


Figure III: Haemagglutination assays – Anti-B monoclonal antibody with blood type A, B, O and AB a) Anti-B with blood type A; b) Anti-B antibody with blood type B; c) Anti-B antibody with blood type O and d) Anti-B antibody with blood type AB. a) and c) indicates no haemagglutination, images b) and d) shows grape-like clusters of cells showing that haemagglutination has occurred.

iv-2 Haemagglutination assay of *F. necrophorum* cells with sheep red blood cells treated with neuraminidase.

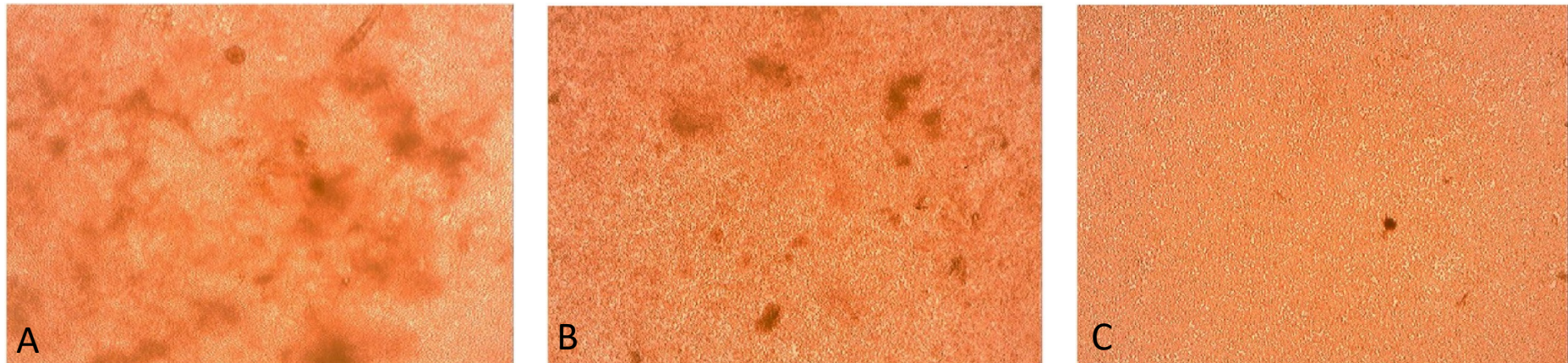


Figure IV: Haemagglutination assays showing results of *F. necrophorum* bacterial cells tested with neuraminidase treated sheep erythrocytes. A) ARU 01; B) JCM 3718 and C) JCM 3724 *F. necrophorum* cells with neuraminidase treated sheep erythrocytes. The results showed that *F. necrophorum* bacterial cells tested all agglutinated with the neuraminidase treated red blood cells.

Table I: Haemagglutination between human and sheep red cells and *F. necrophorum*

ARU 01; JCM 3718; JCM 3724

Agglutinin	Human Red Cells				Sheep Red Cells	
	A	B	0	AB	Native	Desialylated
ARU 01	0	0	0	0	0	3
JCM 3718	0	0	0	0	0	2+
JCM 3724	0	0	0	0	0	2
Anti-A	4	0	0	4	0	0
Anti-B	0	3+	0	3+	0	0

Appendix V: Q-RT-PCR for gene expression

Table II: Real-time PCR results of the first gene (LpxA) of lipid A pathway, showing the melt curve and quantitation analysis of *F. necrophorum* samples:

ARU 01; JCM 3718; JCM 3724; F21 and NC (no template control).

Lpx A		
Strains	CT Values	Melting Temperature
ARU 01	17.82	81.3
JCM 3718	11.74	82
JCM 3724	16.54	81.7
F5	7.46	82
F21	9.5	82
F24	8.49	82
F30	23.2	82
Neg Control	26.44	89
Pos Control	13.45	82

Table III: Real-time PCR results of the second gene (LpxC) of lipid A pathway, showing the melt curve and quantitation analysis of *F. necrophorum* samples:

ARU 01; JCM 3718; JCM 3724; F21 and NC (no template control).

Lpx C		
Strains	CT Values	Melting Temperature
ARU 01	17.05	81.2
JCM 3718	17.43	81.2
JCM 3724	17.23	81.3
F5	7.53	81.5
F21	8.98	81.5
F24	9.29	81.5
F30	8.91	81.5
Neg Control	25.44	87.0
Pos Control	14.10	81.5

Table IV: Real-time PCR results of the third gene (LpxD) of lipid A pathway, showing the melt curve and quantitation analysis of *F. necrophorum* samples:

ARU 01; JCM 3718; JCM 3724; F21 and NC (no template control).

Lpx D		
Strains	CT Values	Melting Temperature
ARU 01	19.59	82.2
JCM 3718	19.34	82
JCM 3724	18.88	82.3
F5	9.56	82.5
F21	9.03	82.5
F24	11.37	82.5
F30	9.97	82.5
Neg Control	26.25	89
Pos Control	14.63	82.5

Table V: Real-time PCR results of the fourth gene (LpxB) of lipid A pathway, showing the melt curve and quantitation analysis of *F. necrophorum* samples:

ARU 01; JCM 3718; JCM 3724; F21, PC (positive control) and NC (no template control).

Lpx B		
Strains	CT Values	Melting Temperature
ARU 01	18.29	79.7
JCM 3718	12.21	80.2
JCM 3724	18.8	80.2
F5	9.13	80
F21	10.36	80.3
F24	10.81	80
F30	9.16	80.3
Neg Control	26.24	88.8
Pos Control	15.08	80.3

Appendix VI: Formulae for estimation of biofilm assays

To ensure reproducibility and repeatability of the all biofilm assays, coefficient of variation (CV) was calculated for replicate assays (Feiler *et al.*, 2014). Standard deviation mean values and CV were determined for data generated from all biofilm assays to determine extent of dispersion between resultant OD values (replicates) using the equation;

$CV (\%) = \sigma/\mu \times 100$; Where σ is the standard deviation and μ is the mean value. CV % was subsequently set at $\leq 10 \%$.

Percentage efficacy of an antibiotic/antimicrobial (also known as antibiotic activity) and residual biofilm biomass for biofilm inhibition and eradication was determined for all MIC replicate assays using the formula;

Antibiotic/Antimicrobial efficacy (%) = $[(A - B) / A] \times 100$

and

Residual biofilm biomass (%) = $100 - \text{Antibiotic/Antimicrobial efficacy} (\%)$

Where A = absorbance of control (antibiotic free culture), B = absorbance of test sample (bacteria with antibiotic). Percentage inhibition (PI) and percentage reduction (PR) of biofilms by an antibiotic/antimicrobial which can also be defined as the efficacy of that antibiotic/antimicrobial were calculated using the formula;

Antibiotic/Antimicrobial efficacy (%) = $[(A - B) / A] \times 100$,

or

PI/PR = $100 - \text{Residual biofilm biomass} (\%)$

Appendix VII: Rpm (speed) to g (RCF)

Table VI: Conversion Table- Speed (rpm) to Relative centrifugal force (g) for Eppendorf centrifuge used in the project.

The radius of this centrifuge is 10 cm and is used with 15 ml tubes.

Speed (RPM)	RCF (g)
1000	112
1500	252
2000	447
2500	699
3000	1006
3500	1370
4000	1789
4500	2264
5000	2795
5500	3382
6000	4025
6500	4724
7000	5478
7500	6289
8000	7155
8500	8078
9000	9056
9500	10090
10000	11180
10500	12326
11000	13528
11500	14786
12000	16099
13000	18894
13500	20376
14000	21913

Table VII: Conversion Table - Speed (rpm) to Relative centrifugal force (g) for Eppendorf centrifuge used in the project.

The radius of this centrifuge is 8 cm and is used with 1.5 ml microfuge tubes.

Speed (RPM)	RCF (g)
1000	89
1500	201
2000	358
2500	559
3000	805
3500	1096
4000	1431
4500	1811
5000	2236
5500	2706
6000	3220
6500	3779
7000	4383
7500	5031
8000	5724
8500	6462
9000	7245
9500	8072
10000	8944
10500	9861
11000	10822
11500	11828
12000	12879
13000	15115
13500	16300
14000	17530

Appendix VIII

Permission granted from the copyright holder for the use of Figure 8.1.

Order License ID: 1040238-1.

References

- Adetunji, V. O. and Isola, T. O. (2011).** Crystal violet binding assay for assessment of biofilm formation by *Listeria monocytogenes* and *Listeria* spp. on wood, steel and glass surfaces. *Global Veterinaria*, **6** (1), 6-10.
- Afrough, B., Dwek, M. V. and Greenwell, P. (2007).** Identification and elimination of false-positives in an ELISA-based system for qualitative assessment of glycoconjugate binding using a selection of plant lectins. *BioTechniques*, **43**, 458-464.
- Agashe, D., Sane, M., Phalnikar, K., Diwan, G.D., Habibullah, A., Martinez-Gomez, N.C. et al. (2016).** Large-effect beneficial synonymous mutations mediate rapid and parallel adaptation in a bacterium *Mol Biol Evol*, **33**, 1542–1553.
- Ahn, S. and Burne, R.A. (2007).** Effects of oxygen on biofilm formation and the AtlA autolysin of *Streptococcus mutans*. *Journal of Bacteriology*, **189**(17), 6293-6302.
- Ahn, S. J., Browngardt, C. M. & Burne, R. A. (2009).** Changes in biochemical and phenotypic properties of *Streptococcus mutans* during growth with aeration. *Applied and environmental microbiology*, **75**, 2517-2527.
- Aliyu, S.H., Marriott, R.K., Curran, M.D., Parmar, S., Bentley, N., Brown, N.M., Brazier, J.S. and Ludlam, H. (2004).** Real-time PCR investigation into the importance of *Fusobacterium necrophorum* as a cause of acute pharyngitis in general practice. *Journal of Medical Microbiology*, **53**(10), 1029–1035.
- Allan, V.J.M., Callow, M.E., Macaskie, L.E. & Paterson-Beedle, M. (2002).** Effect of nutrient limitation on biofilm formation and phosphatase activity of a *Citrobacter* sp. *Microbiology*, **148**(Pt 1), 277–288.
- Amoako, K., Goto, Y. and Shinjo, T. (1993).** Comparison of extracellular enzymes of *Fusobacterium necrophorum* subsp. *necrophorum* and *Fusobacterium necrophorum* subsp. *funduliforme*. *Journal of Clinical Microbiology*, **8**(31), 2244-2247.
- Anderson, G.G. & O'Toole, G.A. (2008).** Innate and induced resistance mechanisms of bacterial biofilms. In *Bacterial Biofilms* (ed. Romeo T.), 85–105. Springer, Heidelberg.

- Atkinson, T. P., Centor, R. M., Xiao, L., Wang, F., Cui, X., Van Der Pol, W., and Waites, K. B. (2018).** Analysis of the tonsillar microbiome in young adults with sore throat reveals a high relative abundance of *Fusobacterium necrophorum* with low diversity. *PLoS one*, **13**(1), e0189423.
- Atlas M.R. (1997).** *Principles of microbiology*, 2nd ed. Dubuque, Iowa: Wm. C. Brown.
- Azeredo, J., Azevedo, N.F., Briandet, R., Cerca, N., Coenye, T., Costa, A.R., Desvaux, M., Di Bonaventura, G., Hébraud, M., Jaglic, Z., Kačániová, M., Knøchel, S., Lourenço, A., Mergulhão, F., Meyer, R.L., Nychas, G., Simões, M., Tresse, O. and Sternberg, C. (2017).** Critical review on biofilm methods, *Critical Reviews in Microbiology*, **43**(3), 313-351.
- Baker, J. S. (1984).** Comparison of various methods for differentiation of staphylococci and micrococci. *Journal of clinical microbiology*, **19** (6), 875-879.
- Bank, S., Nielsen, H.M., Hoyer Mathiasen, B., Christiansen Leth, D., Hagelskjær Kristensen, L. and Prag, J. (2010).** *Fusobacterium necrophorum* - detection and identification on a selective agar. *Apmis*, **118**(12), 994–999.
- Barb, A.W. and Zhou, P. (2008).** Mechanism and inhibition of LpxC: an essential zinc-dependent deacetylase of bacterial lipid A synthesis. *Current pharmaceutical biotechnology*, **9**(1), 9–15.
- Bassler, B.L. (2002).** Small talk. Cell-to-cell communication in bacteria. *Cell*, **109**(4), 421–4.
- Bassler, B.L. and Losick, R. (2006).** Bacterially speaking. *Cell*, **125**(2), 237–246.
- Batty, A., Wren, M.W.D. and Gal, M. (2005).** *Fusobacterium necrophorum* as the cause of recurrent sore throat: comparison of isolates from persistent sore throat syndrome and Lemierre's disease. *J Infect*, **51**(4), 299-306.
- Bax, M., Kuijff, M.L., Heikema, A.P., van Rijs, W., Bruijns, S.C., García-Vallejo, J.J., Crocker, P.R., Jacobs, B.C., van Vliet, S.J. & van Kooyk, Y. (2011).** *Campylobacter jejuni* lipooligosaccharides modulate dendritic cell-mediated T cell polarization in a sialic acid linkage-dependent manner. *Infect. Immun*, **79**, 2681–2689.
- Bennett, K.W. and Eley, A. (1993).** Fusobacteria: new taxonomy and related diseases. *Journal of medical microbiology*, **39**(4), 246–54.
- Bergmann, M., Michaud, G., Visini, R., Jin, X., Gillon, E., Stocker, A., Imberty, A., Darbre, T. and Reymond, J.L. (2016).** Multivalency effects on *Pseudomonas*

aeruginosa biofilm inhibition and dispersal by glycopeptide dendrimers targeting lectin LecA. *Organic & Biomolecular Chemistry*, **14**(1), 138–148.

Bjork, H., Bieber, L., Hedin, K. & Sundqvist, M. (2015). Tonsillar colonisation of *Fusobacterium necrophorum* in patients subjected to tonsillectomy. *BMC infectious diseases*, **15**, 264.

Bouchet, V., Hood, D.W., Li, J., Brisson, J.R., Randle, G.A., Martin, A., Li, Z., Goldstein, R., Schweda, E.K.H., Pelton, S.I., Richards, J.C. & Moxon, E.R. (2003). Host-derived sialic acid is incorporated into *Haemophilus influenzae* lipopolysaccharide and is a major virulence factor in experimental otitis media. *Proc Natl Acad Sci USA*, **100** (15), 8898-8903.

Brackman, G., Cos, P., Maes, L., Nelis, H. J. & Coenye, T. (2011). Quorum Sensing inhibitors increase the susceptibility of bacterial biofilms to antibiotics *in Vitro* and *in Vivo*. *Antimicrob. Agents Chemother.* **55**(6), 2655–2661.

Bradshaw, D.J., Marsh, P.D., Watson, G.K. and Allison, C. (1998). Role of *Fusobacterium nucleatum* and coaggregation in anaerobe survival in planktonic and biofilm oral microbial communities during aeration. *Infection and immunity*, **66**(10), 4729–4732.

Branda, S. S., Vik, Å., Friedman, L. & Kolter, R. (2005). Biofilms: the matrix revisited. *Trends Microbiol*, **13**, 20–26.

Brazier, J.S., Hall, V., Yusuf, E. & Duerden, B.I. (2002). *Fusobacterium necrophorum* infections in England and Wales 1990-2000. *Journal of Medical Microbiology*, **51** (3), 269-272.

Brazier, J.S. (2006). Human infections with *Fusobacterium necrophorum*. *Anaerobe*, **12**(4), 165–172.

Brennan, C.A. and Garrett W.S. (2019). *Fusobacterium nucleatum* — symbiont, opportunist and oncobacterium. *Nature Reviews Microbiology*, **17**, 156–166.

Brink D.R., Lowry S.R., Stock R.A. and Parrott J.C. (1990). Severity of liver abscesses and efficiency of feed utilization of feedlot cattle. *J anim sci*, **68**, 1201-1207.

British Society for Antimicrobial Chemotherapy (2014). *BSAC Methods for Antimicrobial Susceptibility Testing*. (Available from: <http://bsac.org.uk/wp-content/uploads/2012/02/BSAC-disc-susceptibility-testing-method.pdf>). [Accessed: July 2014].

Bugla-Płoskońska G., Rybka J., Futoma-Kołoch B., Cisowska A., Gamian A. and Doroszkiewicz, W. (2010). Sialic acid-containing lipopolysaccharides of *Salmonella* O48 strains--potential role in camouflage and susceptibility to the bactericidal effect of normal human serum. *Microb Ecol*, **59**(3), 601-13.

Burmølle, M., Ren, D., Bjarnsholt, T. and Sørensen, S.J. (2014). Interactions in multispecies biofilms : do they actually matter ? *Trends in Microbiology*, **22**(2), 84–91.

Calcutt, M.J., Foecking, M.F., Nagaraja, T.G. & Stewart, G.C. (2014). Draft genome sequence of *Fusobacterium necrophorum* subsp. *funduliforme* bovine liver abscess isolate B35. *Genome Announc.*, **2**.

Carlier, J.P., Henry, C., Lorin, V. and Rouffignat, K. (1997). Conversion of DL-threonine, D-threonine and 2-oxobutyrate into propionate and 2-hydroxybutyrate by *Fusobacterium* species. *Lett Appl Microbiol*, **25**(5), 371-4.

CDC (Centers for Disease Control and Prevention), (2001). *Issues in Healthcare Settings: CDC's Seven Healthcare Safety Challenges*. United States Department of Health and Human Services: Atlanta, GA, USA.

Centor, R.M., Atkinson, T.P., Ratliff, A.E., Xiao, L., Crabb, D.M., Estrada, C.A., Faircloth, M.B., Oestreich, L., Hatchett, J., Khalife, W. and Waites, K.B. (2015). The clinical presentation of *Fusobacterium*-positive and streptococcal-positive pharyngitis in a university health clinic: A cross-sectional study. *Annals of Internal Medicine*, **162**(4), 241–247.

Chakravorty, S., Helb, D., Burday, M., Connell, N. and Alland, D. (2007). A detailed analysis of 16S ribosomal RNA gene segments for the diagnosis of pathogenic bacteria. *Journal of Microbiological Methods*, **69**(2), 330–339.

Chan, Y. Y. and Chua, K. L. (2005). The *Burkholderia pseudomallei* BpeAB-OprB efflux pump: expression and impact on quorum sensing and virulence. *J. Bacteriol*, **187**, 4707–4719.

Chukwu,O.F., Umezudike, K. A., Kolawole, M., Agu R., Aa S. & Coker A. (2013). Susceptibility pattern of *Prevotella* and *Porphyromonas* species from patients with odontogenic infections in Lagos University Teaching Hospital to amoxicillin. *International Journal of Pharma and Bio Sciences*, **4**(2), B760–B765.

Chun, J., Oren, A., Ventosa, A., Christensen, H., Arahal, D.R., da Costa, M.S., Rooney, A.P., Yi, H., Xu, X.W., De Meyer, S. and Trujillo, M.E. (2018). Proposed minimal standards for the use of genome data for the taxonomy of prokaryotes.

International Journal of Systematic and Evolutionary Microbiology, **68**(1), 461–466.

Clinical Laboratory Standards Institute. (2014). *Performance Standards for Antimicrobial Susceptibility Testing; Twenty–Fourth Informational Supplement*. CLSI document M100–S24. Wayne, PA: Clinical and Laboratory Standards Institute; 2014.

Cochran, W.L., Suh, S.J., McFeters, G.A. and Stewart, P.S. (2000). Role of RpoS and AlgT in *Pseudomonas aeruginosa* biofilm resistance to hydrogen peroxide and monochloramine. *J Appl Microbiol*, **88**(3), 546-553.

Comstock, L.E. and Kasper, D.L. (2006). Bacterial Glycans: Key mediators of diverse host immune responses. *Cell*, **126**(5), 847–850.

Copenhagen-Glazer, S., Sol, A., Abed, J., Naor, R., Zhang, X., Han, Y.W. and Bachrach, G. (2015). Fap2 of *Fusobacterium nucleatum* is a galactose-inhibitable adhesin involved in coaggregation, cell adhesion, and preterm birth. *Infect Immun*, **83**(3), 1104-1113.

Cordero, O.J., and Varela-Calviño, R. (2018). Oral hygiene might prevent cancer. *Heliyon*, **4**(10), e00879.

Cox, M. E. , Kohr, R. J. and Samia, C. K. (1997). Comparison of quality control results with use of anaerobic chambers versus anaerobic jars. *Clinical Infectious Diseases*, **25** (2), S137–S138.

Cotton, L.A., Graham, R.J. and Lee, R.J. (2009). The role of alginate in *P. aeruginosa* PAO1 biofilm structural resistance to gentamicin and ciprofloxacin. *Journal of Experimental Microbiology and Immunology (JEMI)*, **13**, 58-62.

Cramton, S. E., Ulrich, M., Gotz, F. and Doring, G. (2001). Anaerobic conditions induce expression of polysaccharide intercellular adhesin in *Staphylococcus aureus* and *Staphylococcus epidermidis*. *Infect Immun*, **69**, 4079-85.

Cuny, G.D. (2009). A new class of UDP-3- O -(R -3-hydroxymyristol)- N -acetylglucosamine deacetylase (LpxC) inhibitors for the treatment of Gram-negative infections: PCT application WO 2008027466 . *Expert Opinion on Therapeutic Patents*, **19**(6), 893–899.

Dapefrid, A., Lundstrom, B. and Tano, K. (2017). Prevalence of *Fusobacterium necrophorum* in tonsils from patients with chronic tonsillitis. *Acta otolaryngologica*, **137**, 297-301.

Darling, A.E., Mau, B. and Perna, N.T. (2010). progressiveMauve: Multiple genome alignment with gene gain, loss and rearrangement. *PLoS One* **5**, e11147.

- Davies, D. (2003).** Understanding biofilm resistance to antibacterial agents. *Nature Reviews Drug Discovery*, **2**(2), 114–122.
- Davies, D.G., Parsek, M.R., Pearson, J.P., Iglewski, B.H., Costerton, J.W. and Greenberg, E.P. (1998).** The involvement of cell-to-cell signals in the development of a bacterial biofilm. *Science*, **280**(5361), 295–298.
- Dehazya, P. and Coles, R.S. (1980).** Agglutination of Human erythrocytes by *Fusobacterium nucleatum*: factors influencing hemagglutination and some characteristics of the agglutinin. *J Bacteriol*, **143**(1), 205-11.
- DeKeersmaecker, S. C. and Vanderleyden, J. (2003).** Constraints on detection of autoinducer-2 (AI-2) signalling molecules using *Vibrio harveyi* as a reporter. *Microbiology*, **149**, 1953–1956.
- De Witte, C., Flahou, B., Ducatelle, R., Smet, A., De Bruyne, E., Cnockaert, M., Taminiau, B., Daube, G., Vandamme, P. and Haesebrouck, F. (2017).** Detection, isolation and characterization of *Fusobacterium gastroisuis* sp. nov. colonizing the stomach of pigs. *Syst Appl Microbiol*, **40**(1), 42–50.
- Di Bonaventura, G., Stepanović, S., Picciani, C., Pompilio, A. and Piccolomini, R. (2007).** Effect of environmental factors on biofilm formation by clinical *Stenotrophomonas maltophilia* isolates. *Folia Microbiologica*, **52**(1), 86-90.
- Dong, H., Cao, H. and Zheng, H. (2017).** Pathogenic bacteria distributions and drug resistance analysis in 96 cases of neonatal sepsis. *BMC pediatrics*, **17**(1), 44.
- Dong, J.Z., Wang, L.P., Zhang, S.N., Shi, K.Q., Chen, S.L., Yang, N.B., Ni, S.L., Zhu, J.H. and Lu, M.Q. (2014).** LPS pretreatment ameliorates D-galactosamine/lipopolysaccharide-induced acute liver failure in rat. *Int J Clin Exp Pathol*, **7**(11), 7399-408.
- Donlan, R.M. (2001).** Biofilm formation: a clinically relevant microbiological process. *Clinical infectious diseases*, **33**(8), 1387–92.
- Donlan, R.M. and Costerton, J.W. (2002).** Biofilms : survival mechanisms of clinically relevant microorganisms. *Clin Microbiol Rev*, **15**(2), 167-93.
- Donlan, R.M. (2002).** Biofilms: microbial life on surfaces. *Emerging infectious diseases*, **8**(9), 881–90.
- El-Hadedy, D. and El-Nour, S. (2012).** Identification of *Staphylococcus aureus* and *Escherichia coli* isolated from Egyptian food by conventional and molecular methods. *Journal of Genetic Engineering and Biotechnology*, **10** (1), 129-135.

- Emiola, A., George, J. and Andrews, S.S. (2015).** A complete pathway model for lipid A biosynthesis in *Escherichia coli*. *PLoS ONE*, **10**(4). <https://doi.org/10.1371/journal.pone.0121216>.
- Engbrecht, J. and Silverman, M. (1984).** Identification of genes and gene products necessary for bacterial bioluminescence. *Proceedings of the National Academy of Sciences of the United States of America*, **81**(13), 4154–4158.
- Enright, A. J., Van Dongen, S. and Ouzounis, C. A. (2002).** An efficient algorithm for large-scale detection of protein families. *Nucleic acids research*, **30**(7), 1575–1584.
- Esko, J.D. and Sharon, N. (2009).** Microbial Lectins: hemagglutinins, adhesins, and toxins. In *Essentials of glycobiology*. 2nd edition. Varki, A., Cummings, R.D., Esko, J.D. *et al.*, editors. Cold Spring Harbor (NY): Cold Spring Harbor Laboratory Press.
- European Committee on Antimicrobial Susceptibility Testing (2014).** **EUCAST Clinical Breakpoint** (Available from https://eucast.org/ast_of_bacteria/previous_versions_of_documents/)
- Firnberg, E., Labonte, J.W., Gray, J.J. and Ostermeier, M.A. (2014).** A comprehensive, high-resolution map of a gene's fitness landscape. *Mol Biol Evol*, **31**, 1581-92.
- Fletcher, M. (1977).** The effects of culture concentration and age, time and temperature on bacterial attachment to polystyrene. *Can J Microbiol*, **23**, 1–6.
- Fu, L., Niu, B., Zhu, Z., Wu, S. and Li, W. (2012).** CD-HIT: Accelerated for clustering the next-generation sequencing data. *Bioinformatics*, **28**(23), 3150–3152.
- Garcia, M. M., Alexander, D. C. and McKay, K. A. (1975).** Biological characterization of *Fusobacterium necrophorum*. Cell fractions in preparation for toxin and immunization studies. *Infection and immunity*, **11**(4), 609–616.
- Garcia, G.G., Amoako, K.K., Xu, D.L., Inoue, T., Goto, Y. and Shinjo, T. (1999).** Chemical composition of endotoxins produced by *Fusobacterium necrophorum* subsp. *necrophorum* and *F. necrophorum* subsp. *funduliforme*. *Microbios*, **100**(397). 175-9.
- Gee, J.E., Sacchi, C.T., Glass, M.B., De, B.K., Weyant, R.S., Levett, P.N., Whitney, A.M., Hoffmaster, A.R. and Popovic, T. (2003).** Use of 16S rRNA gene sequencing for rapid identification and differentiation of *Burkholderia pseudomallei* and *B. mallei*. *J.Clin.Microbiology*, **41**(10), 4647–4654.

- Goodman, D.B., Church, G.M. and Kosuri, S. (2013).** Causes and effects of N-terminal codon bias in bacterial genes. *Science*, **342**, 475–479.
- Goris, J., Konstantinidis, K.T., Klappenbach, J.A., Coenye, T., Vandamme, P. and Tiedje, J.M. (2007).** DNA-DNA hybridization values and their relationship to whole-genome sequence similarities. *International Journal of Systematic and Evolutionary Microbiology*, **57**(1), 81–91.
- Greiner, L.L., Watanabe, H., Phillips, N.J., Shao, J., Morgan, A., Zaleski, A., Gibson, B.W. and Apicella, M.A. (2004).** Nontypeable *Haemophilus influenzae* strain 2019 produces a biofilm containing N-Acetylneuraminic acid that may mimic sialylated O-Linked glycans. *Infection and immunity*, **72**(7), 4249–4260.
- Gunnarsson A., Mårdh PA., Lundblad A. and Svensson S. (1984).** Oligosaccharide structures mediating agglutination of sheep erythrocytes by *Staphylococcus saprophyticus*. *Infection and Immunity*, **45**(1), 41-6.
- Haas, W., Shepard, B.D and Gilmore, M.S. (2002).** Two-component regulator of *Enterococcus faecalis* cytolysin responds to quorum-sensing autoinduction. *Nature*, **415**, 84–87.
- Haataja, S., Verma, P., Fu, O., Papageorgiou, A.C., Pöysti, S., Pieters, R.J., Nilsson, U.J. and Finne, J. (2018).** Rationally designed chemically modified glycodendrimer inhibits *Streptococcus suis* adhesin SadP at picomolar concentrations. *Chemistry - A European Journal*, **24**(8), 1905–1912.
- Hadfield, J., Croucher, N.J., Goater, R.J., Abudahab, K., Aanensen, D.M. and Harris, S.R. (2017).** Phandango: An interactive viewer for bacterial population genomics. *Bioinformatics*, **34**(2), 292–293.
- Hagelskjaer, L.H., Prag, J., Malczynski, J. and Kristensen, J.H. (1998).** Incidence and clinical epidemiology of necrobacillosis, including Lemierre's syndrome, in Denmark 1990–1995. *Eur J Clin Microbiol Infect Dis*, **17**, 561–5.
- Hajdu, S., Holinka, J., Reichmann, S., Hirschl, A.M., Graninger, W. and Presterl, E. (2010).** Antimicrobial Effects of daptomycin, vancomycin, tigecycline, fosfomicin, and cefamandole on Staphylococcal biofilms. *Antimicrob. Agents Chemother*, **54**(10), 4078.
- Halebian, S., Harris, B., Finegold, S.M. and Rolfei, R.D. (1981).** Rapid method that aids in distinguishing Gram-positive from Gram-negative anaerobic bacteria. *Journal of Clinical Microbiology*, **13** (3), 444-448.

- Hall-Stoodley, L., Costerton, J.W. and Stoodley, P. (2004).** Bacterial biofilms: From the natural environment to infectious diseases. *Nature Reviews Microbiology*, **2**(2), 95–108.
- Hall-Stoodley, L. and Stoodley, P. (2009).** Evolving concepts in biofilm infections. *Cell Microbiol*, **11**, 1034–43.
- Handler, M.Z., Miriovsky, B., Gendelman, H.E. and Sandkovsky, U. (2011).** *Fusobacterium necrophorum* causing infective endocarditis and liver and splenic abscesses. *Rev. Inst. Med. Trop. Sao Paulo*, **53**(3), 169-172.
- Harjai, K., Khandwaha, R.K., Mittal, R. et al. (2005).** Effect of pH on production of virulence factors by biofilm cells of *Pseudomonas aeruginosa*. *Folia Microbiol* (Praha), **50**, 99–102.
- Hayakawa, K., Nagashima, M., Ohta, K., Ohmagari, N. and Tayama, N. (2018).** *Fusobacterium necrophorum* subsp. *funduliforme* in tonsils from various patient populations in Japan. *Japanese Journal of Infectious Diseases*, **71**(5), 365-367.
- Heikema, A.P., Koning, R.I., Rico, S.D. dos S., Rempel, H., Jacobs, B.C., Endtz, H.P., van Wamel, W.J.B. and Samsom, J.N. (2013).** Enhanced, sialoadhesin-dependent uptake of Guillain-Barré syndrome-associated *Campylobacter jejuni* strains by human macrophages. *Infection and Immunity*, **81**(6), 2095–2103.
- Henderson, J.C., O'Brien, J.P., Brodbelt, J.S. and Trent, M.S. (2013).** Isolation and chemical characterization of lipid A from Gram-negative bacteria. *J Vis Exp*, **(79)**, e50623.
- Hentges, D. J., (1996).** Anaerobes: General Characteristics. In: Baron S, editor. Medical Microbiology. 4th edition. Galveston (TX): University of Texas Medical Branch at Galveston. Chapter 17. Available from: <https://www.ncbi.nlm.nih.gov/books/NBK7638/>
- Hibbing, M., Fuqua, C., Parseck, M. and Brook Peterson, S. (2010).** Bacterial competition: surviving and thriving in the microbial jungle. *Nature Reviews Microbiology*, **8** (1), 15 – 25.
- Hochbaum, A.I., Kolodkin-Gal, I., Foulston, L., Kolter, R., Aizenberg, J. and Losick, R. (2011).** Inhibitory effects of D-amino acids on *Staphylococcus aureus* biofilm development. *Journal of Bacteriology*, **193**(20), 5616–5622.
- Hollis, R. J., Bruce, J. L., Fritschel S. J. and Pfaller, M. A. (1999).** Comparative evaluation of an automated ribotyping instrument versus Pulsed-Field gel

electrophoresis for epidemiological investigation of clinical isolates of bacteria. *Diagn Microbiol Infect Dis*, **34**, 263–268.

Holm, K., Collin, M., Hagelskjær-Kristensen, L., Jensen, A. and Rasmussen, M. (2017). Three variants of the *leukotoxin* gene in human isolates of *Fusobacterium necrophorum* subspecies *funduliforme*. *Anaerobe*, **45**, 129–132.

Holm, L. and Rosenström, P. (2010). Dali server: conservation mapping in 3D. *Nucleic acids research*, **38**(Web Server issue), W545–W549.

Holmes, A.H., Moore, L.S.P., Sundsfjord, A., Steinbakk, M., Regmi, S., Karkey, A., Guerin, P.J. and Piddock, L.J. V. (2016). Understanding the mechanisms and drivers of antimicrobial resistance. *Lancet* **387**(10014), 176-187.

Hošťacká, A., Čížnár, I. and Štefkovičová, M. (2010). Temperature and pH affect the production of bacterial biofilm. *Folia Microbiologica*, **55**(1), 75–78.

Hsu S.P., Chen C-C. and Chien C-T. (2016). Pretreatment of sialic acid efficiently prevents lipopolysaccharide-induced acute renal failure and suppresses TLR4/gp91-mediated apoptotic signalling. *Kidney & blood pressure research*, **413**, 267-77.

Hu, M., Zhang, C., Mu, Y., Shen, Q. and Feng, Y. (2010). Indole affects biofilm formation in bacteria. *Indian journal of microbiology*, **50** (4), 362-368.

Huang, S.F., Lin, C.H., Lai, Y.T., Tsai, C.L., Cheng, T.J.R. and Wang, S.K. (2018). Development of *Pseudomonas aeruginosa* lectin LecA inhibitor by using bivalent galactosides supported on polyproline peptide scaffolds. *Chemistry - An Asian Journal*, **13**(6), 686–700.

Huerta-Cepas, J., Szklarczyk, D., Forslund, K., Cook, H., Heller, D., Walter, M.C., Rattei, T., Mende, D.R., Sunagawa, S., Kuhn, M., Jensen, L.J., Von Mering, C. and Bork, P. (2016). EGGNOG 4.5: A hierarchical orthology framework with improved functional annotations for eukaryotic, prokaryotic and viral sequences. *Nucleic Acids Research*, **44**(D1), D286–D293

Huizinga R., Easton AS., Donachie AM., Guthrie J., van Rijs W., Heikema A., Boon L., Samsom, J.N., Jacobs, B.C., Willison, H.J. and Goodyear, C.S. (2012). Sialylation of *Campylobacter jejuni* Lipo-Oligosaccharides: Impact on Phagocytosis and Cytokine Production in Mice. *PLoS ONE*, **7**(3), e34416.

Inoue, T., Kanoe, M., Goto, N., Matsumura, K. and Nakano, K. (1985). Chemical and biological properties of lipopolysaccharides from *Fusobacterium necrophorum* biovar A and biovar B strains. *Jpn J Et Sci*, **47**, 639-645.

- Jamal, M., Ahmad, W., Andleeb, S., Jalil, F., Imran, M., Asif, M., Hussain, T., Ali, M., Rafiq, M. and Atif, M. (2018).** Bacterial biofilm and associated infections. *Journal of the Chinese Medical Association*, **81**(1), 7–11.
- Jang, Y., Choi, Y., Lee, S., Jun, H. and Choi, B. (2012).** Autoinducer 2 of *Fusobacterium nucleatum* as a target molecule to inhibit biofilm formation of periodontopathogens. *Archives of Oral Biology*, **58**(1), 17–27.
- Jefferson, K.K. (2004).** What drives bacteria to produce a biofilm? *FEMS Microbiol Lett*, **236**, 163–73.
- Jensen, A., Kristensen, L.H. and Nielsen, H. (2008).** Minimum requirements for a rapid and reliable routine identification and antibiogram of *Fusobacterium necrophorum*. *Eur J Clin Microbiol Infect Dis*, **27**(7), 557-63.
- Jensen, A., Kristensen, L.H. and Prag, J. (2007).** *Fusobacterium necrophorum*: from tonsillitis to Lemierre's syndrome. *Ugeskr Laeger*, **171**(12), 987-90.
- Jones, C., Virji, M. and Crocker, P.R. (2003).** Recognition of sialylated meningococcal lipopolysaccharide by siglecs expressed on myeloid cells leads to enhanced bacterial uptake. *Molecular Microbiology*, **49**(5), 1213–1225.
- Jones, R.N., Ballou, C. and Biedenbach, D. (2001).** Multi-laboratory assessment of the linezolid spectrum of activity using the Kirby-Bauer disk diffusion method: Report of the Zyvox® Antimicrobial Potency Study (ZAPS) in the United States. *Diagnostic Microbiology and Infectious Disease*. **40** (1-2), 59 – 66.
- Joo, H. and Otto, M. (2012).** Review molecular basis of *in vivo* biofilm formation by bacterial pathogens. *Chemistry & Biology*, **19**(12), 1503–1513.
- Jurcisek, J., Greiner, L., Watanabe, H., Zaleski, A., Apicella, M.A. and Bakaletz, L.O. (2005).** Role of sialic acid and complex carbohydrate biosynthesis in biofilm formation by nontypeable *Haemophilus influenzae* in the Chinchilla middle ear. *Infection and immunity*, **73**(6), 3210–3218.
- Kajiwara, H., Toda, M., Mine, T., Nakada, H., Wariishi, H. and Yamamoto, T. (2010).** Visualization of sialic acid produced on bacterial cell surfaces by lectin staining. *Microbes and Environments*, **25**(3), 152–155.
- Källberg, M., Wang, H., Wang, S., Peng, J., Wang, Z., Lu, H. and Xu, J. (2012).** Template-based protein structure modeling using the RaptorX web server. *Nature protocols*, **7**(8), 1511–1522.

- Kapatral, V., Anderson, I., Ivanova, N., Reznik, G., Los, T., Lykidis, A., Bhattacharyya, A., Bartman, A., Gardner, W., Grechkin, G., Zhu, L., Vasieva, O., Chu, L., Kogan, Y., Chaga, O., Goltsman, E., Bernal, A., Larsen, N., Souza, M. D. et al. (2002).** Genome sequence and analysis of the oral bacterium *Fusobacterium nucleatum* Strain ATCC 25586. *Journal of bacteriology*, **184**(7), 2005–2018.
- Kapatral, V., Ivanova, N., Anderson, I., Reznik, G., Bhattacharyya, A., Gardner, W.L., Mikhailova, N., Lapidus, A., Larsen, N., D'Souza, M., Walunas, T., Haselkorn, R., Overbeek, R. and Kyrpides, N. (2003).** Genome analysis of *F. nucleatum* subsp. *vincentii* and its comparison with the genome of *F. nucleatum* ATCC 25586. *Genome Res*, **13**(6A), 1180–1189.
- Karpathy, S.E., Qin, X., Gioia, J., Jiang, H., Liu, Y., Petrosino, J.F., Yerrapragada, S., Fox, G.E., Haake, S.K., Weinstock, G.M. and Highlander, S.K. (2007).** Genome sequence of *Fusobacterium nucleatum* subspecies *polymorphum* - A genetically tractable fusobacterium. *PLoS ONE*, **2**(8).
- Katoh, K., Misawa, K., Kuma, K-I. and Miyata, T. (2002).** MAFFT: a novel method for rapid multiple sequence alignment based on fast Fourier transform. *Nucleic Acids Res*, **30**, 3059–3066.
- Kawsar, S.M.A., Takeuchi, T., Kasai, K. ichi, Fujii, Y., Matsumoto, R., Yasumitsu, H. and Ozeki, Y. (2009).** Glycan-binding profile of a D-galactose binding lectin purified from the annelid, *Perinereis nuntia* ver. *vallata*. *Comparative Biochemistry and Physiology - B Biochemistry and Molecular Biology*, **152**(4), 382–389.
- Keren, I., Kaldalu, N., Spoering, A., Wang, Y. and Lewis, K. (2004).** Persister cells and tolerance to antimicrobials. *FEMS Microbiology Letters*, **230** (1), 13–18.
- Keren, I., Mulcahy, L.R. and Lewis, K. (2012).** Persister eradication: lessons from the world of natural products. *Methods Enzymol.*, **517**, 387-406.
- Kim, D., Song, L., Breitwieser, F.P. and Salzberg, S.L. (2016).** Centrifuge: rapid and sensitive classification of metagenomic sequences. *Genome Res*, **26**, 1721–1729.
- Kirby, A., Garner, K. and Levin, B. (2012).** The relative contributions of physical structure and cell density to antibiotic susceptibility in bacteria in biofilms. *Antimicrobial Agents and Chemotherapy*, **56** (6), 2967 – 2975.

- Klug, T.E., Rusan, M., Fuursted, K., Ovesen, T. and Jorgensen A.W. (2016).** A systematic review of *Fusobacterium necrophorum* positive acute tonsillitis: prevalence, methods of detection, patient characteristics, and the usefulness of the Centor score. *Eur J Clin Microbiol Infect Dis.*, **35**(12), 1903-1912.
- Kolenbrander, P.E. (2011).** Multispecies communities: interspecies interactions influence growth on saliva as sole nutritional source. *Int J Oral Sci.*, **3**, 49-54.
- Koressaar, T. and Remm, M. (2007).** Enhancements and modifications of primer design program Primer3. *Bioinformatics*, **23**(10), 1289-91.
- Kristensen, L.H. and Prag, J. (2000).** Human Necrobacillosis, with emphasis on Lemierre's Syndrome. *Clin Infect Dis.* **31**(2), 524-32.
- Kudla, G., Murray, A. W., Tollervey, D. and Plotkin, J. B. (2009).** Coding-sequence determinants of gene expression in *Escherichia coli*. *Science (New York, N. Y.)*, **324**(5924), 255–258.
- Lagesen, K., Hallin, P., Rødland, A., Staerfeldt, H.-H., Rognes, T. and Ussery, D.W. (2007).** RNAmmer: consistent and rapid annotation of ribosomal RNA genes. *Nucleic Acids Research*, **35**(9), 3100–3108.
- Lange, R. P., Locher, H. H., Wyss, P. C. and Then, R. L. (2007).** The targets of currently used antibacterial agents: lessons for drug discovery. *Current pharmaceutical design*, **13**, 3140-3154.
- Langworth, B.F. (1977).** *Fusobacterium necrophorum*: Its characteristics and role as an animal pathogen. *Bacteriological Reviews*, **41**(2), 373-390.
- Lê, S., Josse, J. and Husson, F. (2008).** FactoMineR: an R package for multivariate analysis. *J Stat Softw* **25**(1), 1-18.
- Lee, I., Kim, Y.O., Park, S.C. and Chun, J. (2016).** OrthoANI: An improved algorithm and software for calculating average nucleotide identity. *International Journal of Systematic and Evolutionary Microbiology*, **66**(2), 1100–1103.
- Lerner, K. L. and Lerner. B.W. (2003).** *World of microbiology and immunology*. Detroit: Gale, ©2003
- Lesman-Movshovich, E., Lerrer, B. and Gilboa-Garber, N. (2003).** Blocking of *Pseudomonas aeruginosa* lectins by human milk glycans. *Canadian Journal of Microbiology* **49**(3), 230-235.
- Lewis, A.L., Robinson, L.S., Agarwal, K. and Lewis, W.G. (2016).** Discovery and characterization of *de novo* sialic acid biosynthesis in the phylum *Fusobacterium*. *Glycobiology*, **26**(10), 1107–1119.

- Lewis, K. (2001).** Riddle of biofilm resistance. *Antimicrob Agents Chemother*, **45**, 999-1007.
- Lewis, K., (2007).** Persister cells, dormancy and infectious disease. *Nature Reviews Microbiology*, **5**(1), 48–56.
- Li, G-W., Oh, E. and Weissman, J.S. (2012).** The anti-Shine-Dalgarno sequence drives translational pausing and codon choice in bacteria. *Nature* **484**, 538–541.
- Licking, E. (1999).** Getting a grip on bacterial slime. *Business Week* 13 September, 98 – 100.
- Liu, Y. and Burne, R. A. (2011).** The major autolysin of *Streptococcus gordonii* is subject to complex regulation and modulates stress tolerance, biofilm formation, and extracellular-DNA release. *J Bacteriol*, **193**, 2826-37.
- Löfmark, S., Edlund, C. and Nord, C. (2010).** Metronidazole is still the drug of choice for treatment of anaerobic infections. *Clin Infect Dis.* **50** (1), S16 – S23. Doi: 10.1086/647939.
- Loo, C.Y., Corliss, D.A. and Ganeshkumar, N., (2000).** *Streptococcus gordonii* biofilm formation : identification of genes that code for biofilm phenotypes. *Journal of Bacteriology*, **182**(5), 1374–1382.
- López, D., Vlamakis, H. and Kolter, R., (2010).** Biofilms. *Cold Spring Harb Perspect Biol*, **2**, 1–11.
- Lyster, C., Kristensen, L. H., Prag, J. and Jensen, A. (2019).** Complete genome sequences of two isolates of *Fusobacterium necrophorum* subsp. *funduliforme*, obtained from blood from patients with Lemierre's Syndrome. *Microbiology resource announcements*, **8**(4), e01577-18.
- Ma, L., Lu, H., Sprinkle, A., Pamek, M. and Wozniak, D. (2007).** *Pseudomonas aeruginosa* Psl Is a Galactose- and Mannose-Rich exopolysaccharide. *Journal of Bacteriology*, **189**(22), 8353-8356.
- Macher, B.A. and Galili, U., (2008).** The Gal α 1,3Gal β 1,4GlcNAc-R (α -Gal) epitope: a carbohydrate of unique evolution and clinical relevance. *Biochim Biophys Acta.* **1780**(2), 75–88.
- Maeshima N., and Fernandez R. C., (2013).** Recognition of lipid A variants by the TLR4-MD-2 receptor complex. *Frontiers in Cellular and Infection Microbiology.* **3**, 3.
- Mah, T.C. and Toole, G.A.O., (2001).** Mechanisms of biofilm resistance to antimicrobial agents. *Trends Microbiol*, **9**(1), 34–39.

Mailhe, M., Ricaboni, D., Vitton, V., Benezech, A., Dubourg, G., Michelle, C., Andrieu, C., Armstrong, N., Bittar, F., Fournier, P.E., Raoult, D., and Million, M. (2016). Noncontiguous finished genome sequence and description of *Fusobacterium massiliense* sp. nov. isolated from human duodenum. *New Microbes New Infect*, **16**, 3–12.

Mangan, D.F., Novak, M.J., Vora, S.A., Mourad, J. and Kriger, P.S., (1989). Lectin like interactions of *Fusobacterium nucleatum* with human neutrophils. *Infection and Immunity*, **57**(11), 3601–3611.

McDougald, D., Rice, S.A., Barraud, N., Steinberg, P.D. and Kjelleberg, S. (2012). Should we stay or should we go: mechanisms and ecological consequences for biofilm dispersal. *Nat Rev Microbiol*, **10**, 39-50.

Merritt, J. H., Kadouri, D. E., & O'Toole, G. A. (2005). Growing and analyzing static biofilms. *Current protocols in microbiology*, Chapter 1, Unit–1B.1.

Merritt, J.H., Kadouri, D.E. and Toole, G.A.O., (2011). Growing and analyzing static biofilms. *Curr Protoc Microbiol*. Chapter 1:Unit 1B.1, 1-18.

Metzger, L.E., and Raetz, C.R., (2010). An Alternative Route for UDP-Diacylglycosamine hydrolysis in bacterial lipid A biosynthesis. *Biochemistry*, **49**(31), 6715-6726.

Metzger, L.E., Lee, J.K, Finer-Moore J.S., Raetz, CR., and Stroud R.M.,(2012). LpxI structures reveal how a lipid A precursor is synthesized. *Nat Struct Mol Biol*, **19**(11),1132-8.

Millar, B.C., Jiru, X., Moore, J.E., and Earle, J.A.P., (2000). A simple and sensitive method to extract bacterial, yeast and fungal DNA from blood culture material. *Journal of Microbiological Methods*, **42**, 139–147.

Miller M.B, and .Bassler, B.L., (2001). Quorum sensing in bacteria. *Annual Review of Microbiology*, **55**, 165–99.

Mohammed, A., Nerland, A.H., Al-haroni, M. and Bakken, V. (2013). Polymeric matrix , and treatment of peridontitis. *Journal of Oral Microbiology*, **1**(5), 1–9.

Moons, P., Van Houdt, R., Aertsen, A., Vanoirbeek, K., Engelborghs, Y. and Michiels, C.W. (2006). Role of quorum sensing and antimicrobial component production by *Serratia plymuthica* in formation of biofilms, including mixed biofilms with *Escherichia coli*. *Applied and Environmental Microbiology*, **72**(11), 7294–7300.

- Morgenstein, A.A., Citron, D.M. and Finegold, S.M. (1981).** New medium selective for *Fusobacterium* species and differential for *Fusobacterium necrophorum*. *J Clin Microbiol*, **13**(4), 666–669.
- Mouricout, M., Petit, J.M., Carias, J.R., and Genius, R.J. (1990).** Glycoprotein glycans that inhibit adhesion of *Escherichia coli* mediated by K99 fimbriae: Treatment of experimental colibacillosis. *Infection and immunity*, **58**, 98-106.
- Munoz, A., Alonso, B., Alvarez, O., Llovo, J. (2003).** Lectin typing of five medically important *Candida* species. *Mycoses*, **46** (3-4), 85–89.
- Munoz, A., Alvarez, O., Alonso, B., Llovo, J. (1999).** Lectin typing of methicillin-resistant *Staphylococcus aureus*. *Journal of Medical Microbiology*, **48**(5), 495–499.
- Murray, P.A., Kern, D.G. and Winkler, J.R. (1988).** Identification of a galactose-binding lectin on *Fusobacterium nucleatum* FN-2. *Infection and Immunity*, **56**(5), 1314–1319.
- Nagaraja, T., and Cbengappa, M. (1998).** Liver abscesses in feedlot cattle: a review. *Journal of Animal Science*, **76**(1), 287-298.
- Nagaraja, T. G., Galyean, M.L., and Cole. N.A. (1998).** Nutrition and disease. *Vet. Clin. North Am. Food Anim. Pract*, **14**, 257–277.
- Narayanan, S., Nagaraja, T.G., Okwumabua, O., Staats, J., Chengappa, M.M. and Oberst, R.D. (1997).** Ribotyping to compare *Fusobacterium necrophorum* isolates from bovine liver abscesses, ruminal walls, and ruminal contents. *Applied and Environmental Microbiology*, **63**(12), 4671–4678.
- Narongwanichgarn, W., Kawaguchi, E., Misawa, N., Goto, Y., and Haga, T. (2001).** Differentiation of *Fusobacterium necrophorum* subspecies from bovine pathological lesions by RAPD-PCR. *Vet Microbiol*, **1**, 383–388.
- Ng, W.L., and Bassler B. L. (2009).** Bacterial quorum-sensing network architectures. *Annu. Rev. Genet*, **43**, 197–222.
- Nicholson, L.A., Morrow, C.J., Corner, L.A. and Hodgson, A.L.M. (1994).** Phylogenetic relationship of *Fusobacterium necrophorum* A, AB, and B biotypes base upon 16S rRNA gene sequence analysis. *Int J Syst Bacteriol*, **44**, 315–319.
- NIH, National Heart, Lung, and Blood Institute. (2002-12-20).** Research on microbial biofilms (PA-03-047).
- Nobbs, A., Lamont, R. and Jenkinson, H. (2009).** *Streptococcus* adherence and colonization. *Microbiology and Molecular Biology Reviews*, **73**(3), 407-450.

- Nord, C.E., (1995).** The role of anaerobic bacteria in recurrent episodes of sinusitis and tonsillitis. *Clinical Infectious Diseases*, **20**(6), 1512–1524.
- Nostro, A., Cellini, L., Di Giulio, M., D'Arrigo, M., Marino, A., Blanco, A.R., Favaloro, A., Cutroneo, G. and Bisignano, G., (2012).** Effect of alkaline pH on staphylococcal biofilm formation. *APMIS*, **120**(9), 733–742.
- Ofek, I., Hasty, D. L., and Sharon, N. (2003).** Anti-adhesion therapy of bacterial diseases: prospects and problems. *FEMS Immunology and Medical Microbiology*, **38**, 181-191.
- O'Toole, G.A., (2011).** Microtiter dish biofilm formation assay. *Journal of Visualized Experiments: JoVE*, (47), 2437.
- O'Toole, G. A., Pratt, L. A., Watnick, P. I., Newman, D. K., Weaver, V. B., & Kolter, R. (1999).** Genetic approaches to study of biofilms. *Methods in Enzymology*, **310**, 91–109.
- Ohlsson, J., Larsson, A., Haataja, S., Alajääski, J., Stenlund, P., Pinkner, J.S., Hultgren, S.J., Jukka, F., Kihlberg, J. and Nilsson, U.J., (2005).** Structure-activity relationships of galabioside derivatives as inhibitors of *E. coli* and *S. suis* adhesins: Nanomolar inhibitors of *S. suis* adhesins. *Organic and Biomolecular Chemistry*, **3**(5), 886–900.
- Okahashi, N., Koga, T., Nishihara, T., Fujiwara, T., and Hamada, S. (1988).** Immunobiological properties of lipopolysaccharides isolated from *Fusobacterium nucleatum* and *F. necrophorum*. *J Gen Microbiol*, **134**(6), 1707-15.
- Okwumabua, O., Tan, Z., Staats, J., Oberst, R.D., Chengappa, M.M. and Nagaraja, T.G., (1996).** Ribotyping to differentiate *Fusobacterium necrophorum* subsp. *necrophorum* and *F. necrophorum* subsp. *fundiliforme* isolated from bovine ruminal contents and liver abscesses. *Applied and Environmental Microbiology*, **62**(2), 469–472.
- Ondov, B.D., Bergman, N.H. and Phillippy, A.M., (2011).** Interactive metagenomic visualization in a Web browser. *BMC Bioinformatics*, **12**, 385.
- Opiyo, S.O., Pardy, R.L., Moriyama, H. and Moriyama, E.N., (2010).** Evolution of the Kdo2-lipid A biosynthesis in bacteria. *BMC Evolutionary Biology*, **10**(1), 362.
- Page, A.J., Cummins, C.A., Hunt, M., Wong, V.K., Reuter, S., Holden, M.T.G., Fookes, M., Falush, D., Keane, J.A. and Parkhill, J., (2015).** Roary: rapid large-scale prokaryote pan genome analysis. *Bioinformatics*, **31**, 3691–3693.

Page, A.J., Taylor, B., Delaney, A.J., Soares, J., Seemann, T., Keane, J.A. and Harris, S.R., (2016). SNP-sites: rapid efficient extraction of SNPs from multi-FASTA alignments. *Microb Genom* **2**, e000056.

Park, S.N., Kong, S.W., Kim, H.S., Park, M.S., Lee, J.W., Cho, E., Lim, Y.K., Choi, M.H., Chang, Y.H., Shin, J.H., Park, H.S., Choi, S.H., and Kook, J.K. (2012a). Draft genome sequence of *Fusobacterium nucleatum* ChDC F128, isolated from a periodontitis lesion. *J Bacteriol*, **194**, 6322–6323.

Park, S.N., Kong, S.W., Park, M.S., Lee, J.W., Cho, E., Lim, Y.K., Choi, M.H., Kim, H.S., Chang, Y.H., Shin, J.H., Park, H.S., Choi, S.H., and Kook, J.K. (2012b). Draft genome sequence of *Fusobacterium nucleatum* subsp. *fusiforme* ATCC 51190^T. *J Bacteriol*, **194**, 5445–5446.

Parsek, M.R., & Greenberg, E.P. (2005). Sociomicrobiology: the connections between quorum sensing and biofilms. *Trends Microbiol*, **13**(1), 27-33.

Pawlak, A., Rybka, J., Dudek, B., Krzyżewska, E., Rybka, W., Kędziora, A., Klaus, E. and Bugla-Płoskońska, G. (2017). *Salmonella* O48 serum resistance is connected with the elongation of the lipopolysaccharide O-antigen containing sialic acid. *International Journal of Molecular Sciences*, **18**(10), 2022.

Persson, G.R., and Imfeld, T. (2008). Periodontitis and cardiovascular disease. *Ther Umsch*, **65**(2),121-6.

Pett, E., Saeed, K., and Dryden, M. (2014). *Fusobacterium* species infections: clinical spectrum and outcomes at a district general hospital. *Infection*, **42**(2), 363-70.

Petti, C.A., Polage, C.R., and Schreckenberger, P. (2005). The role of 16S *rRNA* gene sequencing in identification of microorganisms misidentified by conventional methods. *J Clin Microbiol*, **43**, 6123–5.

Powers, M.J., and Trent M.S. (2018). Phospholipid retention in the absence of asymmetry strengthens the outer membrane permeability barrier to last-resort antibiotics. *Proc Natl Acad Sci USA*, **115** (36), E8518-E8527.

Price, M.N., Dehal, P.S., and Arkin, A.P. (2009). FastTree: computing large minimum evolution trees with profiles instead of a distance matrix. *Mol Biol Evol*, **26**, 1641–1650.

Pye, C.C., Yu, A.A. and Weese, J.S. (2013). Evaluation of biofilm production by *Pseudomonas aeruginosa* from canine ears and the impact of biofilm on antimicrobial susceptibility *in vitro*. *Vet Dermatol*, **24**(4), 446-9.

- Rachmaninov, O., Zinger-Yosovich, K.D., and Gilboa-Garber, N. (2012).** Preventing *Pseudomonas aeruginosa* and *Chromobacterium violaceum* infections by anti-adhesion-active components of edible seeds. *Nutrition Journal* **11**,10-17.
- Raina S., Vizio D.D., Odell M., Clements M., Vanhulle S., and Keshavarz T. (2009).** Microbial quorum sensing: a tool or a target for antimicrobial therapy? *Biotechnol Appl Biochem*, **54**, 65–84.
- Richter, M., and Rosselló-Móra, R. (2009).** Shifting the genomic gold standard for the prokaryotic species definition. *Proc Natl Acad Sci USA*, **106**, 19126–19131.
- Riordan, T., (2007).** Human infection with *Fusobacterium necrophorum* (Necrobacillosis), with a focus on Lemierre's syndrome. *Clinical microbiology reviews*, **20**(4), 622–59.
- Römling, U. and Balsalobre, C. (2012).** Biofilm infections, their resilience to therapy and innovative treatment strategies. *Journal of Internal Medicine*, **272**(6), 541–561.
- Rosano G.L., and Ceccarelli E.A. (2009).** Rare codon content affects the solubility of recombinant proteins in a codon bias-adjusted *Escherichia coli* strain. *Microb. Cell Fact*, **8**, 41.
- Rosen, G., Nisinov, I., Helcer, M. and Sela, M.N. (2003).** *Actinobacillus actinomycetemcomitans* serotype b lipopolysaccharide mediates coaggregation with *Fusobacterium nucleatum*. *Infect Immun*, **71**, 3652–3656.
- Rosen, G. and Sela, M.N. (2006).** Coaggregation of *Porphyromonas gingivalis* and *Fusobacterium nucleatum* PK 1594 is mediated by capsular polysaccharide and lipopolysaccharide. *FEMS Microbiol Lett*, **256**(2), 304-10.
- Rudi, K., Skulberg, O.M., Larsen, F., and Jakobsen, K.S. (1997).** Strain characterization and classification of oxyphotobacteria in clone cultures on the basis of 16S rRNA sequences from the variable regions V6, V7, and V8. *Applied and Environmental Microbiology*, **63**(7), 2593–2599.
- Sanders, B. E., Umana, A., Lemkul, J. A., and Slade, D. J. (2018).** FusoPortal: an interactive repository of hybrid MinION-Sequenced *Fusobacterium* Genomes Improves Gene Identification and Characterization. *mSphere*, **3**(4), e00228-18.
- Sasmal, D., Guhathakurta, B., Ghosh, A. N., Pal, C.R., and Datta, A. (1999).** Purification of a mannose/glucose-specific hemagglutinin/lectin from a *Vibrio cholerae* 01 strain. *FEMS Immunology and Medical Microbiology*, **23**(3), 221-227.

- Schachter, B. (2003).** Slimy business - The biotechnology of biofilms. *Nature Biotechnology*, **21**(4), 361–365.
- Scheffers, D. J. and Pinho, M. G. (2005).** Bacterial cell wall synthesis: new insights from localization studies. *Microbiology and Molecular Biology Reviews*, **69**, 585-607.
- Schliep, K.P. (2011).** phangorn: phylogenetic analysis in R. *Bioinformatics*, **27**, 592–593.
- Seemann, T. (2014).** Prokka: rapid prokaryotic genome annotation. *Bioinformatics*, **30**, 2068–2069.
- Segata, N., Börnigen, D., Morgan, X.C., and Huttenhower, C. (2013).** PhyloPhlAn is a new method for improved phylogenetic and taxonomic placement of microbes. *Nat Commun*, **4**, 2304.
- Seshadri, R., Leahy, S.C., Attwood, G.T., Teh, K.H., Lambie, S.C., Cookson, A.L., Eloe-Fadrosh, E.A., Pavlopoulos, G.A., Hadjithomas, M., Varghese, N.J., and Paez-Espino, D., Hungate1000 project collaborators, ... Kelly, W.J. (2018).** Cultivation and sequencing of rumen microbiome members from the Hungate1000 Collection. *Nature Biotechnology*, **36**(4), 359–367.
- Severi, E., Randle, G., Kivlin, P., and Whitfield, K. (2005).** Sialic acid transport in *Haemophilus influenzae* is essential for lipopolysaccharide sialylation and serum resistance and is dependent on a novel tripartite ATP-independent periplasmic transporter: Sialic acid TRAP transporter in *Haemophilus influenzae*. *Molecular Microbiology* **8**(4),1173-1185.
- Severi, E., Mueller, A., Potts, J.R., Leech, A., Williamson, D., Wilson, K.S., and Thomas G.H. (2008).** Sialic acid mutarotation is catalyzed by the *Escherichia coli* beta-propeller protein YjhT. *J. Biol. Chem*, **283**, 4841-4849.
- Shaniztki, B., Hurwitz, D., Smorodinsky, N., Ganeshkumar, N. and Weiss, E.I. (1997).** Identification of a *Fusobacterium nucleatum* PK1594 Galactose-Binding Adhesin which mediates coaggregation with periopathogenic bacteria and hemagglutination. *Infect Immun*, **65**(12),5231-7.
- Sharp, P.M. and Li, W.H. (1987).** The Codon Adaptation Index--a measure of directional synonymous codon usage bias, and its potential applications. *Nucleic Acids Res*, **15**, 1281–1295.
- Shinjo, T., Fujisawa, T., and Mitsuoka, T. (1991).** Proposal of two subspecies of *Fusobacterium necrophorum* (Flügge) Moore and Holdeman: *Fusobacterium necrophorum* subsp. *necrophorum* subsp. nov., nom. rev. (ex Flügge 1886), and

Fusobacterium necrophorum subsp. *funduliforme* subsp. nov., nom. rev. (ex Hallé 1898). *Int J Syst Bacteriol*, **41**(3), 395-7.

Simon, P.C. and Stovell, P.L. (1971). Isolation of *Sphaerophorus necrophorus* from bovine hepatic abscesses in British Columbia. *Canadian Journal of Comparative Medicine*, **35**, 103–106.

Slifkin, M., and Doyle, R. J. (1990). Lectins and their application to clinical microbiology. *Clinical microbiology reviews*, **3**(3), 197–218.

Sonnenwirth, A.C., Yin, E.T., Sarmiento, E.M., and Wessler, S. (1972). Bacteroidaceae endotoxin detection by Limulus assay. *Am J Clin Nutr*, **25**(12), 1452-4.

Sørensen, M.A., and Pedersen, S. (1991). Absolute *in vivo* translation rates of individual codons in *Escherichia coli*: The two glutamic acid codons GAA and GAG are translated with a threefold difference in rate. *Journal of Molecular Biology*, **222**, (2), 265-280.

Soto, S.M. (2013). Role of efflux pumps in the antibiotic resistance of bacteria embedded in a biofilm. *Virulence*, **4**(3), 223–229.

Spinola, S.M., Li, W., Fortney, K.R., Janowicz, D.M., Zwickl, B., Katz, B.P. and Munson, R.S. (2012). Sialylation of lipooligosaccharides is dispensable for the virulence of *Haemophilus ducreyi* in Humans. S. R. Blanke, ed. *Infection and Immunity*, **80**(2), 679–687.

Stanley, N.R. and Lazazzera, B.A. (2004). MicroReview: Environmental signals and regulatory pathways that influence biofilm formation. *Mol Microbiol*, **52**, 917–924.

Stapper, A.P., Narasimhan, G., Ohman, D.E., Barakat, J., Hentzer, M., Molin, S., Kharazmi, A., Høiby, N. and Mathee, K. (2004). Alginate production affects *Pseudomonas aeruginosa* biofilm development and architecture, but is not essential for biofilm formation. *Journal of Medical Microbiology*, **53**(7), 679–690.

Stepanović, S., Vukovic, D., Jezek, P., Pavlovic, M., and Svabic-Vlahovic.M. (2001). Influence of dynamic conditions on biofilm formation by staphylococci. *Eur. J. Clin. Microbiol. Infect. Dis*, **20**, 502–504.

Stewart, P.S. and Costerton, J.W. (2001). Antibiotic resistance of bacteria in biofilms. *Lancet*, **358**, 135–138.

Stoodley, P., Nistico, L., Johnson, S., Lasko, L. A., Baratz, M., Gahlot, V., Ehrlich, G.D., and Kathju, S. (2008). Direct demonstration of viable *Staphylococcus aureus* biofilms in an infected total joint arthroplasty. A case

report. *The Journal of bone and joint surgery. American volume*, **90**(8), 1751–1758.

Swords, W.E., Moore, M.L., Godzicki, L., Bukofzer, G., Mitten, M.J. and Voncannon, J. (2004). Sialylation of lipooligosaccharides promotes biofilm formation by nontypeable *Haemophilus influenzae*. *Infection and immunity*, **72**(1), 106–113.

Taj, Y., Essa, F., Aziz, F. and Kazmi, S. U. (2011). Study on biofilm-forming properties of clinical isolates of *Staphylococcus aureus*. *The Journal of Infection in Developing Countries*, **6**, 403-409.

Tan, Y., Gong, F., Li, S., Ji, S., Lu, Y., Gao, H., Xu, H. and Zhang, Y. (2010). Brief report: A new profile of terminal N-acetylglucosamines glycans on pig red blood cells and different expression of α -galactose on Sika deer red blood cells and nucleated cells. *Glycoconjugate Journal*, **27**(4), 427–433.

Tan, Z.L., Nagaraja, T.G. and Chengappa, M.M. (1996). *Fusobacterium necrophorum* infections: Virulence factors, pathogenic mechanism and control measures. *Veterinary Research Communications*, **20**(2), 113–140.

Tille, P., (2013). Bailey and Scott's Diagnostic Microbiology. 13th Edition. eBook ISBN:9780323277426.

Tomaras, A.P., McPherson, C.J., Kuhn, M., Carifa, A., Mullins, L., George, D., Desbonnet, C., Eidem, T.M., Montgomery, J.I., Brown, M.F., Reilly, U., Miller, A.A. and O'Donnell, J.P. (2014). LpxC inhibitors as new antibacterial agents and tools for studying regulation of lipid A biosynthesis in Gram-negative pathogens. *MBio*. **5**(5), e01551-14.

Untergasser, A., Cutcutache, I., Koressaar, T., Ye, J., Faircloth, B. C., Remm, M., and Rozen, S. G. (2012). Primer3--new capabilities and interfaces. *Nucleic acids research*, **40**(15), e115.

Uslu, C., Taysi, S., Akcay, F., Sutbeyaz, M.Y. and Bakan, N. (2003). Serum free and bound sialic acid and alpha-1-acid glycoprotein in patients with laryngeal cancer. *Annals of Clinical and Laboratory Science*, **33**(2), 156–159.

Varki, A., Freeze, H.H., and Gagneux, P. (2009). Evolution of glycan diversity. In: *Essentials of Glycobiology*. 2nd edition. Varki, A., Cummings, R.D., Esko, J.D., et al., editors. Cold Spring Harbor (NY): Cold Spring Harbor Laboratory Press.

Vimr, E.R., Kalivoda, K.A., Deszo, E.L. and Steenbergen, S.M. (2004). Diversity of microbial sialic acid metabolism. *Microbiology and molecular biology reviews*: *MMBR*, **68**(1), 132–53.

- Vinogradov, E., St. Michael, F., Homma, K., Sharma, A. and Cox, A.D. (2017).** Structure of the LPS O-chain from *Fusobacterium nucleatum* strain 10953, containing sialic acid. *Carbohydrate Research*, **440–441**, 38–42.
- Vlamakis, H., Aguilar, C., Losick, R. and Kolter, R. (2008).** Control of cell fate by the formation of an architecturally complex bacterial community. *Genes and Development*, **22**(7), 945–953.
- Vogel, U., Claus, H., Heinze, G. and Frosch, M. (1999).** Role of lipopolysaccharide sialylation in serum resistance of serogroup B and C meningococcal disease isolates. *Infection and Immunity*, **67**(2), 954–957.
- Vu, B., Chen, M., Crawford, R.J. and Ivanova, E.P. (2009).** Bacterial extracellular polysaccharides involved in biofilm formation. *Molecules* **14**, 2535–2554.
- Walters, M. C., 3rd, Roe, F., Bugnicourt, A., Franklin, M. J. and Stewart, P. S. (2003).** Contributions of antibiotic penetration, oxygen limitation, and low metabolic activity to tolerance of *Pseudomonas aeruginosa* biofilms to ciprofloxacin and tobramycin. *Antimicrobial agents and chemotherapy*, **47**(1), 317–323.
- Wang, B. and Anzai, J.I. (2015).** Recent progress in lectin-based biosensors. *Materials (Basel, Switzerland)*, **8**(12), 8590–8607.
- Wang, X. and Quinn, P.J. (2010).** Lipopolysaccharide: Biosynthetic pathway and structure modification. *Progress in lipid research*, **49**(2), 97–107.
- Weiss, E.I., Shaniztki, B., Dotan, M., Ganeshkumar, N., Kolenbrander, P.E. and Metzger, Z. (2000).** Attachment of *Fusobacterium nucleatum* PK1594 to mammalian cells and its coaggregation with periodontopathogenic bacteria are mediated by the same galactose-binding adhesin. *Oral Microbiology and Immunology*, **15**(6), 371–377.
- Wright, W.F, Shiner, C.N. and Ribes, J.A. (2012).** Lemierre’s syndrome. *South Med J.* **105**(5), 283-8.
- Wu, H., Zeng, M. and Fives-Taylor, P. (2007).** The glycan moieties and the N-terminal polypeptide backbone of a fimbria-associated adhesin, Fap1, play distinct roles in the biofilm development of *Streptococcus parasanguinis*. *Infection and Immunity*, **75**(5), 2181–2188.
- Yoneda, M., Kato, S., Mawatari, H., Kiriko hi, H., Imajo, K., Fujita, K., Endo, H., Takahashi, H., Inamori, M., Kobayashi, N., Kubota, K., Saito, S., Tohnai, I., Watanuki, K., Wada, K., Maeda, S. and Akajima, A. (2011).** Liver

abscess caused by periodontal bacterial infection with *Fusobacterium necrophorum*. *Hepatology Research*, **41**(2), 194-196.

Yoneda, S., Loeser, B., Feng, J., Dmytryk, J., Qi, F. and Merritt, J. (2014). Ubiquitous sialometabolism present among oral fusobacteria. *PLoS ONE*, **9**(6), e99263.

Yuki, N., Suzuki, K., Koga, M., Nishimoto, Y., Odaka, M., Hirata, K., Taguchi, K., Miyatake, T., Furukawa, K., Kobata, T. and Yamada, M. (2004). Carbohydrate mimicry between human ganglioside GM1 and *Campylobacter jejuni* lipooligosaccharide causes Guillain-Barré Syndrome. *Proc. Natl. Acad. Sci. USA*, **101**, 11404–11409.

Yusuf, E., Halewyck, S., Wybo, I., Piérard, D. and Gordts, F. (2015). *Fusobacterium necrophorum* and other *Fusobacterium* spp. isolated from head and neck infections: A 10-year epidemiology study in an academic hospital. *Anaerobe*, **34**, 120-4.

Zaric, S.S., Lappin, M.J., Fulton, C.R., Lundy, F.T., Coulter, W.A. and Irwin, C.R. (2017). Sialylation of *Porphyromonas gingivalis* LPS and its effect on bacterial-host interactions. *Innate Immunity*, **23**(3), 319–326.

Zhang, Y. (2014) Persisters, persistent infections and the Yin–Yang model. *Emerging Microbes and Infection*. **3**, e3.

Zhang, S.L., Wang, S.N. and Miao, C.Y. (2017). Influence of microbiota on intestinal immune system in ulcerative colitis and its intervention. *Frontiers in Immunol*, **8**, 1674.

Zhang, F., Nagaraja, T.G., George, D. and Stewart, G.C. (2006). The two major subspecies of *Fusobacterium necrophorum* have distinct leukotoxin operon promoter regions. *Veterinary Microbiology*, **112**(1), 73–78.

Zhou, H., Bennett, G. and Hickford, J.G.H. (2009). Variation in *Fusobacterium necrophorum* strains present on the hooves of footrot infected sheep , goats and cattle. *Veterinary Microbiology*, **135**, 363–367.

Zhou, M. and Wu, H. (2009). Glycosylation and biogenesis of a family of serine-rich bacterial adhesins. *Microbiology*, **155**(2), 317–327.